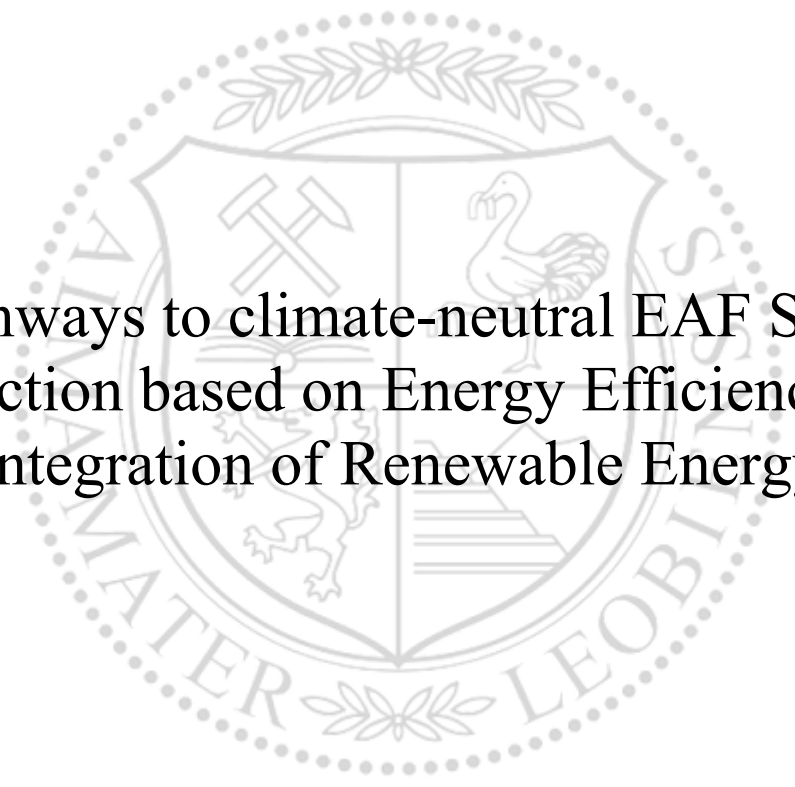




Chair of Energy Network Technology

Doctoral Thesis



Pathways to climate-neutral EAF Steel  
Production based on Energy Efficiency and  
Integration of Renewable Energy

Dipl.-Ing. Johannes Mathias Dock, BSc

August 2022



**AFFIDAVIT**

I declare on oath that I wrote this thesis independently, did not use other than the specified sources and aids, and did not otherwise use any unauthorized aids.

I declare that I have read, understood, and complied with the guidelines of the senate of the Montanuniversität Leoben for "Good Scientific Practice".

Furthermore, I declare that the electronic and printed version of the submitted thesis are identical, both, formally and with regard to content.

Date 16.08.2022

---

Signature Author  
Johannes Mathias Dock

## **ABSTRACT**

The iron and steel industry is accountable for a major share of global carbon dioxide emissions. Meeting the targets of the United Nations and the European Union to mitigate global warming requires a sharp reduction in greenhouse gas emissions. The transition from coal to renewable electric power as the main energy source allows for a major reduction of carbon dioxide emissions in steel production. This suggests a shift from the integrated process route involving blast furnace and converter to electric arc furnace-based production processes. The production of primary steel via direct reduction and secondary steel via the recycling of steel scrap enables low-carbon dioxide steelmaking. Both process routes entail the operation of an EAF steel mill.

Electric steel production is characterized by a high share of electric power in the total energy consumption. Thus, the provision of renewable electricity for the operation of the electric arc furnace and other aggregates represents an initial step towards carbon dioxide neutral steel production. However, a considerable amount of energy is supplied in the form of fossil fuels such as natural gas and coal. Three approaches are considered for reducing direct carbon dioxide emissions from the combustion of fossil fuels: fuel saving, carbon capture and substitution of energy carriers. The optimal implementation and the evaluation of these measures demands a holistic consideration of the entire production process, its energy supply and its interaction with the overall energy system.

Within the scope of the present thesis, potential approaches to reduce carbon dioxide emissions in electric steel production were investigated. First, a component- and time-resolved energy system model of an existing EAF steel mill was created based on measured data. This model generates energy-related key performance indicators and load profiles of energy carriers and industrial gases. Second, the energy system model was utilized to perform a techno-economic evaluation of a range of proposed energy efficiency and carbon dioxide emission reduction measures. Third, an optimization model was developed to analyze different options for flexible on-site production of oxygen, hydrogen and synthetic natural gas. Thus, the impact of the electricity price-driven operation of a power-to-gas plant on the steel mill and the overall energy system was analyzed.

Based on the defined research questions, the proposed options were assessed with regard to energy consumption, demand side flexibility, carbon dioxide emission reduction and economic viability. Eventually, the thesis outlines a potential pathway leading to the carbon dioxide-neutral energy supply of an EAF steel mill and identifies the enabling framework.

## KURZFASSUNG

Die Eisen- und Stahlindustrie ist für einen großen Teil der weltweiten Kohlendioxidemissionen verantwortlich. Um die Ziele der Vereinten Nationen und der Europäischen Union zur Eindämmung der globalen Erwärmung zu erreichen, muss der Ausstoß an Treibhausgasen drastisch reduziert werden. Der Übergang von Kohle zu Strom aus erneuerbaren Energiequellen als Hauptenergiequelle ermöglicht eine erhebliche Verringerung der Kohlendioxidemissionen in der Stahlproduktion. Dies bedeutet eine Verlagerung der Stahlproduktion weg von der integrierten Prozessroute mit Hochofen und Konverter hin zu Produktionsprozessen, welche auf dem Einsatz von Elektrolichtbogenöfen basieren. Sowohl die Erzeugung von Primärstahl durch Direktreduktion als auch von Sekundärstahl durch das Recycling von Stahlschrott ermöglicht eine kohlendioxidarme Stahlerzeugung.

Die Elektrostahlerzeugung ist durch einen hohen Anteil von elektrischer Energie am Gesamtenergieverbrauch gekennzeichnet, ein erheblicher Teil der Energie wird jedoch in Form fossiler Brennstoffe bereitgestellt. Die klimaneutrale Stahlproduktion erfordert daher die Bereitstellung von Strom aus erneuerbaren Energiequellen und die Verringerung direkter Kohlendioxidemissionen durch Brennstoffeinsparung, Carbon Capture and Utilization und Substitution fossiler Energieträger. Die optimale Implementierung und Bewertung dieser Maßnahmen erfordert eine holistische Betrachtung des gesamten Produktionsprozesses, der Energiebereitstellung und deren Interaktion mit dem übergeordneten Energiesystem.

Im Rahmen der vorliegenden Arbeit wurden vielversprechende Ansätze zur Reduktion der Kohlendioxidemissionen in der Elektrostahlerzeugung untersucht. Basierend auf Messdaten wurde ein komponenten- und zeitaufgelöstes Energiesystemmodell eines bestehenden Elektrostahlwerks erstellt. Dieses generiert energietechnische Kennzahlen und Lastprofile von Energieträgern und Gasen. Das Modell wurde genutzt, um eine techno-ökonomische Bewertung einer Reihe von Maßnahmen zur Senkung des Energieverbrauchs und der Kohlendioxidemissionen vorzunehmen. Weiters wurde ein Optimierungsmodell entwickelt, um verschiedene Optionen für eine flexible Vor-Ort-Produktion von Sauerstoff, Wasserstoff und synthetischem Methan zu analysieren. So wurden die Auswirkungen der strompreisgetriebenen Fahrweise einer Power-to-Gas-Anlage auf das Stahlwerk und das übergeordnete Energiesystem analysiert.

Auf Grundlage der formulierten Forschungsfragen wurden die vorgeschlagenen Optionen im Hinblick auf Energieverbrauch, Lastflexibilität, Kohlendioxidemissionen und Wirtschaftlichkeit bewertet. Schließlich zeigt die vorliegende Arbeit einen möglichen Pfad zur kohlendioxidneutralen Energieversorgung eines Elektrostahlwerkes und die dafür notwendigen Rahmenbedingungen auf.

## **ACKNOWLEDGEMENT**

At this point, I want to express my gratitude to the people, without whom this thesis would not have been possible.

First, I would like to thank my parents, Andrea and Johannes Dock, for enabling my studies and supporting me in every way throughout my academic career. Then, I want to thank my girlfriend Laura who was a great listener, advisor, proofreader and motivator during the doctoral studies. Moreover, I am grateful to my family and friends for their interest in my work and their moral support.

Special thanks go to my supervisor Thomas Kienberger and my mentor Markus Haider for the guidance in my scientific work. I would also like to thank the colleagues at the chair of Energy Network Technology for the professional as well as the witty discussions. In this context, the daily coffee breaks with Matthias deserve a special mention. It was a pleasure to work with this great team!

# CONTENTS

- Nomenclature..... I**
- List of figures ..... III**
- List of tables ..... V**
- 1 Introduction..... 1**
- 2 Context and Research Need ..... 4**
  - 2.1 EAF steel production process, energy demand and carbon dioxide emissions ..... 4
  - 2.2 Energy system models of EAF steel mills..... 7
  - 2.3 Reduction of carbon dioxide emissions..... 8
    - 2.3.1 Reduction of direct carbon dioxide emissions ..... 9
    - 2.3.2 Reduction of indirect carbon dioxide emissions ..... 14
  - 2.4 Research need..... 18
- 3 Methodology for the Assessment of Measures towards climate-neutral EAF Steel Production..... 20**
  - 3.1 Approach and outline of the thesis ..... 20
  - 3.2 Energy system model of the EAF steel mill..... 21
  - 3.3 Energy efficiency measures and CCU ..... 23
  - 3.4 Demand side management and RES integration ..... 24
  - 3.5 Overall assessment ..... 26
- 4 Results and Discussion ..... 28**
  - 4.1 Time- and component resolved energy demand ..... 28
  - 4.2 Energy consumption ..... 30
  - 4.3 Demand side management..... 32
  - 4.4 Carbon dioxide emissions ..... 34
  - 4.5 Economic assessment ..... 37
  - 4.6 Impact of extreme events..... 40
- 5 Conclusion and Outlook ..... 41**
  - 5.1 Conclusion..... 41

## Contents

---

5.2 Summary and Outlook .....	44
<b>6 References .....</b>	<b>46</b>
<b>Appendix A: Peer-reviewed scientific articles .....</b>	<b>54</b>
Article A1.....	54
Article A2.....	55
Article A3.....	56
<b>Appendix B: Further scientific dissemination .....</b>	<b>57</b>

## NOMENCLATURE

### Abbreviations

AEC	Alkaline electrolysis cell
BF	Blast furnace
BOF	Basic oxygen furnace
CAPEX	Capital expenditures
CCU	Carbon capture and utilization
CCS	Carbon capture and storage
CRC	Clausius Rankine Cycle
DR	Direct reduction
DRI	Direct reduced iron
DSM	Demand side management
EAF	Electric arc furnace
ETS	Emission trading system
GHGP	Greenhouse gas protocol
KPI	Key performance indicator
LCOO	Levelized cost of oxygen
LCOH	Levelized cost of hydrogen
LF	Ladle furnace
LH	Ladle heater
MILP	Mixed integer linear programming
OPEX	Operational expenditures
ORC	Organic Rankine Cycle
PEMEC	Proton exchange membrane electrolysis cell
PSA	Pressure swing adsorption
RES	Renewable energy sources



## Nomenclature

---

SEC	Specific energy consumption
SNG	Synthetic natural gas
SOEC	Solid oxide electrolysis cell
SR	Smelting reduction
TES	Thermal energy storage
VD	Vacuum degassing
VOD	Vacuum oxygen decarburization
WHR	Waste heat recovery

## Indices

HHV	Higher heating value
LHV	Lower heating value
el	electric
ref	reference

## LIST OF FIGURES

Figure 1: Estimated shares of future steel production technologies in the European Union according to production data from EUROFER [6] and future scenarios from Material Economics (ME) [10], IEA (SDS: Sustainable Development, STEPS: Stated Policies) [7], BCG [17] and ICF - Fraunhofer [18].	3
Figure 2: Schematic energy balance of an electric arc furnace.	4
Figure 3: Temperature curves of ladle heating programs for drying and preheating as well as an annealing program.	5
Figure 4: Final energy demand and direct carbon dioxide emissions of an EAF steel mill [24].	7
Figure 5: Available heat in relation to exhaust gas temperature for the stoichiometric combustion of methane with air and oxygen.	10
Figure 6: Demand side management measures and their impact on process quality and timing (TOU: time of use, DR: demand reserve, SR: spinning reserve) [62].	15
Figure 7: Excerpt of a hybrid energy system comprising of an electricity and natural gas system.	17
Figure 8: Applied approach for the development of a carbon dioxide emission reduction strategy EAF steel production, published scientific journal articles (A1-A4) and conference proceedings (C1-C2).	21
Figure 9: Schematic representation of the energy system of the EAF steel mill.	22
Figure 10: Process integration concept [24][24].	23
Figure 11: Optimization model for the implementation of different scenarios for flexible oxygen, hydrogen and SNG production [56].	25
Figure 12: Profile (A) and duration curve (B) of historical and forecasted electricity spot market prices for the years 2020 (blue), 2030 (orange) and 2050 (grey) [56].	27
Figure 13: Load profile for electric energy, natural gas and coal generated by the energy system model [22].	28
Figure 14: Waste heat load profile generated by the energy system model [22,24].	29
Figure 15: Load profile for oxygen and carbon dioxide generated by the energy system model [56].	30
Figure 16: Final and total specific energy consumption and gas sales for the different scenarios related to the reference scenario REF 2020.	32
Figure 17: Assessment of the demand side management potential of different oxygen and hydrogen supply systems including pressure swing adsorption (PSA) and electrolysis (PEM) in 2050 [56].	33

List of figures

---

Figure 18: Energy-related specific carbon dioxide emissions broken down by scopes related to the reference scenario REF 2020. .... 36

Figure 19: Composition of energy costs and revenues for different investigated scenarios related to the reference scenario REF 2020. .... 37

Figure 20: Projected development of the hydrogen sales price, natural gas price [56]. The latter includes emission allowances, charges and taxes. .... 39

## LIST OF TABLES

Table 1: Specific energy demand and carbon dioxide emissions of different steel production routes [7–10].....	2
Table 2: Projected energy, emission allowance and gas prices for the years 2020, 2030 and 2050 [56]. .....	27
Table 3: Impact of CO <sub>2</sub> emission reduction measures on natural gas, final energy and total energy consumption (based on scenario REF 2020).....	32
Table 4: Flexibility indicators of the PSA unit (EFF 2020) and electrolysis plant (SNG 2030 and PEM 2050) [56].....	34
Table 5: Reduction potential of different measures based on the total CO <sub>2</sub> emissions broken down by emission scopes (referred to the scenario REF 2020).....	36
Table 6: Impact of the extreme price situation on costs for oxygen, hydrogen and natural gas. ....	40
Table A 1: Author contribution statement for article A1.....	54
Table A 2: Author contribution statement for article A2.....	55
Table A 3: Author contribution statement for article A3.....	56

# 1 INTRODUCTION

In 2019, the steel industry in the European Union (EU-27) consumed 578 TWh of total energy [1] and emitted 146 Mt of carbon dioxide [2]. Steel production accounted for 5.0 % [1] of the primary energy consumption and 5.5 % of the total anthropogenic carbon dioxide emissions in the EU. In order to meet the goals set by the Paris Agreement adopted under the UNFCCC [3] and reach climate neutrality by the year 2050, the EU is committed to reduce the domestic greenhouse gas emissions by 55 % until 2030 compared to 1990 [4]. Therefore, the European steel industry faces the major challenge of cutting its CO<sub>2</sub> emissions by 80 to 95 % related to 1990 over the next two decades [5].

Currently, the crude steel production in Europe is based on two main process routes: In 2020, 57 % of European crude steel was produced from iron ore by the primary process route via blast furnace (BF) and basic oxygen furnace (BOF). The remaining 43 % are produced from steel scrap in the secondary route via the electric arc furnace (EAF) [6]. Mainly due to the energy- and emission-intensive reduction of iron ore in the blast furnace, producing one ton of steel via BF-BOF route consumes roughly five times more energy [7–9] and generates about four times more carbon dioxide emissions than recycling steel scrap in EAF steelmaking [7–10]. However, the potential of secondary steel production is limited by the availability and quality of steel scrap [10].

One alternative to the reduction of iron ore using coke in the blast furnace is the direct reduction (DR) with natural gas. In the MIDREX process, natural gas is reformed into carbon monoxide as well as hydrogen and fed into a shaft furnace to reduce the counter flowing iron ore in solid state [11]. The product, direct reduced iron (DRI), is then used as a feedstock in the EAF. The energy consumption of this process route is comparable to that of the BF-BOF route [7,9]. Given the lower carbon content of natural gas compared to coke in the blast furnace, the CO<sub>2</sub>-emissions are reduced by one third in the DR-EAF route [7–10]. The substitution of natural gas by hydrogen from renewable energy sources (RES) in direct reduction (HDR-EAF) represents a promising technology for CO<sub>2</sub>-neutral steelmaking [8–10,12]. However, a number of studies estimate that the electric energy consumption in the steel industry will quadruple due to the demand for hydrogen electrolysis [5].

Smelting reduction (SR) is a primary steel production route that combines the gasification of coal with the reduction and melting of iron ore [13]. The COREX [14] process comprises two reactors: First, the iron ore is reduced to DRI in a reduction shaft and, second, melted in a melter-gasifier. Subsequently, the produced so-called liquid pig iron is processed to crude steel in a BOF or in an EAF. Deploying SR processes has the potential to reduce the energy demand and the carbon dioxide emissions by around 20 % compared to the blast furnace

route [8–10]. The project SuSteel [15] investigates the reduction of iron ore and melting in a single-step process through a hydrogen plasma that is generated by an electric arc. This novel technology is expected to enable CO<sub>2</sub> emission-free steel production, at present. However, the process is still at the basic research stage, with direct CO<sub>2</sub> emissions expected within the range of the electric arc furnace [16].

**Table 1: Specific energy demand and carbon dioxide emissions of different steel production routes [7–10].**

Process route	Specific energy demand	Specific carbon dioxide emissions
	kWh/t <sub>crude steel</sub>	kgCO <sub>2</sub> /t <sub>crude steel</sub>
BF-BOF	4 900 – 5 900	1 600 – 2 200
Scrap-EAF	600 – 1 200	300 – 600
DR-EAF	4 800 – 5 800	600 – 1 500
HDR-EAF	4 100	0 – 25
SR-BOF	4 000	1 200 – 3 500

Table 1 outlines the ranges for specific energy consumption and carbon dioxide emissions of the above-mentioned steel production routes as reported in literature. From the present point of view, two routes qualify for climate-neutral steel production anyway: The Scrap-EAF and HDR-EAF process route.

It is difficult to predict which of the currently applied processes will prevail and which emerging technologies will have significance in future steel production. However, it is likely that there will be a mix of different steelmaking routes. Figure 1 summarizes several studies concerning future steel production technologies, which to some extent predict rather divergent technology mixes. Yet a common aspect of all the studies is that, irrespective the future technology mix and raw material feedstock, EAF steelmaking (Scrap-EAF and HDR/DR-EAF) is estimated to account for a significant share on the overall steel production in 2050.

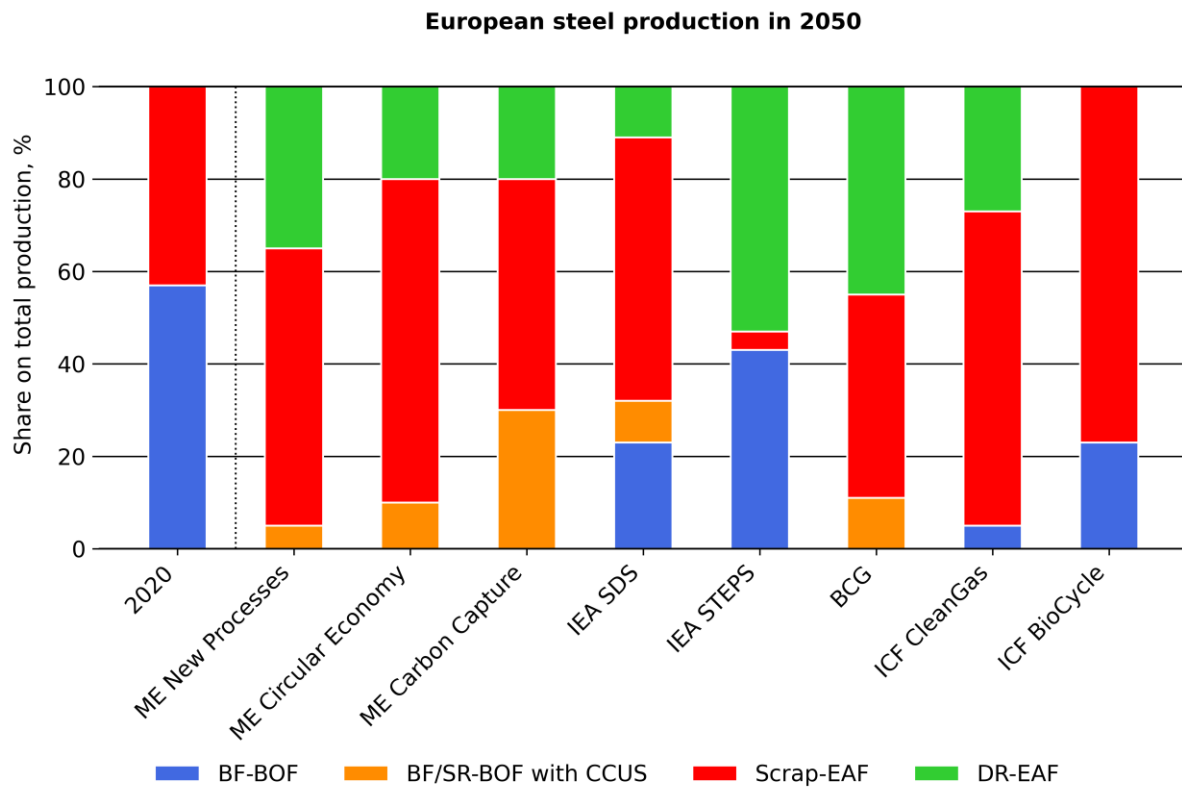


**Figure 1: Estimated shares of future steel production technologies in the European Union according to production data from EUROFER [6] and future scenarios from Material Economics (ME) [10], IEA (SDS: Sustainable Development, STEPS: Stated Policies) [7], BCG [17] and ICF - Fraunhofer [18].**

Independent if a scrap- or DRI-based EAF route is applied, it is necessary to investigate the energy saving and carbon dioxide emission reduction potential of the individual overall production processes. Hence, this doctoral thesis aims to identify suitable CO<sub>2</sub> reduction technologies and investigate their optimal implementation in the EAF steel mill. Furthermore, their impact on the energy consumption, demand side management potential, carbon dioxide emissions and energy provision costs is analyzed. The linking of the obtained results with existing research work and the expected evolution of the higher-level energy system indicates a viable pathway for climate-neutral EAF steel production through 2050.

## 2 CONTEXT AND RESEARCH NEED

The following chapter describes the EAF steel production route, its most important energy consumers and the carbon dioxide emissions associated with the production process. Furthermore, it gives an overview of existing energy system models for EAF steel mills and describes their respective strengths and limitations. Also, the state of technology regarding the reduction of direct and indirect CO<sub>2</sub> emissions is presented. Finally, in view of the requirements of the production process, the available technology and the existing scientific work, further need for scientific investigation is derived in the form of research questions.

### 2.1 EAF steel production process, energy demand and carbon dioxide emissions

Steel production by the EAF route as considered in this thesis comprises the following process steps:

- Primary metallurgy,
- Secondary metallurgy,
- Casting and
- Heat treatment.

The most energy-intensive process step is melting in the electric arc furnace which is referred to as primary metallurgy. The feedstock consists of steel scrap, DRI or a mixture of both. The energy input occurs mainly through the electrodes in the form of electrical energy. Natural gas burners in the furnace as well as injected coal can support the melting process (Figure 2) [19].

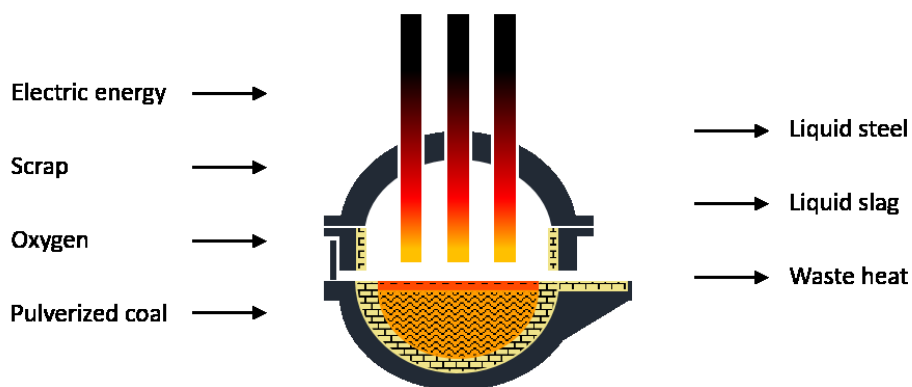


**Figure 2: Schematic energy balance of an electric arc furnace.**

In the EAF, oxygen fulfills three main functions: First, it enables additional energy input through exothermic oxidation reactions of scrap components and coal as well as the utilization of Oxyfuel burners [20]. Second, oxygen is injected for the refining of liquid steel and third, it



allows for the re-burning of combustible gases generated during scrap melting [19]. Therefore, oxygen not only fulfills metallurgical functions such as decarburization but also promotes exothermic reactions in the furnace that significantly reduce the electric energy consumption. Besides providing additional energy, coal is introduced into the furnace as a carburization and slag foaming agent during charging or during the process via lances in pulverized form [21]. Once the molten steel has reached the specified temperature and chemical composition, it is tapped into steel mill ladles.

Steel mill ladles are refractory-lined transport and treatment vessels for liquid steel. In order to prevent thermal shock in the refractory and to reduce the tapping temperature as well as the reheating times in secondary metallurgy, the ladles are heated prior to tapping [19]. The so-called ladle heaters generally serve two distinct purposes:

- Ladle drying refers to the process of removing moisture from the refractory after the relining. Figure 3 depicts the heating schedule which follows material-dependent temperature ramp rates. Heating is carried out in the vertical ladle position to avoid the displacement of the new lining.
- Ladle preheating involves raising and maintaining the ladle temperature between two operation cycles. Preheating allows for steeper heating rates and is conducted in horizontal heating stations to enable access to the installations at the ladle bottom for maintenance.

Due to high preheating temperatures and long operation times, the ladle heaters account for a significant share of total natural gas demand and carbon dioxide emissions in the EAF steel mill [22].

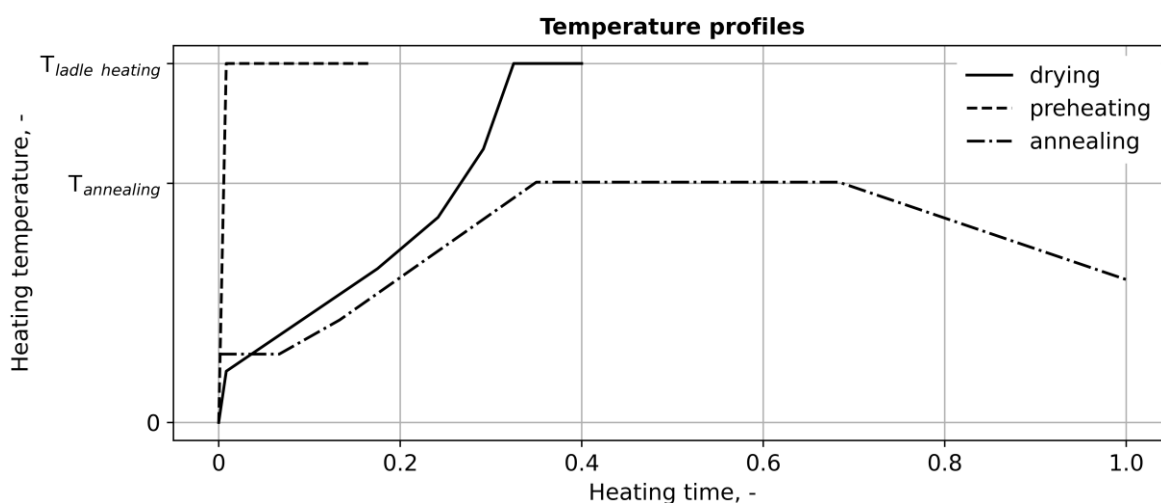


**Figure 3: Temperature curves of ladle heating programs for drying and preheating as well as an annealing program.**

Secondary metallurgy involves processes to further adjust the chemical composition of the steel melt such as decarburation, deoxidation, desulphurization, alloying, homogenization and degassing. During secondary metallurgical processing the ladle furnace (LF) is used to hold the required temperature of the steel melt. Analogous to the EAF, electrodes introduce electric energy into the liquid steel, whereby the steelmaking ladle serves as a furnace vessel. Stainless and special steels are additionally subjected to vacuum treatments such as vacuum oxygen decarburization (VOD) or vacuum degassing (VD). Steam ejector pumps generate the vacuum required for both treatments, resulting in a steam demand.

Subsequently, when the steel meets the predetermined quality, continuous- or ingot casting takes place depending on the plant configuration and required products. Finally, in some steel mills the produced steel blocks or billets are heat-treated in natural gas-fired annealing furnaces to adjust their physical properties. Similar to ladle heating, heat treatment is carried out according to predefined temperature profiles for heating-up and cooling the steel products (see Figure 3). Depending on the applied metallurgical treatments, the production of one ton of steel based on the best available technologies results in the consumption of 404 to 748 kWh of electric energy and 14 to 417 kWh of fossil fuels. Additionally, EAF steelmaking consumes 33 to 360 kg of steam, 3 to 28 kg of coal and 7 to 93 kg of oxygen and directly emits 72 to 180 kg CO<sub>2</sub> [23]. Adding indirect emissions related to the supply of electric power and raw materials, total CO<sub>2</sub> emissions reach up to 600 kg per ton of steel [8].

Figure 4 summarizes the distribution of the final energy demand according to energy carriers and consumers as well as the direct carbon dioxide emissions generated by the combustion of fossil fuels in the EAF steel mill, which was analysed in the course of this thesis. Process steam is mainly required for the vacuum generation through ejector pumps in VD and VOD treatments. For the sake of completeness, coal is stated as an energy carrier, though it is blown into the electric arc furnace in pulverized form merely for slag foaming. In addition to energy supply via electricity and fossil fuels, there is a substantial consumption of oxygen, which, as mentioned above, is highly relevant for the operation of the EAF steel mill.

**Energy consumption and carbon dioxide emissions**

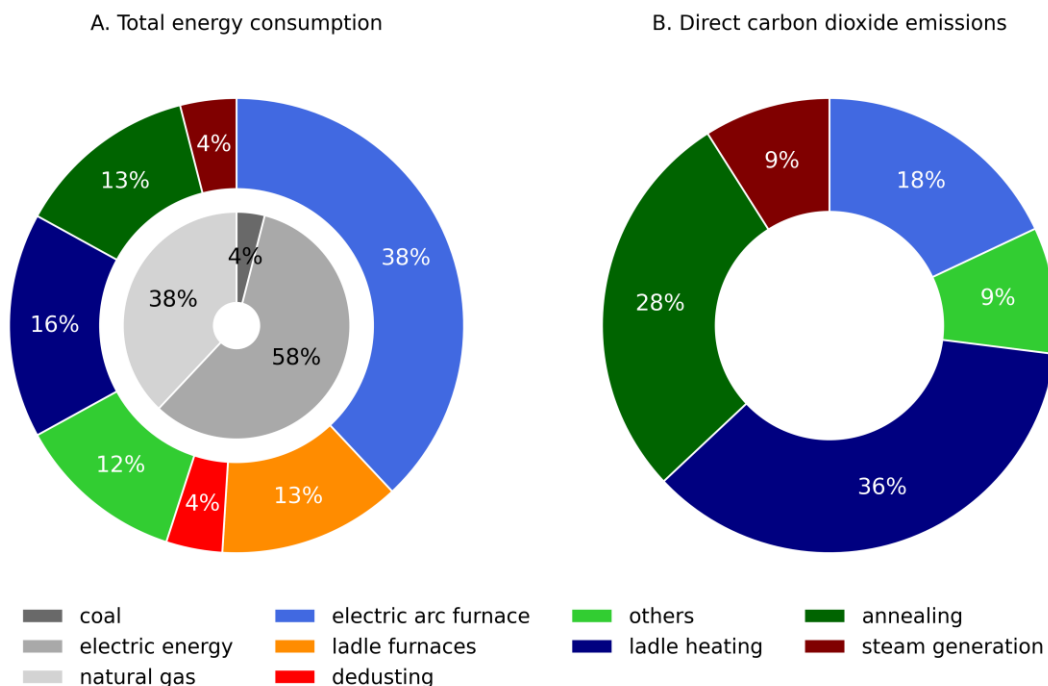


Figure 4: Final energy demand and direct carbon dioxide emissions of an EAF steel mill [24].

## 2.2 Energy system models of EAF steel mills

For highly integrated industrial energy systems, the optimal implementation and assessment of new technologies requires the application of holistic energy system models [22]. Depending on their modelling approach, such models can be subdivided into several groups: For the case of EAF steel mills, thermodynamic models depict the behaviour of individual aggregates such as electric arc or ladle furnaces based on mass and energy balances by application of the first and/or second law of thermodynamics [25–27]. Data-driven models deploy machine-learning tools such as artificial neural networks or regression for predicting the future energy consumption from historical data [28–30]. Process models enable the detailed description of fluid flow, heat transfer as well as chemical reactions and therefore require a profound understanding of the underlying principles and occurring phenomena [31]. In agent-based models, several aggregates such as the individual steel mill processes are implemented as interacting agents [32]. These agents operate independently and lack information about the status of the entire system, but cooperate with each other using a predetermined negotiation protocol.

EAF steel production involves subsequent batch processes resulting in a strongly fluctuating energy demand. Therefore, the energy system model will have to reflect the time-dependent energy demand. In addition, the optimal integration and evaluation of new technologies calls

for a holistic consideration of all system components, energy carriers and relevant process gases. Furthermore, the high complexity and inhomogeneity of the production process for high-alloy steels requires the ability to adapt the production process batch by batch. Several models are suitable for the accurate prognosis of the energy consumption of individual aggregates, but do not reflect any time-resolved behaviour. Other models are capable to generate load profiles but require the knowledge of certain process parameters and predefined load profiles of the sub-processes prior to calculation. To the best of the author's knowledge, solely the model described within the framework of this thesis allows for the holistic modeling of the time- and component-resolved energy consumption of the EAF steel mill. The developed model generates load profiles for energy carriers, gases, waste heat and carbon dioxide emissions [22].

### 2.3 Reduction of carbon dioxide emissions

After identifying the principal energy consumers and emission sources, it is necessary to explore the options for decarbonizing the production process. According to the classification of the *Greenhouse Gas Protocol* (GHGP), the carbon dioxide emissions are subdivided in three categories [33]:

- Scope 1 (direct) emissions that are generated in the steel mill, e.g. by the combustion of fossil energy carriers,
- Scope 2 (indirect) emissions from the generation of supplied electricity and
- Scope 3 (indirect) emissions that are not caused by the company but are a consequence of its activities, e.g. the extraction of raw materials.

For instance, oxygen is consumed in the EAF steel mill, but produced elsewhere and thus contributes to scope 3 emissions. Since this thesis directs its focus exclusively on the energy system of the steel mill, both scope 1 and scope 2 emissions are fully addressed, but scope 3 emissions are discussed only for oxygen generated off-site.

Based on the assessment of technological and political drivers for CO<sub>2</sub> emission mitigation by Rissman et al. [34], this thesis addresses four crucial supply-side measures:

- Energy efficiency,
- Carbon capture,
- Electrification and
- Substitution of fossil fuels.

In the following, based on the GHGP classification, energy efficiency and carbon capture are considered for direct emission reduction, whereas electrification and fossil fuel substitution is regarded as an indirect reduction measure.

### 2.3.1 Reduction of direct carbon dioxide emissions

Options for direct CO<sub>2</sub> emission reduction include the conservation of fossil fuels through energy efficiency measures and the capture of carbon dioxide from the flue gas. The following section describes available emission mitigation strategies for the EAF steel mill.

#### 2.3.1.1 Energy efficiency

In its report *European Union 2020*, the International Energy Agency ranks the improvement of energy efficiency as a first priority to reaching net-zero emissions in 2050 [35]. The conservation of fossil fuels contributes directly to the reduction of fuel-related CO<sub>2</sub> emissions. Energy efficiency measures can involve the application of new technologies, the improvement of the system design and efficient process control [34].

**Oxyfuel technology** is referred to combustion of fuels with pure oxygen. When combusting fuels such as natural gas, coal or hydrogen with ambient air, the major part of the air, mainly nitrogen, does not participate in the oxidation reaction. Nitrogen limits the heat transfer to the product and increases the flue gas heat flow. In contrast, combustion with oxygen increases the adiabatic flame temperature as well as the share of available heat and reduces the flue gas volume along with the associated heat losses [36]. Furthermore, studies show that the high concentration of the radiant gases carbon dioxide and water vapour in the flue gas improves the heat transfer [37]. Therefore, Oxyfuel combustion reduces the fuel consumption, particularly in processes with low thermal efficiency and the corresponding high flue gas temperatures [36]. Derived from the general energy balance, the thermal efficiency ( $\eta$ ) of a combustion process is determined by equation (1), where  $\dot{m}_{fuel}$  and  $\dot{m}_{flue\ gas}$  represent the mass flow rates of fuel and flue gas,  $\bar{c}_{p,flue\ gas}$  and  $T_{flue\ gas}$  the isobaric heat capacity and temperature of the flue gas,  $T_{ref}$  the reference temperature, and  $LHV$  the lower heating value of the fuel.

$$\eta = 1 - \frac{\dot{m}_{flue\ gas} \cdot \bar{c}_{p,flue\ gas}(T) \cdot (T_{flue\ gas} - T_{ref})}{\dot{m}_{fuel} \cdot LHV} \quad (1)$$

Figure 5 shows the thermal efficiency for the combustion of natural gas with air and pure oxygen in relation to the flue gas temperature as well as the potential efficiency increase ( $\Delta\eta$ ) for different steel mill processes and their mean flue gas temperature.

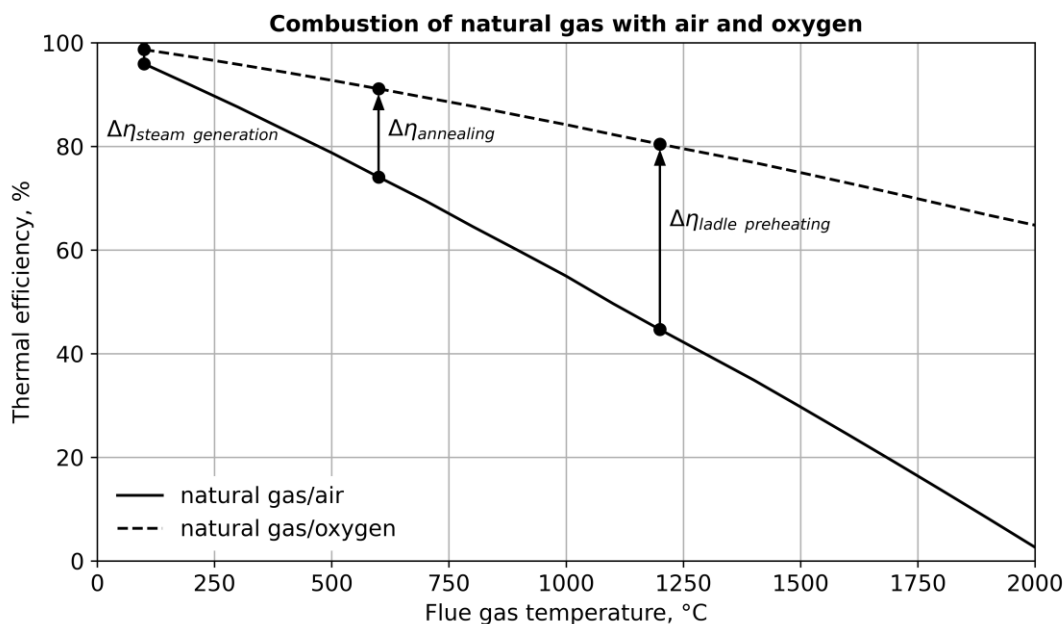


**Figure 5: Available heat in relation to exhaust gas temperature for the stoichiometric combustion of methane with air and oxygen.**

In the steel industry, Oxyfuel solutions have the potential to yield an increase in throughput capacity, fuel savings and reduction of both CO<sub>2</sub> and NO<sub>x</sub> emissions. Areas of application in the EAF steel mill are the electric arc furnace, vessel preheating as well as reheating and heat treatment furnaces [38]. From an energetic point of view, oxygen blowing and/or the operation of Oxyfuel burners in the EAF promote the melting of scrap, thus reducing electricity consumption and increasing productivity [19,38]. Thereby, electric energy is substituted by chemical energy from exothermic oxidation reactions of scrap components and supplied fuels such as natural gas or coal. A combined exploitation of both chemical and electric energy increases the total power input into the furnace and reduces the tap-to-tap time [19]. However, for the production of stainless steels, the injection of oxygen leads to the oxidation of valuable alloying elements, such as chromium [20]. This requires a compromise between saving electrical energy through oxygen blowing and limiting the loss of alloying metals. The mixed injection of oxygen and carbon dioxide is expected to prevent both excessive overheating and oxidation of alloying elements [39]. However, studies on industrial-scale experiments have not yet been published. In view of their high preheating temperatures exceeding 1 000 °C and long holding periods of several hours, the ladle heaters are particularly suitable for a conversion to Oxyfuel combustion [22] (Figure 5). On the one hand, Oxyfuel ladle preheating yields fuel as well as emission savings of up to 50 % [38] and increases heating rates as well as achievable heating temperatures [19,38]. On the other hand, the oxygen demand of the steel mill increases significantly.

Since steel production involves the application of high temperature processes, high amounts of waste heat at high temperature levels [22] occur. Therefore, studies on energy efficiency enhancement in the iron and steel industry consistently include suggestions for **waste heat recovery** [40]. Leveraging heat recovery opportunities not only reduces the energy consumption and direct carbon dioxide emissions but also saves costs. The appropriate recovery technology depends primarily on the temperature and type of recovered fluid. Waste heat sources in the steel industry lie within the medium to high temperature range (200°C to 1200°C). High dust loads, high recovery costs or the lack of a suitable sinks often limit their utilization [41].

In a typical electric arc furnace, about one third of the energy input is discharged through the off-gas at temperatures up to 1 200 °C [42]. Most of this heat is dissipated by means of a water cooled hot gas duct in order to allow subsequent flue gas treatment. Hot gas ducts are usually operated at cooling water temperatures well below 100 °C, thus the recovered energy can solely be used for low-exergy applications such as space heating. To enhance the waste heat exploitation, in the literature there are three approaches to harness the sensible heat from EAF off-gas: scrap preheating, steam production and power generation. Heating the steel scrap prior to charging saves electric energy and shortens the melting time, but promotes the formation of volatile organic compounds (VOC) and dioxins in the exhaust gas [43,44]. Furthermore, scrap preheating implies the implementation of a suitable charging system such as a conveyor belt or a vertical shaft at the electric arc furnace [44]. Since the electric arc furnace investigated in this thesis does not provide these features, we will focus on the latter waste heat applications. Several concepts exist for the recovery of waste heat from the EAF off-gas for steam and power generation, addressing the following common challenges [42,45–48]:

- High off-gas velocities,
- High dust loads,
- Gas temperature fluctuations,
- Mass flow fluctuations,
- High-temperature corrosion and
- Intermittent operation of the EAF.

The first option is to use the EAF waste heat for process steam generation [47]. Potential consumers of steam are the ejector pumps of the secondary metallurgical vacuum treatments [22,43]. One concept is to adapt the cooling system and raise the temperature and pressure of the cooling water [47] in order to produce low-pressure steam. For balancing the fluctuating heat supply and demand, the concept includes a pressurized thermocline storage tank. Results from dynamic simulations of the proposed system layout with a process simulation software

indicate that the thermocline storage enables a constant steam supply rate, despite the fluctuating waste heat load at the EAF. Hence, it is possible to substitute fossil fuel-fired steam generators, save primary energy and reduce carbon dioxide emissions [47]. In other concepts, as an alternative to pressurized water cooling evaporative cooling is applied. Therefore, the hot gas duct is replaced by a waste heat boiler. Ruths steam buffers decouple supply and demand, enabling a continuous steam mass flow to the steam consumers [42,46]. In order to overcome shortcomings such as the limited temperature of heat extraction and low thermal storage density, alternative concepts are currently developed involving the application of different heat transport and thermal energy storage (TES) media [42,48–50].

The second option for the utilization of waste heat is power generation, in particular when a suitable steam or heat consumer is not available. Power can be generated either by Clausius Rankine Cycle (CRC) or by Organic Rankine Cycle (ORC) plants. In the ORC process water is replaced by an organic working fluid, which entails a number of advantages [51]: On the one hand, the reduced evaporation temperature of the organic fluid allows the production of electricity from waste heat at lower temperatures. On the other hand, the compact system layout and modular design facilitates the utilization of small, decentralized energy sources. However, because of the lower application temperature, the maximum efficiency of ORC processes is significantly lower than that of CRCs. For both, Clausius Rankine Cycle and Organic Rankine Cycle concepts, the heat from the off-gas is transferred to a steam or thermal oil cycle. In order to buffer the intermittent waste heat source and to allow for constant power generation, the implementation of a TES is indispensable. Subsequently, the steam is either expanded directly [42] or, similar to thermal oil, acts as a heat transfer fluid for the ORC process [46,50,52].

**Air preheating** represents a technology to reduce fuel consumption and decrease the exhaust gas temperature of combustion-based processes. Thereby, the hot flue gas discharged from the furnace preheats the cold air prior to combustion through a regenerator or a recuperator [41]. Air preheating reduces the exhaust gas losses and the required heat input of the furnace. In regenerative air preheating, flue gas and combustion air flow alternately through the regenerator, whereby heat is extracted from the flue gas, stored in a high heat capacity material and then transferred to the combustion air. In recuperative preheating, both gases flow through the heat exchanger simultaneously, but are structurally separated. Given the high flue gas temperatures, air preheating provides an energy saving potential for the annealing furnaces and ladle heaters. For the former, air preheating by regenerators or recuperative burners is state of the art technology. Research on the optimal implementation of air preheating systems for ladle heaters is still ongoing. Studies indicate that the installation of a recuperator raises the combustion air temperature by 200 °C, thus saving up to 35 % of



natural gas and carbon dioxide emissions [53]. However, due to the high number of individual units, equipping ladle heating stations with such systems requires significant investment.

Finally, it should be emphasized that energy efficiency is not only achieved by the optimization of individual plant components but also, more importantly, by an **integrated system design** [34]. A holistic view on the respective energy system is therefore crucial in order to assess the effects of the implemented measures on one another and on the overall system. For instance, deploying Oxyfuel combustion will on the one hand result in fuel savings and enable the separation and utilization of carbon dioxide, but on the other hand, it will reduce the flue gas flow rate and thus the available amount of usable waste heat.

### *2.3.1.2 Carbon capture, utilization and storage*

Depending on the point of carbon separation, the most mature carbon capture processes are generally categorized in three different technologies [54]:

- Pre-combustion sequestration and capture,
- Post-combustion sequestration and capture and
- Oxyfuel combustion, sequestration and capture.

Pre-combustion capture technologies are applied in integrated gasification combined cycle (IGCC) power plants. The carbon is removed from the fuel before combustion which requires additional process steps. In a first step, the fuel is gasified with oxygen or water as gasification agent. Then, the produced carbon monoxide is converted via the water gas shift (WGS) reaction towards CO<sub>2</sub>, which allows that most of the carbon content of the fuel can be removed by subsequent scrubbing. In post-combustion, the CO<sub>2</sub> is removed from the flue gas by scrubbing processes or membranes [55]. This process is especially suitable as end-of-pipe solution for re-powering concepts.

Oxyfuel combustion generates a flue gas containing mainly carbon dioxide and water vapour, which facilitates the separation of CO<sub>2</sub> through condensation. Deploying the Oxyfuel technology for ladle heating offers a range of advantages [24]: First, Oxyfuel ladle heating results in significant natural gas savings, thus reducing fuel costs and carbon dioxide emissions. Second, the separation of carbon dioxide from the flue gas converts climate-critical emissions into a valuable product, which is otherwise purchased. This two-fold emission reduction, consisting of the conservation of fossil fuels and the capturing of the generated carbon dioxide, clearly fosters the application of the Oxyfuel technology.

**Carbon capture and utilization** (CCU) refers to the separation of carbon dioxide and its subsequent utilization. Carbon capture and storage (CCS) describes the permanent storage of the separated carbon dioxide in underground storages such as depleted natural gas reservoirs [55]. In the context of the EAF steel mill, the recovery of CO<sub>2</sub> is considered for the following

applications: the neutralization of alkaline wastewater [24], the treatment of cooling water and SNG production via methanation (see 2.3.2.2) [56]. A further potential sink for carbon dioxide is the mixed blowing of O<sub>2</sub> and CO<sub>2</sub> in the EAF [39,57]. However, given the resulting increase in electrical energy consumption and the lack of an impact on the CO<sub>2</sub> balance of the steel mill, this option is excluded from the scope of this thesis.

### **2.3.2 Reduction of indirect carbon dioxide emissions**

The transition from the BF-BOF steelmaking to DR-EAF or Scrap-EAF production routes results in an enhanced electrification of steel production. The energy supply of the production process shifts from coal and coke to electricity and hydrogen generated from renewable power. Supplying the process with renewable electricity therefore offers the potential for the reduction of indirect CO<sub>2</sub> emissions. However, this implies the need for an enhanced integration of renewable energies into the overall energy system. Since not all processes can be electrified, there is a need to substitute fossil fuels such as natural gas with climate-neutral alternatives. The following section shows how these two objectives can be combined.

#### *2.3.2.1 Renewable electricity*

Climate neutrality within the energy system necessitates the transition from fossil fuels to renewable energy sources for power generation. In 2020 electricity accounted for 23 % of the final energy consumption [1] and 20 % of the net CO<sub>2</sub> emissions in the European Union. The goal to reach net-zero carbon dioxide emissions in 2050 [4] is only achievable with a substantial expansion of renewable generation capacity, mainly wind and solar [35]. In 2020 the share of renewable energy sources in electricity production reached 38 % in the EU [1]. For the first time, more electricity was generated from renewable sources than fossil fuels and the carbon intensity for power generation decreased to 226 g/kWh [58]. The recent increase in the share of renewables is mainly due to the cut in coal-fired power generation and the growing share of wind and photovoltaics.

Compared to coal, oil, gas and nuclear power generation, renewable energies such as photovoltaics and wind power feature volatile generation profiles. A higher share of fluctuating RES in the power supply mix as well as a fluctuating energy demand implies increased requirements for the energy system. The provision of large power generation and grid capacities is necessary to cover peak loads and secure the energy supply. However, the availability of this reserve capacity margin leads to a low average utilization of power plants and transmission networks [59]. Therefore, the discrepancy between generation and demand needs to be compensated by the provision of flexibility options. A wide scope of measures is necessary to enable the integration of the increasing share of volatile renewable power generation into the energy system [35]:

- Implementation of energy storage capacity,
- Improvement of the power grid,
- Deployment of flexible power generation and
- Provision of demand side flexibility.

An efficient way to secure the energy supply and provide flexibility to the power system is to apply **demand side management (DSM)**. DSM describes the concept of matching the demand with the available volatile supply through active load management of dispatchable energy consumers [60]. Load management involves either reducing the energy consumption or shifting the energy demand to a later time [61]. The implementation of DSM measures allows for minimizing the reserve capacity margin and the efficient operation of transmission as well as distribution grids [59]. This facilitates the enhanced integration of intermittent renewable energy sources such as photovoltaics and wind into existing energy systems. For that reason, the provision of load flexibility by industrial processes contributes to the reduction of the specific carbon dioxide emissions of electric energy in order to reach a climate-neutral power system.

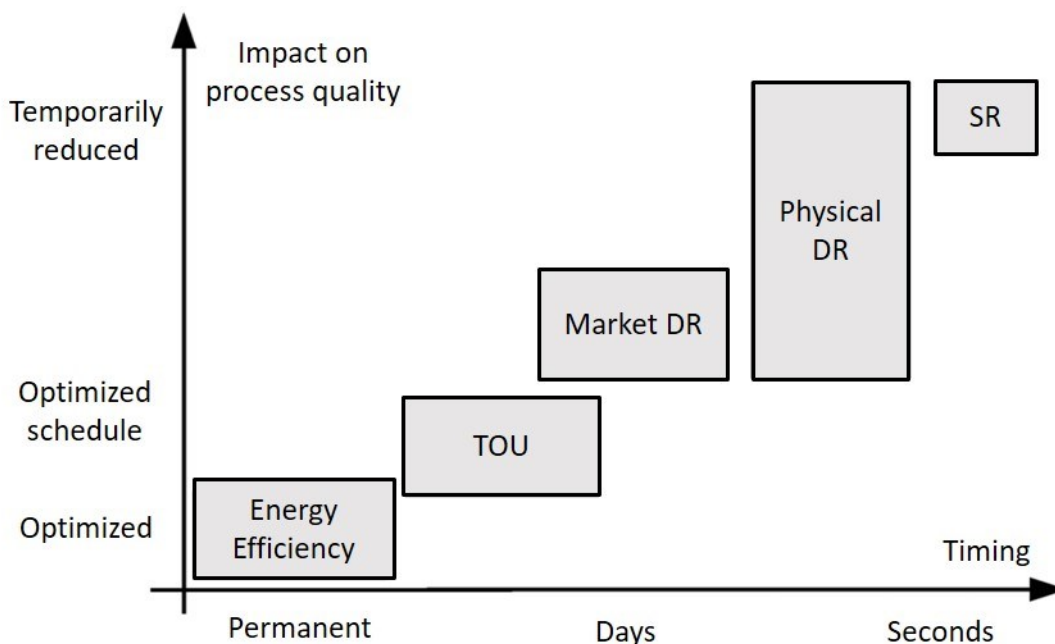


**Figure 6: Demand side management measures and their impact on process quality and timing (TOU: time of use, DR: demand reserve, SR: spinning reserve) [62].**

Figure 6 classifies different types of DSM according to their effect on the individual production process and their temporal horizon. Energy efficiency measures, as described in section 2.3.1.1, lead to sustained energy and CO<sub>2</sub> emission savings with very little or no impact on the process quality. Time of use (TOU) DSM involves re-arranging the production schedule to periods of lower electricity price tariffs. The dynamic shifting or shedding of loads based on

price or command signals is referred to as demand response. Market demand response reacts to electricity price signals on the day-ahead or real-time pricing market, while physical demand response acts in the event of overloaded grid infrastructure such as power lines and transformers. The spinning reserve, also denoted as primary and secondary control, aims to stabilize and restore the grid frequency. Consumers can act as a virtual spinning reserve by reducing the load, when the frequency drops and increasing the load when the frequency rises [62].

Besides the previously explained effect DSM has the ability to enable energy cost optimization in EAF steel mills [63]. The following flexibility options have been identified: Electricity-powered furnaces such as electric arc and ladle furnaces operate in batches and thus allow for rescheduling between each batch. As the largest electricity consumer in the steel mill the EAF particularly stands in the focus of the DSM studies. The furnace can respond to varying electricity prices either by shifting the operation schedule or by adjusting the load. In literature, load scheduling models based on mixed integer linear programming (MILP) are applied on a theoretical basis, enabling the plant owner to comply with predefined load curves and to operate the equipment at minimal cost [64,65]. In practice, a lack of information on future batches severely limits the accurate forecasting of electricity consumption profiles. In an industrial environment, batch weights, scrap quality and composition, tap-to-tap times, delays due to malfunctioning or occupied equipment and maintenance activities as well as the highly fluctuating load profile of the EAF can only be estimated. Robust scheduling tools that are capable to handle these significant uncertainties need to be developed. Moreover, load shifting in steel mill aggregates is limited to several minutes, but impairs subsequent production processes such as secondary metallurgy and casting, and has a negative impact on the steel production output and the plant utilization [63].

In contrast, the coupling of the steel mill with interrelated processes such as oxygen production allows for demand side management without affecting the core steelmaking process [66]. Since oxygen and natural gas play a fundamental role in steel production, the on-site operation of an electrolysis plant for the combined production of hydrogen and oxygen might enable the provision of flexibility for the integration of fluctuating RES, the supply of the steel mill with by-product oxygen and the generation of a climate-neutral fuel [67,68].

### 2.3.2.2 *Renewable direct fuels*

**Power-to-gas** (PtG) refers to the production of gases such as hydrogen or synthetic methane from electric energy by electrolysis and subsequent methanation with carbon dioxide. PtG plants are crucial elements in hybrid energy systems, which are characterized by the interconnection of electric, gas and heat systems. Figure 7 presents a cutout of a hybrid system consisting of an electric and a gas system, which are interconnected by a PtG plant. By

harnessing the synergies between the individual infrastructures, hybrid energy systems enable the enhanced integration of renewable energy. They provide flexibility for balancing supply and demand, promote electrification of private-, commercial- and industrial processes, offer higher resilience and increase the security of supply [69]. For the integration of PtG technologies in the gas system, three configurations are considered, which might coexist depending on local conditions:

- Feed-in of hydrogen into a dedicated hydrogen infrastructure,
- Feed-in of hydrogen into the natural gas grid,
- Feed-in of synthetic natural gas into the natural gas grid.

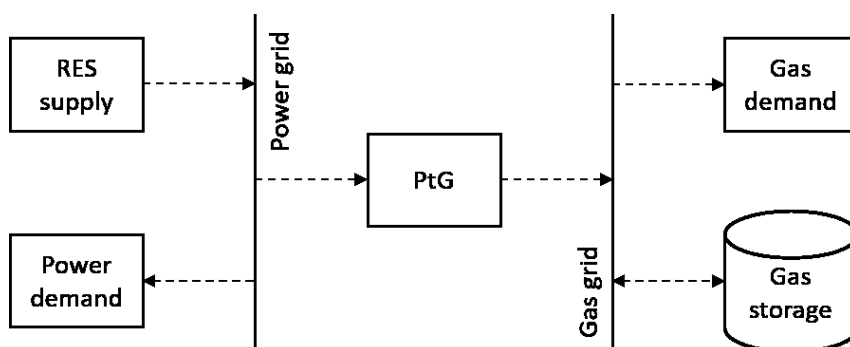


**Figure 7: Excerpt of a hybrid energy system comprising of an electricity and natural gas system.**

Considering historical energy and emission allowance prices, the production costs for both renewable hydrogen and SNG substantially exceeded those of conventional natural gas [70]. Hydrogen as an energy carrier appeared economically viable solely in narrow parts of the transport sector such as heavy duty trucks or train applications, compared to electrification, but would require the development of a completely new infrastructure. At present and in future, there is a strong case for preliminary using the existing natural gas infrastructure for a mix of natural gas, SNG, bio-methane and hydrogen.

On the one hand, the economic framework conditions support the partial replacement of natural gas: In the short term, the war in Ukraine and the associated economic consequences have triggered a substantial increase in natural gas prices, which is assessed in section 4.6. In the long term, the politically intended rise of CO<sub>2</sub> emission allowance prices will significantly add to the costs for natural gas utilization. Both effects promote the substitution of natural gas with RES.

On the other hand, the admixture of renewable and climate-neutral gases into the natural gas network will gradually reduce CO<sub>2</sub> emissions in the gas sector and enable the transformation to an hydrogen-only system in the long term [69]. The effect of natural gas/hydrogen blends on industrial furnaces is intensively investigated. Studies indicate that the combustion of gas blends with up to 100 % hydrogen lead to reduced flue gas losses, but to increased NO<sub>x</sub>

emissions both for air-staged- and flameless combustion. Additionally, the combustion of hydrogen or gas mixtures requires the adaption of the air fuel ratio control [71].

Moreover, carbon dioxide neutral EAF steelmaking requires the **substitution of coal**, which plays a crucial role particularly in the foamed slag method. Essentially, there are two alternatives to coal: secondary fuels such as waste plastics and rubber or biomass [21].

## 2.4 Research need

Within section 2.3 of this thesis, the most relevant measures for the reduction of carbon dioxide emissions in EAF steel mills are presented. Regarding the design, implementation and operational optimization of energy efficiency technologies such as Oxyfuel combustion and waste heat recovery, a wide range of studies has been carried out. Due to its high energy consumption, the EAF lies in the main focus of research efforts, particularly in the field of waste heat recovery and electric energy savings. However, climate-neutral steel production through the EAF route requires a package of complementary measures. Besides the implementation of energy efficient and emission-reducing technologies in the steel mill, the interaction of the mill with the higher-level electricity and gas networks across all energy carriers is crucial. The optimal design, integration and operation of these technologies in an existing EAF steel mill as well as the assessment of their effect on demand side management, carbon dioxide emissions and energy costs calls for further investigation.

From the literature review the following technologies emerged as most relevant to address:

- Oxyfuel ladle heating,
- CCU for water neutralization and methanation,
- Waste heat recovery from the ladle heaters and the EAF,
- DSM through flexible hydrogen and/or oxygen production and
- Substitution of natural gas by SNG and/or hydrogen.

In the light of these considerations, this thesis raises the following research question:

*What are suitable system solutions concerning the integration of Oxyfuel combustion, CCU, Waste heat recovery, DSM and fuel substitution for the reduction of CO<sub>2</sub> emissions in EAF steel production and what are the enabling framework conditions?*

From this overarching research question the following sub-questions are derived:

1. *What is the impact of the proposed measures on the energy consumption of the production process?*
2. *What is the impact of the proposed measures on the demand side flexibility provided by the industrial energy system?*

3. *What is the impact of the proposed measures on the energy-related direct and indirect carbon dioxide emissions of the steel mill?*
4. *What economic framework conditions are required for the viable implementation of the proposed measures?*

## 3 METHODOLOGY FOR THE ASSESSMENT OF MEASURES TOWARDS CLIMATE-NEUTRAL EAF STEEL PRODUCTION

The following chapter provides an overview on the pursued approach to address the research topics defined in section 2.4 and summarizes the main findings of the three research studies.

### 3.1 Approach and outline of the thesis

Based on the CO<sub>2</sub> emission reduction measures listed in section 2.4, the approach outlined in Figure 8 was developed. It allows for a comprehensive review of the status quo, enables the optimal integration of the above-mentioned technologies in existing production processes and the investigation of their impact on the overall energy system. The aim is to provide answers to the research questions defined in section 2.4. The pursued approach is structured as follows:

- First, an adaptive **energy system model of the EAF steel** mill is developed (section 3.2). It allows for the holistic analysis of the energy demand with particular regard to energy efficiency, CCU and DSM. In addition to time-resolved load profiles for energy sources and gases, the model is supposed to provide energy-related key performance indicators (KPI). The established energy system model serves as a basis for the subsequent studies.
- Second, **energy efficiency measures and CCU** are investigated in a techno-economic case study (section 3.3). Different concepts for Oxyfuel combustion, waste heat recovery as well as CO<sub>2</sub> sequestration and mill-internal utilization are implemented into the developed energy system model. These measures are then evaluated with regard to energy consumption, costs and CO<sub>2</sub> emission savings.
- Third, a study on the **demand side management potential and RES integration** through the flexible on-site production of oxygen, hydrogen, and/or SNG is conducted (section 3.4). Based on the previously generated load profiles of the steel mill, the layout and operation of a power-to-gas plant is optimized. Different plant layouts are assessed in terms of DSM potential, fossil fuel substitution and CO<sub>2</sub> emission reduction.

Based on the findings of the above-mentioned studies, three scenarios are developed in this thesis, which, all together offer a potential path to climate-neutral EAF steel production (section 3.5). These scenarios are subjected to a thorough analysis and discussion concerning their impact on the energy consumption (section 4.2), DSM potential (section 4.3) and CO<sub>2</sub> emissions (section 4.4) as well as their economic viability (section 4.5). Finally, the thesis



concludes with the answers to the research questions (section 5.1) as well as a summary and outlook (section 5.2).

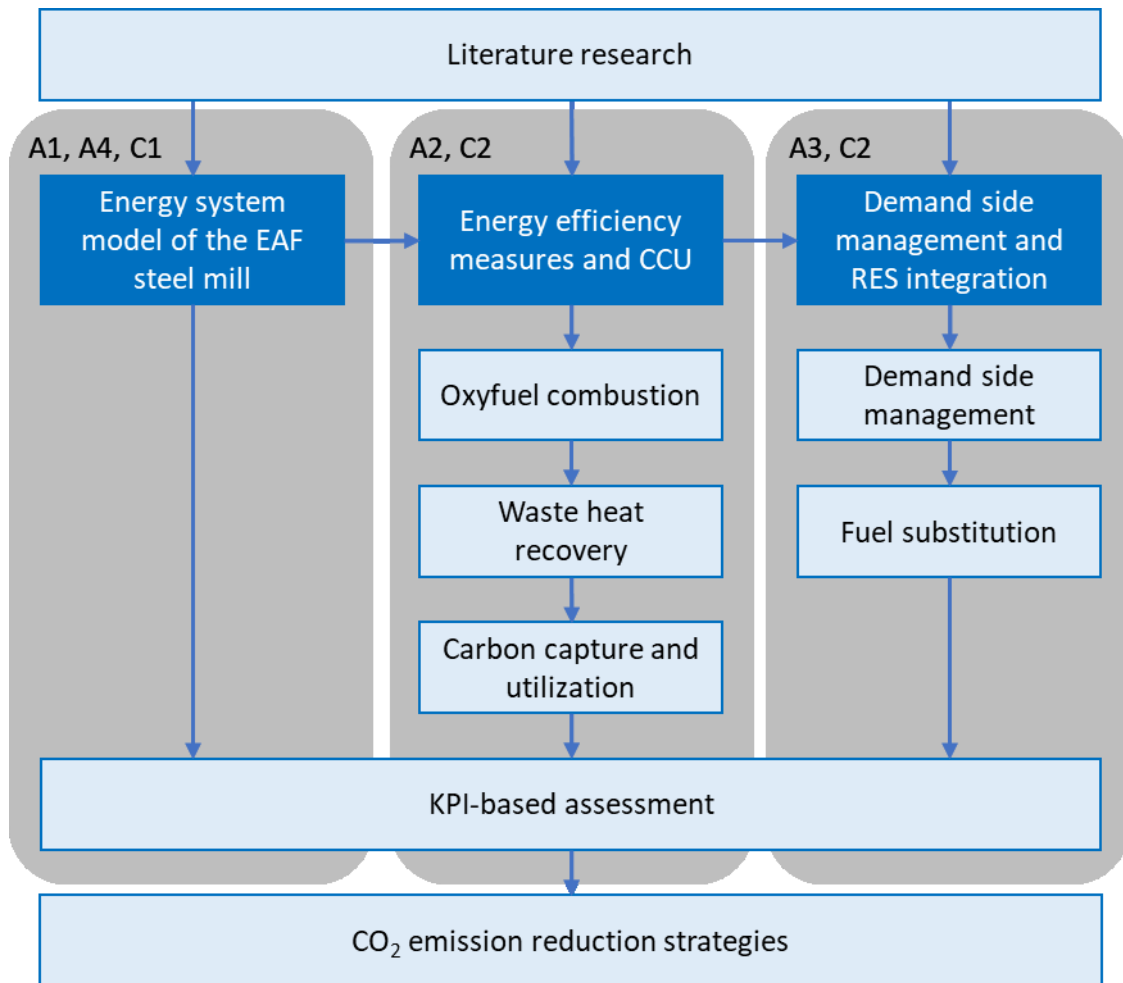


**Figure 8: Applied approach for the development of a carbon dioxide emission reduction strategy EAF steel production, published scientific journal articles (A1-A4) and conference proceedings (C1-C2).**

This thesis is based on three peer-reviewed scientific journal articles (A1, A2, A3) [22,24,56], as well as several further scientific contributions in journals and conference proceedings (A4, C1, C2) [72–74]. Studies existing in literature that are relevant to the climate-neutral electric steel production complete the scope of the present work. The underlying research studies are cited at the appropriate places.

### 3.2 Energy system model of the EAF steel mill

The batch production process of different steel grades and variable production times in the EAF steel mill leads to a strongly fluctuating energy demand. Assessing the overall impact of the implementation of new technologies into the highly integrated production process requires time-resolved analysis and modelling of the considered energy system. Therefore, a study on the characterization and the modelling of the energy system of an EAF steel mill was carried out in the article *Time- and component-resolved energy system model of an electric*



Figure 9 gives an overview over the modelled energy system. The modular design allows the modification of existing system components and the implementation of additional equipment such as further processing units, carbon dioxide and heat recovery plants as well as buffer storages [22].

### 3.3 Energy efficiency measures and CCU

With a share of 38 % of the final energy demand of the steel mill, natural gas is the second most important energy carrier and the principal source of direct carbon dioxide emissions (see Figure 4). The conservation of natural gas by applying Oxyfuel combustion was identified as the first field of action for CO<sub>2</sub> reduction. The second field concerns the sequestration and mill-internal utilization of carbon dioxide from flue gas. A third field of action is saving natural gas by the recovery and utilization of waste heat. The article *Techno-economic case study on Oxyfuel technology implementation in EAF steel mills – concepts for waste heat recovery and carbon dioxide utilization* [24] addresses the implementation of novel technologies in the production processes of an existing steel mill. For the case study, the previously developed energy system model of the investigated steel mill is adapted: A part of the energy- and emission-intensive ladle heaters is equipped with Oxyfuel-burners and a carbon dioxide separation system. Additionally, heat recovery systems as well as buffer storages for heat and carbon dioxide are integrated, as depicted in Figure 10.

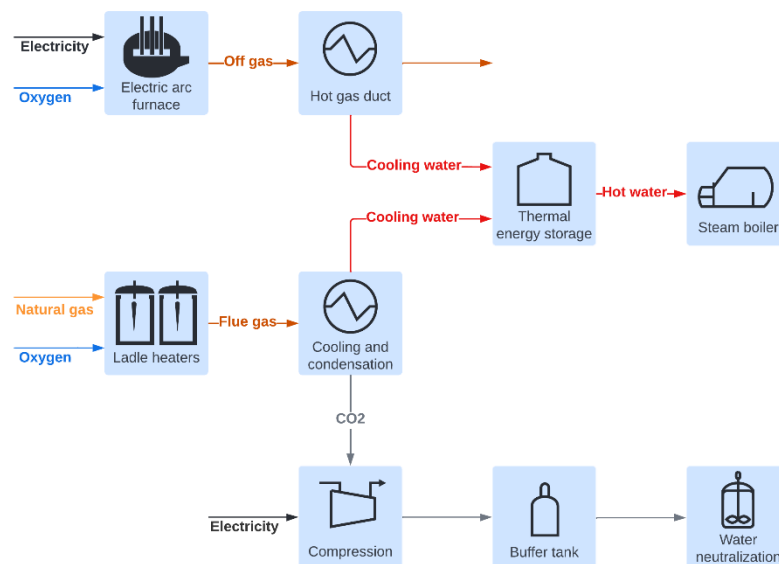


Figure 10: Process integration concept [24][24].

In the course of this thesis, the proposed efficiency measures are referred to as:

- Oxyfuel ladle preheating,
- Ladle heater waste heat recovery,

- Electric arc furnace waste heat recovery and
- Carbon dioxide utilization.

The case study aims to optimize the technical design of the proposed measures, to assess the energy, cost and CO<sub>2</sub> emission saving potential and to identify the required economic framework conditions for their implementation. First, a simple simulation approach is used to determine the appropriate capacity for the buffer storages: Simulation runs under variation of the storage capacities and subsequent economic analysis lead to the system configuration with minimum annual costs for ladle heating and steam generation. Annual costs include the annuity for the CAPEX of new equipment and the cost for electricity, natural gas, emission allowances as well as for the purchased oxygen and carbon dioxide. Second, the reductions in natural gas consumption, direct CO<sub>2</sub> emissions and annual energy cost of the economically optimized scenarios are evaluated. Finally, a sensitivity analysis demonstrates the economic prerequisites for the profitable implementation of the investigated measures.

### **3.4 Demand side management and RES integration**

More than 50 % of the energy demand for EAF steel production is consumed in form of electric energy. Consequently, the climate-neutral EAF steel mill requires the supply of carbon dioxide neutral electricity. In order to enable the integration of volatile renewable energy sources into the production process, a study on the demand side management potential was conducted in the article *Provision of demand side flexibility through the integration of power-to-gas technologies in the electric steel mill* [56]. In this article, the electricity price-driven oxygen production via pressure swing adsorption and the integration of an electrolysis based power-to-gas plant are identified as promising flexibility options. Due to the high oxygen demand of the steel mill and the technologically simple storage, the production of gases such as oxygen, hydrogen and SNG represents a strong flexibility option to be implemented on the high-level power grid (110 kV). Besides that, decoupling of supply and demand through buffer storages ensures that the flexible management of the electricity demand has no negative effect on the steel production process. In contrast, the temporal shifting of the electric load of individual aggregates in the main production process, such as the electric arc furnace, is complex. Due to the highly integrated batch processes, load shifting of such processes has a significant impact on the production output, energy efficiency, product quality as well as scheduling and resource planning. In this work, this is not considered.

Three scenarios based on technologies that operate decoupled from the core-production process are investigated:

- Oxygen production via Pressure Swing Adsorption (scenario PSA),
- Co-production of hydrogen and oxygen using PEM electrolysis (scenario PEM) and

- Co-production of hydrogen and oxygen using PEM electrolysis and subsequent methanation for SNG production (scenario SNG).

These scenarios are investigated using an optimization model, which covers the oxygen and hydrogen production plants as well as all relevant auxiliary equipment, energy carriers and gases. Figure 11 depicts the structure of the optimization model for the three implementation scenarios.

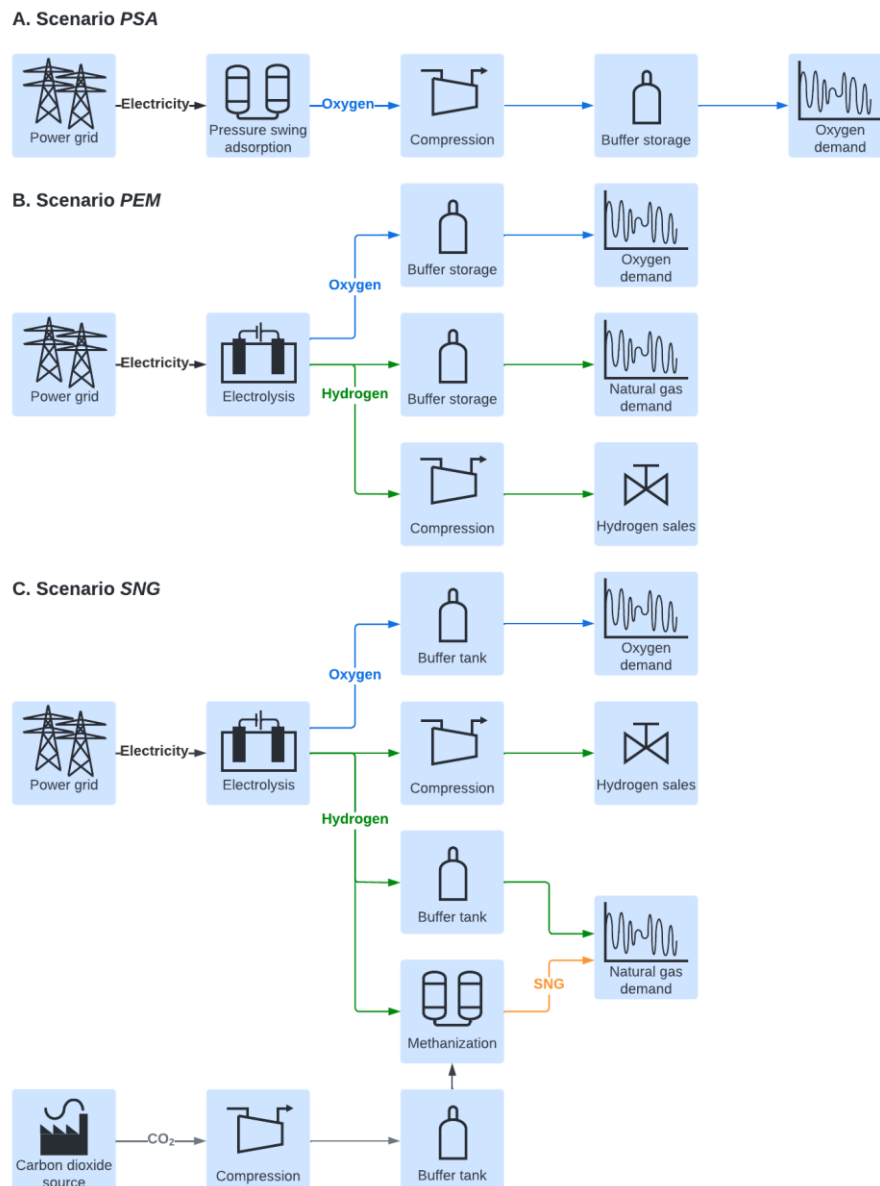


**Figure 11: Optimization model for the implementation of different scenarios for flexible oxygen, hydrogen and SNG production [56].**

The load profiles generated with the previously described energy system model serve as an input for the time-resolved natural gas and oxygen demand as well as carbon dioxide generation. The objective of the optimization is minimizing the sum of investment, energy and

oxygen cost under fluctuating power prices. In this way, the effects on the energy consumption and CO<sub>2</sub> emissions of the steel mill as well as the provision of flexibility for the power grid are investigated and operating strategies for the deployed systems are derived. A comparative analysis of the individual scenarios with anticipated CAPEX and energy prices for the years 2020, 2030 and 2050 demonstrates the required technical and economic framework conditions.

### 3.5 Overall assessment

Considering the research questions defined in section 2.4, the above-mentioned energy efficiency and flexibility measures are evaluated regarding potential energy savings, provision of demand side flexibility, carbon dioxide emission reduction and economic viability. The analysis shown here is based on three scenarios derived from the articles A2 [24] and A3 [56]:

- The energy efficiency scenario EFF 2020 involves the measures proposed in article A2 including the transition to Oxyfuel ladle heating, carbon dioxide capture and utilization for water neutralization as well as waste heat recovery. The resulting optimized energy and oxygen demand profiles serve as basis for the subsequent scenarios. The oxygen is supplied by the flexible operation of an on-site PSA plant.
- Scenario SNG 2030 investigates the implementation of a power-to-gas plant into the steel mill, consisting of a PEM electrolysis and a methanation unit. The electricity price-driven operation of the electrolyzer needs to cover the oxygen demand of the steel mill and generates hydrogen. Due to the lack of a dedicated hydrogen infrastructure, the admixture of hydrogen into the gas system of the mill is limited to 20 %<sub>vol</sub> in each time interval. The methanation of carbon dioxide generated by the Oxyfuel ladle heaters increases the internal utilization of hydrogen. Excess hydrogen is either consumed in the steel mill in compliance with the admixture limit or injected into the gas grid. Since the production capacity of the power-to-gas plant is small compared to the transmission capacity of large natural gas lines, the admixture limit is not considered for the infeed into the gas grid.
- In the PEM 2050 scenario, assuming a complete conversion of the overall natural gas infrastructure to hydrogen, solely the PEM electrolysis is deployed. Again, the electrolysis unit meets the oxygen demand. Additionally, we postulate that by 2050 the gas infrastructure is designed for operation on 100 %<sub>vol</sub> hydrogen.

Each of these three scenarios is benchmarked against the reference scenario (REF 2020), which represents the current status in the analyzed steel mill. Throughout the analysis, the final energy consumption and total energy consumption are compared in the different scenarios. The former only considers the consumption of energy carriers in the production

process, whereas the latter also takes into account the electrical energy required to produce oxygen and hydrogen. In terms of emissions, the benchmarking includes direct (scope 1) and indirect (scope 2 and 3) carbon dioxide emissions. Load flexibility is determined considering the nominal power, the annual full load hours and the average electricity price of the power-to-gas plant. The economic analysis includes the energy carriers electric energy, natural gas, hydrogen and SNG. Moreover, the cost of oxygen for metallurgy and combustion, the acquired CO<sub>2</sub> emission certificates as well as the capital costs arising from additionally implemented equipment are considered. Given the projected costs for energy, emission allowances and gases through 2050, the economic performance of the individual scenarios is compared based on data for the years 2020, 2030 and 2050. Table 4 summarizes the commodity prices for the economic assessment that are considered constant. Figure 12 depicts the applied volatile prices for the electricity price-driven optimization of the PSA and PtG plants.

**Table 2: Projected energy, emission allowance and gas prices for the years 2020, 2030 and 2050 [56].**

Commodity	Unit	2020	2030	2050	Ref
Electric energy (mean)	EUR/MWh	33	62	82	[75–77]
Natural gas	EUR/MWh	13	12	11	[78]
Hydrogen	EUR/MWh	146	93	103	[79]
Oxygen	EUR/t	77	93	103	[56]
Emission allowances	EUR/t	24	130	250	[78,80–82]

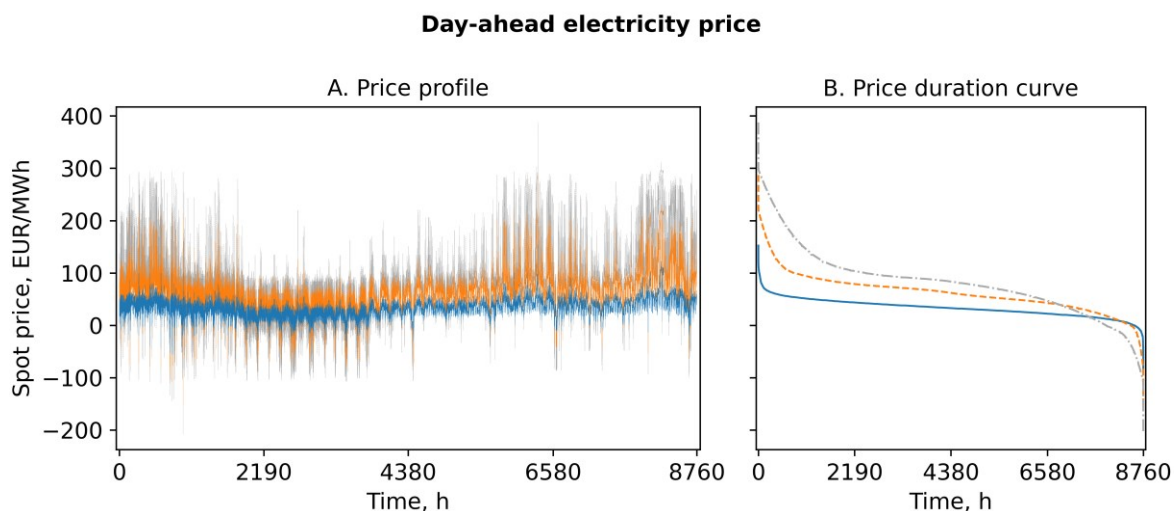


**Figure 12: Profile (A) and duration curve (B) of historical and forecasted electricity spot market prices for the years 2020 (blue), 2030 (orange) and 2050 (grey) [56].**

## 4 RESULTS AND DISCUSSION

The following chapter summarizes the most relevant results of the conducted research studies and puts them into a common context. First, the results of the energy system analysis are presented. Then, in order to provide robust answers to the stated research questions, the findings from the case studies are evaluated in terms of energy consumption, carbon dioxide emissions and economic impact.

### 4.1 Time- and component resolved energy demand

The primary objective of the energy system model is to map the individual energy consumers of the production process in the investigated steel mill. This allows for the generation of synthetic load profiles for electric energy, natural gas, coal, oxygen, carbon dioxide as well as profiles for waste heat. Based on the data obtained from on-site measurements, the model generates representative minute-resolved load profiles over arbitrary observation periods. The following figures present the load profiles generated by the energy system model in a temporal resolution of 15 minutes over a period of four weeks. The loads are normalized to the respective maximum power or mass flow.

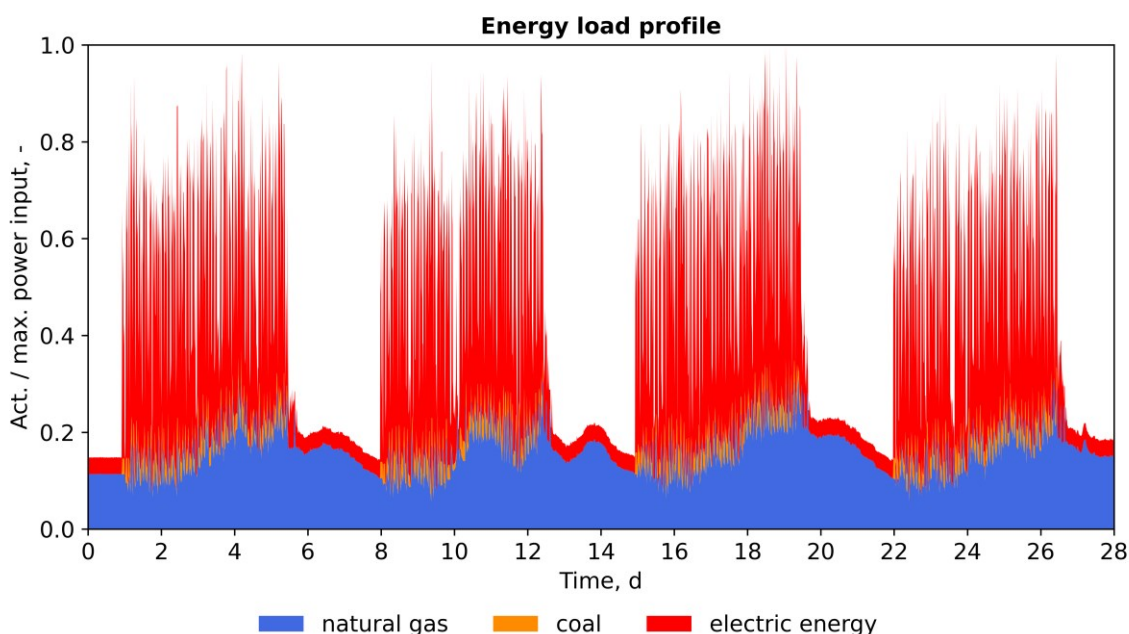


**Figure 13: Load profile for electric energy, natural gas and coal generated by the energy system model [22].**

With a consumption of 38 % of the total energy demand, the electric arc furnace clearly dominates the electric load profile. Due to its batch operation, the remaining processes such as secondary metallurgy, annealing or ladle heating follow a certain periodicity, resulting in strongly fluctuating energy demand (Figure 13). The intermittency of the EAF operation also affects the natural gas load profile, which is mainly determined by the ladle heaters and the



heat treatment furnaces. Coal accounts only for a minor share of the total energy input but contributes a considerable portion to the direct carbon dioxide emissions due to its high carbon content.

The major natural gas consumers such as the ladle heaters and heat treatment furnaces account for most of the waste heat generated in the form of hot exhaust gases. A further part of the waste heat, primarily from the cooling panels and the hot gas duct of the EAF, is discharged through cooling water. Due to the wide range of process temperatures, the available waste heat streams feature different exergetic levels. The holding temperatures of ladle heaters and annealing furnaces exceed 600 °C, whereas heat-up temperatures lie in the medium temperature range from 200 to 600 °C. In contrast to the high EAF off-gas temperature, the coolant temperatures are limited to well below 100 °C during standard operation under atmospheric pressure. Resulting from the fluctuating energy input, the production of waste heat is intermittent as well (Figure 14). Hence, the use of thermal energy storage systems is imperative for the efficient recovery of waste heat.

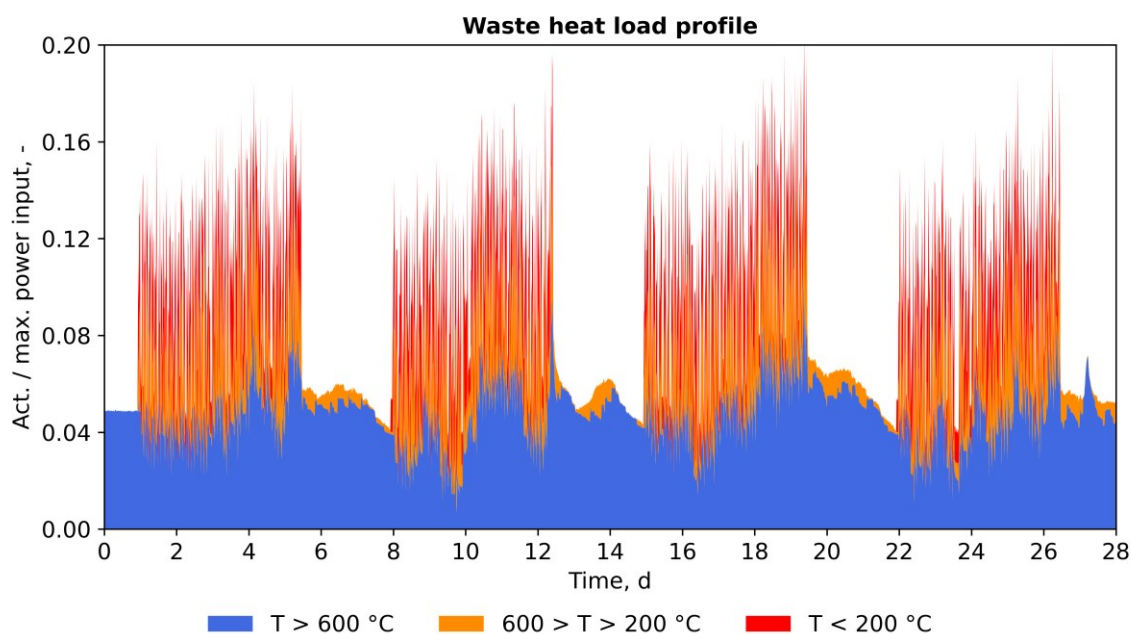


**Figure 14: Waste heat load profile generated by the energy system model [22,24].**

EAF steel production is associated with a considerable oxygen demand. Again, the biggest consumer is the electric arc furnace followed by the vacuum oxygen decarburization units and minor consumers such as the cutting torches. The load profile reflects this situation: oxygen is blown into the EAF at high mass flow rates resulting in intermittent demand peaks. Since not every batch is subjected to VOD and the treatment is carried out at lower mass flow rates, the associated peaks are smaller and occur irregularly. A base load represents frequent operation of minor consumers, whereas on the weekends, the steel production and therefore oxygen consumption is shut down (Figure 15). The carbon dioxide load profile results mainly from the

demand for neutralization of wastewater from the vacuum treatments and, to a smaller extent, from the regular injection of CO<sub>2</sub> into the cooling water. The latter is needed to avoid the precipitation of dissolved minerals. Both the total consumption and the required mass flow rates are much lower compared to oxygen.

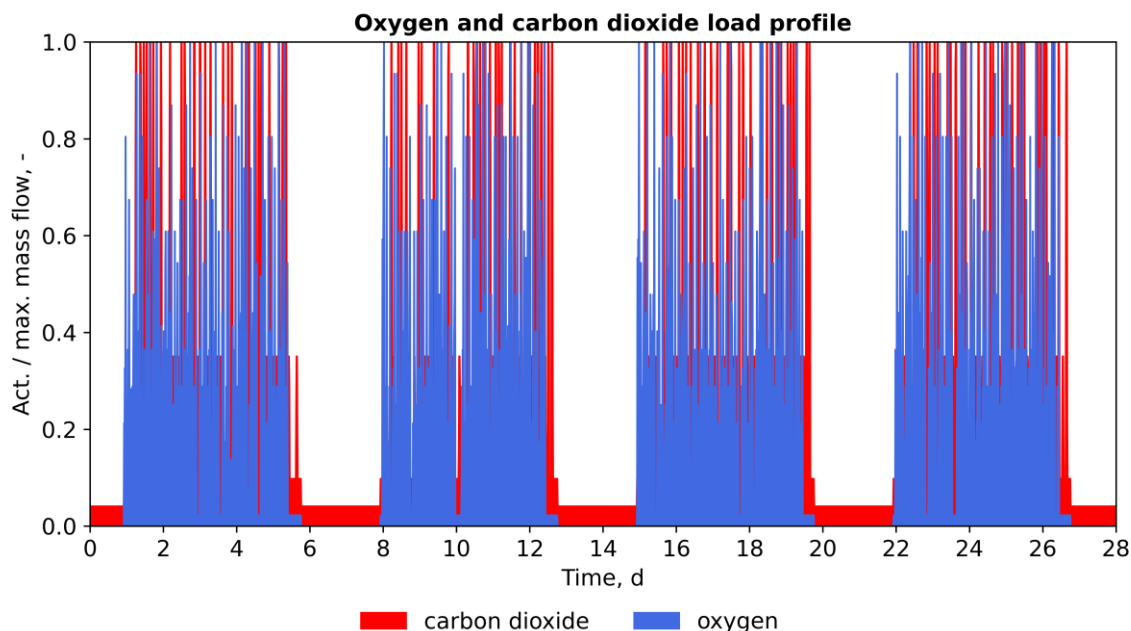


**Figure 15: Load profile for oxygen and carbon dioxide generated by the energy system model [56].**

In addition to the load profiles, the energy system model determines energy-related KPIs such as specific energy consumption and carbon dioxide emissions. The calculated specific energy and oxygen demand as well as the specific emissions for the investigated mill based on one ton of produced steel lie within the literature values given in section 2.1. Considering the good agreement of synthetic and measured load profiles as well as the plausibility of the generated KPIs compared to literature values, we assume that the energy system model provides representative data. The extension option to include additional processes and the capability of holistic energy system analysis enable the assessment of energy efficiency measures and the identification of flexibility options in the subsequent studies.

## 4.2 Energy consumption

The first objective of the techno-economic case study [24] was the investigation of effects of the transition from natural gas/air-fired to Oxyfuel burners. Figure 5 indicates that due to the high process and exhaust gas temperatures, the highest gain in thermal efficiency is achieved for Oxyfuel ladle preheating. According to scenario EFF 2020, the conversion of all ladle heaters, except those required for ladle drying, to Oxyfuel-technology reduces the natural gas consumption of the steel mill by 10 %. These savings are accompanied by an increase of the oxygen consumption by 55 % resulting in an additional energy consumption due to oxygen

production. Assuming a SEC of 0.49 kWh/kg<sub>O<sub>2</sub></sub> [56], saving 1 kWh<sub>HHV</sub> of natural gas translates to the consumption of 0.13 kWh of electrical energy for oxygen production. Considering the energy demand for oxygen production, the total energy savings are reduced by 11 %. In addition to fuel savings, Oxyfuel combustion offers the opportunity for energy-efficient carbon dioxide recovery.

Furthermore, the case study indicates that harnessing the large waste heat recovery potential leads to significant natural gas savings: The exploitation of the ladle heater waste heat for feed water preheating in the process steam boiler effects a reduction of 1 % of the overall natural gas consumption. The additional integration of the cooling system of the EAF hot gas duct provides sufficient thermal energy for the entire steam production, reducing the natural gas consumption of the steel mill by 4 % in total. However, the implementation of such a system is costly and technically complex as it requires the installation of substantial heat storage capacity and the replacement of the hot gas duct. The main challenges lie in the highly fluctuating mass flow rate and temperature as well as the high dust load of the EAF exhaust gas.

The implementation of power-to-gas technologies does not have an impact on the final energy consumption, since the fuel demand still must be covered. Due to the production of SNG and hydrogen, a part of the total energy consumption is shifting from natural gas to electricity. In the SNG 2030 scenario, synthetic methane from electrolysis and methanation substitutes part of the natural gas, but increases the total energy consumption. The produced SNG is consumed mill-internally to reduce the natural gas consumption and CO<sub>2</sub> emissions. The shortfall in CO<sub>2</sub> supply and the admixture limit of 20 %<sub>vol</sub> for the internal infrastructure cause a hydrogen surplus, which is sold through injection into the gas grid.

The scenario PEM 2050 enables the complete substitution of natural gas by hydrogen. The power-to-gas plant supplies a major part of the consumption, the remaining part is procured from the grid. Due to the electricity price- and oxygen demand-driven operation of the electrolyzer, this scenario involves a temporary overproduction and thus the sale of hydrogen into the grid. The absence of the methanation step results in an overall efficiency improvement of the PtG plant and therefore a smaller impact on the total energy consumption (see Figure 16).

In summary, the investigated energy efficiency measures (*EFF 2020*) lead to the conservation of 30 % of the natural gas consumption, corresponding to 11 % of the final SEC for the production of one ton of steel (see Table 3). Given their limited efficiency, the application of electrolysis and methanation increases the total energy consumption, while omitting the electricity consumption for oxygen production and partially substituting natural gas by

climate-neutral gases. The feed-in of excess hydrogen increases the proportion of renewable gases in the grid.

**Table 3: Impact of CO<sub>2</sub> emission reduction measures on natural gas, final energy and total energy consumption (based on scenario REF 2020).**

Measure	Scenario	Natural gas	Final energy	Total energy
Oxyfuel ladle preheating	EFF 2020	-20 %	-7 %	-7 %
Waste heat recovery	EFF 2020	-10 %	-4 %	-4 %
Oxygen production	EFF 2020	-	-	+2 % <sup>1</sup>
SNG production	SNG 2030	-14 %	-	+7 %
Hydrogen production	PEM 2050	-33 %	-	+2 %

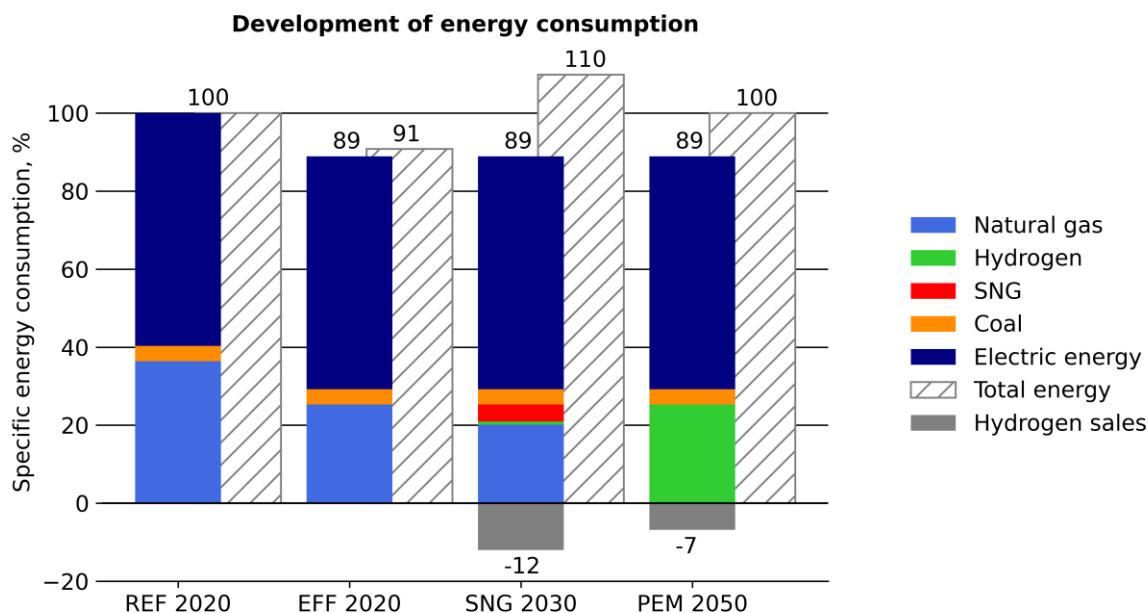


**Figure 16: Final and total specific energy consumption and gas sales for the different scenarios related to the reference scenario REF 2020.**

### 4.3 Demand side management

In view of the high electricity consumption of EAF steelmaking, the provision of load flexibility for the power grid is crucial for the integration of fluctuating renewable generation. Operating the EAF as a DSM asset by shifting the production schedule requires considerable logistical as well as organizational effort and is not considered in this work. In contrast, the on-site production of oxygen was identified as a feasible flexibility option. Oxygen is required in large

<sup>1</sup> Assuming an SEC of 0.49 kWh/kg for oxygen production.

quantities in the steelmaking process, is easily stored, and can be produced from ambient air or water at any location using electrical energy. Pressure swing adsorption (PSA) represents a flexible oxygen source, but PEM-based power-to-gas plants for hydrogen or SNG production feature a higher dispatchable power and additionally produce CO<sub>2</sub> emission-neutral fuels [56].

In order to compare the flexibility potential of the individual scenarios, the optimized nominal power, full-load hours and electricity prices are considered. Figure 17 shows the forecasted ordered duration curve for the year 2050, the annual average price, the effective average price ( $p_{effective\ average}$ ) and the ordered average price ( $p_{ordered\ average}$ ) for the PEM and the PSA unit.

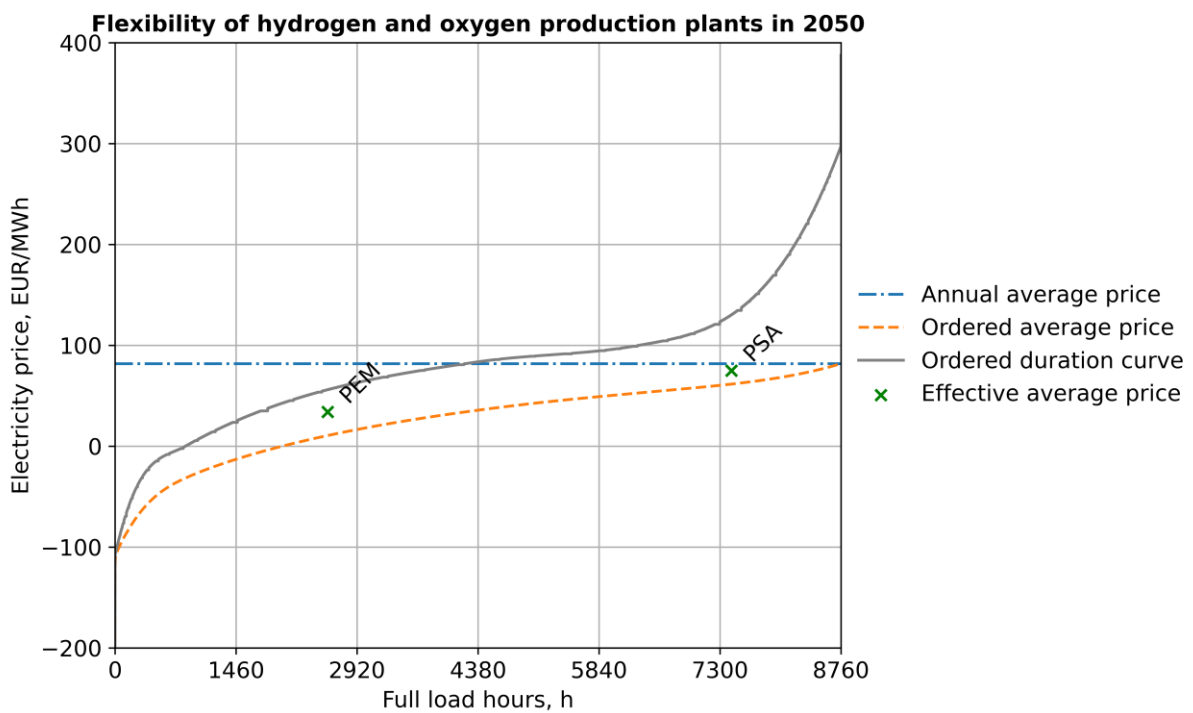


**Figure 17: Assessment of the demand side management potential of different oxygen and hydrogen supply systems including pressure swing adsorption (PSA) and electrolysis (PEM) in 2050 [56].**

The effective average price is an optimization result and represents the actual mean price of the electricity supplied to the power-to-gas plant during operation. The ordered average indicates the theoretical minimum price that would be achieved by operating the plant at full load solely during the cheapest hours. These indicators are determined from the quarter-hourly power prices ( $p_{EE}$ ), the quarter-hourly electricity demand ( $D_{EE}$ ) and the ordered duration curve ( $DC_{EE}$ ) (see equations (2) and (3)).

$$p_{effective\ average}(t) = \frac{\sum_{n=1}^t p_{EE}(n) \cdot D_{EE}(n)}{\sum_{n=1}^t D_{EE}(n)} \quad (2)$$

$$p_{ordered\ average}(t) = \frac{1}{t} \cdot \sum_{n=1}^t DC_{EE}(n) \quad (3)$$

In scenario EFF 2020, due to the high share of the CAPEX on the total cost, the optimized design and operation of the PSA unit is characterized by a low rated power and high full-load hours (see Table 4). The optimal implementation strategy is to minimize the total investment costs by minimizing the oxygen production and storage capacity. In contrast, in both the SNG 2030 and PEM 2050 scenario, the higher share of the energy cost enables an electricity price-driven operation of the electrolysis unit, resulting in high rated power and low full-load hours. The increasing amplitude and frequency of price fluctuations from 2030 to 2050 intensifies this effect, leading to even higher storage and production capacities and lower full-load hours.

**Table 4: Flexibility indicators of the PSA unit (EFF 2020) and electrolysis plant (SNG 2030 and PEM 2050) [56].**

KPI	Unit	EFF 2020	SNG 2030	PEM 2050
Nominal power	kW	400	15 100	20 000
Full load hours	hrs	7 440	3 740	2 570
Annual average electricity price	EUR/MWh	33	62	82
Ordered average electricity price	EUR/MWh	28	32	11
Effective average electricity price	EUR/MWh	49	41	34

The comparison of electricity costs in Table 4 confirms these findings. In the EFF 2020 scenario, the effective average price lies above, whereas in the SNG 2030 scenario, it falls below the annual average price, close to the ordered average, which represents the theoretical minimum. Scenario PEM 2050 reflects the limitations of the proposed power-to-gas system. In order to profit from periods of low electricity prices, the full-load hours of the electrolysis unit continue to decline from 2030 to 2050. Nevertheless, due to the coupled oxygen supply, the plant is not able to fully adapt its operation to the time windows of the cheapest prices. Therefore, the effective price diverges from the ordered average. With the expansion of renewable generation, seasonal price variations that cannot be balanced by the plant-internal storages will increase, highlighting the complementary need for seasonal storage systems.

#### 4.4 Carbon dioxide emissions

When determining the CO<sub>2</sub> balance of the production process, it is necessary to distinguish between the carbon dioxide emissions of different scopes (see section 2.3). The high natural gas and electricity consumption causes scope 1 and scope 2 emissions, whereas emissions generated by oxygen production are assigned to scope 3 in the reference scenario.

The most cost-efficient measure for the mitigation of scope 1 emissions is the reduction of fuel consumption by enhancing the energy efficiency of production processes. In scenario EFF 2020, the natural gas savings associated with the implementation of Oxyfuel combustion and the recovery of the waste heat from the ladle heaters and the electric arc furnace account for a total emission reduction of 12 %. The additional consumption for Oxyfuel combustion increases the emissions related to oxygen production. Furthermore, these emissions are transferred to scope 2 due to the on-site production through a PSA unit, thereby reducing the considered energy-related scope 3 emissions to zero.

Though contracts for the supply of electricity with a higher share of renewables are available, the scope 2 emissions in this thesis are determined based on the specific greenhouse gas emissions of the Austrian electricity sector of 143 g CO<sub>2</sub>/kWh in 2020 [83]. As a consequence of the additional oxygen demand for oxyfuel combustion in scenario EFF 2020, scope 2 emissions will initially increase. At this point, it should be noted that Oxyfuel combustion leads to a considerable CO<sub>2</sub> emission reduction not only for a low-emission generation mix but also for electricity with very high specific emissions. From the year 2030 on, the Austrian federal government aims to supply 100 % renewable electricity [84], resulting in the elimination of scope 2 emissions for electricity consumption.<sup>2</sup> The supply of climate-neutral electricity alone eliminates 50 % of the total CO<sub>2</sub> emissions of the steel mill.

With the transition to carbon dioxide emission-free electric power, only scope 1 emissions from fossil fuels will remain. These emissions are gradually reduced through the implementation of power-to-gas plants and an increase in the share of renewable gas in the public gas grid. SNG production via methanation and limits for the admixture of hydrogen into the gas grid, as assumed in scenario SNG 2030, allow for the utilization of the existing infrastructure. However, the labeling of climate-neutral gases is necessary for gas trading and for the accounting of CO<sub>2</sub> emission allowances. Since the feed-in of SNG and hydrogen reduces CO<sub>2</sub> emissions in the higher-level energy system, this reduction should be attributed to the steel mill. From this point on, the definition of scope 2 is supplemented by those CO<sub>2</sub> emission reductions that are caused by the injection of climate-neutral gases into the grid. The conversion of hydrogen to methane is associated with additional capital costs and losses, which is why in the long term the transformation to a dedicated hydrogen infrastructure, as assumed in the scenario PEM 2050 seems to be reasonable.

---

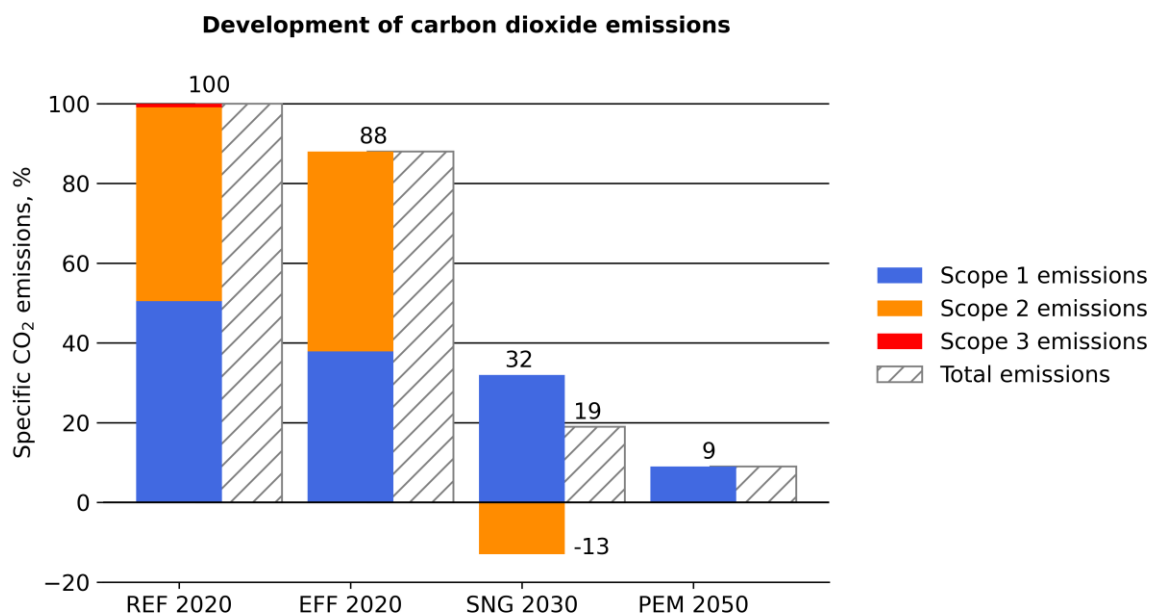
<sup>2</sup> Even power from 100 % renewable generation has specific CO<sub>2</sub> emissions greater than zero. Nevertheless, the author stipulates that electricity-based scope 2 emissions are omitted when producing electricity from RES.

Table 5 summarizes the effect of the proposed reduction measures on the emissions of scope 1, 2 and 3. Resulting from the proposed plant-internal measures, a total CO<sub>2</sub> emission reduction of 41 % is achieved by the year 2050.

**Table 5: Reduction potential of different measures based on the total CO<sub>2</sub> emissions broken down by emission scopes (referred to the scenario REF 2020).**

Measure	Scenario	Scope 1	Scope 2	Scope 3	Total
Oxyfuel ladle heating	EFF 2020	-8 %	-	+1 %	-7 %
Waste heat recovery	EFF 2020	-4 %	-	-	-4 %
Carbon dioxide utilization	EFF 2020	-1 %	-	-	-1 %
Oxygen production	EFF 2020	-	+2 %	-2 %	-
SNG production	SNG 2030	-5 %	-14 %	-	-19 %
Hydrogen production	PEM 2050	-12 %	-8 %	-	-20 %
Coal substitution	-	-9 %	-	-	-9 %

With additional external measures such as the supply of renewable electricity and the conversion of the natural gas network to climate-neutral gases, net-zero energy-related CO<sub>2</sub> emissions are achievable. Figure 18 outlines a potential CO<sub>2</sub> emission reduction path towards a nearly climate-neutral EAF steel production in 2050 including mill-internal measures as well as the prospective development of the higher-level energy system.



**Figure 18: Energy-related specific carbon dioxide emissions broken down by scopes related to the reference scenario REF 2020.**



### 4.5 Economic assessment

The case studies conducted in the articles A2 [24] and A3 [56] include an evaluation of the energy and investment costs for individual plant components: In article A2, three different technology implementation scenarios are analysed under varying economic framework conditions. Article A3 addresses the optimal integration and assessment of flexible oxygen production and power-to-gas plants based on projected energy costs. In view of the expected cost decrease for electrolysis units and rising prices for electricity and emission certificates, the economic analysis covers different economic conditions. From the year 2020 to 2050, evolving prices for the relevant energy carriers and CO<sub>2</sub> emission allowances as well as capital expenditures (CAPEX) for PtG plants are considered. The CAPEX are allocated to the annual energy costs according to the annuity method based on the individual useful life of the assets (between 10 and 20 years) and a calculatory interest rate of 4 %. The assumed price developments are based on several high-level reports. Figure 19 illustrates the development of the specific energy costs upon implementation of the proposed scenarios compared to the reference scenario. The reference scenarios represent the maintenance of the status quo under increasing prices.

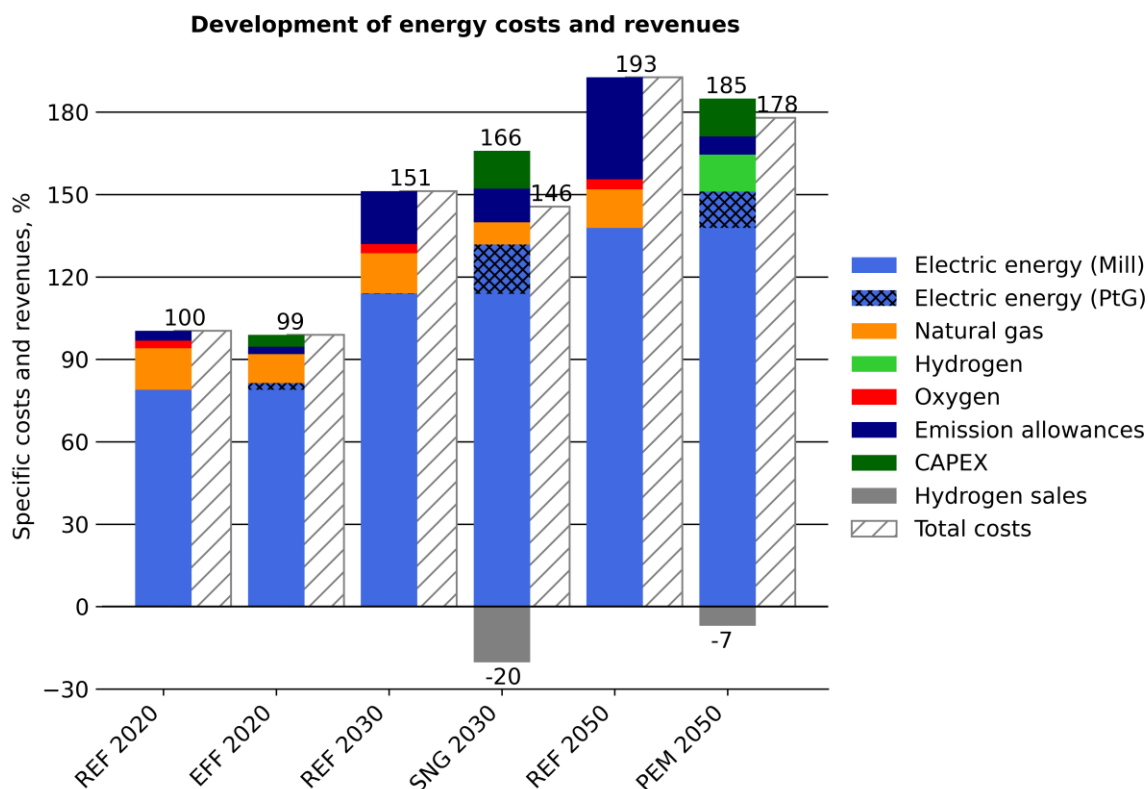


**Figure 19: Composition of energy costs and revenues for different investigated scenarios related to the reference scenario REF 2020.**

The scenario EFF 2020 provides an evaluation regarding the economic viability of energy efficiency measures and CCU: First, the scenario is characterized by a shift of the costs from

natural gas and emission allowances to CAPEX. Second, compared to the reference scenarios for 2020, 2030 and 2050, the implementation of Oxyfuel ladle heaters results in a substantial cost reduction. Savings from the reduced fuel consumption and CO<sub>2</sub> emissions outweigh the costs for the necessary adaption of the ladle heaters, the control equipment as well as the additional oxygen supply. Considering the rising energy and emission allowance prices, the more capital-intensive carbon dioxide utilization and waste heat recovery concepts are profitable as well. Third, in the light of rising prices for natural gas and CO<sub>2</sub> emission certificates, the beneficial impact of implementing fuel-saving technologies on total costs is growing from 2020 to 2050.

In the scenario SNG 2030, on the one side, rising electricity prices and the higher demand due to electrolysis lead to a significant increase in electricity costs. On the other side, the utilization of the generated SNG and hydrogen reduces the expenditures for natural gas as well as emission allowances. Hydrogen sales and the utilization of co-produced oxygen compensates the additional electricity cost.

The PEM 2050 scenario is characterized by a further increase in the average electricity price. However, costs for purchased electricity do not increase in the same range, since the high price variability allows for the exploitation of low electricity prices. In addition, the highly fluctuating electricity price with annually constant gas prices allows for the optimization of energy costs by arbitrage operation: When electricity prices are low, surplus hydrogen is fed into the gas grid; when electricity prices are high, the gas demand of the steelmaking processes is supplied from the gas grid. Due to the conversion of the gas system, the natural gas consumption falls to zero, eliminating natural gas and associated emission allowance costs. Moreover, the increased internal use of hydrogen reduces hydrogen sales.

Due to reasons of complexity associated with an increased total energy consumption and simultaneous hydrogen sales in the scenarios SNG 2030 and PEM 2050, the economic conditions for hydrogen production, self-supply and grid injection need to be studied in more detail. The solid lines in Figure 20 depict the projected development of hydrogen sales and natural gas purchase prices as well as the levelized cost of hydrogen (LCOH) achieved in the case study [56]. The dashed lines represent a 20 % deviation margin. The hydrogen sales price is based on the projected production cost for green hydrogen [79]. The natural gas price includes energy, grid charges, taxes and the costs for CO<sub>2</sub> emission allowances [78,80,81]. The LCOH is derived from the optimization results and incorporates CAPEX, OPEX and energy costs for electrolysis and oxygen storage as well as the cost savings from by-product oxygen utilization in the steel mill. The latter is valued with the oxygen price given in Table 2.

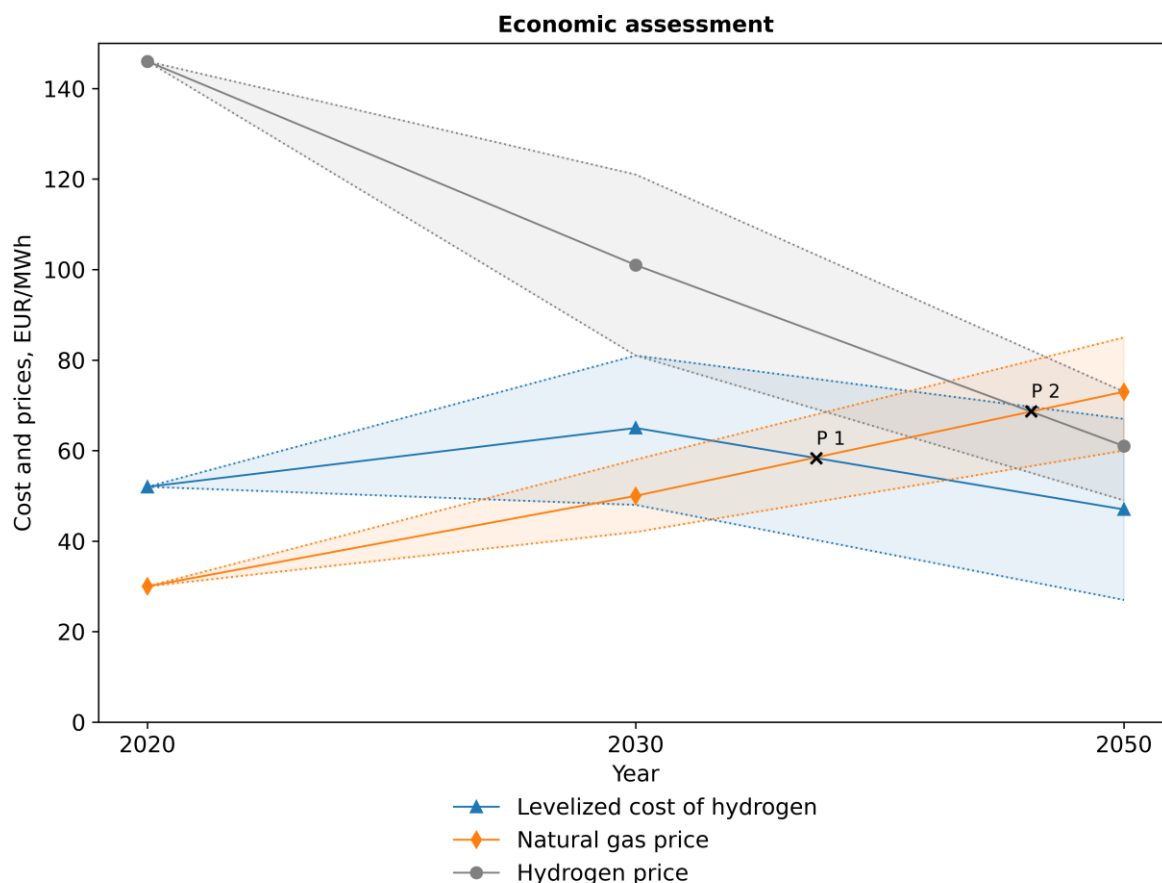


**Figure 20: Projected development of the hydrogen sales price, natural gas price [56]. The latter includes emission allowances, charges and taxes.**

The displayed price situation allows the following conclusions to be drawn: In 2020, the sales price for renewable hydrogen was significantly higher than the LCOH obtained from our study. However, since the price of natural gas including emission allowances is well below the LCOH, hydrogen injection into the gas grid is not profitable. As the cost for electricity already exceeds the natural gas price, either markets for renewable hydrogen sales must be established or feed-in must be subsidized. A similar situation emerges for 2030, with LCOH, natural gas price and hydrogen price continuing to converge. The injection of the generated hydrogen into the gas grid remains economically unviable without subsidies. However, under the projected increase in emission allowance prices, an investment subsidy might represent a suitable instrument to push the LCOH below the cost of natural gas. Ultimately, between 2030 and 2050, the situation arises that, firstly, the costs for on-site produced hydrogen fall below those for purchased natural gas (P1) and, secondly, the feed-in of hydrogen into the gas grid becomes profitable (P2). Starting at P1, the substitution of natural gas by hydrogen is economically viable, whereas from P2 onwards, the full conversion of the gas system to becomes feasible. Consequently, the PEM 2050 scenario involves a complete transition from natural gas to hydrogen to cover the gas demand of the production process.

In summary, the results from the presented case studies indicate that the energy costs will rise in all scenarios, but less sharply for the implementation of energy efficiency and DSM measures than under continuation of the status quo. The amortization periods for the investments range from 3.0 years for the EFF 2020 scenario to 2.5 and 0.9 years for SNG 2030 and PEM 2050 respectively.

## 4.6 Impact of extreme events

As a consequence of the after-effects of the Coronavirus crisis as well as the war in Ukraine, energy prices rose dramatically within the last months. In June 2022, the day-ahead prices for natural gas and electric energy reached 103 EUR/MWh [85] and 180 EUR/MWh [86], respectively. Emission allowances were traded at 83 EUR/t<sub>CO2</sub> [87]. The price forecasts applied in this work are subject to a high degree of uncertainty. Since these forecasts constitute an important foundation of this thesis, this situation requires a more detailed assessment. Therefore, the existing scenarios are re-evaluated applying the present energy and emission allowance prices.

Table 6 demonstrates the impact of this extreme price environment in the first six months of 2022 on the LCOO, LCOH and the total natural gas cost including charges and taxes as well as the cost for emission allowances compared to the predicted values in the scenarios. In the scenario EFF 2022, the high natural gas and emission allowance price has a positive effect on the economic viability of the implemented efficiency measures: The reduction in total annual energy costs increases from 1 to 7 % and the amortization period decreases from 3.0 to 0.2 years. However, the situation is different for the SNG 2022 and PEM 2022 scenarios: Due to the high electricity prices, production costs for oxygen and hydrogen rise dramatically. Even though the cost of natural gas increases as well, it remains far below the LCOH. Consequently, the proposed substitution of natural gas by hydrogen is not economically viable under the current energy price regime.

**Table 6: Impact of the extreme price situation on costs for oxygen, hydrogen and natural gas.**

KPI	EFF 2020	EFF 2022	SNG 2030	SNG 2022	PEM 2050	PEM 2022
LCOO	77	180	93	180	103	180
LCOH	-	-	66	266	47	268
Natural gas cost	30	150	50	150	73	150

## 5 CONCLUSION AND OUTLOOK

The last chapter presents the most important findings related to the research questions (see section 2.4), deduces a comprehensive CO<sub>2</sub> emission reduction pathway and gives an outlook on future research needs.

### 5.1 Conclusion

The conclusion provides answers to the research questions with reference to both the energy efficiency measures and the flexibility options.

*1. What is the impact of the proposed measures on the total energy consumption of the production process?*

The transition from the conventional integrated route via BF and BOF to the Scrap-EAF and DR-EAF route implies the electrification of the steelmaking process. Electric energy and natural gas substitute coal and coke as the main energy sources. This transition leads to a substantial cut in CO<sub>2</sub> emissions, but achieving climate-neutral steel production requires extensive emission reduction measures.

First, the most cost-efficient emission reduction measure is the conservation of fossil fuels by improving the energy efficiency of the applied production facilities. In high-temperature processes such as ladle heating, Oxyfuel combustion leads to significant fuel savings, which by far exceed the power consumption for oxygen production. The implementation of heat recovery systems results in energy conservation through the cascading utilization of energy: Waste heat from combustion processes and cooling systems substitutes natural gas for hot water and process steam generation. In the considered EAF steel mill, the measures integrated in scenario EFF 2020 result in a reduction of 11 % of the total energy consumption and 12 % of total CO<sub>2</sub> emissions. Hence, investments in energy efficiency measures constitute a hedge against rising prices for energy and emission allowances.

Second, in view of the remaining gas demand of the production process, it is essential to replace natural gas by climate-neutral alternatives such as SNG, biomethane or hydrogen. The integration of a PtG plant into the energy system of the steel mill allows for an energy-efficient oxygen supply and the production of a climate-neutral fuel. Thus, the synthetization of gases by PtG technologies such as electrolysis and methanation enables the indirect electrification of combustion processes, while substituting 14 % (SNG 2030) to 33 % (PEM 2050) of the natural gas consumption. SNG and hydrogen is either consumed plant-internally or sold externally, thus reducing the purchase of gas or generating revenues. The production of hydrogen is preferable to that of SNG, since the limited efficiency of methanation results in

energy losses. Therefore, the advancement of the infrastructure towards a gas system with high hydrogen levels appears reasonable.

Third, direct and indirect electrification will increase the electric energy consumption of the steel mill by 44 % (SNG 2030) and 39 % (PEM 2050). Climate-neutral steel production requires the supply of the production process and the PtG plant with CO<sub>2</sub> emission-free generated electricity. Hence, the decarbonization of the power system is a key prerequisite for the zero-emission steel mill.

### *2. What is the impact of the proposed measures on the load flexibility provided by the industrial energy system?*

The proposed energy efficiency measures effectively reduce the energy demand, but do not provide any flexibility. Flexible on-site oxygen production was identified as a feasible option for DSM. Regarding PSA-based O<sub>2</sub> production, the high share of CAPEX in oxygen production costs dictates a high level of plant utilization, resulting in low O<sub>2</sub> production plant and storage capacity, but high full-load hours. Even highly fluctuating energy prices do not compensate the additional investment costs for higher-capacity plants. Furthermore, the oxygen demand-governed plant design in combination with the low specific energy consumption provides low dispatchable power compared to the nominal load of the EAF steel mill. In contrast, the electrolysis unit holds a considerable DSM potential. The relatively high share of energy costs in the hydrogen and oxygen production costs entails a high dependence of the economic efficiency on the electricity price. The exploitation of favorable energy prices allows for large-capacity plants and low full-load hours. Due to the high specific energy demand and the low full-load hours, the proposed electrolysis plant provides a high dispatchable load.

### *3. What is the impact of proposed measures on the energy-related direct and indirect carbon dioxide emissions of the steel mill?*

As a consequence of the fuel savings, the application of both Oxyfuel combustion and waste heat recovery effects a direct emission reduction of 12 % at the ladle heaters and the steam generator (EFF 2020). However, depending on the specific CO<sub>2</sub> emissions of the supplied electricity, indirect emissions arise from the oxygen production process. The deployment of CCU can completely prevent the emission of CO<sub>2</sub> generated during Oxyfuel combustion. The neutralization of alkaline wastewater and the methanation of hydrogen emerge as suitable applications for the captured carbon dioxide.

PtG plants contribute to the reduction of carbon dioxide emissions on several levels: On the one hand, their energy price-driven operation provides load flexibility for the enhanced integration of RES into the energy system, thus contributing to the reduction of indirect emissions. On the other hand, electrolysis and methanation units generate climate-neutral

fuels. In the scenarios SNG 2030 and PEM 2050, the mill-internal utilization of SNG and hydrogen reduces the direct emissions by 5 and 12 %, while their external sale leads to negative indirect emissions of 14 and 8 % respectively. Furthermore, the utilization of the by-product satisfies the oxygen demand for metallurgical processes and Oxyfuel combustion, thus reducing the total energy consumption and indirect CO<sub>2</sub> emissions.

#### *4. What economical and political framework conditions are required for the economically viable implementation of the proposed system solutions?*

The drive to increase energy efficiency is fueled by high energy- and/or CO<sub>2</sub> emission allowance prices. The more expensive the saved energy becomes, the shorter the amortization period for investments in efficient technologies. Regarding Oxyfuel combustion and waste heat utilization, the gross price of natural gas including energy, emission allowances and taxes is the decisive factor in determining whether the implementation of new equipment is economically viable.

Due to the aftermath of the Covid-19 pandemic and the war in Ukraine, the energy share of the natural gas price has soared within a few months. As a result, investments that were not considered economically viable a year ago are now profitable. The situation is similar for climate-neutral gases: Rising natural gas prices and falling specific investment costs for electrolysis plants are causing the spread between hydrogen production costs and natural gas prices to tighten. This creates conducive conditions for the economically viable operation of PtG plants.

The emission trading system (ETS), the policy instrument designed to encourage industrial companies to save fossil fuels and switch to climate-neutral energy sources, achieves a similar effect as high natural gas prices. By periodically reducing the volume of emission allowances, the certificate prices have risen to a level where they affect investment decisions and the selection of energy sources. However, zero-emission steelmaking will not be enforced solely by pushing CO<sub>2</sub> emission allowance prices. There are certain requirements for the higher-level energy system as well:

First, there is the expansion of renewable power generation to supply the future highly electrified steelmaking processes with CO<sub>2</sub>-free electricity. The present work demonstrates that steel mills are capable of supporting the expansion of fluctuating RES by providing flexibility, but that requires the development of generation capacity on the supply side. At this point, it should also be emphasized that advantageous price situations resulting from a surplus of renewable electricity are essential for the economic operation of PtG plants. In this context, it is not the annual average price of electrical energy that is decisive, but rather the existence of extreme price situations. The case study shows that a strongly fluctuating electricity price

with a higher average price is more favorable for the operation of electrolysis plants than a slightly fluctuating electricity price with a lower average price.

Second, to promote the deployment of PtG plants and the feed-in of SNG and hydrogen into the gas grid, it is necessary to create an appropriate market for climate-neutral gases. The presence of a mix of natural gas, SNG, hydrogen and biomethane in the gas grid will trigger a need for the labeling of these gases. The trade of certificates for gases of different origin allows for the introduction of different price regimes for renewable and climate-neutral gases. Individual tariffs and pricing enable the profitable feed-in of climate-neutral gases into the gas grid at an earlier stage. Purchasing carbon-neutral gases could result in benefits for the consumer such as the elimination of scope 1 CO<sub>2</sub> emissions and the exclusion from the ETS. A further instrument to accelerate the introduction of climate-neutral gases into the energy system is the funding of investments in power-to-gas plants and hydrogen-ready infrastructure in the industry. The former allows the operators of power-to-gas plants to trade renewable gases at market prices without subsidized feed-in tariffs. The latter encourages the early adopters among industrial consumers to implement hydrogen technologies at an earlier stage.

Third, the flexibility options in the presented scenarios are operated electricity price-driven. According to the current power price structure, the only varying component of the electricity price is the commodity price. Consequently, the operation strategy of the plants is based entirely on the supply and demand situation on the electricity market, but does not take into account the status of the power grid. For the grid-supporting operation of PtG plants, a supplementary indicator such as variable grid charges depending on the local network load could be imposed in addition to the time-varying commodity prices. One solution for the spatial splitting of the electricity market would be the transition from zonal pricing to nodal pricing.

## 5.2 Summary and Outlook

The present thesis contributes to the scientific knowledge by developing a methodology for the holistic, time- and component-resolved modelling of the energy system of an EAF steel mill. Further achievements involve the identification of suitable CO<sub>2</sub> emission reduction measures, the analysis of their optimal implementation and operation as well as the assessment of their impact on the energy system of an existing steel mill. Based on the presented findings, not only answers to critical research questions are derived, but also a potential pathway to climate-neutral EAF steel production is outlined:

The first step in reducing CO<sub>2</sub> emissions in EAF steelmaking is improving the energy efficiency of the steel mill processes. Investments in efficiency measures such as Oxyfuel combustion



and waste heat recovery are already cost-effective today and will become more so as energy and CO<sub>2</sub> emission allowance prices increase. From this perspective, they represent a hedge against rising energy prices. The second step focuses on providing flexibility to the higher-level power grid to facilitate the expansion of RES. This is accompanied by the gradual conversion to a climate-neutral gas supply through injection of mill-internally generated SNG and hydrogen into the gas system. The methanation of hydrogen from electrolysis using captured CO<sub>2</sub> from Oxyfuel combustion enables the utilization of climate-neutral SNG in the steel mill without major challenges to the infrastructure. By utilizing the co-produced oxygen from the electrolysis unit in the steel mill, the LCOH is significantly reduced. The intermediate methanation route is necessary as long as the grid and consumer infrastructure limits the admixture of hydrogen. The third step involves the complete transition of the gas system to operation on 100 % hydrogen. Between the years 2030 and 2050, the LCOH is projected to fall below the price of natural gas including emission allowances. When the substitution of natural gas with hydrogen from renewable electricity becomes economically viable, it might be appropriate to convert the infrastructure to operate on pure hydrogen, thus paving the way to a climate-neutral gas system.

The potential emission reduction path outlined in this thesis is based on a portfolio of various technologies that have hitherto been investigated to a great extent. Most of the considered technologies have been industrially applied for several years, whereas none of the technologies is still in the basic research stage. On a technological level, future research potential lies primarily in the optimal deployment of waste heat recovery systems for direct fuel savings, further development of electrolysis systems to increase efficiency and reduce manufacturing costs and the design of a gas infrastructure that allows for a shift of the gas system to a gas mix with high concentrations of hydrogen. However, the most pressing questions arise at an energy-systemic level. This thesis illustrates that CO<sub>2</sub> emission reduction measures such as energy efficiency, electrification, carbon capture, and fuel substitution do not end at the mill fence, but interact with the overarching energy system. An overall system analysis across multiple industries is essential to determine what the energy system is capable of providing and what needs to be contributed from industrial consumers on the path to climate neutrality. The course for the future of our energy system is laid today, now is the time to make sure it is headed in the right direction.

## 6 REFERENCES

- [1] Eurostat, Energy balance sheets, 2022.
- [2] European Environment Agency, National emissions reported to the UNFCCC and to the EU Greenhouse Gas Monitoring Mechanism, 25th 2022.  
<https://www.eea.europa.eu/data-and-maps/data/national-emissions-reported-to-the-unfccc-and-to-the-eu-greenhouse-gas-monitoring-mechanism-17> (accessed 10th March, 2022).
- [3] United Nations Framework Convention of Climate Change (Ed.), United Nations Framework Convention on Climate Change: Adoption of the Paris agreement, United Nations, Paris, 2015.
- [4] Regulation (EU) 2021/1119 of the European Parliament and of the Council of 30th June 2021 establishing the framework for achieving climate neutrality and amending Regulations (EC) No 401/2009 and (EU) 2018/1999: European Climate Law, in: Official Journal of the European Union.
- [5] Eurofer, Low carbon roadmap: Pathways to a CO<sub>2</sub>-neutral European steel industry, Brussels, 2019.
- [6] Eurofer, European steel in figures. Covering 2011 - 2019, Brussels, 2020.
- [7] International Energy Agency, Iron and Steel Technology Roadmap, Paris, 2020.
- [8] A. Toktarova, I. Karlsson, J. Rootzén, L. Göransson, M. Odenberger, F. Johnsson, Pathways for Low-Carbon Transition of the Steel Industry—A Swedish Case Study, *Energies* 13 (2020) 3840. <https://doi.org/10.3390/en13153840>.
- [9] M. Arens, E. Worrell, W. Eichhammer, A. Hasanbeigi, Q. Zhang, Pathways to a low-carbon iron and steel industry in the medium-term – the case of Germany, *Journal of Cleaner Production* 163 (2017) 84–98. <https://doi.org/10.1016/j.jclepro.2015.12.097>.
- [10] Material Economics, Industrial Transformation 2050 - Pathways to Net-Zero Emissions from EU Heavy Industry, 2019.
- [11] T. Battle, U. Srivastava, J. Kopfle, R. Hunter, The Direct Reduction of Iron, in: *Treatise on process metallurgy*, Elsevier, Kidlington, Oxford, U.K, Waltham, Mass, 2014, pp. 89–176.
- [12] A. Sasiain, K. Rechberger, A. Spanlang, I. Kofler, H. Wolfmeir, C. Harris, T. Bürgler, Green Hydrogen as Decarbonization Element for the Steel Industry, *Berg Huettenmaenn Monatsh* 165 (2020) 232–236. <https://doi.org/10.1007/s00501-020-00968-1>.

## References

---

- [13] B. Anameric, S.K. Kawatra, Direct iron smelting reduction processes, *Mineral Processing and Extractive Metallurgy Review* 30 (2008) 1–51.  
<https://doi.org/10.1080/08827500802043490>.
- [14] Primetals Technologies, COREX: Efficient and environmentally friendly smelting reduction, 2021. <https://www.primetals.com/portfolio/ironmaking/corexr>.
- [15] Voestalpine AG, Breakthrough Technologies: SuSteel, 2022.  
<https://www.voestalpine.com/greentecsteel/en/breakthrough-technologies/> (accessed 3rd June, 2022).
- [16] Masab Naseri Seftejani, Reduction of hematite using hydrogen plasma smelting reduction. Doctoral thesis, Leoben, 2020.
- [17] The Boston Consulting Group (BCG), Steel Institute VDEh, Steel's contribution to a low-carbon Europe 2050: Technical and economic analysis of the sector's CO<sub>2</sub> abatement potential, 2013.
- [18] ICF Consulting Services Limited, Fraunhofer Institute for Systems and Innovation Research, Industrial innovation: Pathways to deep decarbonisation of industry: Part 2: Scenario analysis and pathways to deep decarbonisation, 2019.
- [19] N. Docquier, M. Grant, K. Kaiser, 22. Ferrous Metals, in: C.E. Baukal (Ed.), *Oxygen-enhanced combustion*, secondnd ed., CRC Press, Boca Raton, 2013, pp. 531–555.
- [20] Jorge Madias, *Electric Furnace Steelmaking*, in: *Treatise on process metallurgy*, Elsevier, Kidlington, Oxford, U.K, Waltham, Mass, 2014, pp. 271–300.
- [21] T. Echterhof, Review on the Use of Alternative Carbon Sources in EAF Steelmaking, *Metals* 11 (2021) 222. <https://doi.org/10.3390/met11020222>.
- [22] J. Dock, D. Janz, J. Weiss, A. Marschnig, T. Kienberger, Time- and component-resolved energy system model of an electric steel mill, *Cleaner Engineering and Technology* 4 (2021) 100223. <https://doi.org/10.1016/j.clet.2021.100223>.
- [23] R. Remus, Best available techniques (BAT) reference document for iron and steel production: Industrial emissions directive 2010/75/EU (integrated pollution prevention and control), Publications Office of the European Union, Luxembourg, 2013.
- [24] J. Dock, T. Kienberger, Techno-economic case study on Oxyfuel technology implementation in EAF steel mills – Concepts for waste heat recovery and carbon dioxide utilization, *Cleaner Engineering and Technology* 9 (2022) 100525.  
<https://doi.org/10.1016/j.clet.2022.100525>.

- [25] M. Kirschen, K. Badr, H. Pfeifer, Influence of direct reduced iron on the energy balance of the electric arc furnace in steel industry, *Energy* 36 (2011) 6146–6155.  
<https://doi.org/10.1016/j.energy.2011.07.050>.
- [26] Ü. Çamdalı, M. Tunç, Modelling of electric energy consumption in the AC electric arc furnace, *Int. J. Energy Res.* 26 (2002) 935–947. <https://doi.org/10.1002/er.829>.
- [27] Ü. Çamdalı, M. Tunç, Energy and exergy analysis of a ladle furnace, *Canadian Metallurgical Quarterly* 42 (2003) 439–446.  
<https://doi.org/10.1179/cmq.2003.42.4.439>.
- [28] C. Chen, Y. Liu, M. Kumar, J. Qin, Energy Consumption Modelling Using Deep Learning Technique — A Case Study of EAF, *Procedia CIRP* 72 (2018) 1063–1068.  
<https://doi.org/10.1016/j.procir.2018.03.095>.
- [29] D. Gajic, I. Savic-Gajic, I. Savic, O. Georgieva, S. Di Gennaro, Modelling of electrical energy consumption in an electric arc furnace using artificial neural networks, *Energy* 108 (2016) 132–139. <https://doi.org/10.1016/j.energy.2015.07.068>.
- [30] M. Kovačič, K. Stopar, R. Vertnik, B. Šarler, Comprehensive Electric Arc Furnace Electric Energy Consumption Modeling: A Pilot Study, *Energies* 12 (2019) 2142.  
<https://doi.org/10.3390/en12112142>.
- [31] T. Hay, V.-V. Visuri, M. Aula, T. Echterhof, A Review of Mathematical Process Models for the Electric Arc Furnace Process, *steel research int.* 92 (2021) 2000395.  
<https://doi.org/10.1002/srin.202000395>.
- [32] M.F. Zarandi, P. Ahmadpour, Fuzzy agent-based expert system for steel making process, *Expert Systems with Applications* 36 (2009) 9539–9547.  
<https://doi.org/10.1016/j.eswa.2008.10.084>.
- [33] World Resources Institute, World Business Council for Sustainable Development, The greenhouse gas protocol. <https://ghgprotocol.org/standards> (accessed 19th November, 2021).
- [34] J. Rissman, C. Bataille, E. Masanet, N. Aden, W.R. Morrow, N. Zhou, N. Elliott, R. Dell, N. Heeren, B. Huckestein, J. Cresko, S.A. Miller, J. Roy, P. Fennell, B. Cremmins, T. Koch Blank, D. Hone, E.D. Williams, S. de La Rue Can, B. Sisson, M. Williams, J. Katzenberger, D. Burtraw, G. Sethi, H. Ping, D. Danielson, H. Lu, T. Lorber, J. Dinkel, J. Helseth, Technologies and policies to decarbonize global industry: Review and assessment of mitigation drivers through 2070, *Applied Energy* 266 (2020) 114848.  
<https://doi.org/10.1016/j.apenergy.2020.114848>.
- [35] International Energy Agency, European Union 2020: Energy Policy Review, 2020.

- [36] C.E. Baukal, 2. Fundamentals, in: C.E. Baukal (Ed.), *Oxygen-enhanced combustion*, secondnd ed., CRC Press, Boca Raton, 2013, pp. 25–43.
- [37] C.E. Baukal, 10. Heat Transfer, in: C.E. Baukal (Ed.), *Oxygen-enhanced combustion*, secondnd ed., CRC Press, Boca Raton, 2013, pp. 197–234.
- [38] J. von Scheele, *Oxyfuel Combustion in the Steel Industry: Energy Efficiency and Decrease of CO<sub>2</sub> Emissions*, in: J. Palm (Ed.), *Energy Efficiency*, Sciyo, 2010.
- [39] G. Wei, R. Zhu, X. Wu, K. Dong, L. Yang, R. Liu, Technological Innovations of Carbon Dioxide Injection in EAF-LF Steelmaking, *JOM* 70 (2018) 969–976.  
<https://doi.org/10.1007/s11837-018-2814-3>.
- [40] K. He, L. Wang, A review of energy use and energy-efficient technologies for the iron and steel industry, *Renewable and Sustainable Energy Reviews* 70 (2017) 1022–1039.  
<https://doi.org/10.1016/j.rser.2016.12.007>.
- [41] H. Jouhara, N. Khordehgah, S. Almahmoud, B. Delpech, A. Chauhan, S.A. Tassou, Waste heat recovery technologies and applications, *Thermal Science and Engineering Progress* 6 (2018) 268–289. <https://doi.org/10.1016/j.tsep.2018.04.017>.
- [42] T. Steinparzer, M. Haider, F. Zauner, G. Enickl, M. Michele-Naussed, A.C. Horn, Electric Arc Furnace Off-Gas Heat Recovery and Experience with a Testing Plant, *steel research int.* 85 (2014) 519–526. <https://doi.org/10.1002/srin.201300228>.
- [43] L.-z. Yang, T. Jiang, G.-h. Li, Y.-f. Guo, F. Chen, Present Situation and Prospect of EAF Gas Waste Heat Utilization Technology, *High Temperature Materials and Processes* 37 (2018) 357–363. <https://doi.org/10.1515/htmp-2016-0218>.
- [44] B. Lee, I. Sohn, Review of Innovative Energy Savings Technology for the Electric Arc Furnace, *JOM* 66 (2014) 1581–1594. <https://doi.org/10.1007/s11837-014-1092-y>.
- [45] G. Hartfuß, M. Schmid, G. Scheffknecht, Off-Gas Waste Heat Recovery for Electric Arc Furnace Steelmaking Using Calcium Hydroxide (Ca(OH)<sub>2</sub>) Dehydration, *steel research int.* 91 (2020) 2000048. <https://doi.org/10.1002/srin.202000048>.
- [46] M. Ramirez, M. Epelde, M.G. de Arteche, A. Panizza, A. Hammerschmid, M. Baresi, N. Monti, Performance evaluation of an ORC unit integrated to a waste heat recovery system in a steel mill, *Energy Procedia* 129 (2017) 535–542.  
<https://doi.org/10.1016/j.egypro.2017.09.183>.
- [47] T. Keplinger, M. Haider, T. Steinparzer, A. Patrejko, P. Trunner, M. Haselgrübler, Dynamic simulation of an electric arc furnace waste heat recovery system for steam production, *Applied Thermal Engineering* 135 (2018) 188–196.  
<https://doi.org/10.1016/j.applthermaleng.2018.02.060>.

- [48] I. Ortega-Fernández, J. Rodríguez-Aseguinolaza, Thermal energy storage for waste heat recovery in the steelworks: The case study of the REslag project, *Applied Energy* 237 (2019) 708–719. <https://doi.org/10.1016/j.apenergy.2019.01.007>.
- [49] M. Haider, A. Werner, An overview of state of the art and research in the fields of sensible, latent and thermo-chemical thermal energy storage, *Elektrotech. Inftech.* 130 (2013) 153–160. <https://doi.org/10.1007/s00502-013-0151-3>.
- [50] R. Pili, A. Romagnoli, H. Spliethoff, C. Wieland, Techno-Economic Analysis of Waste Heat Recovery with ORC from Fluctuating Industrial Sources, *Energy Procedia* 129 (2017) 503–510. <https://doi.org/10.1016/j.egypro.2017.09.170>.
- [51] S. Quoilin, M. van den Broek, S. Declaye, P. Dewallef, V. Lemort, Techno-economic survey of Organic Rankine Cycle (ORC) systems, *Renewable and Sustainable Energy Reviews* 22 (2013) 168–186. <https://doi.org/10.1016/j.rser.2013.01.028>.
- [52] S. Lecompte, O. Oyewunmi, C. Markides, M. Lazova, A. Kaya, M. van den Broek, M. de Paepe, Case Study of an Organic Rankine Cycle (ORC) for Waste Heat Recovery from an Electric Arc Furnace (EAF), *Energies* 10 (2017) 649. <https://doi.org/10.3390/en10050649>.
- [53] W. Moch, W. Adler, M.A. Gregor, Investigations and measures to reduce emissions and energy consumption during the preheating of steel ladles, Publications Office, Luxembourg, 2008.
- [54] T. Wall, Y. Liu, C. Spero, L. Elliott, S. Khare, R. Rathnam, F. Zeenathal, B. Moghtaderi, B. Buhre, C. Sheng, R. Gupta, T. Yamada, K. Makino, J. Yu, An overview on oxyfuel coal combustion—State of the art research and technology development, *Chemical Engineering Research and Design* 87 (2009) 1003–1016. <https://doi.org/10.1016/j.cherd.2009.02.005>.
- [55] H. Mikulčić, I. Ridjan Skov, D.F. Dominković, S.R. Wan Alwi, Z.A. Manan, R. Tan, N. Duić, S.N. Hidayah Mohamad, X. Wang, Flexible Carbon Capture and Utilization technologies in future energy systems and the utilization pathways of captured CO<sub>2</sub>, *Renewable and Sustainable Energy Reviews* 114 (2019) 109338. <https://doi.org/10.1016/j.rser.2019.109338>.
- [56] J. Dock, S. Wallner, A. Traupmann, T. Kienberger, Provision of Demand-Side Flexibility through the Integration of Power-to-Gas Technologies in an Electric Steel Mill, *Energies* 15 (2022) 5815. <https://doi.org/10.3390/en15165815>.

- [57] H. Wang, H. Yu, L. Teng, S. Seetharaman, Evaluation on material and heat balance of EAF processes with introduction of CO<sub>2</sub>, *J min metall B Metall* 52 (2016) 1–8. <https://doi.org/10.2298/JMMB150627002W>.
- [58] Agora Energiewende, Ember, The European Power Sector in 2020: Up-to-Date Analysis on the Electricity Transition, 2021.
- [59] G. Strbac, Demand side management: Benefits and challenges, *Energy Policy* 36 (2008) 4419–4426. <https://doi.org/10.1016/j.enpol.2008.09.030>.
- [60] P. Warren, A review of demand-side management policy in the UK, *Renewable and Sustainable Energy Reviews* 29 (2014) 941–951. <https://doi.org/10.1016/j.rser.2013.09.009>.
- [61] M. Paulus, F. Borggrefe, The potential of demand-side management in energy-intensive industries for electricity markets in Germany, *Applied Energy* 88 (2011) 432–441. <https://doi.org/10.1016/j.apenergy.2010.03.017>.
- [62] P. Palensky, D. Dietrich, Demand Side Management: Demand Response, Intelligent Energy Systems, and Smart Loads, *IEEE Trans. Ind. Inf.* 7 (2011) 381–388. <https://doi.org/10.1109/TII.2011.2158841>.
- [63] F. Marchiori, A. Belloni, M. Benini, S. Cateni, V. Colla, A. Ebel, M. Lupinelli, G. Nastasi, M. Neuer, C. Pietrosanti, A. Vignali, Integrated Dynamic Energy Management for Steel Production, *Energy Procedia* 105 (2017) 2772–2777. <https://doi.org/10.1016/j.egypro.2017.03.597>.
- [64] G.D. Ave, J. Hernandez, I. Harjunkoski, L. Onofri, S. Engell, Demand Side Management Scheduling Formulation for a Steel Plant Considering Electrode Degradation, *IFAC-PapersOnLine* 52 (2019) 691–696. <https://doi.org/10.1016/j.ifacol.2019.06.143>.
- [65] K. Nolde, M. Morari, Electrical load tracking scheduling of a steel plant, *Computers & Chemical Engineering* 34 (2010) 1899–1903. <https://doi.org/10.1016/j.compchemeng.2010.01.011>.
- [66] Q. Zhang, I.E. Grossmann, Enterprise-wide optimization for industrial demand side management: Fundamentals, advances, and perspectives, *Chemical Engineering Research and Design* 116 (2016) 114–131. <https://doi.org/10.1016/j.cherd.2016.10.006>.
- [67] T. Kato, M. Kubota, N. Kobayashi, Y. Suzuoki, Effective utilization of by-product oxygen from electrolysis hydrogen production, *Energy* 30 (2005) 2580–2595. <https://doi.org/10.1016/j.energy.2004.07.004>.
- [68] J. Gorre, F. Ruoss, H. Karjunen, J. Schaffert, T. Tynjälä, Cost benefits of optimizing hydrogen storage and methanation capacities for Power-to-Gas plants in dynamic

- operation, *Applied Energy* 257 (2020) 113967.  
<https://doi.org/10.1016/j.apenergy.2019.113967>.
- [69] ENTSOG, 2050 Roadmap for gas grids, Brussels, 2021.
- [70] S. Schiebahn, T. Grube, M. Robinius, V. Tietze, B. Kumar, D. Stolten, Power to gas: Technological overview, systems analysis and economic assessment for a case study in Germany, *International Journal of Hydrogen Energy* 40 (2015) 4285–4294.  
<https://doi.org/10.1016/j.ijhydene.2015.01.123>.
- [71] M. Mayrhofer, M. Koller, P. Seemann, R. Prieler, C. Hochenauer, Assessment of natural gas/hydrogen blends as an alternative fuel for industrial heat treatment furnaces, *International Journal of Hydrogen Energy* 46 (2021) 21672–21686.  
<https://doi.org/10.1016/j.ijhydene.2021.03.228>.
- [72] J. Dock, T. Kienberger, Klimaneutrale Elektrostahlproduktion durch Energieeffizienz und Integration Erneuerbarer Energie, *Elektrotech. Inftech.* Under review (2022).
- [73] J. Dock, D. Janz, T. Kienberger, Modellierung des Lastprofils eines Elektrolichtbogenofens mittels Markov-Ketten, in: 16. Symposium Energieinnovation 2020, Graz, 2020.
- [74] J. Dock, S. Wallner, T. Kienberger, Energieeffizienz und Flexibilität bei der Elektrostahlproduktion, in: 17. Symposium Energieinnovation, Graz, 2022.
- [75] Austrian Power Grid AG, EXAA day-ahead prices 2020.  
<https://www.apg.at/de/markt/Markttransparenz/Uebertragung/EXAA-Spotmarkt> (accessed 21st December, 2021).
- [76] Energy Brainpool, Trends in the development of electricity prices – EU Energy Outlook 2050. <https://blog.energybrainpool.com/en/trends-in-the-development-of-electricity-prices-eu-energy-outlook-2050/> (accessed 16th February, 2022).
- [77] Energy Brainpool, Update: EU Energy Outlook 2050 - How will Europe evolve over the next 30 years? <https://blog.energybrainpool.com/en/update-eu-energy-outlook-2050-how-will-europe-evolve-over-the-next-30-years/> (accessed 16th February, 2022).
- [78] International Energy Agency, *World Energy Outlook 2021*, Paris, 2021.
- [79] R. Cvetkovska, P. Nagovnak, T. Kienberger, Pathways for ramping-up hydrogen into the natural gas system, in: 17. Symposium Energieinnovation, Graz, 2022.
- [80] R.C. Pietzcker, S. Osorio, R. Rodrigues, Tightening EU ETS targets in line with the European Green Deal: Impacts on the decarbonization of the EU power sector, *Applied Energy* 293 (2021) 116914. <https://doi.org/10.1016/j.apenergy.2021.116914>.



- 
- [81] European Commission, A Clean Planet for all - A European long-term strategic vision for a prosperous, modern, competitive and climate neutral economy: In-depth analysis in support of the commission communication COM (2018) 773, 28th 2018.
- [82] European Energy Exchange AG, Emission Spot Primary Market Auction Report 2020. <https://www.eex.com/en/market-data/environmental-markets/eua-primary-auction-spot-download> (accessed 21st December, 2021).
- [83] Ember, Emissions intensity: Austria. <https://ember-climate.org/data/data-explorer/> (accessed 16th May, 2022).
- [84] Austrian Federal Ministry for Climate Action, Environment, Energy, Mobility, Innovation and Technology, Mission 2030. [https://www.bmk.gv.at/ministerium/ziele\\_agenda2030/13.html](https://www.bmk.gv.at/ministerium/ziele_agenda2030/13.html) (accessed 16th May, 2022).
- [85] European Energy Exchange AG, Neutral gas price: NGP price history. <https://www.powernext.com/spot-market-data> (accessed 22nd July, 2022).
- [86] Austrian Power Grid AG, EXAA day-ahead prices 2022. <https://www.apg.at/de/markt/Markttransparenz/Uebertragung/EXAA-Spotmarkt> (accessed 22nd July, 2022).
- [87] European Energy Exchange AG, Emission Spot Primary Market Auction Report 2022. <https://www.eex.com/en/market-data/environmental-markets/eua-primary-auction-spot-download> (accessed 22nd July, 2022).

## APPENDIX A: PEER-REVIEWED SCIENTIFIC ARTICLES

### Article A1

J. Dock, D. Janz, J. Weiss, A. Marschnig, T. Kienberger, Time- and component-resolved energy system model of an electric steel mill, Cleaner Engineering and Technology 4 (2021) 100223. <https://doi.org/10.1016/j.clet.2021.100223>.

Submitted: 28<sup>th</sup> January, 2021

Published: 29<sup>th</sup> July, 2021

**Table A 1: Author contribution statement for article A1.**

Activity	Contributing authors
Conceptualization	J. Dock, T. Kienberger
Methodology	J. Dock, J. Weiss, A. Marschnig
Data curation	J. Dock, D. Janz
Software development and validation	J. Dock, J. Weiss, A. Marschnig
Modelling	J. Dock, J. Weiss, A. Marschnig
Investigation and analysis	J. Dock, D. Janz, J. Weiss, A. Marschnig
Visualization	J. Dock
Writing (original draft)	J. Dock
Writing (review and editing)	J. Dock, T. Kienberger

## Article A2

J. Dock, T. Kienberger, Techno-economic case study on Oxyfuel technology implementation in EAF steel mills – Concepts for waste heat recovery and carbon dioxide utilization, *Cleaner Engineering and Technology* 9 (2022) 100525. <https://doi.org/10.1016/j.clet.2022.100525>.

Submitted: 12<sup>th</sup> October, 2021

Published: 29<sup>th</sup> June, 2022

**Table A 2: Author contribution statement for article A2.**

<b>Activity</b>	<b>Contributing authors</b>
Conceptualization	J. Dock, T. Kienberger
Methodology	J. Dock, T. Kienberger
Data curation	J. Dock
Software development and validation	J. Dock
Modelling	J. Dock
Investigation and analysis	J. Dock
Visualization	J. Dock
Writing (original draft)	J. Dock
Writing (review and editing)	J. Dock, T. Kienberger

### Article A3

J. Dock, S. Wallner, A. Traupmann, T. Kienberger, Provision of Demand-Side Flexibility through the Integration of Power-to-Gas Technologies in an Electric Steel Mill, *Energies* 15 (2022) 5815. <https://doi.org/10.3390/en15165815>.

Submitted: 14<sup>th</sup> July, 2022

Published: 10<sup>th</sup> August, 2022

**Table A 3: Author contribution statement for article A3.**

Activity	Contributing authors
Conceptualization	J. Dock, T. Kienberger
Methodology	J. Dock, S.Wallner, T. Kienberger
Data curation	J. Dock, S.Wallner, A. Traupmann
Software development and validation	J. Dock, S.Wallner
Modelling	J. Dock, S.Wallner
Investigation and analysis	J. Dock, S.Wallner, A.Traupmann
Visualization	J. Dock
Writing (original draft)	J. Dock, A.Traupmann
Writing (review and editing)	J. Dock, T. Kienberger

## **APPENDIX B: FURTHER SCIENTIFIC DISSEMINATION**

J. Dock, D. Janz, J. Weiss, A. Marschnig, M. Rahnama Mobarakeh, Zeitlich aufgelöste Modellierung des Energieverbrauchs bei der Elektrostahlproduktion, *e & i Elektrotechnik und Informationstechnik* 138, 274-280 (2021). <https://doi.org/10.1007/s00502-021-00895-0>.

J. Dock, D. Janz, T. Kienberger, Modellierung des Lastprofils eines Elektrolichtbogenofens mittels Markov-Ketten, in: 16. Symposium Energieinnovation 2020, Graz, 2020.

J. Dock, S. Wallner, T. Kienberger, Energieeffizienz und Flexibilität in der Elektrostahlproduktion, in: 17. Symposium Energieinnovation 2022, Graz, 2022.



## Time- and component-resolved energy system model of an electric steel mill

Johannes Dock<sup>a,\*</sup>, Daniel Janz<sup>b</sup>, Jakob Weiss<sup>a</sup>, Aaron Marschnig<sup>a</sup>, Thomas Kienberger<sup>a</sup>

<sup>a</sup> Chair of Energy Network Technology, Montanuniversitaet Leoben, Franz-Josef-Straße 18, 8700, Leoben, Austria

<sup>b</sup> Breitenfeld Edelstahl AG, Breitenfeldstraße 22, 8662, St.Barbara-Mitterdorf, Austria

### ARTICLE INFO

#### Keywords:

Energy system  
Steel production  
Electric arc furnace  
Markov chain

### ABSTRACT

Steel production is a highly energy- and emission-intensive process. Compared to the production via the integrated route, the melting of recycled steel scrap and directly reduced iron in an electric arc furnace operated on green power constitutes a way to reduce energy consumption and CO<sub>2</sub>-emissions. However, there is still potential to reduce energy consumption and CO<sub>2</sub>-emissions in electric arc furnace steel production by introducing new sub-processes, optimal operational design, and integration of renewable energy sources. For complex industrial processes, this potential can only be determined using models of the entire system. The batch operation, changing process parameters, and strongly fluctuating energy consumption require a holistic, temporally, and technologically resolved model. Within the scope of this paper, we describe an energy system model of an electric arc furnace steel mill. It allows assessing the optimal implementation of novel technologies and system integration of renewable energy sources using a reduced set of input parameters. The modular design facilitates the extension of the model, and the option of specifying several input parameters enables the model to be adopted for other electric steel mills.

### 1. Introduction

With a final energy consumption of 569 TWh, the European iron and steel industry is not only one of the largest energy consumers but also one of the most relevant industrial emitters of carbon dioxide (Eurostat, 2018). It is estimated that this industry sector is responsible for 4–7% of anthropogenic CO<sub>2</sub>-emissions in the European Union (Pardo et al., 2015). To comply with the Paris Agreement of the UNFCCC (United Nations Framework Convention on Climate Change), measures to increase energy efficiency and reduce greenhouse gas emissions are strongly required (United Nations Framework Convention of Climate Change, 2015).

Main steel production routes are the integrated process route (blast furnace/converter) and the electric arc furnace route (steel scrap/electric arc furnace). Compared to the energy- and emission-intensive blast furnace route the latter represents an option for low carbon emission steel production: instead of reducing iron ore to pig iron, recycled steel scrap is remelted in an electric arc furnace (EAF), which saves energy and CO<sub>2</sub>-emissions. In 2019, 41.4% of the European steel was produced using the EAF route (Eurofer, 2020).

An alternative is the processing of direct reduced iron (DRI) in an EAF. Due to the direct reduction step, this process route entails no

energetic benefits but the use of natural gas as a reducing agent results in a reduction of CO<sub>2</sub> emissions by about 18% (Arens et al., 2017). Powering electric arc furnaces with electric energy from renewable energy sources further decreases the CO<sub>2</sub>-intensity of the process. According to Bhaskar et al. (2020), hydrogen direct reduction of iron ore and steel production via HDRI-EAF-route represents a viable alternative to the integrated steelmaking route but economic feasibility depends on the future cost of electrolyzers and electricity. Sasiain et al. (2020) conclude that the CO<sub>2</sub>-reduction potential of HDRI-EAF steelmaking is related to the decarbonization of the electricity sector.

#### 1.1. EAF steelmaking – state of the art

In their study, Zarandi and Ahmadpour (2009) describe EAF steelmaking based on the following process steps:

- Remelting (primary metallurgy),
- Ladle metallurgy (secondary metallurgy),
- Ingot casting.

Fig. 1 represents the sub-processes of the EAF steelmaking process and shows the principal steelmaking components in the steel mill investigated in this work.

\* Corresponding author.

E-mail addresses: [johannes.dock@unileoben.ac.at](mailto:johannes.dock@unileoben.ac.at) (J. Dock), [daniel.janz@breitenfeld.at](mailto:daniel.janz@breitenfeld.at) (D. Janz).

<https://doi.org/10.1016/j.clet.2021.100223>

Received 28 January 2021; Received in revised form 29 June 2021; Accepted 22 July 2021

Available online 24 July 2021

2666-7908/© 2021 The Authors.

Published by Elsevier Ltd.

This is an open access article under the CC BY-NC-ND license

(<http://creativecommons.org/licenses/by-nc-nd/4.0/>).

Symbols			
$Prob\{X\}$	probability	$\dot{m}$	mass flow
$X$	random variable	$\bar{c}_p$	isobaric heat capacity
$P_{ij}$	transition probability	$T$	temperature
$P_{ij, cum}$	cumulative transition probability	$T_{ref}$	reference temperature
$P$	transition probability matrix	$\dot{Q}_{use}$	useful heat flow
$P_{electric}, P_{el}$	electric power	$LHV$	lower heating value
$P_{thermal}, P_{th}$	thermal power	$\eta$	efficiency
$P_{waste\ heat\ power}, P_{wh}$	waste heat power	$P$	active power
$E$	energy consumption	$Q$	reactive power
$m_{scrap}$	mass of steel scrap	$S$	apparent power
$\dot{H}$	enthalpy flow rate	$\cos(\phi)$	power factor
$h$	specific enthalpy	$EEI$	energy efficiency index
$\dot{Q}_{cooling}$	cooling power	$SEC$	specific energy consumption

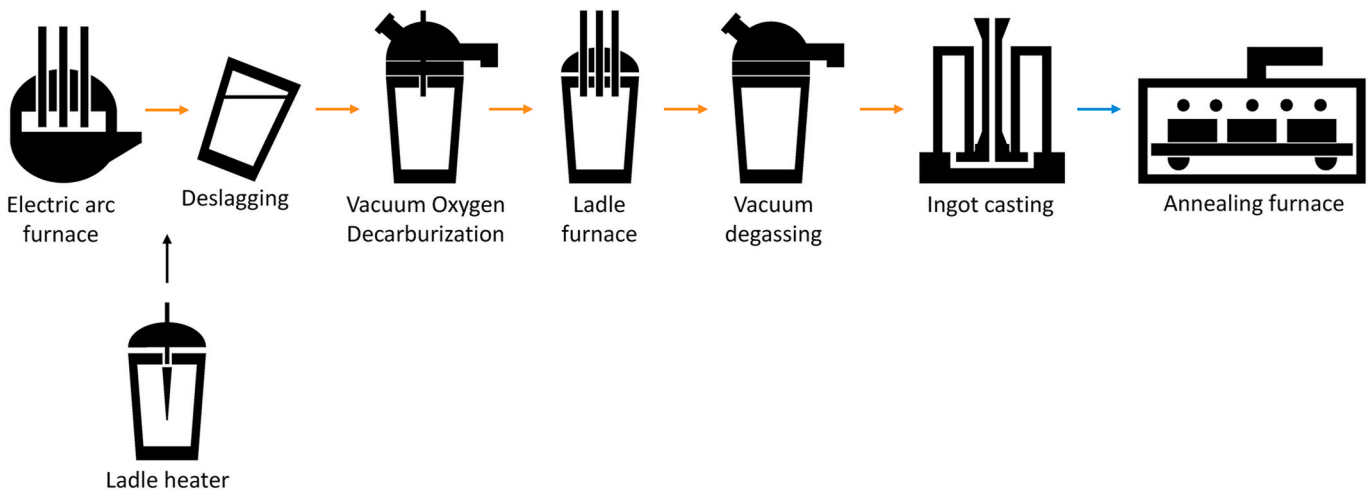


Fig. 1. Steelmaking process in the investigated steel mill.

The function of the electric arc furnace is to melt steel scrap into liquid steel. This requires heat input into the material, which is mainly driven by the radiant heat of the electric arc (Blesl and Kessler, 2013). Unlike many other electric arc furnaces, the furnace described here does not have any additional gas burners for further energy input.

So-called ladles are used as transport and treatment vessels for liquid steel. Before the tapping procedure begins, ladles are preheated to avoid damage to the refractory, remove any humidity and prevent excessive cooling of the steel melt. Natural gas burners preheat the ladles up to more than 1000 °C.

After tapping, the liquid steel is subjected to ladle or secondary metallurgy. The required steel quality and composition determine the treatments that have to be carried out. Production steps within secondary metallurgy are (Zarandi and Ahmadpour, 2009):

- Heating,
- Desulphurization,
- Deoxidation,
- Degassing,
- Decarburization,
- Homogenization,
- Composition adjustment,
- Removal of non-metallic inclusions.

The product-specific application of ladle treatments affects the use of

the ladle furnace. Its principal purpose is to adjust the steel melt temperature throughout secondary metallurgical processes and for casting. In analogy to the electric arc furnace, three carbon electrodes enable the energy transfer into the liquid steel.

For the production of high-alloy and special steels, which are produced in the investigated steel mill, vacuum degassing (VD) and vacuum oxygen decarburization (VOD) are applied to remove dissolved gases or in the case of the VOD process residual carbon concentrations from the steel melt.

When the steel meets the required composition, quality, and casting temperature, in the steel mill considered in this study, it is cast in ingots. Finally, the properties of the solidified steel ingots are adjusted by heat treatment in annealing furnaces.

### 1.2. Energy system modeling corresponding to EAF steelmaking

In energy intensive industries, investments in new technologies and equipment have a clear effect on energy efficiency. Gajdzik and Sroka (2021) use economic models to prove the correlation between investments and the resource and energy intensity in the steel industry. In their study on energy efficiency trends, Wolniak et al. (2020) confirm that an increase in investment leads to a decrease in energy consumption. They find that full automation and flexibilization of production processes in the context of industry 4.0 holds particular potential to reduce the energy intensity. Pardo Martinez (Pardo et al., 2015) analysis

of the energy efficiency in German and Colombian manufacturing industries demonstrates that energy demand is a decisive factor in technology development. However, an investment decision requires well-conducted preliminary studies for an accurate assessment of the current energy system and potential savings (Johansson, 2015).

Energy system models aim to estimate the impact of technological developments on the overall energy consumption of a process to evaluate investment decisions and policy designs. For energy demand models, there are two basic modeling approaches: top-down and bottom-up. Bottom-up models are characterized by their detailed representation of technologies, whereas top-down models are limited to aggregated representations of the system. This results in a loss of information about the applied technologies (Fleiter et al., 2011).

In bottom-up approaches, thermodynamic methods are often used to model the energy consumption of steel mill components. Based on mass and energy balances, Kirschen et al. (2011) developed an energy model of an electric arc furnace to investigate the impact of inserting DRI on the energy efficiency of the electric arc furnace. Camdali and Tunc (Çamdali and Tunc, 2002) studied the effect of several process properties on the energy consumption of an EAF using the first law of thermodynamics. In another publication, they perform an energy and exergy analysis on a ladle furnace considering also the second law of thermodynamics (Çamdali and Tunc, 2003).

Another approach to predict energy demand is data-driven modeling. Chen et al. (2018) propose a deep learning model to predict the daily energy consumption of an EAF using data from an existing steel mill. Gajic et al. (2016) use an artificial neural network to study the effect of steel scrap composition on specific electric energy consumption. Kovacic et al. (Kovačić et al., 2019) present two approaches for the prediction of EAF energy demand. A linear regression model, as well as a generic programming model, were applied to determine energy consumption.

Carlsson et al. (2019) present a structured description of the existing statistical models for predicting EAF energy consumption. In contrast to other mathematical modeling approaches, the result of statistical models is based on weighted decisions derived from known exemplary data. The study covers linear regression models as well as neural networks and investigates the influence of different input variables such as time, chemical reactions, temperature as well as complexity and treatment of data. The conclusion states that process knowledge is indispensable for the development of a practice-oriented model. Regarding the design of new models, attention should be paid to the predictive performance for future batches and the robustness of the model.

In their review article, Hay et al. (2021) give an overview over process models for the electric arc furnace process. Process models are characterized as a middle ground between the statistical energy consumption models and the CFD (computational fluid dynamics) models. The considered models enable the description of heat transfer, melting process and chemical reactions. The authors conclude that existing process models are suitable for describing and understanding the underlying principles of different processes.

Zarandi and Ahmadpour (2009) present an agent-based expert system for the EAF steelmaking process. Matino et al. (2016) describe a process model including the process route, the gas supply network, and water treatment. In a scenario analysis (Matino et al., 2017), this virtual electric steel mill is used to obtain key performance indicators (KPI) such as electric energy consumption or carbon dioxide emissions. In his article, Atabay (2017) presents a mathematical model to economically optimize industrial energy systems. Ziębik and Gładysz (Ziębik and Gładysz, 2018) applied Input-Output-Analysis on the system level to assess its energy and exergy efficiency. In a case study, they used a nonlinear mathematical model to analyze the energy management of an integrated steel plant.

### 1.3. Research need

For complex industrial energy systems, such as an electric steel mill, operation optimization, implementation of energy efficiency measures and new processes, as well as identification of flexibility options for the integration of renewable energy sources or demand-side management require the application of holistic, time- and technology-resolved energy system models. These models must allow for predicting the effects of changes in the production process on energy demand, the superior energy grid, and the resulting carbon dioxide emissions.

Some of the energy consumption models mentioned in chapter 1.2 are capable of predicting the future energy demand of individual steel mill components (Çamdali and Tunc, 2002, 2003; Carlsson et al., 2019; Chen et al., 2018; Gajic et al., 2016; Hay et al., 2021; Kirschen et al., 2011; Kovačić et al., 2019). These models do not allow time-resolved calculations to investigate the effects of renewable energy sources as well as waste heat and product gas utilization in terms of process integration. Hence, their use is inappropriate for representing complex process chains as part of an energy system.

Other above-mentioned models are capable of predicting and assessing the energy consumption and environmental impact of an entire production process consisting of several sub-processes (Matino et al., 2016; Zarandi and Ahmadpour, 2009). However, these models do not provide any time-resolved energy consumption profiles either.

There are models that consider the temporal behavior of an overall energy system (Atabay, 2017; Ziębik and Gładysz, 2018) such as an electric steel mill but their application requires specific knowledge, for instance, provided by measurement results, of the temporally resolved energy consumption of the sub-processes as melting, ladle preheating or vacuum treatments. It has to be mentioned that the load profiles of the sub-processes change depending on implemented technology and pre-defined operating parameters.

Electric steelmaking consists of a series of energy-intensive batch processes, such as melting, refining, alloying, decarburization, or degassing (see Fig. 1). Hence, the energy consumption of the equipment, as well as of the entire steel mill, is strongly fluctuating. It is therefore necessary for the overall energy system model of the steel mill to reflect the time-dependent behavior of the energy demand and the interdependencies of the processes of the different steel mill components.

However, to the best of our knowledge, no study exists that allows for comprehensive time-resolved modeling of an overall electric steel mill together with generic component models providing accurate results with only minor demand of directly measured data. The objective of this study is to present an energy system model of an electric steel mill, which is suitable to assess the impact of technological developments on the temporally resolved energy demand. Therefore, we aim for a modeling approach that allows us to generate generic synthetic load profiles.

The paper is structured as follows: chapter 2 introduces the methods applied to construct the sub-models (2.1) and presents the structure of the energy system model (2.2). In chapter 3, we apply our generic approach to model the components (3.1) and the overall energy system (3.2) of an existing steel mill based on actual process parameters. Chapter 4 addresses the evaluation and discussion of the results. The conclusion (chapter 5) sums up the results.

## 2. Modeling approach

In this section, we first identify major energy consumers and analyze their operational and load characteristics. Then, we introduce appropriate methodologies to generate synthetic load profiles, which are applied in chapter 3 and discussed in chapter 4.

### 2.1. Modeling of sub-components

In order to model generically valid synthetic load profiles of the



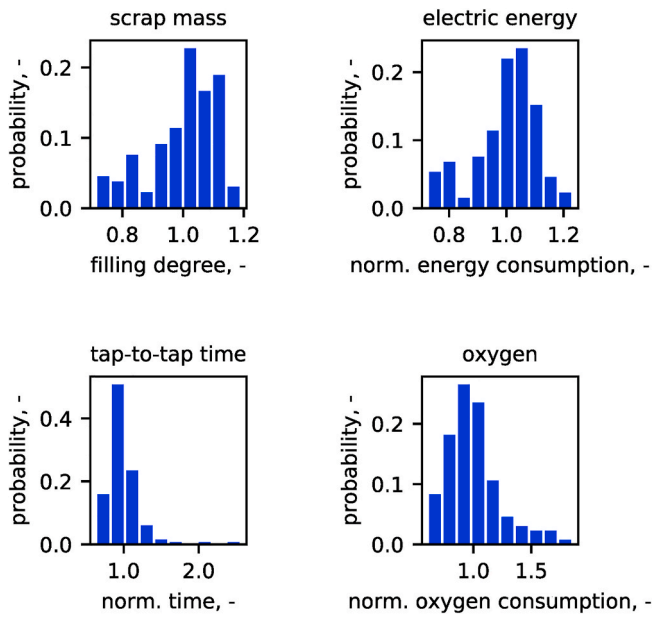


Fig. 2. Production data of the electric arc furnace.

considered system components (Fig. 1), their actual time-resolved energy demand and waste heat flows are obtained. Three-phase power analyzers (Artemes AM-15-PLOG) recorded the values of active, reactive, and apparent power consumed by the production facilities. Natural gas consumption was measured using the on-site turbine flow meters and logged by data loggers (DataTaker DT85). The waste heat flow of the electric arc furnace was determined based on temperature, composition, volume flow, and pressure measurements of the exhaust gas stream. For other components, we calculated waste heat flows by using mass and energy balances.

To build the sub-models as well as the overall energy system model, we chose Python as the programming language (Guido van Rossum, 2020). Advantages of the language are its versatility, the availability of comprehensive documentation and tutorials, and its wide range of powerful libraries. Libraries used within the scope of this work are Pandas, NumPy and Matplotlib.

Individual energy consumers of the energy system are integrated into the model in the form of sub-models. These sub-models are represented in the code by classes containing individual properties and a method for the generation of load profiles. The basic framework for each sub-model is an operational model, which is coupled with time-resolved load profiles to form an energy consumption model.

Depending on their individual load and operation characteristics, we pursued different modeling approaches. Therefore, the sub-models are grouped into components with predefined load profiles (ladle heaters, vacuum treatment units, small consumers), strongly fluctuating load profiles (electric arc furnace, ladle furnace), and dependent load profiles (induced draft fans).

In the following chapters, two modeling approaches that are substantial for the present work are explained: stochastic modeling of process parameters and load profile generation based on Markov chains.

### 2.1.1. Stochastic modeling

There is a common aspect regarding the production processes observed in the steel mill: processes often vary substantially in terms of process duration and energy consumption. As a representative example, Fig. 2 shows histograms of the process parameters of the electric arc furnace including scrap mass, electric energy consumption, tap-to-tap time, and oxygen consumption. The values are presented relative to the mean value, which is therefore 1.0. For each parameter, the ordinate indicates the probability of occurrence.

Table 1

Pearson correlation coefficients between electric energy consumption and measured process parameters.

Correlation coefficient (Pearson):		
Energy consumption	kWh	1.00
Scrap mass	t	0.89
Oxygen consumption	m <sup>3</sup> <sub>Norm</sub>	-0.32
Tap-to-tap time	min	0.16
Chromium content at tapping	%	-0.21
Tapping temperature	°C	-0.33

Investigations on process parameters of the secondary metallurgical processes and the preheating of steelmaking ladles deliver similar results: depending on the used type of scrap, the required steel quality, and the availability of processing units and operating personnel, different process durations and energy consumptions follow.

In order to generate representative load profiles and calculate realistic KPIs, we have to take into account decisive process parameters. For the EAF, we identified scrap mass and tap-to-tap time as vital input parameters. In our model, they are determined stochastically by drawing samples from measured distributions using Python’s mathematical module *random* (Guido van Rossum, 2020). Since we did not find any significant correlation between the remaining process parameters and the energy consumption for the considered electric arc furnace based on the available data, these parameters are determined separately (see Table 1).

In this manner, we determine the varying process durations of secondary metallurgical processes (3.1.2.2), the initial cycle count of the steelmaking ladles (3.1.4.2), and which batches are subjected to vacuum oxygen decarburization (3.1.5.2) or annealing (3.1.6.2). Stochastically determined parameters such as tap-to-tap time and scrap mass also serve as input values for generating Markov chains (see 2.1.2).

### 2.1.2. Markov chains

Markov chains serve to predict future states of a system based on historical data. In the field of energy technology, they are frequently used to model synthetic load or generation profiles. In their studies, Nijhuis et al. (2016), Collin et al. (2014), and McKenna et al. (2015) apply Markov chains to generate occupancy and demand profiles of households. These profiles are used to develop load models for the residential sector. Shamshad et al. (2005) and Ma et al. (2018) use Markov chains in their wind speed models in order to estimate wind power potentials, while Carpinone et al. (2015) introduce a model for very-short-term wind power forecasting. Wang and Infield (2018) investigate the impact of electric vehicle charging on the distribution network using driving patterns generated by Markov Chain Monte Carlo (MCMC) simulation.

Physical processes, such as temporally resolved load profiles, often represent a sequence of discrete states. If the state of the system to be described in the next time step depends exclusively on the status at the current point in time and not on previous events, it satisfies the so-called Markov property (see equation (1)) (Stewart, 2009).

$$Prob\{X_{n+1} = x_{n+1} | X_n = x_n, X_{n-1} = x_{n-1}, \dots, X_0 = x_0\} = Prob\{X_{n+1} = x_{n+1} | X_n = x_n\} \tag{1}$$

In an observed sequence of states, there is a certain probability that the system changes from one state (*i*) to another (*j*) (equation (2)).  $p_{ij}(n)$  is the probability that the system shifts from state *i* to state *j* within one time step (*n*).

$$p_{ij}(n) = Prob\{X_{n+1} = j | X_n = i\} \tag{2}$$

For the construction of a Markov chain, these probabilities are arranged in a matrix. The so-called transition probability matrix has the following form (3):

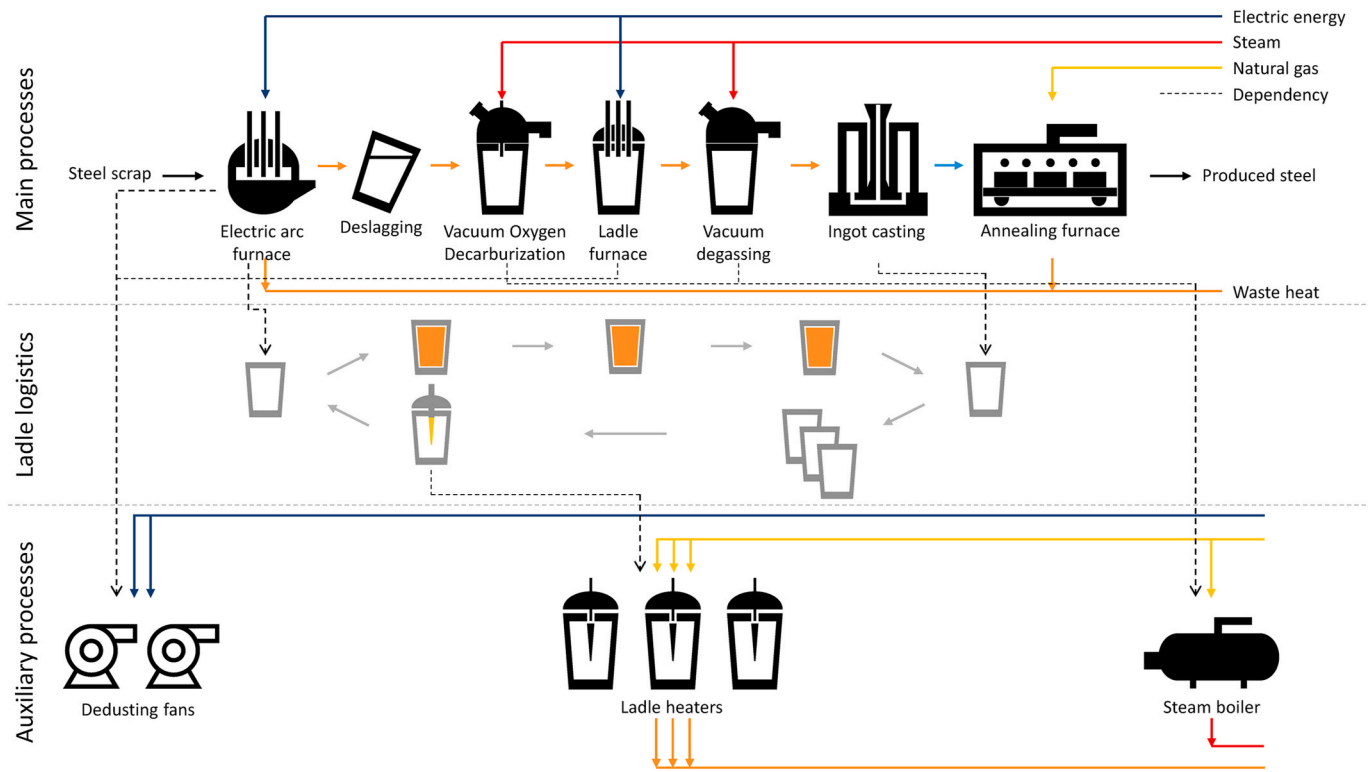


Fig. 3. Overview over the energy system model.

$$P(n) = \begin{pmatrix} p_{00}(n) & p_{01}(n) & \dots & p_{0j}(n) & \dots \\ p_{10}(n) & p_{11}(n) & \dots & p_{1j}(n) & \dots \\ \vdots & \vdots & \ddots & \vdots & \ddots \\ p_{i0}(n) & p_{i1}(n) & \dots & p_{ij}(n) & \dots \\ \vdots & \vdots & \vdots & \vdots & \ddots \end{pmatrix} \quad (3)$$

Each element of matrix  $P(n)$  satisfies the properties  $0 \leq p_{ij}(n) \leq 1$  and  $\sum_{all j} p_{ij}(n) = 1$ . To construct a Markov chain, these probabilities are cumulated for each row according to equation (4).

$$p_{ij, cum} = \sum_{k=0}^j p_{ik} \quad (4)$$

If we give an initial state as the starting point and draw a discrete random number  $z$  ( $0 \leq z \leq 1$ ), the cumulated transition probability matrix leads to the next state, which then serves as the initial state for the following time step. Stewart (2009) gives a detailed description of Markov chains, their construction, and application.

This principle can be applied to the modeling of synthetic load profiles of the electric arc furnace or other fluctuating energy consumers. Within our model, the electric load of the electric arc and ladle furnaces, as well as the EAF off-gas temperature, were modeled using Markov chains. Therefore, the nominal power of the electric arc furnace and the ladle furnaces are divided into intervals. These power intervals represent the possible states that the furnaces may be in during operation.

By counting the transitions between different power levels and division by the total number of transitions in the measured load profile, the model generates a transition probability matrix. Due to their different characteristics, separate matrices are calculated for the EAF process phases melting and refining as well as for the ladle furnaces. Similarly, the exhaust gas temperature range of the EAF is segmented into intervals and a corresponding transition probability matrix is generated. The transition probability matrix of the EAF melting phase is included in the supplementary material.

### 2.2. Energy system model

The main objective of the present work is to develop a holistic, time-resolved model of the industrial energy system of an EAF steel mill, containing several energy carriers. Therefore, all sub-models described in chapter 3.1 are merged to form an energy system model of the steel mill. Simulation time steps have a length of 60 s corresponding to the temporal resolution of the three-phase power measurements and the natural gas consumption data.

Fig. 3 provides an overview of the overall energy system model of the steel mill. For better clarity, we divide the occurring processes into a main process sequence and several auxiliary processes. Along the main process chain, the steelmaking batches pass through the steel mill following the procedure described below.

The first process steps of steelmaking are melting and refining of scrap in the electric arc furnace. We synthesize the strongly fluctuating load profile of the EAF in the form of a Markov chain. After a time delay for tapping and deslagging, the model transfers the batch to a queue for secondary metallurgical processes.

For every time step, the secondary metallurgy module iterates through this queue of batches waiting for treatment and assigns them to available ladle furnaces, vacuum oxygen decarburization, or vacuum degassing units. Then, the model iterates through the list of ladle furnaces, VD, and VOD units, retrieves current load levels, stops finished processes, and adds the batches to the queue. Once a batch has been processed, it is transferred to a casting queue.

Auxiliary processes are dependent on the main production processes: the electrical power of the fans is determined by the operation of the electric arc furnace, and the natural gas demand of the steam boiler is related to the steam demand of the vacuum processes. The ladle logistics model enables the connection of the ladle heaters with the production process. Fig. 3 indicates the dependencies between the main and auxiliary processes by dashed lines.

Load profiles of the entire system and output values are calculated following equations (5)–(7).

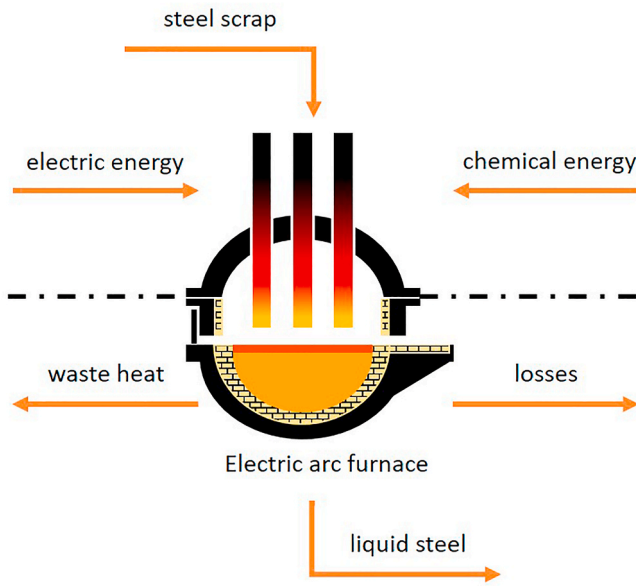


Fig. 4. Energy balance of an electric arc furnace.

$$P_{electric}(t) = P_{el, EAF}(t) + P_{el, ladle\ furnace}(t) + P_{el, fans}(t) + P_{el, base\ load}(t) \quad (5)$$

$$P_{thermal}(t) = P_{th, ladle\ heating}(t) + P_{th, annealing}(t) + P_{th, steam\ generation}(t) + P_{th, base\ load}(t) \quad (6)$$

$$P_{waste\ heat}(t) = P_{wh, EAF}(t) + P_{wh, ladle\ heating}(t) + P_{wh, annealing}(t) \quad (7)$$

In analogy to active power (5), reactive and apparent power of individual consumers are summed up as well. In the case of natural gas-fired consumers, the model takes into account not only thermal power but also temperature levels at which the off-gas leaves the respective unit. For the steam boiler, the annealing furnaces, and the ladle heaters, a distinction is made between useful and final energy consumption.

### 3. Electric steel mill model

According to the approach discussed in chapter 2, we have developed component models as well as the overall system for modeling a specific electric steel mill. Process parameters from the investigated steel mill serve as a basis for the model. However, the described approach can be applied to any steel mill with a similar configuration. Since we cannot publish the actual consumption data, the load and waste heat profiles are shown in normalized form. For individual units, it was required to normalize process times and temperatures as well.

#### 3.1. Sub-models

In chapter 3.1, models of the individual steel mill components are developed following the procedure:

- Data analysis,
- Modeling,
- Presentation of results.

##### 3.1.1. Electric arc furnace

As the melting unit, the electric arc furnace is the centerpiece of the steel mill. Due to its energy consumption and its high nominal power, the EAF represents an important component of the energy system model.

**3.1.1.1. Data analysis.** Given the temporal and energetic dependency of other sub-processes on EAF operation, proper modeling of this

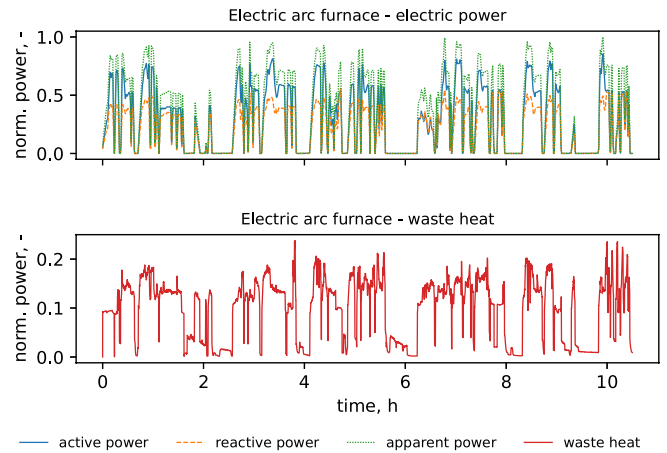


Fig. 5. Electric load profile (top) and waste heat profile (bottom) of an electric arc furnace.

component is essential for the overall steel mill model. During the processing of one batch of steel the following process steps are applied:

- Preparation and charging,
- Melting,
- Refining and
- Tapping.

Electric energy input takes place within the melting phases or refining and amounts to 404–748 kWh/t of liquid steel according to literature (Remus, 2013). Total specific heat input is considerably higher at 512 to 883 kWh/t, including chemical energy from exothermic oxidation reactions of particular scrap components and natural gas burners. Outputs are the latent and the sensible heat of the liquid steel and slag, off-gas enthalpy, and further losses like heat conduction through the furnace vessel and cooling water losses (Fig. 4) (Kirschen et al., 2009).

The theoretical minimum energy demand is equal to the specific enthalpy difference for melting and superheating of steel. At a tapping

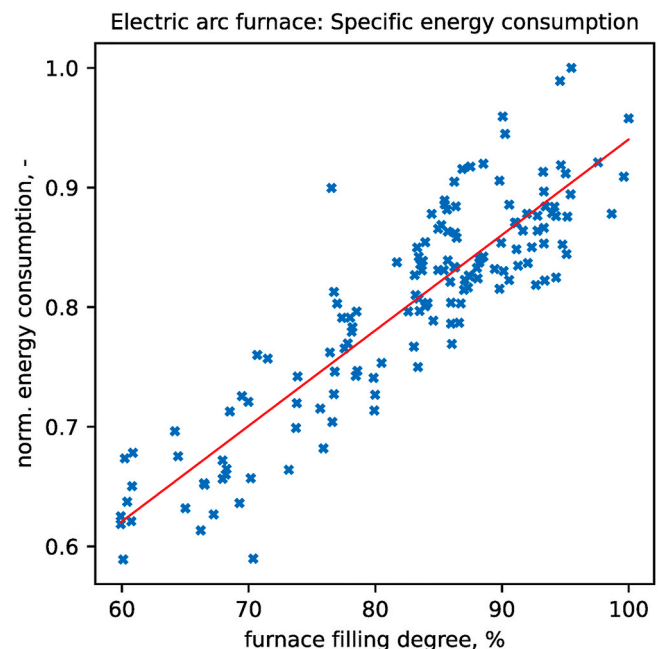


Fig. 6. Estimation of the EAF energy consumption based on the scrap mass using linear regression.

temperature of 1600 °C, specific enthalpy amounts to 361 kWh/t for carbon steels and 372 kWh/t for stainless steels (Kirschen et al., 2009).

In the course of the energy system analysis of the investigated steel plant, we obtained three-phase, time-resolved power measurements for 130 batches. Along with minute-resolved active, reactive, and apparent power values, the tap-to-tap time, which indicates the time interval between two tapping procedures, as well as scrap mass, tapping temperature, and carbon content of the melt were analyzed.

Fig. 5 represents the normalized measured electric load profile as well as the measured exhaust heat flow of the electric arc furnace. Active, reactive, and apparent power values, as well as the waste heat flow, are indicated in relation to the nominal apparent power of the furnace transformer.

It was shown that there is an approximately linear relationship (see Fig. 6) between the amount of scrap charged and the electrical energy used. However, the temporal behavior of the load profile and the occurrence of load peaks as well as the tap-to-tap time cannot be determined from the above-mentioned data, but rather corresponds to stochastic behavior.

Linear regression was applied to obtain an equation, which is then used in the model to calculate the amount of energy based on the scrap mass.

$$E = a \cdot m_{scrap} + b \quad (8)$$

Equation (8) describes the relationship between scrap mass ( $m_{scrap}$ ) and energy input ( $E$ ). Parameter  $a$  represents the variable part of the energy consumption, which depends on the scrap mass, while  $b$  represents the constant part. Both figures are characteristic for the observed furnace.

A relation between measured active, reactive, and apparent power was found with the aid of linear regression. This means that we have observed approximately constant factors between active and reactive as well as between active and apparent power.

Between 12 and 56% of the total energy input leave the electric arc furnace as waste heat via the cooling system and the exhaust gas (Kirschen et al., 2009). Steinparzer et al. (2014) present a furnace with exhaust gas losses of 226 kWh/t. Their investigations suggest that part of this heat can be recovered at the hot-gas duct via heat exchangers (Keplinger et al., 2018; Steinparzer et al., 2014).

These figures are consistent with the observations made within the context of the present work. Our calculations show that 13% of the supplied electric energy exits the furnace via exhaust gas and 40% via the cooling system. A reference to the amount of electrical energy input is reasonable in this case since the furnace is not equipped with natural gas burners. Exhaust gas temperatures range up to 740 °C, while the water of the cooling system discharges waste heat at 90 °C.

The waste heat flow varies significantly due to fluctuating exhaust gas temperatures and mass flow rates (see Fig. 5), whereby the former is mainly affected by the energy input.

**3.1.1.2. Modeling.** The structure of the model for generating synthetic load profiles for electric arc furnaces can be divided into four parts, which are explained in more detail below:

- Calculation of the energy demand,
- Specification of the tap-to-tap time,
- Construction of the Markov Chains and
- Sequencing of the load profiles.

In order to compute the load profile, it is necessary to define a number of input variables. These are the scrap mass, tap-to-tap time, specific oxygen demand, and the transition probability matrices generated from observation sequences (see chapter 2.1.2).

For each batch, the required energy input is calculated according to equation (8) and allocated to a Markov chain (see chapter 2.1.2). Once

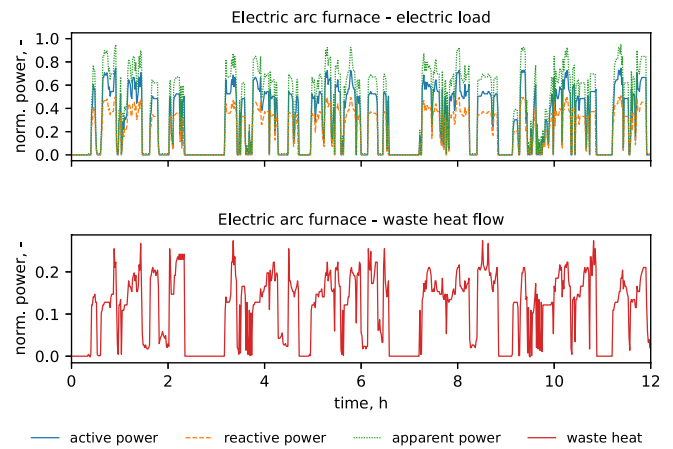


Fig. 7. Synthetic electric load profile (top) and waste heat profile (bottom) of the electric arc furnace.

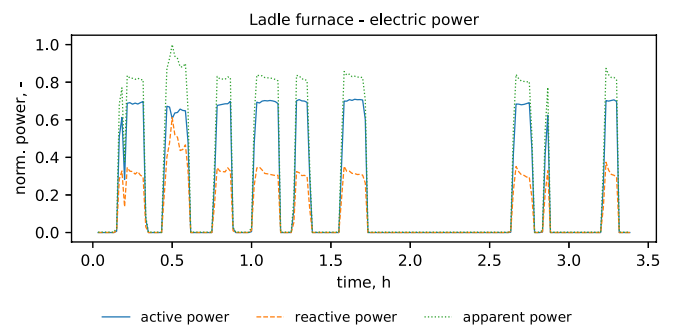


Fig. 8. Measured electric load profile of a ladle furnace.

the length of the chain corresponds to the previously specified tap-to-tap time, the Markov chain is transferred to the load profile of the electric arc furnace. Reactive and apparent power for each time step is calculated from the active power profile using the power factors referred to in section 3.1.1.1.

Based on the electric load profile, the model determines the load profile of the exhaust fans (see 3.1.3.2). The waste heat flow exiting the electric arc furnace ( $\dot{H}$ ) is defined by mass flow rate ( $\dot{m}$ ), mean specific heat capacity ( $\bar{c}_p(T)$ ) and temperature ( $T$ ) of the exhaust gas and the power of the cooling system ( $\dot{Q}_{cooling}$ ) according to equation (9). In our model, the reference temperature ( $T_{ref}$ ) is defined as input parameter.

$$\dot{H} = \dot{m} \cdot \bar{c}_p(t) \cdot (T - T_{ref}) + \dot{Q}_{cooling} \quad (9)$$

Since the mass flow is directly related to the exhaust fan operation, it is calculated based on the fan capacity (see 3.1.3.1). The strongly fluctuating temperature ( $T$ ) is determined over a Markov chain (see 2.1.2). The cooling system operates at a constant level and is set to nominal power during power-on periods of the electric arc furnace.

**3.1.1.3. Result.** Fig. 7 represents the load profile of the EAF for 12 hours of steel production. As before, active, reactive, and apparent power, as well as waste heat flow are displayed relative to the nominal apparent power of the furnace transformer. Contrary to Fig. 5, the power dissipated by the cooling system is included in the waste heat flow. We will discuss the accordance between measured and simulated power characteristics (Figs. 5 and 7) in chapter 4.

**3.1.2. Ladle furnace**

The main function of the ladle furnace is to keep the steel at the required temperature level during subsequent refining processes. These

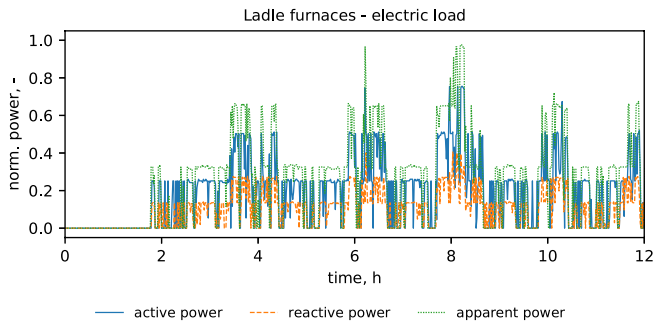


Fig. 9. Synthetic electric load profile of four ladle furnaces.

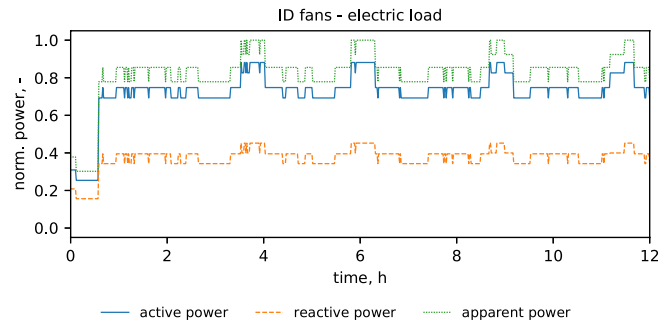


Fig. 11. Aggregated load profile of the EAF- and dedusting fans.

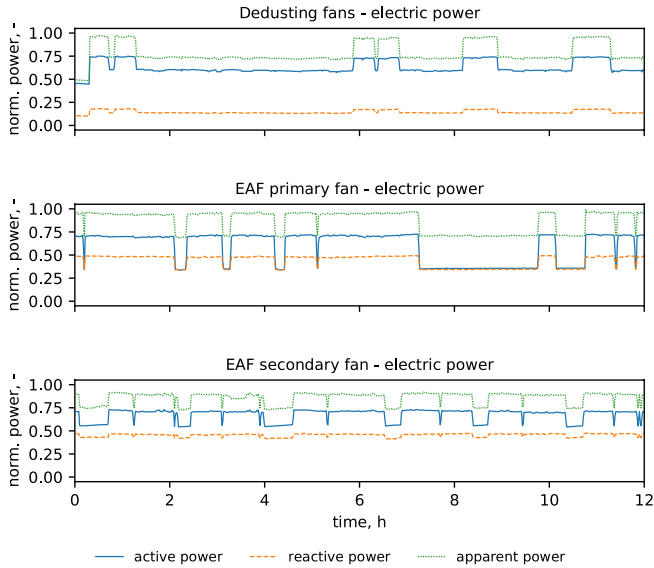


Fig. 10. Load profile of the dedusting fans (top) and EAF fans (bottom).

include desulfurization, alloying, homogenization, deoxidation as well as degassing and are referred to as secondary or ladle metallurgy (Remus, 2013).

3.1.2.1. *Data analysis.* Fig. 8 depicts the active, reactive, and apparent power demand of the ladle furnace relative to its nominal apparent power for one steel batch. The functional principle of the ladle furnace is similar to that of the electric arc furnace, whereby it is intended solely for heating the molten steel bath. Therefore, the power rating is lower and the power input is more uniform.

The load profile of the ladle furnace reflects ladle metallurgical processes, hence energy supply is repeatedly interrupted. During these phases raw materials such as alloying elements are added, treatments are carried out and samples are taken. Subsequently, the required casting temperature needs to be adjusted in most cases.

In order to model the process, we subdivide it into three parts: heating phase one, degassing, and heating phase two.

3.1.2.2. *Modeling.* Since the applied secondary metallurgical treatments during heating phases one and two and their time sequences vary considerably, the operating periods and energy consumption of the ladle furnace differ as well. For this reason, a Markov chain was used to model the load profile of the ladle furnace during these two process phases, similar to that of the electric arc furnace (chapter 2.1.2).

In order to generate the aggregated load profile of the ladle furnaces, the model iterates through the list of furnaces (see chapter 2.2) and retrieves their current load level.

3.1.2.3. *Result.* Fig. 9 shows the synthetic electric load profile of the four available ladle furnaces and a simulation time of 12 hours. Electric power is represented relative to the nominal apparent power of the ladle furnace.

### 3.1.3. Induced draft fans

Given their portion on the total energy consumption, the following fans are included in our analysis: two induced draft fans, the primary and secondary exhaust fans, are in place to absorb the EAF off-gas directly from the furnace vessel and a canopy hood (exhaust fans). The two steel mill buildings are equipped with a powerful dust extraction system, driven by four fans (dedusting fans).

3.1.3.1. *Data analysis.* During steel production, which is for the steel mill considered in this work the case for a maximum of five days per week, the production halls must be dedusted. Therefore, dedusting fans run whenever the steel mill is in operation. In one of the buildings, the dedusting system operates at constant load. In the second building, fans are mainly running at partial load (53%) and powered up to full load only when casting is in progress. The measured load profiles (Fig. 10) indicate the load peaks during casting and the shutdown of the dedusting system during the weekend.

The nominal power of the two exhaust fans is lower and the actual power level is coupled to the electric energy input into the EAF. The fans are controlled stepwise so that full power is only available during melting and refining. While the furnace is not consuming electrical power, fan power is reduced to partial load, which is 80% and 50% of the full load for the primary and secondary exhaust fan (see Fig. 10). After the final tapping at the electric arc furnace, the blowers are shut down for the weekend.

The mean power factors, which indicate the ratio of active to apparent power, are 0.92 for the dedusting fans and 0.74 for the exhaust fans.

3.1.3.2. *Modeling.* Following the findings described in the previous chapter, the electric load for the dedusting fans was set to nominal power during production and to zero during downtimes of the steel mill. During the casting procedure, the power of one of the dedusting fans is ramped up.

The active power demand of the exhaust fans was coupled to the load profile of the electric arc furnace according to the operational behavior described in chapter 3.1.3.1. During power-on times, the fan is operated at full power, during power-off times, fan power is reduced to partial load. After final tapping, the fan power is set to zero.

Once the active power has been determined, the model calculates reactive and apparent power using the power factors ( $\cos(\phi)$ ) given in 3.1.3.1 and equations (10) and (11), where  $P$  represents the active,  $Q$  the reactive and  $S$  the apparent power.

$$Q = P \cdot \tan(\arccos(\cos(\phi))) \tag{10}$$

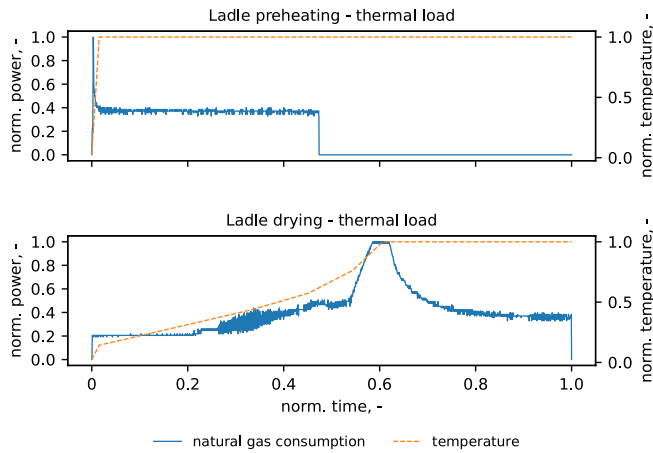


Fig. 12. Measured load profiles and corresponding temperature curves for ladle drying (top) and preheating (bottom).

$$S = \frac{P}{\cos(\phi)} \quad (11)$$

3.1.3.3. *Result.* Fig. 11 shows the aggregated electric load profile of the ID fans, including the EAF-fans as well as the dedusting fans relative to nominal apparent power.

### 3.1.4. Ladle heaters

Ladle heaters serve two purposes: on one hand, they preheat ladles to their operating temperature (ladle preheating). On the other hand, repaired or relined ladles have to be heat-treated for more than 30 h before returning to service (ladle drying).

3.1.4.1. *Data analysis.* The natural gas consumption profiles of three different ladle heater types installed in the steel mill were measured during the ladle preheating and ladle drying processes. Fig. 12 describes natural gas consumption in relation to nominal burner load and corresponding normalized temperature curves. The final temperature for both heat-treatment and preheating exceeds 1000 °C.

An energy balance establishes the relationship between thermal load ( $P_{thermal}$ ), which equals the energy input in form of natural gas and waste heat flow ( $P_{waste\ heat}$ ).

$$\dot{Q}_{use}(t) = P_{thermal}(t) - P_{waste\ heat}(t) \quad (12)$$

$\dot{Q}_{use}$  represents the useful heat and was determined from equation (12). Thermal load and waste heat flow are defined according to equations (13) and (14), where  $\dot{m}_{natural\ gas}$  is the fuel mass flow and  $LHV_{natural\ gas}$  its lower heating value.

$$P_{thermal}(t) = \dot{m}_{natural\ gas} \cdot LHV_{natural\ gas} \quad (13)$$

Waste heat flow rate is the product of mass flow rate ( $\dot{m}_{fluegas}$ ), average specific heat capacity ( $c_{pm, fluegas}(T)$ ) and temperature difference of the flue gas.

$$P_{waste\ heat}(t) = \dot{m}_{fluegas} \cdot \bar{c}_{p, fluegas}(T) \cdot (T_{fluegas} - T_{reference}) \quad (14)$$

3.1.4.2. *Modeling.* For the calculation of the overall load profile for ladle heating, it is necessary to investigate the temporally resolved positions and states of the individual steel ladles. An operational model was developed in order to simulate the states of the ladles in the steel mill.

According to our operational model, there are five possible states for a steel mill ladle: preheating, operation, maintenance, drying, and waiting. Preheating means that a ladle heater preheats the ladle to operating temperature prior to its next operation cycle. Between the

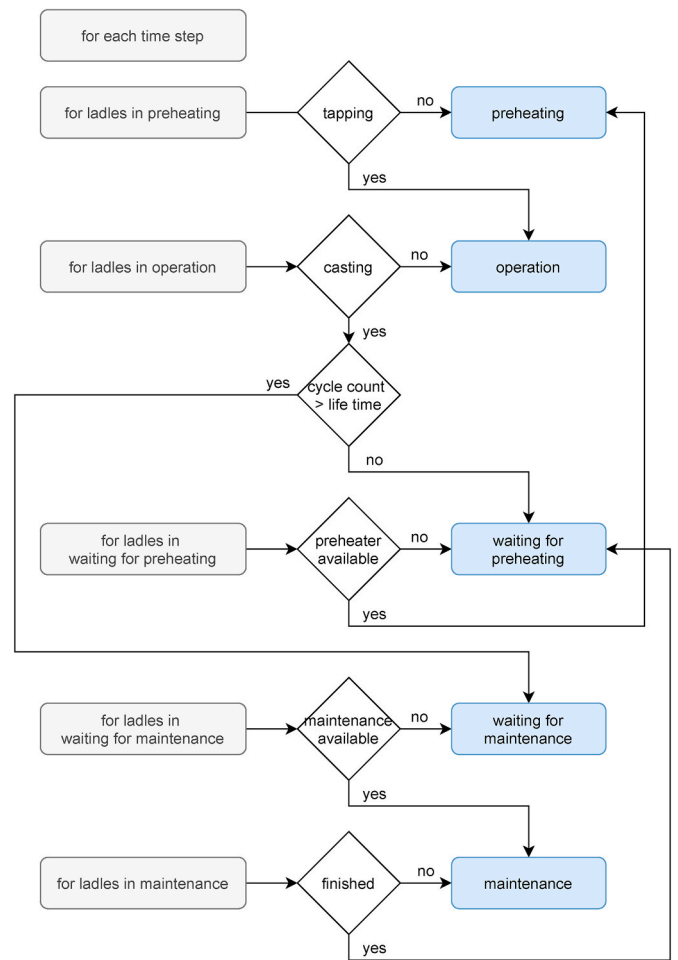


Fig. 13. Flow chart of the operational model.

tapping process at the electric arc furnace and ingot casting, the ladle is in operation.

After a certain number of operation cycles, the ladle is relined, dried, and reheated to operating temperature. Maintenance and drying are thus the third and fourth ladle state. If there is no ladle heater or maintenance position available at the current time step, the state of the ladle is defined as waiting.

In the subsequent time steps, the waiting queue is serviced according to the "first in first out" principle. During a production week, the number of simultaneously operated ladle heaters is limited to seven, while during weekends, a maximum of four heaters is in use.

During the initialization of the model, a list of steelmaking ladles is created. The number of ladles is defined as an input parameter. According to chapter 2.1.1, the random function of Python assigns states, cycle counts, and refractory lining types to these ladles as properties. The model distinguishes between linings for standard batches and batches that require a VOD treatment.

Fig. 13 shows a flow chart of the operational model, which provides the basis for the ladle heater sub-model. Thermal energy demand or waste heat generation occurs in two situations: when a ladle is dried after repair or relining, or when it is preheated for its utilization. The individual thermal load and waste heat profiles for preheating and drying are aggregated to obtain the overall thermal load profile as well as the waste heat profile.

3.1.4.3. *Result.* Fig. 14 shows the aggregated thermal load and the waste heat profile of the ladle heaters for a simulation time of 12 hours relative to the maximum thermal power. It consists of several temporally

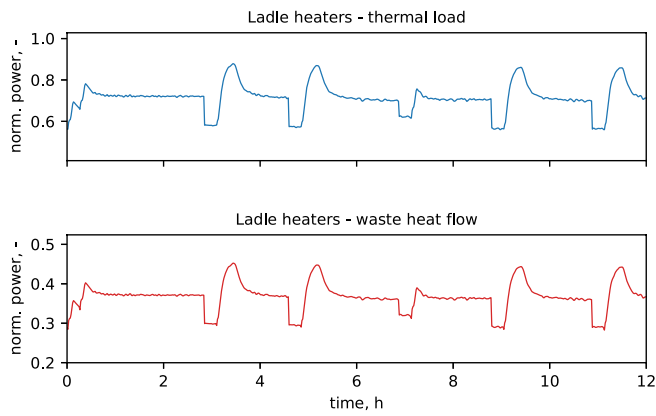


Fig. 14. Thermal load profile for ladle heating.

staggered drying and preheating processes. The aggregated profile has its minimum during the weekends when the number of preheated ladles decreases.

### 3.1.5. Vacuum treatments

Vacuum treatments (VOD – Vacuum oxygen decarburization and VD – Vacuum degassing) are performed to further increase steel purity. In order to remove gasses from the liquid steel, steam ejector pumps generate a vacuum. The process steam is provided by two industrial steam boilers.

**3.1.5.1. Data analysis.** Due to different processing sequences and steam mass flows, we distinguish between VD- and VOD-processes for the modeling of time-resolved steam consumption. Vacuum oxygen decarburization is situated downstream the EAF-process and subsequent slag removal, while vacuum degassing represents the last purification step before casting. Further differences concern process duration and oxygen consumption associated with the VOD-process.

Data collected with regard to vacuum treatments include the steam parameters, mass flows, and processing times. Moreover, the oxygen demand for the oxygen decarburization process was determined. In our study, all batches are subjected to degassing, while vacuum decarburization is only necessary for 7% of all produced batches.

In order to obtain the useful energy demand, we estimated the enthalpy flow rate ( $\dot{H}_{steam}$ ) from the mass flow rate ( $\dot{m}_{steam}$ ) and the steam parameters temperature and pressure (equation (15)).

$$\dot{H}_{steam} = \dot{m}_{steam} \cdot h_{steam} \quad (15)$$

Specific enthalpy ( $h_{steam}$ ) was obtained from a steam table according to IAPWS 1995 (Wagner and Pruf, 2002).

Division of the enthalpy flow by the boiler efficiency results in the thermal load required for process steam generation (see equation (16)). In their paper, Saidur et al. (2010) quote energy efficiencies in the range of 62–94% for industrial steam boilers. In our model, we assume a constant steam boiler efficiency of 94%.

$$P_{thermal} = \frac{\dot{H}_{steam}}{\eta_{steam\ generator}} \quad (16)$$

**3.1.5.2. Modeling.** In order to calculate the load profiles for vacuum oxygen decarburization (VOD) and vacuum degassing (VD), the first task addresses modeling the process steam demand. Vacuum treatment schedules depend on the operating periods of the electric arc furnace and the ladle furnace (see chapter 2.2).

Analogous to the ladle furnace, the model generates the steam load profile by iterating through the list of VD and VOD units and retrieves their current steam demand. In a further step, it converts the aggregated steam demand into natural gas consumption based on the steam boiler

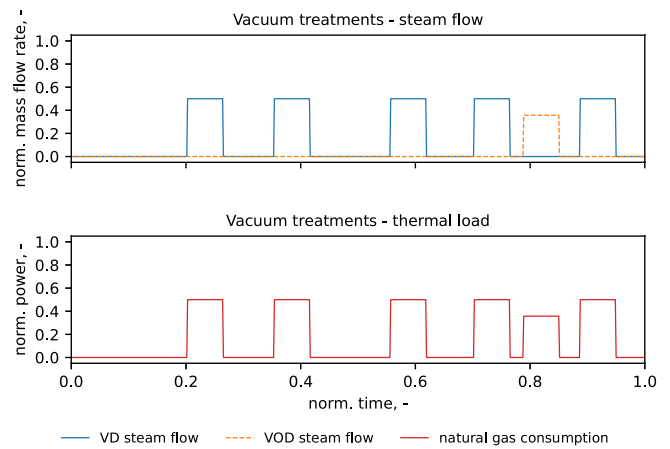


Fig. 15. Consumption load profiles of the vacuum treatments.

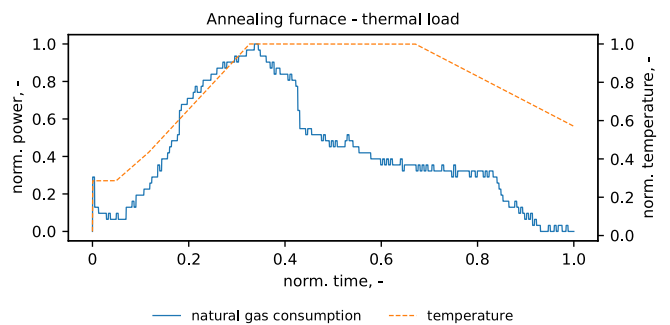


Fig. 16. Measured load and temperature profile of the annealing program.

efficiency.

**3.1.5.3. Result.** Fig. 15 represents the enthalpy flow of steam caused by the vacuum treatments and the corresponding thermal load of the process steam boiler.

### 3.1.6. Annealing furnaces

When the steel has the required composition and temperature, it is cast into ingots. Annealing refers to a heat treatment process that adjusts the required physical properties of the steel ingots for subsequent processing.

**3.1.6.1. Data analysis.** In order to adjust the required steel properties, ingots are heat-treated in annealing furnaces. The heating and cooling process follows a predefined temperature profile. There are various annealing programs, but we focused on the modeling of only one representative program. In the steel mill that is described in this study, 85% of the ingots are subjected to annealing.

The annealing furnaces under examination are natural gas/cold air-fired bogie hearth furnaces. For several weeks, the natural gas consumption of one of the annealing furnaces was measured. Fig. 16 describes the load profile and the normalized profile of the interior furnace temperature for an annealing batch of 105 t.

**3.1.6.2. Modeling.** The results of the data analysis suggest the following modeling approach: After a randomly drawn cooling time, the cast steel batches that are designated for heat treatment are added to a pool. When the mass of batches in the pool exceeds the furnace capacity, the ingots are assigned to an available furnace and the annealing process is started.

For each time step, the model iterates through the furnace list, retrieves the heating power, and adds it to the total load profile. After completion of the treatment, the batch is added to a list of finished

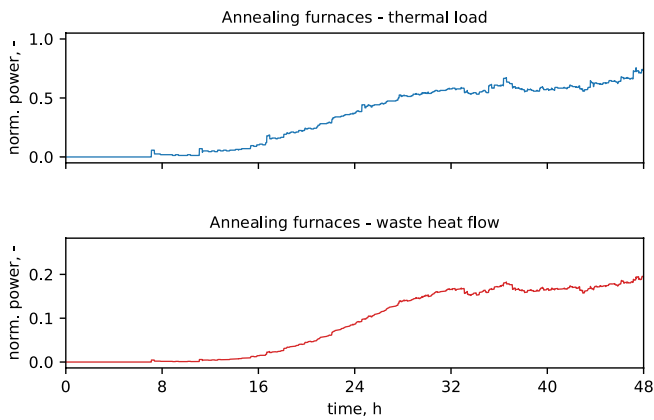


Fig. 17. Aggregated load profile of the annealing furnaces.

batches and the furnace is available for the next heat.

Analogous to the ladle heaters, the waste heat flow is calculated by applying equations (12), (13), and (14).

3.1.6.3. Results. The result is a combined load and waste heat flow profile for the heat treatment furnaces in the steel mill (Fig. 17).

3.1.7. Other consumers

The processes described in the previous chapters consume 88% of the annual energy consumption. The remaining energy demand of 12% relates to several smaller consumers. In view of the substantial measurement and modeling effort involved, we will not provide a detailed characterization of these loads and consider them baseload.

This load is implemented into the energy system model of the electric steel plant as a separate sub-model. The electric baseload accounts for 4% of the maximum electric load, while the thermal baseload amounts to 6% of the maximum thermal load.

3.2. Energy system model

The simulation of the overall steel mill described in chapter 3.1

provides not only representative time-resolved load profiles of the individual consumers and the resulting aggregate load profile of the steel mill but also energy-related analyses and performance indicators. These results are presented in the following chapter.

3.2.1. Energy consumption

An important objective of the steel mill model is to produce representative, time-resolved load profiles. Fig. 18 shows the aggregated, temporally resolved demand of final energy carriers electric energy and natural gas.

Fig. 19 gives an overview of the major steel mill components and their share of final energy consumption. With a proportion of 36% of the total energy consumption or more than 50% of the electric energy demand, the EAF is the biggest energy consumer in the steel mill. The electric energy for ladle furnaces and dedusting amounts to 13% and 4% respectively. Despite being an auxiliary process, drying and preheating the steelmaking ladles accounts for 17% of the total energy demand.

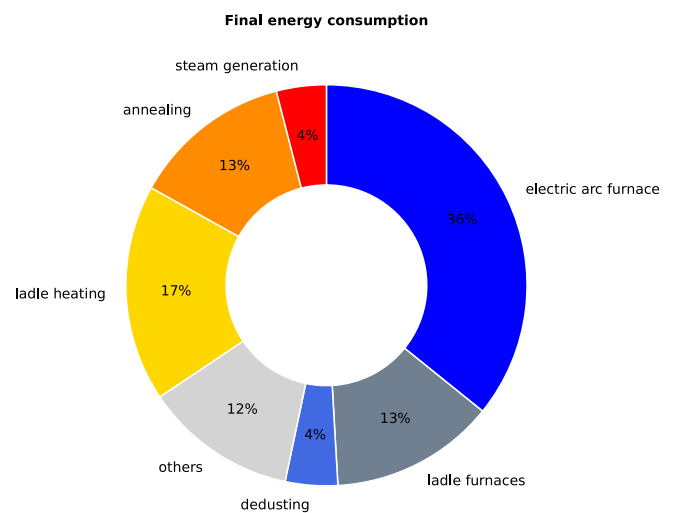


Fig. 19. Distribution of final energy demand.

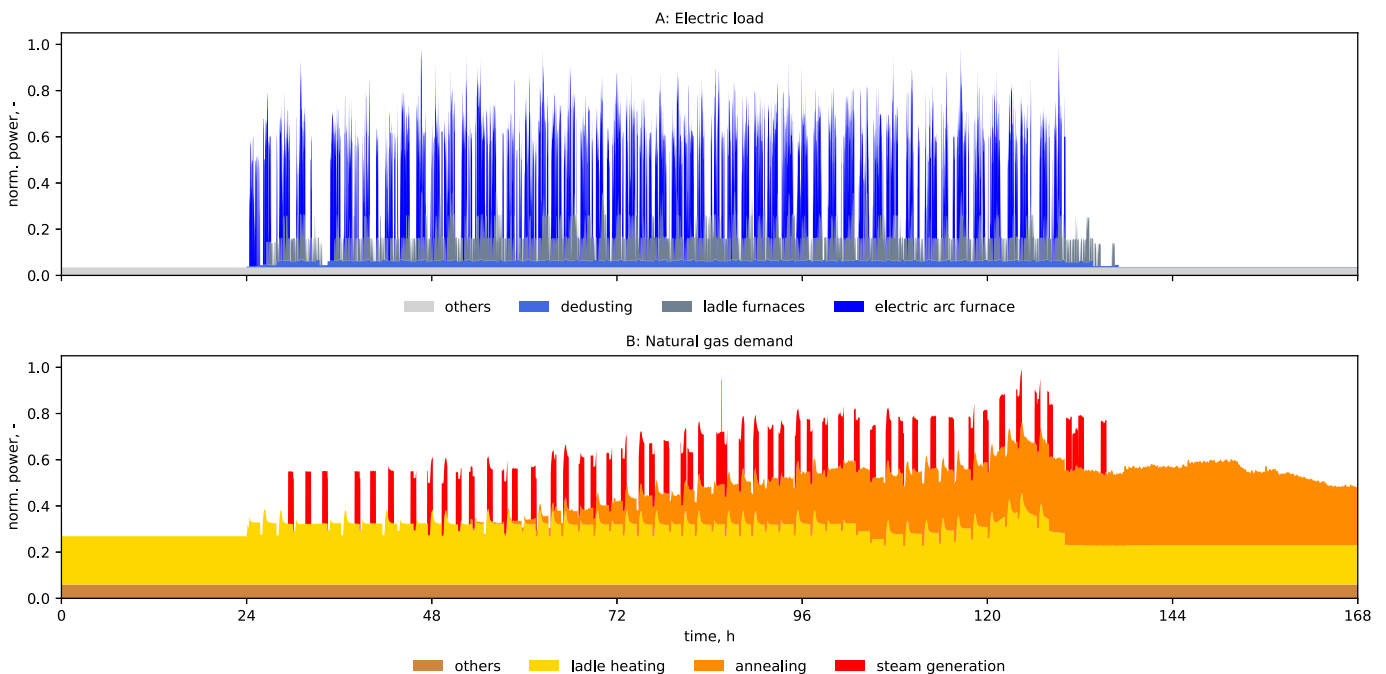


Fig. 18. Overall load profiles for final energy carriers.



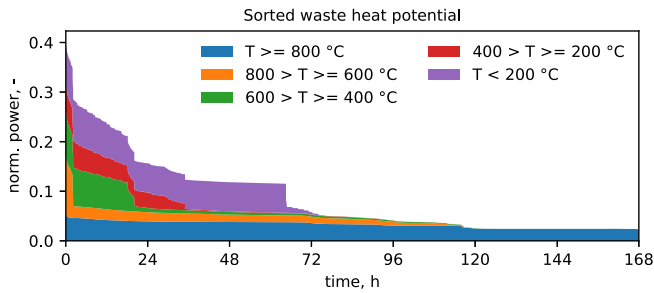


Fig. 20. Sorted duration line of the theoretical waste heat potential.

Natural gas consumption amounts to 13% for annealing and 4% for steam generation. 12% of the overall final energy consumption of the steel mill is required for the remaining processes.

A benchmark value is used to evaluate the energy consumption and thus the energy efficiency of the production process. The ratio of simulated specific energy consumption ( $SEC_{simulation}$ ) and the reference value ( $SEC_{reference}$ ) of 1183 kWh/t of product (Arens et al., 2017) results in an energy efficiency index (EEI) of 0.8 (see equation (17)). Consequently, the benchmark suggests an energy saving potential of 20%.

$$EEI = \frac{SEC_{simulation}}{SEC_{reference}} \quad (17)$$

### 3.2.2. Waste heat recovery potential

A major goal of the model is the identification of optimization potentials. In their framework for industrial waste heat utilization, Woolley et al. (2018) define three quantitative descriptors for waste heat streams: temperature, available energy, and temporal availability. Furthermore, they consider qualitative properties such as spatial availability, carrier medium, and contamination.

The present model analyses the waste heat potential based on the mentioned quantitative properties. Hence, waste heat flow rates are resolved not only temporally but also with respect to temperature. Sorted duration lines are well suited for a concise presentation of time-resolved waste heat.

Fig. 20 shows the theoretical waste heat power relative to the

maximum power input containing natural gas flow and electric load. The observation period covers one week. The amount of waste heat fluctuates considerably due to the batch operation of the production processes and is available at different temperature levels.

The theoretical heat recovery potential of the system amounts to 28% of the overall final energy consumption. In the diagram, the waste heat potential is categorized in four levels: under 400 °C, from 400 to 600 °C, from 600 to 800 °C and higher than 800 °C. Because of its intermittent operation, the electric arc furnace generates a highly fluctuating waste heat flow with respect to temperature and time. The high availability of waste heat at relatively high temperature levels above 800 °C results from the continuous operation of the ladle heaters. Medium-temperature waste heat is generated at the annealing furnaces and the electric arc furnace. The cooling system of the EAF discharges heat at a comparatively low temperature level.

## 4. Discussion

Representative synthetic load profiles are expected to be consistent with the observed profiles. Therefore, we want to compare the measured and simulated time series using duration lines. Fig. 21 illustrates the ordered duration lines of the electrical power of the electric arc furnace, the ladle furnace, the ID fans, and the natural gas consumption of one of the ladle heaters for one week.

A statistical analysis of the measured and simulated load profiles yields the following normalized values for the arithmetic mean and standard deviation (Table 2).

Not only the time-resolved but also the cumulative energy

Table 2  
Results of the statistical analysis of the load.

Load profile	Normalized arithmetic mean		Normalized standard deviation	
	Measurement	Simulation	Measurement	Simulation
Electric arc furnace	0.41	0.38	0.33	0.34
Ladle furnace	0.21	0.18	0.38	0.37
EAF primary fan	0.89	0.92	0.10	0.10
Dedusting fan	0.66	0.65	0.21	0.20

## Load profile analysis

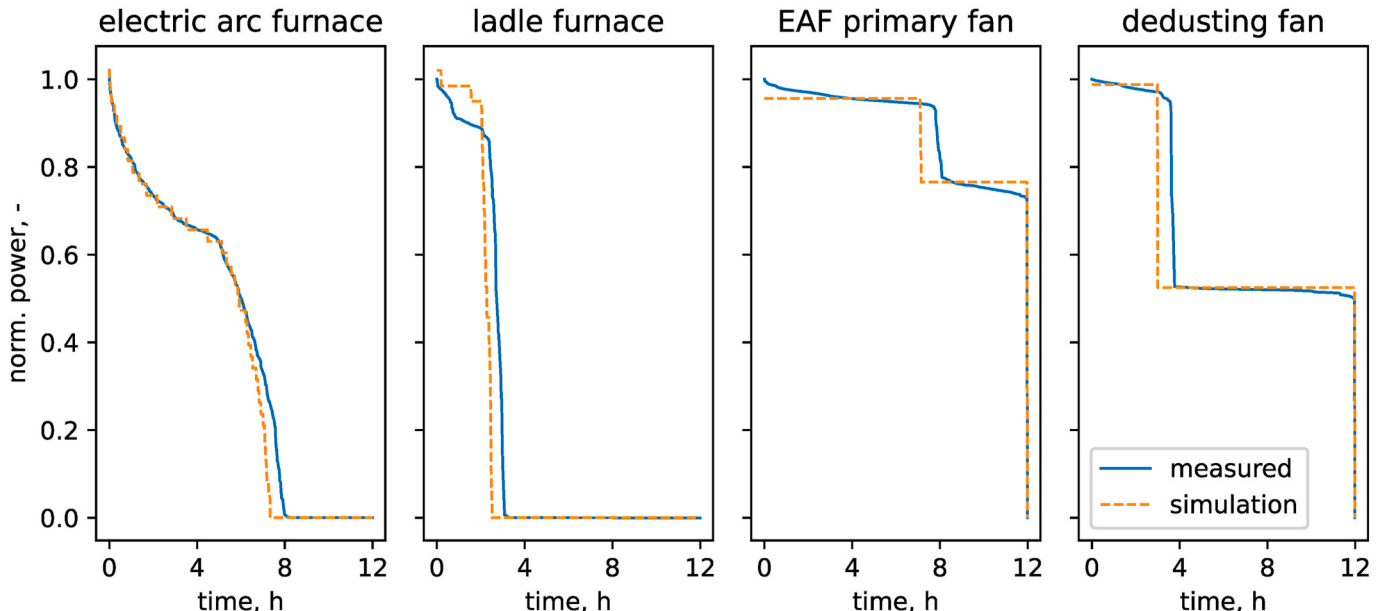


Fig. 21. Statistical analysis of electric load and waste heat profiles.

**Table 3**

Deviation of simulated from actual specific energy consumption.

Component	MAPE
Electric arc furnace	3.9%
Ladle furnaces	8.0%
Annealing furnaces	2.2%
Dedusting fans	6.5%
Ladle heaters	1.0%
Steam boiler	2.9%
Others	10.9%
Overall energy system	1.6%

consumption gives an indication of the validity of the model. The comparison of the simulated and the actual consumption of the individual components is of particular interest. For the considered steel mill, the actual values of the year 2018 are compared to the results of a simulation over four production weeks.

Since the produced volume of steel per week varies slightly, the specific energy consumption related to the produced steel mass in kWh/t is more revealing. In the following Table 3, the deviations of the simulated from the actual specific energy consumptions over five simulation runs are given as mean absolute percentage errors (MAPE). The value for the overall energy system represents the error for the specific energy consumption of the entire production process.

## 5. Conclusion

The model presented in this article is capable of generating synthetic consumption load profiles of individual components as well as of the most relevant overall electric steel mill configurations based on a limited amount of input data. The representative load profiles and performance indicators provide a basis for the evaluation of energy efficiency measures and the integration of renewable energy sources.

The model includes the electric arc furnace, ladle furnaces, vacuum treatment units, and auxiliary aggregates such as ladle heaters and ID fans. It covers electricity, natural gas, and waste heat flows and calculates energy-related KPIs such as total and specific energy consumption, waste heat recovery potential as well as the energy efficiency index of the steel mill.

The indicators we apply to evaluate the industrial energy system are above all the specific energy consumption and the associated specific carbon dioxide emissions of the individual process steps and of the entire production route. The comparison with a benchmark value provides a quantitative statement on potential for energy efficiency improvement.

Due to the design of the model, it is possible to scale the production volume and to add further process steps, and integrate novel technologies into the production process without any restructuring. Therefore, the model is qualified to simulate changes in the production process and assess its impact on the overall system.

The analysis of the synthetic load profiles and the specific energy consumption values generated by the model shows that the simulation results are representative for the investigated steel mill. Quantitative evaluation of the simulated specific energy consumption results in a mean absolute percentage error of less than 2%.

## Declaration of competing interest

The authors declare that they have no known competing financial interests or personal relationships that could have appeared to influence the work reported in this paper.

## Acknowledgments

This work was carried out as part of the OxySteel project. OxySteel is a subproject of NEFI – New Energy for Industry, a flagship region funded

by the Climate and Energy Funds Austria.

## Appendix A. Supplementary data

Supplementary data to this article can be found online at <https://doi.org/10.1016/j.clet.2021.100223>.

## References

- Arens, M., Worrell, E., Eichhammer, W., Hasanbeigi, A., Zhang, Q., 2017. Pathways to a low-carbon iron and steel industry in the medium-term – the case of Germany. *J. Clean. Prod.* 163, 84–98. <https://doi.org/10.1016/j.jclepro.2015.12.097>.
- Atabay, D., 2017. An open-source model for optimal design and operation of industrial energy systems. *Energy* 121, 803–821. <https://doi.org/10.1016/j.energy.2017.01.030>.
- Bhaskar, A., Assadi, M., Nikpey Somehsaraei, H., 2020. Decarbonization of the iron and steel industry with direct reduction of iron ore with green hydrogen. *Energies* 13, 758. <https://doi.org/10.3390/en13030758>.
- Blesl, M., Kessler, A., 2013. *Energieeffizienz in der Industrie*. Springer-Vieweg, Berlin, p. 350.
- Çamdali, Ü., Tunç, M., 2002. Modelling of electric energy consumption in the AC electric arc furnace. *Int. J. Energy Res.* 26, 935–947. <https://doi.org/10.1002/er.829>.
- Çamdali, Ü., Tunç, M., 2003. Energy and exergy analysis of a ladle furnace. *Canadian Metallurgical Quarterly* 42, 439–446. <https://doi.org/10.1179/cm.2003.42.4.439>.
- Carlsson, L.S., Samuelsson, P.B., Jönsson, P.G., 2019. Predicting the electrical energy consumption of electric arc furnaces using statistical modeling. *Metals* 9, 959. <https://doi.org/10.3390/met9090959>.
- Carpinone, A., Giorgio, M., Langella, R., Testa, A., 2015. Markov chain modeling for very-short-term wind power forecasting. *Elec. Power Syst. Res.* 122, 152–158. <https://doi.org/10.1016/j.epsr.2014.12.025>.
- Chen, C., Liu, Y., Kumar, M., Qin, J., 2018. Energy consumption modelling using deep learning technique — a case study of EAF. *Procedia CIRP* 72, 1063–1068. <https://doi.org/10.1016/j.procir.2018.03.095>.
- Collin, A.J., Tzarakakis, G., Kiprakis, A.E., McLaughlin, S., 2014. Development of low-voltage load models for the residential load sector. *IEEE Trans. Power Syst.* 29, 2180–2188. <https://doi.org/10.1109/TPWRS.2014.2301949>.
- Eurofer, 2020. *European Steel in Figures. Covering 2011 - 2019*, Brussels. (Accessed 12 May 2021).
- Eurostat, 2018. *Energy Balance Sheets: 2016 Data*. Luxembourg.
- Fleiter, T., Worrell, E., Eichhammer, W., 2011. Barriers to energy efficiency in industrial bottom-up energy demand models—a review. *Renew. Sustain. Energy Rev.* 15, 3099–3111. <https://doi.org/10.1016/j.rser.2011.03.025>.
- Gajdzik, B., Sroka, W., 2021. Resource intensity vs. Investment in production installations—the case of the steel industry in Poland. *Energies* 14, 443. <https://doi.org/10.3390/en14020443>.
- Gajic, D., Savic-Gajic, I., Savic, I., Georgieva, O., Di Gennaro, S., 2016. Modelling of electrical energy consumption in an electric arc furnace using artificial neural networks. *Energy* 108, 132–139. <https://doi.org/10.1016/j.energy.2015.07.068>.
- Guido van Rossum, 2020. *The python library reference. Release 3, 7, 8rc1*.
- Hay, T., Visuri, V.-V., Aula, M., Echterhof, T., 2021. A review of mathematical process models for the electric arc furnace process. *steel research int* 92, 2000395. <https://doi.org/10.1002/srin.202000395>.
- Johansson, M.T., 2015. Improved energy efficiency within the Swedish steel industry—the importance of energy management and networking. *Energy Efficiency* 8, 713–744. <https://doi.org/10.1007/s12053-014-9317-z>.
- Keplinger, T., Haider, M., Steinparzer, T., Patrejkó, A., Trunner, P., Haselgrübler, M., 2018. Dynamic simulation of an electric arc furnace waste heat recovery system for steam production. *Appl. Therm. Eng.* 135, 188–196. <https://doi.org/10.1016/j.applthermaleng.2018.02.060>.
- Kirschen, M., Badr, K., Pfeifer, H., 2011. Influence of direct reduced iron on the energy balance of the electric arc furnace in steel industry. *Energy* 36, 6146–6155. <https://doi.org/10.1016/j.energy.2011.07.050>.
- Kirschen, M., Risonarta, V., Pfeifer, H., 2009. Energy efficiency and the influence of gas burners to the energy related carbon dioxide emissions of electric arc furnaces in steel industry. *Energy* 34, 1065–1072. <https://doi.org/10.1016/j.energy.2009.04.015>.
- Kovačić, M., Stopar, K., Vertnik, R., Šarler, B., 2019. Comprehensive electric arc furnace electric energy consumption modeling: a pilot study. *Energies* 12, 2142. <https://doi.org/10.3390/en12112142>.
- Ma, J., Fouladirad, M., Grall, A., 2018. Flexible wind speed generation model: Markov chain with an embedded diffusion process. *Energy* 164, 316–328. <https://doi.org/10.1016/j.energy.2018.08.212>.
- Matino, I., Alcamisi, E., Colla, V., Baragiola, S., Moni, P., 2016. Process modelling and simulation of electric arc furnace steelmaking to allow prognostic evaluations of process environmental and energy impacts. *Matériaux Tech.* 104 <https://doi.org/10.1051/mattech/2016004>.
- Matino, I., Colla, V., Baragiola, S., 2017. Electric energy consumption and environmental impact in unconventional EAF steelmaking scenarios. *Energy Procedia* 105, 3636–3641. <https://doi.org/10.1016/j.egypro.2017.03.839>.
- McKenna, E., Krawczynski, M., Thomson, M., 2015. Four-state domestic building occupancy model for energy demand simulations. *Energy Build.* 96, 30–39. <https://doi.org/10.1016/j.enbuild.2015.03.013>.

- Nijhuis, M., Gibescu, M., Cobben, J.F.G., 2016. Bottom-up Markov chain Monte Carlo approach for scenario based residential load modelling with publicly available data. *Energy Build.* 112, 121–129. <https://doi.org/10.1016/j.enbuild.2015.12.004>.
- Pardo, N., Moya, J.A., Vatopoulos, K., 2015. Prospective Scenarios on Energy Efficiency and CO<sub>2</sub> Emissions in the EU Iron & Steel Industry: Re-edition. Publications Office, Luxembourg, p. 48.
- Pardo Martínez, C.I., 2015. Estimating and analyzing energy efficiency in German and Colombian manufacturing industries using DEA and data panel analysis. Part I: energy-intensive sectors. *Energy Sources B Energy Econ. Plann.* 10, 322–331. <https://doi.org/10.1080/15567249.2010.540625>.
- Remus, R., 2013. Best Available Techniques (BAT) Reference Document for Iron and Steel Production: Industrial Emissions Directive 2010/75/EU (Integrated Pollution Prevention and Control). Publications Office of the European Union, Luxembourg, p. 17.
- Saidur, R., Ahamed, J.U., Masjuki, H.H., 2010. Energy, exergy and economic analysis of industrial boilers. *Energy Pol.* 38, 2188–2197. <https://doi.org/10.1016/j.enpol.2009.11.087>.
- Sasiain, A., Rechberger, K., Spanlang, A., Kofler, I., Wolfmeir, H., Harris, C., Bürgler, T., 2020. Green hydrogen as decarbonization element for the steel industry. *Berg Huettenmaenn Monatsh* 165, 232–236. <https://doi.org/10.1007/s00501-020-00968-1>.
- Shamshad, A., Bawadi, M., Wanhussin, W., Majid, T., Sanusi, S., 2005. First and second order Markov chain models for synthetic generation of wind speed time series. *Energy* 30, 693–708. <https://doi.org/10.1016/j.energy.2004.05.026>.
- Steinparzer, T., Haider, M., Zauner, F., Enickl, G., Michele-Naussed, M., Horn, A.C., 2014. electric arc furnace off-gas heat recovery and experience with a testing plant. *steel research int* 85, 519–526. <https://doi.org/10.1002/srin.201300228>.
- Stewart, W., 2009. *Probability, Markov Chains, Queues, and Simulation: the Mathematical Basis of Performance Modeling*. Princeton University Press, Oxford, p. 758. Princeton (N.J.).
- United Nations Framework Convention of Climate Change (Ed.), 2015. *United Nations Framework Convention on Climate Change: Adoption of the Paris Agreement*. United Nations, Paris.
- Wagner, W., Pruß, A., 2002. The IAPWS formulation 1995 for the thermodynamic properties of ordinary water substance for general and scientific use. *J. Phys. Chem. Ref. Data* 31, 387–535. <https://doi.org/10.1063/1.1461829>.
- Wang, Y., Infield, D., 2018. Markov chain Monte Carlo simulation of electric vehicle use for network integration studies. *Int. J. Electr. Power Energy Syst.* 99, 85–94. <https://doi.org/10.1016/j.ijepes.2018.01.008>.
- Wolniak, R., Saniuk, S., Grabowska, S., Gajdzik, B., 2020. Identification of energy efficiency trends in the context of the development of industry 4.0 using the polish steel sector as an example. *Energies* 13, 2867. <https://doi.org/10.3390/en13112867>.
- Woolley, E., Luo, Y., Simeone, A., 2018. Industrial waste heat recovery: a systematic approach. *Sustainable Energy Technologies and Assessments* 29, 50–59. <https://doi.org/10.1016/j.seta.2018.07.001>.
- Zarandi, M.F., Ahmadpour, P., 2009. Fuzzy agent-based expert system for steel making process. *Expert Syst. Appl.* 36, 9539–9547. <https://doi.org/10.1016/j.eswa.2008.10.084>.
- Ziębik, A., Gładysz, P., 2018. Systems approach to energy and exergy analyses. *Energy* 165, 396–407. <https://doi.org/10.1016/j.energy.2018.08.214>.



# Techno-economic case study on Oxyfuel technology implementation in EAF steel mills – Concepts for waste heat recovery and carbon dioxide utilization

Johannes Dock<sup>\*</sup>, Thomas Kienberger

Chair of Energy Network Technology, Montanuniversitaet Leoben, Franz-Josef-Straße 18, 8700, Leoben, Austria

## ABSTRACT

Compared to integrated steel production via blast furnace and basic oxygen furnace, the electric arc furnace route saves energy and carbon dioxide emissions. While the major part of the energy is provided in the form of electric power, a substantial fraction of thermal energy is supplied by the combustion of direct fuels.

In the present study, we describe available options for increasing the energy efficiency and cut down on carbon dioxide emissions in electric arc furnace steel mills. Based on these technologies, we develop possible process layouts including the transition to Oxyfuel ladle preheating, on-site utilization of the CO<sub>2</sub>-rich product gas and off-gas heat as well as the recovery of waste heat from the hot gas duct of the electric arc furnace for process steam production.

With the aid of an energy system model, a case study is carried out to determine the potential for fuel savings as well as carbon dioxide and waste heat utilization. In a technical assessment, we investigate the relationship between the storage capacities, the carbon dioxide and waste heat utilization ratios as well as the fuel and CO<sub>2</sub> emission savings. The subsequent economic analysis yields the optimum system layout under different framework conditions.

## 1. Introduction

The European steel industry had an annual final energy consumption of 309 TWh in 2018 (Eurostat (European Commission), 2020) and is today responsible for 4–7% of the anthropogenic carbon dioxide emissions in the EU (Pardo et al., 2015). Steel production using an electric arc furnace (EAF) enables both the recycling of steel scrap and the processing of directly reduced iron. Compared to the integrated steel production (blast furnace (BF)/basic oxygen furnace (BOF)) the secondary process route (scrap/EAF) reduces the CO<sub>2</sub>-emissions by 63–73%. The application of the direct reduction route (DRI/EAF) results in a decrease of the CO<sub>2</sub>-intensity of 41–68%, whereas direct reduction using hydrogen (HDRI/EAF) is expected to cut emissions by up to 99% (Toktarova et al., 2020).

However, the actual carbon dioxide emissions associated with the production of one ton of steel via the EAF route depend primarily on two main factors: The specific CO<sub>2</sub> emissions of the power grid (Sasiain et al., 2020) and the energy efficiency of the applied production processes (Quader et al., 2015). Within EAF steel production, particularly the generation of process heat from fossil fuels offers significant potential for reducing the energy consumption and thus the carbon dioxide emissions of the process.

### 1.1. Production process and energy consumption

Steel production via the EAF route consists of the main process steps melting, refining, steel and slag tapping, decarburization, ladle treatments and casting (Remus, 2013).

The EAF melts the introduced steel scrap through the input of electrical and chemical energy. In the refining process, the liquid steel is decarburized by oxygen blowing. Then, the steel is tapped into a preheated steelmaking ladle and unwanted scrap components are removed with the slag. For high-alloy steels, vacuum oxygen decarburization (VOD) is applied. Ladle metallurgy involves the process steps of desulphurization, alloying, homogenization and degassing and aims to adjust the required chemical composition (Remus, 2013). In the investigated mill, the steel is cast into ingots, which are heat-treated to enhance the material properties of the steel product. An alternative option is continuous casting to produce steel billets.

Most of these process steps require the input of substantial amounts of energy. According to literature, the mean specific energy consumption for EAF steelmaking amounts to 1178 kWh per ton of product (Arens et al., 2017). Depending on scrap and product quality as well as applied production processes, the production of one ton of steel requires about 5–65 m<sup>3</sup> of oxygen and 3–28 kg of coal (Remus, 2013).

A recent study conducted by the authors at an Austrian steel mill

<sup>\*</sup> Corresponding author.

E-mail addresses: [johannes.dock@unileoben.ac.at](mailto:johannes.dock@unileoben.ac.at) (J. Dock), [evt@unileoben.ac.at](mailto:evt@unileoben.ac.at) (T. Kienberger).

showed that about 58% of the final energy consumption is supplied in the form of electric energy, while the remaining 42% are provided by direct fuels (Fig. 1) (Dock et al., 2021). Electrical energy is mainly used to power the electric arc furnace, the ladle furnaces and the dedusting systems. Preheating of the steel mill ladles using natural gas burners is the second most energy-intensive process step. Further major natural gas consumers are the heat treatment furnaces and the process steam generation for vacuum treatments. The remaining minor electricity and natural gas consumers are subsumed under the term *others*. Pulverized coal is only used in the EAF and acts as a slag foaming agent.

Concerning the accounting of carbon dioxide emissions, the Greenhouse Gas Protocol (World Resources Institute and World Business Council for Sustainable Development, 2021) specifies three scopes. Scope 1 or direct emissions refers to greenhouse gases that are emitted by company-operated facilities. By multiplying the consumption values of the steel mill under consideration for natural gas and pulverized coal by their respective specific CO<sub>2</sub> emissions, we obtain scope 1 carbon dioxide emissions of the production process. Fig. 1 shows that ladle heaters are not only the biggest consumers of natural gas, but also the most important emitters of CO<sub>2</sub>.

1.2. Decarbonization and energy efficiency measures

In EAF steel production, a major part of the process heat is generated by burning fossil direct fuels. Combustion processes, such as ladle preheating, are the main source of scope 1 CO<sub>2</sub> emissions in the considered steel mill (see 1.1). Moreover, individual processes, i.e. scrap melting in the EAF generate waste heat, which is currently not exploited, neither in the steel mill nor for external use.

In this article, we therefore focus on the implementation of the following energy efficiency measures, which we consider technically feasible under the given conditions:

- Oxyfuel-combustion,
- CO<sub>2</sub>-capture and utilization (CCU),
- Waste heat recovery.

Properly deployed, these technologies have the potential to reduce not only energy consumption, but also production costs and carbon dioxide emissions.

1.2.1. Oxyfuel combustion

Compared to combustion with air, the Oxyfuel technology, the combustion of natural gas with pure oxygen, represents an effective measure to reduce fuel consumption and CO<sub>2</sub> emissions. First, the absence of nitrogen in the combustion process increases the thermal efficiency, because a higher portion of energy is transferred to the heating good instead of heating the nitrogen in the combustion air (Baukal and Baukal, 2013a). Second, the high concentration of the radiant gases CO<sub>2</sub> and H<sub>2</sub>O in the Oxyfuel flue gas results in increased thermal radiation, thus improving the heat transfer (Baukal and Baukal, 2013b). Consequently, less fuel is required for a given heating load. In addition, scope 1 carbon dioxide emissions decrease proportionally to the decreasing fuel consumption (Baukal, 2013). However, the overall emission reduction depends on the applied oxygen production technology and the specific carbon dioxide emissions in the electricity mix.

Within the studies conducted by Stanger et al. (2015), Wall et al. (2013) as well as Gibbins and Chalmers (2008), Oxyfuel combustion is considered as key technology for capturing CO<sub>2</sub> from fossil-fired power plants. Burning coal or natural gas with pure oxygen produces a flue gas mainly consisting of water vapor and carbon dioxide, which is separated by dehydration (H<sub>2</sub>O condensation) and purification. Stanger et al. (2015) give an overview over the technical advances in Oxyfuel technology for coal- and gas-fired power plants. Apart from demonstration on industrial level, the authors identify research needs in terms of higher integration, alternative oxygen sources, innovative combustion

Energy consumption and carbon dioxide emissions

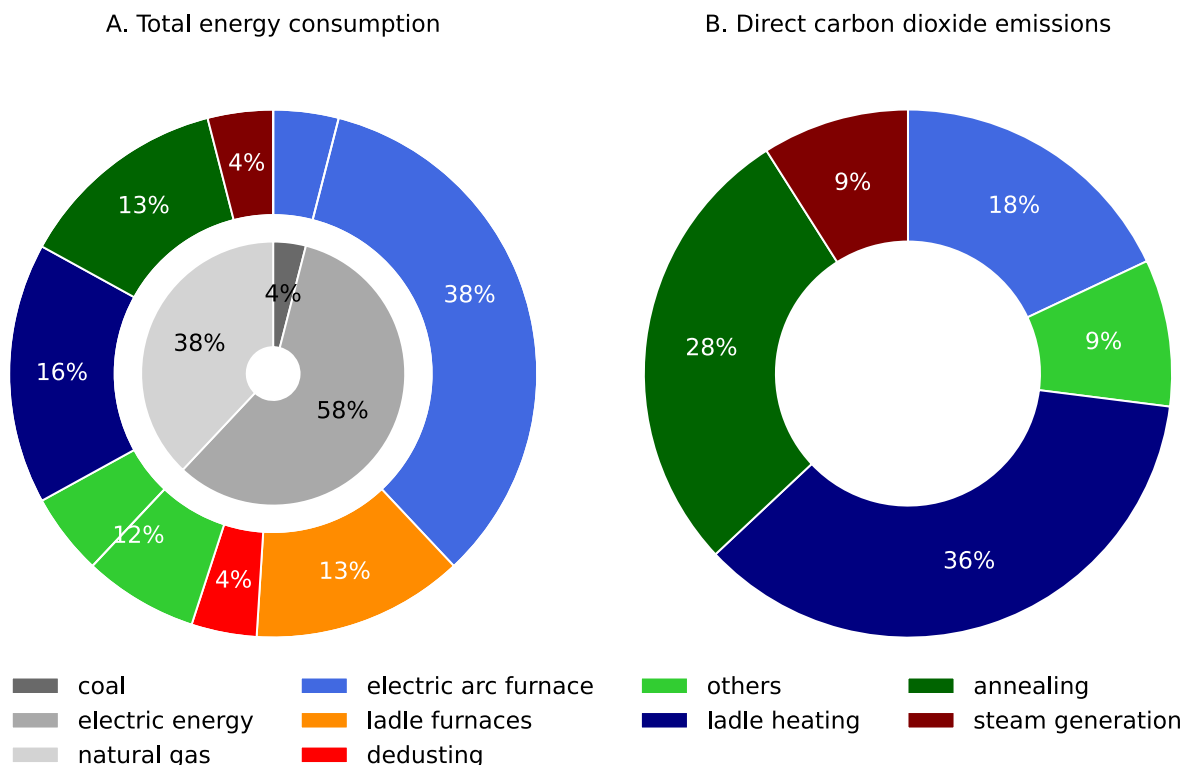


Fig. 1. Final energy consumption (A) and scope 1 carbon dioxide emissions (B) of main consumers in the electric steel mill.

processes as well as improvement of energy efficiency and reduction of installation costs and risks.

Regarding the steel industry, von Scheele (von Scheele and Palm, 2010) identifies the hot stoves of the blast furnace, the electric arc furnace, the reheating furnace, vessel preheating and strip processing as feasible areas of application for Oxyfuel combustion. According to his work, positive effects range from increased throughput capacities, fuel savings and increased material yield to reduced CO<sub>2</sub> and NO<sub>x</sub> emissions. For vessel preheating, the fuel consumption and the associated CO<sub>2</sub> emissions may be reduced by around 50% (von Scheele and Palm, 2010).

In steel mills, ladle heaters are deployed to dry and preheat the steelmaking lades prior to their utilization. As indicated in Fig. 1, they represent major consumers of natural gas and thus contribute significantly to the overall CO<sub>2</sub>-emissions. According to Docquier et al. (2013), the conversion of a natural gas/air-fired ladle heating station to Oxyfuel-combustion results not only in fuel savings but also shorter heating times and higher achievable end temperatures. Due to higher preheating temperatures, the required tapping temperature decreases resulting in enhanced productivity, furnace life and energy efficiency. As state-of-the-art technology, Oxyfuel ladle heating is available from major equipment manufacturers such as Messer (Messer Americas, 2019) or Linde (Linde AG, 2017). Ladle heating with OXIPYR burners is expected to bring fuel savings of up to 55%, uniform heating, shorter heating cycles and lower NO<sub>x</sub> emissions (Messer Americas, 2019). In order to lower the flame temperature and ensure uniform heating, the flame is diluted by flue gas, referred to as flameless Oxyfuel combustion. Similarly, substantially shorter heating times, fuel savings, extended refractory lifetime, and lower feasible EAF tapping temperatures have been reported for OXYGON burners compared to the combustion with air (Linde AG, 2017).

### 1.2.2. Carbon dioxide utilization in steelmaking

Combusting natural gas with pure oxygen generates a flue gas with a high concentration of carbon dioxide and water (see 2.2.1). Condensation of the water vapor produces a CO<sub>2</sub>-rich gas that can be recovered for other processes. The separation and utilization of carbon dioxide from the flue gas transforms climate-relevant emissions into a valuable resource. In the iron and steel industry, carbon dioxide utilization has positive effects on metallurgical processes and has the potential to reduce overall carbon dioxide emissions (Wei et al., 2018). The review article by Dong and Wang (2019) discusses promising fields of application for carbon dioxide including top- and bottom-blowing in the BOF and the argon oxygen decarburization (AOD) converter, the ladle furnace and the EAF, injection into the blast furnace as well as CO<sub>2</sub> circulation in combustion processes. In light of the extensive research on the positive effects of carbon dioxide deployment in ferrous metallurgy processes, the authors project an overall CO<sub>2</sub> utilization potential of more than 100 kg/t of steel.

In their article, Zhu et al. (2020) review the beneficial effect of carbon dioxide on the EAF and BOF process and propose a route for the utilization of steel mill-generated CO<sub>2</sub>. Laboratory (Li et al., 2017) and industrial scale (Lv et al., 2012) experiments were conducted to investigate the utilization of carbon dioxide in the basic oxygen furnace. BOF steelmaking involves dust production in the range of 13–32 kg/t of steel that consists mainly of iron and its oxides (Ray et al., 1997). Li et al. (2017) prove that the dust is generated as a consequence of the entrainment of carbon monoxide bubbles and evaporation of elements. The introduction of CO<sub>2</sub> as an oxidant allows decarburization while controlling the temperature of the steel bath. Using a mixture of oxygen and carbon dioxide as top-blowing gas in the converter and substitution of nitrogen and argon by carbon dioxide for bottom blowing reduces dust generation and iron loss, promotes the removal of nitrogen and phosphorous from liquid steel and saves oxygen. Zhu et al. (2020) assume a consumption of 10–13 kg CO<sub>2</sub>/t of steel for top-blowing at 10 %<sub>vol</sub> CO<sub>2</sub> and full substitution of oxygen by CO<sub>2</sub> for bottom blowing in

BOF steelmaking.

Similarly, the electric arc furnace is a promising field of application for recovered carbon dioxide. According to Wei et al. (2018), current research focuses on the utilization of CO<sub>2</sub> for mixed blowing, submerged injection as well as bottom blowing in the EAF and the ladle furnace. In mixed blowing, instead of pure oxygen, an O<sub>2</sub>/CO<sub>2</sub> mixture is injected into the EAF through a blowing lance. Compared to blowing with pure oxygen during the refining phase, endothermic reactions of CO<sub>2</sub> with elements in the liquid steel bath reduce the generation of hot spots and therefore limit the evaporation of iron and other elements (Wei et al., 2018). In their research article, Wang et al. (2016) establish an energy and material balance to investigate the impact of carbon dioxide injection into the EAF. The authors find that oxygen blowing with an increasing proportion of CO<sub>2</sub> increases the electric energy consumption. However, they argue that this effect is outweighed by enhanced decarburization and chromium retention. According to the literature, reasonable mixing ratios of carbon dioxide and oxygen range from 5 %<sub>vol</sub> (Wei et al., 2018) to 50 %<sub>vol</sub> (Wang et al., 2016) of CO<sub>2</sub>.

Certain steel production steps such as vacuum treatments (VD and VOD) cause alkaline wastewater. Before discharge into a sewage system, the pH-value of the wastewater must be reduced to a neutral level. Water neutralization using carbon dioxide is an environmentally friendly alternative to conventional treatments based on mineral acids. Compared to acids, the advantages include safer handling, precise pH control, prevention of excessive acidification as well as low investment and operational costs (Messer North America Inc, 2021).

Furthermore, CO<sub>2</sub> serves as a neutralizer for the water in the cooling circuits of the steel mill. Since natural water tends to lime scale build-up, the cooling water needs to be treated to avoid plugging in the cooling equipment. Water hardness results from dissolved minerals such as calcium and magnesium. Carbonation of the cooling water with CO<sub>2</sub> represents an inexpensive and safe method to remove calcium and magnesium ions and reduce the pH-value to a neutral level (Ahn et al., 2018). Hart et al. (2011) describe the successful application of carbon dioxide to prevent scale build-up in a heat exchanger of a pulp mill.

### 1.2.3. Waste heat utilization in steel mills

In their review on energy use and energy efficient technologies, He and Wang (2017) describe the significant potential of waste heat utilization in the steel industry. For EAF steelmaking, they recommend the recovery of EAF waste heat for electricity production and cite energy savings of 130 kWh/t of steel. The electric arc furnace is not only the largest energy consumer, but also a considerable source of waste heat. In an electric arc furnace, the heat dissipated by the cooling system and the sensible heat of the off-gas account for 20–30% of the overall energy input (Steinparzer et al., 2014). For a 120 t furnace, the energy of the off-gas amounts to 226 kWh/t of steel at temperatures up to 1200 °C (Steinparzer et al., 2014), however typical outlet temperatures for EAF cooling systems lie around 50 °C (Gharib Mombeni et al., 2016).

Yang et al. (2018) elaborate on the possibilities to recycle the sensible heat of the EAF exhaust gas. Scrap preheating, steam production and eventual electricity generation via a steam turbine are presented as relatively mature technologies. However, fluctuations in EAF off-gas temperature and mass flow as well as its high dust content pose a challenge for steam and electricity generation. The authors consider the ejector pumps of the vacuum degassing system as potential consumers of the generated steam. Ramirez et al. (2017) present a waste heat recovery plant for the electric arc furnace of a special steel mill using Organic Rankine Cycle (ORC) technology. The furnace exhaust gas is used to produce saturated steam in a heat recovery unit. This steam supplies heat to an ORC process and a district heating network. In order to compensate for the discontinuous heat availability, the EAF and the consumers are decoupled by a steam accumulator. Due to the implementation of the plant, the authors estimate annual savings of 7990 t of CO<sub>2</sub> and 40 360 MWh of electricity and heat. Keplinger et al. (2018) present a dynamic simulation model for the recovery of EAF waste heat

for steam production. The hot gas duct, which has the function to cool the off-gas for its subsequent treatment serves as a heat source. Due to the batch operation of the electric arc furnace, a thermocline storage is integrated into the system to compensate temperature and mass flow fluctuations. Depending on the load situation of the EAF, the waste heat steam generator is supplied with hot water from the storage tank or directly from the hot gas duct. Therefore, the cooling system is operated at an elevated water outlet temperature of 200 °C. Simulation results indicate that the presented concept is a feasible option for EAF waste heat recovery and that the thermocline storage system is capable of decoupling the time-variable heat supply and demand (Keplinger et al., 2018).

Waste heat recovery from ladle preheating has not yet been investigated to the same extent as for the electric arc furnace. Moch et al. (2008) conduct their research on ways to decrease energy consumption and emissions of ladle heaters. As part of the project, two ladle-heating stations are equipped with a rotating regenerator and a recuperator, respectively, for air preheating. Long-term observations indicate that these measures reduce natural gas consumption by 20–35%.

The authors are not aware of any studies on the utilization of waste heat from ladle heaters apart from air preheating.

### 1.3. Research need and structure of the work

The articles cited in chapter 1.2 demonstrate that the proposed technologies are suitable for reducing energy consumption and CO<sub>2</sub> emissions in EAF steelmaking. Scientific studies and implementation reports are available for Oxyfuel combustion, carbon dioxide utilization for steelmaking and water treatment processes as well as waste heat recovery in the steel industry.

However, to the authors' knowledge, at present there is no publication addressing the holistic implementation of the technologies mentioned in section 1.2 in an existing steel mill. We aim to understand, how energy saving and emission abatement technologies need to be integrated into the production processes to achieve the optimal effect for the overall energy system of an EAF steel mill. For this purpose, this study investigates the process integration of selected energy efficiency and CO<sub>2</sub> emission reduction technologies into an existing EAF steel mill.

The implementation of Oxyfuel and CCU technologies as well as waste heat recovery systems into batch production processes with highly fluctuating loads requires a time-resolved analysis. By using a steady-state simulation approach with a temporal resolution of 1 min, we integrate different feasible options into an energy system model of the steel mill and evaluate their impact in terms of overall energy efficiency, economic viability and carbon dioxide emissions.

Due to their significant natural gas consumption (see 1.1) and high operating temperatures, we focus on the conversion of air-fired ladle heaters to Oxyfuel-combustion. Within the present work, we investigate possibilities of waste heat recovery from the ladle heaters and the EAF as well as carbon dioxide separation and utilization in the steel production process. The objective is to develop viable concepts for reducing fuel consumption and CO<sub>2</sub> emissions in order to enable a low-CO<sub>2</sub> production process. Therefore, we compare the results of three integration scenarios on a technical and economic level.

In our study, we proceed as follows: First, we develop scenarios for the implementation of the presented technologies (2.1). Second, we introduce our model, which includes the energy system of the steel mill, Oxyfuel combustion, carbon capture equipment and storages (2.2). Additionally, we explain the cost-model used for our economic assessment. Based on each technology's potential, we carry out a technical (3.1) and an economic (3.2) assessment. A sensitivity analysis highlights the conditions under which investments in the examined technologies are economically viable (4). Finally, chapter 5 summarizes the key outcomes and gives a conclusion.

## 2. Methods

### 2.1. Scenario development

Due to long heating times and high operating temperatures, ladle heaters account for a major share on the final energy consumption of the steel mill. As stated in chapter 1.3, Oxyfuel-combustion offers the potential to significantly reduce the natural gas consumption of the ladle heaters. Therefore, this study focuses on the installation of Oxyfuel burners for preheating the steel mill ladles. As part of the burner conversion, the horizontal ladle heaters will be replaced by the vertical alternative. Measurements indicate that vertical heaters consume about one third less fuel due to improved flue gas routing in the ladle. The conversion from natural gas/air to natural gas/oxygen burners is associated with a considerable additional oxygen consumption (see Table 3). However, due to the metallurgical processes the steel mill already requires large volumes of oxygen, which are supplied by deliveries and storage tanks. Hence, we assume that the additional consumption through Oxyfuel combustion is met by the existing supply system.

Additionally, we intend to exploit the CO<sub>2</sub>-rich off gas generated by the Oxyfuel combustion process through the integration of a carbon dioxide separation and utilization system. Due to different types of deployed ladles and varying conditions of the upper ladle rims, a gap remains between the lid and the ladle, thus preventing airtight heating operation. However, the burner is operated at an overpressure, which will reduce the false air volumes to a minimum. In view of the proposed CO<sub>2</sub> application options, we assume that the gas treatment system generates a product gas of adequate purity, even in the case of minor false air inflow. For our case study, we consider the following in-plant carbon dioxide sinks: the neutralization of alkaline wastewater and cooling water in the cooling systems as well as the mixed injection of oxygen and carbon dioxide during refining in the electric arc furnace. Since both the wastewater neutralization and the cooling water conditioning using purchased CO<sub>2</sub> are already implemented in the considered mill, the existing infrastructure can be deployed in this case. In the latter case, the CO<sub>2</sub> is fed into the oxygen line ahead of the oxygen manipulator and then blown into the EAF through the injection lance. Prior to injection into the supply network and subsequent utilization, it is required to cool the exhaust gas, separate the water and compress the product gas to the operating pressure of the CO<sub>2</sub> supply network. To balance the fluctuating CO<sub>2</sub>-demand, especially for mixed blowing in the EAF, we implement a buffer tank into the CO<sub>2</sub> supply system (see Fig. 2).

Condensation of the exhaust gas not only increases the carbon dioxide concentration in the product gas but also allows the recovery of waste heat. The ladle heaters are equipped with an exhaust gas condenser with an integrated heat exchanger that transfers the exhaust gas heat to the cooling water. Subsequently, the hot cooling water is used in the process steam boiler for feed water preheating. In an extended scenario, we evaluate the waste heat recovery from the hot gas duct at the electric arc furnace. The water-cooled duct dissipates the major part of the heat in the EAF exhaust gas. The recovered heat from the hot gas duct will be used for steam generation in the steel mill. For this scenario, the installation of a thermal energy storage is inevitable to balance the waste heat generation and steam demand (see Fig. 2).

As described in chapter 1.2.3, within the scope of their study, Keplinger et al. (2018) present a suitable system for the recovery of waste heat from the EAF hot gas duct for steam production. Increasing the water temperature and pressure in the cooling system requires the replacement of the duct. The additional equipment consists of a pressurized hot water storage, a kettle evaporator, pumps and a pressurization system.

In order to assess the technical and economic feasibility and the necessary framework conditions, we will investigate three scenarios:

- Scenario D: The starting point is a demonstration scenario in which half of the ladle heaters are converted to Oxyfuel technology. The

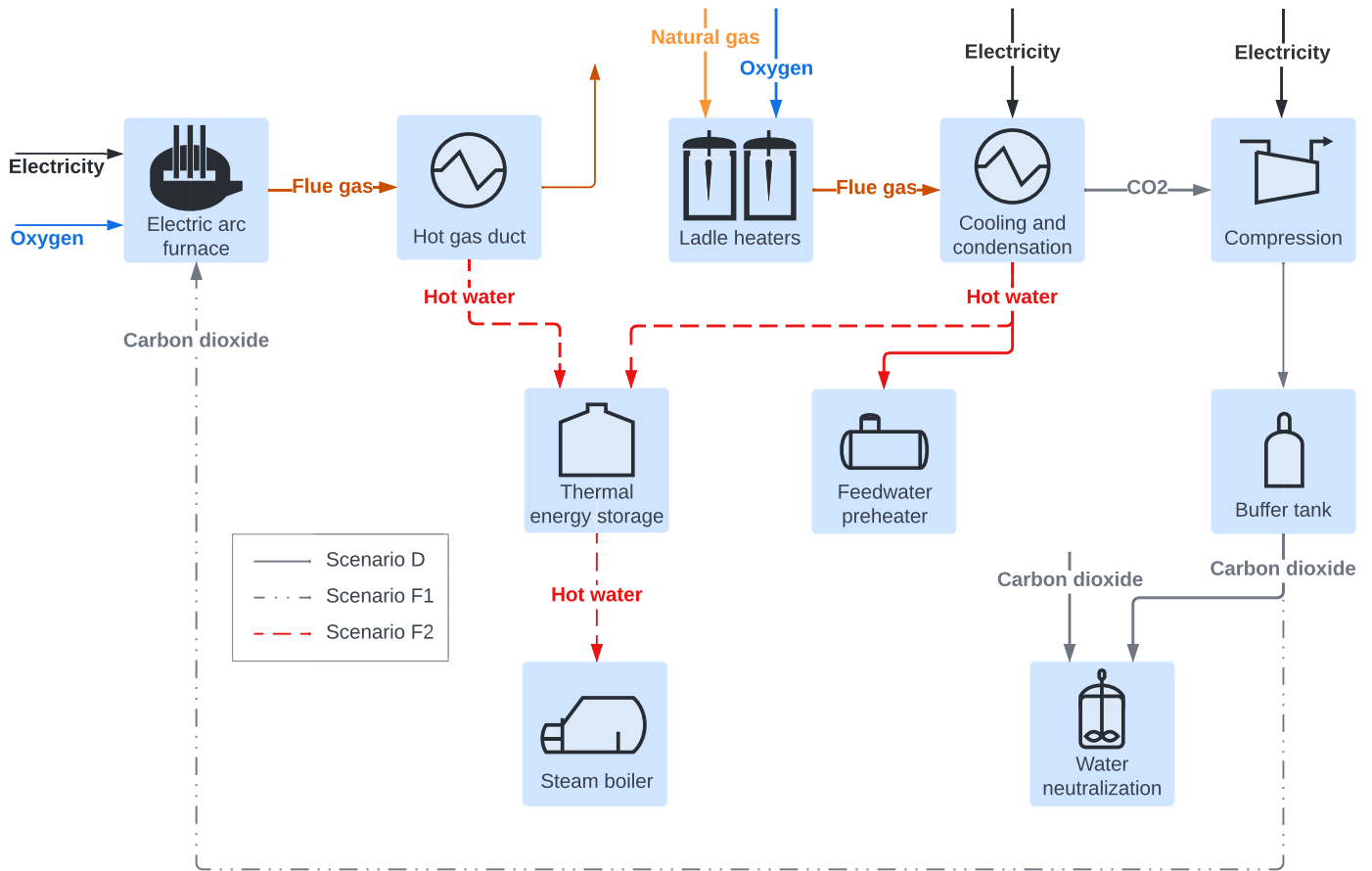


Fig. 2. Process layouts for the simulation scenarios.

generated carbon dioxide and waste heat are recovered and utilized plant-internally for water treatment. For this simulation, we stipulate that Oxyfuel ladle heaters, if available, are deployed preferentially.

- Scenario F1: In a first future scenario, we analyze the complete conversion of all ladle heaters to Oxyfuel technology. Analogous to the demonstration scenario, we aim to recover both CO<sub>2</sub> and waste heat. In addition to water treatment, the produced carbon dioxide is deployed for mixed blowing in the electric arc furnace.
- Scenario F2: The second future scenario, based on F1, deals with the additional recovery of waste heat from the EAF hot gas duct for steam generation.

Fig. 2 provides an overview over the considered waste heat and carbon dioxide flows. The simulation results are evaluated based on a reference scenario (R), which reflects the status quo in the steel mill. Table 1 summarizes the main features of the investigated scenarios.

2.2. Energy system model

In order to evaluate the implementation of efficiency measures in an existing EAF steel mill, we deploy the energy system model presented in a study by Dock et al., 2021. This preceding work describes the

Table 1  
Considered implementation scenarios.

	R	D	F1	F2
Number of Oxyfuel ladle heaters	0	2/4	4/4	4/4
Water neutralization	-	X	X	X
O <sub>2</sub> /CO <sub>2</sub> mixed blowing	-	-	X	X
Feed water preheating (LH)	-	X	X	X
Steam generation (LH + EAF)	-	-	-	X

development of a model that generates time-resolved, synthetic load and waste heat profiles of sub-processes as well as the overall steel mill. The model covers the electric arc furnace, ladle furnaces, vacuum treatments, ladle heaters, annealing furnaces, as well as the dedusting and steam generation system. Due to its modular design, the model allows sub-processes to be added or system configurations to be modified. Therefore, we are able to represent different process designs and operational strategies within the scope of the present case study.

As part of this work, the energy system model is extended to include Oxyfuel combustion, production and demand profiles for carbon dioxide, buffer storages for carbon dioxide and thermal energy as well as a tool for basic economic analysis.

2.2.1. Ladle heating

In order to implement an Oxyfuel ladle heater in our energy system model, it is necessary to determine the actual flow rates of natural gas, oxygen, waste heat and carbon dioxide for every time step. We estimate these values by applying a simple process model based on the time-resolved thermal load and waste heat profiles of the mentioned steel mill model.

Our starting point is the following heat balance, where  $\dot{Q}_{thermal}$  is the thermal power input,  $\dot{Q}_{useful}$  the thermal power that is used to heat the ladle, and  $\dot{Q}_{waste\ heat}$  the thermal power of the exhaust gas.

$$\dot{Q}_{thermal}(t) = \dot{Q}_{useful}(t) + \dot{Q}_{waste\ heat}(t) \tag{1}$$

Provided the fuel and the oxidant are supplied at reference temperature, the thermal power and the waste heat flow are defined by equations (2) and (3).  $\dot{m}_{ng}$  and  $\dot{m}_{fg}$  are the mass flow rates of natural gas and flue gas,  $NCV$  is the net calorific value of natural gas.  $c_{p, fg}$ ,  $T_{fg}$  and  $T_{amb}$  are the mean specific isobaric heat capacity in  $\frac{kJ}{kg \cdot K}$  as well as



temperatures of the flue gas and the ambient air in  $K$ .

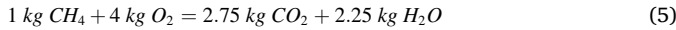
$$\dot{Q}_{thermal}(t) = \dot{m}_{ng}(t) \cdot NCV \quad (2)$$

$$\dot{Q}_{waste\ heat}(t) = \dot{m}_{fg}(t) \cdot c_{p, fg} \cdot (T_{fg} - T_{amb})(t) \quad (3)$$

The mass flow of the flue gas can be determined by establishing the mass balance (4).

$$\dot{m}_{fg} = \dot{m}_{ng} + \dot{m}_{ox} \quad (4)$$

Derived from the reaction equation for the combustion of 1 kg of methane (5), which is the main combustible constituent of natural gas, the oxidant mass flow is calculated according to equation (6), where  $x_{CH_4, ng}$  and  $x_{O_2, ox}$  are the mass fractions of methane in the fuel and oxygen in the oxidant, and  $\lambda$  is the air-fuel equivalence ratio.



$$\dot{m}_{ox} = \dot{m}_{ng} \cdot \lambda \cdot \frac{4 \cdot x_{CH_4, ng}}{x_{O_2, ox}} \quad (6)$$

Since the ladle heating program follows a specified temperature profile and we know the associated time-resolved thermal power input (equation (2)) and waste heat power (equation (3)), we are able to determine the time-resolved useful power (equation (1)). By applying the above equations and substituting air by pure oxygen as oxidant, we obtain the new mass flow rates for natural gas, oxygen, and exhaust gas resulting from the transition to Oxyfuel combustion. Combustion of natural gas with oxygen decreases the exhaust gas mass flow compared to combusting with air, while the useful heat profile determined by the heating program remains unchanged. This leads to a significant reduction in exhaust gas losses, thermal power input and thus natural gas consumption.

We obtain the mass flow rate of carbon dioxide ( $\dot{m}_{CO_2}$ ) in the exhaust gas from the mass balance for carbon dioxide (7), where  $x_{CO_2, ox}$  and  $x_{CO_2, ng}$  are the mass fractions of carbon dioxide in the oxidation medium and in the fuel.  $x_{CH_4, ng} \cdot 2.75$  represents the generation of  $CO_2$  due to methane combustion.

$$\dot{m}_{CO_2} = x_{CO_2, ox} \cdot \dot{m}_{ox} + (x_{CO_2, ng} + 2.75 \cdot x_{CH_4, ng}) \cdot \dot{m}_{ng} \quad (7)$$

Fig. 3 shows the normalized natural gas and resulting carbon dioxide flow for ladle preheating with a conventional and an Oxyfuel burner.

### 2.2.2. Carbon dioxide utilization

In our study, the captured  $CO_2$ -rich product gas recovered from the Oxyfuel combustion is provided for neutralization in the wastewater treatment plant, injection into the cooling system and refining in the electric arc furnace. In order to determine the required capacity of the buffer tank, we consider the following carbon dioxide demand profile (Fig. 4).

The carbon dioxide demand profile was created by adapting the energy system model of the EAF steel mill (Dock et al., 2021). Its modular structure allows for implementation of the  $CO_2$  consumers.  $CO_2$  consumption occurs mainly during two process steps that are defined in the steel mill model: oxygen blowing at the EAF and wastewater discharge from the vacuum treatments. The required amount of  $CO_2$  for wastewater neutralization is known from measurements, while that for EAF-injection is derived from the oxygen demand of the EAF using a fixed mixing ratio of 25 %<sub>vol</sub> carbon dioxide.

An analysis of the third  $CO_2$  sink, the injection into the cooling water of the EAF and various other installations, indicated a frequent consumption of small quantities for periods of less than a minute. Therefore, the total consumption was averaged over the operating hours of the individual installations and implemented into the model as a continuous demand.

### 2.2.3. EAF hot gas duct

Compared to the energy system model the authors presented in (Dock et al., 2021), the model of the EAF cooling system is modified to increase the accuracy of the simulation results. Instead of averaging the cooling power during an entire EAF production cycle, in the improved model used in this work, we represent the individual process phases in the load profile. Based on time-resolved measurements of the cooling power, we determined mean power levels for the process phases *melting* and *refining* as well as the time intervals between, referred to here as *power off*. The process phases as well as the associated cooling power levels are displayed in Fig. 5 B.

In order to model the fluctuating waste heat profile, the ordered duration line of the measured waste heat profile is divided into intervals, which are assigned to certain process phases based on the previously defined mean power levels. During the simulation, for every time step, a power value is drawn randomly from the distribution of power levels in the respective process phase. This results in the synthetic profile of the cooling power for one week presented in Fig. 5 A relative to the nominal EAF transformer power in kVA. A comparison of the sorted duration lines over 12 h of operation indicates the good agreement between the measured and simulated waste heat profile (see Fig. 5 B).

### 2.2.4. Carbon dioxide and thermal energy storage

Chapter 1.2 describes the need for storage systems to balance the temporal variability of both the demand and generation of waste heat and carbon dioxide. Both storages are implemented into the energy system model using the following properties: storage capacity, state of charge (SOC) at simulation start as well as associated sinks and sources.

According to equations (8) and (9), the SOC of the carbon dioxide ( $m$ ) and the thermal energy storage ( $Q$ ) are determined for every simulation time step ( $\Delta t$ ).  $\dot{m}_{inflow}$  and  $\dot{m}_{outflow}$  refer to mass flow rates during feed-in and discharge of the carbon dioxide storage, while  $\dot{Q}_{inflow}$  and  $\dot{Q}_{outflow}$

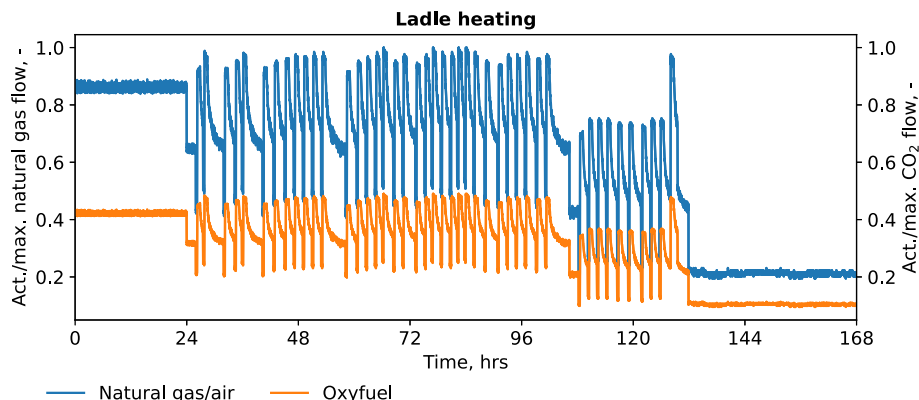


Fig. 3. Normalized natural gas and carbon dioxide flow profile of Oxyfuel and conventional combustion for ladle preheating.

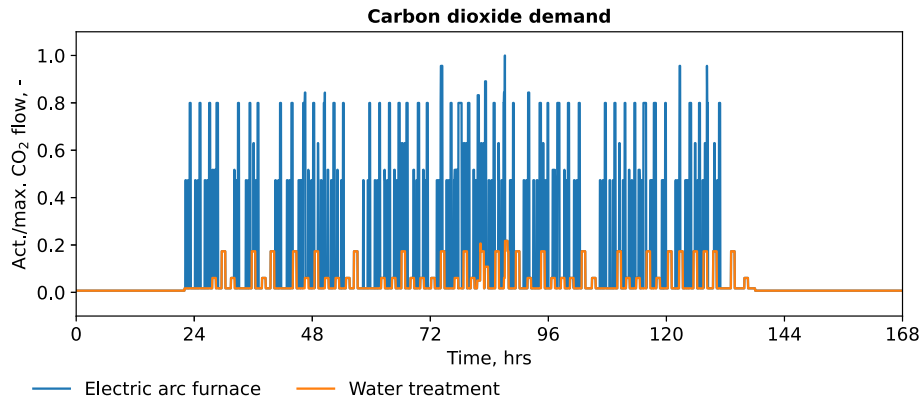


Fig. 4. Normalized carbon dioxide consumption profile.

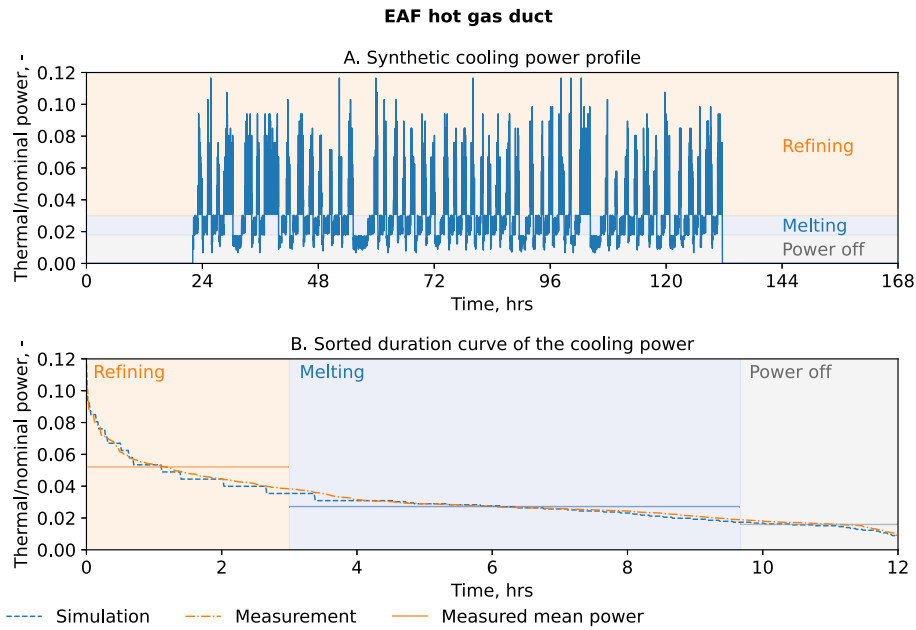


Fig. 5. Ordered duration line of the hot gas duct cooling power.

represent the heat flow rate for loading and discharging the thermal energy storage (TES).  $\dot{Q}_{loss}$  denotes the loss rates of the TES (see equation (11)).

$$m(t) = m(t-1) + (\dot{m}_{inflow}(t) - \dot{m}_{outflow}(t)) \cdot \Delta t \quad (8)$$

$$Q(t) = Q(t-1) + (\dot{Q}_{inflow}(t) - \dot{Q}_{outflow}(t) - \dot{Q}_{loss}(t)) \cdot \Delta t \quad (9)$$

Assuming operation at constant pressure, the amount of stored energy ( $Q_{max}$ ) in a sensible TES is given by the following equation (10), where  $m$  is the mass of the storage medium,  $c_p$  its mean isobaric heat capacity.  $T_{max}$  is the maximum and  $T_{min}$  the minimum storage temperature. The maximum storage temperature and therefore the storage capacity is limited by the evaporation temperature of the storage medium. Consequently, pressurized storage tanks allow operation at higher temperatures than atmospheric storages.

$$Q_{max} = m \cdot c_p \cdot (T_{max} - T_{min}) \quad (10)$$

We determine the energy losses of the TES using equation (11) (Verein Deutscher Ingenieure VDI-Gesellschaft Verfahrenstechnik Chemieingenieurwesen VDI-W ä rmeatlas, 2013). The heat loss rate ( $\dot{Q}_{loss}$ ) is dependent on the overall heat transfer coefficient ( $k$ ) and the surface of the storage tank ( $A$ ) as well as the current temperature

difference between storage medium ( $T_{storage}$ ) and ambient ( $T_{amb}$ ).

$$\dot{Q}_{loss}(t) = k \cdot A \cdot (T_{storage}(t) - T_{amb}) \quad (11)$$

### 2.2.5. CO<sub>2</sub> sequestration

In order to recover the carbon dioxide from Oxyfuel combustion, the flue gas has to be cooled. Therefore, the implementation of a cooling system is necessary, which causes additional energy consumption and costs. Part of the recovered heat is exploited by the steam boiler, while excess heat is dissipated in a cooling tower. The waste heat ( $\dot{Q}$ ) is transferred to the cooling water, which has the volume flow rate  $\dot{V}$ , the density  $\rho$ , the specific heat capacity  $\bar{c}_p$  as well as a temperature range between in- ( $T_{in}$ ) and outflow ( $T_{out}$ ). Given the temperature range, the required water flow is calculated by rearranging equation (12). Based on the volume flow rate, the electric power ( $P_{el}$ ) of the circulation pump can be estimated according to equation (13) (Baehr and Kabelac, 2012), where  $\eta$  is the isentropic efficiency,  $\dot{V}$  the volume flow rate and  $\Delta p$  is the pressure difference that the pump needs to provide.

$$\dot{Q} = \dot{V} \cdot \rho \cdot \bar{c}_p \cdot (T_{out} - T_{in}) \quad (12)$$

$$P_{el} = \frac{1}{\eta} \cdot \dot{V} \cdot \Delta p \quad (13)$$

After the flue gas treatment, the generated CO<sub>2</sub>-rich product gas has to be compressed and stored in a buffer tank. To enable the flow to the consumers, the buffer tank has to operate at a higher pressure than the carbon dioxide network of the steel mill. In our study, carbon dioxide is stored between 5 and 20 bar, which implies a maximum output pressure of 20 bar. Therefore, we apply a two-stage compression of 1–5 bar and 5–20 bar, respectively, with the actual discharge pressure depending on the state of charge of the CO<sub>2</sub> tank. In the sequestration process, the compressor represents a significant energy consumer and thus cost factor that we want to integrate in our model. The electric compressor power ( $P_{el}$ ) was calculated as indicated in equation (14) (Baehr and Kabelac, 2012) considering a pressure increase from inlet ( $p_{in}$ ) to outlet pressure ( $p_{out}$ ). Here,  $\eta$  is the isentropic efficiency,  $\dot{m}$  the mass flow of product gas,  $\kappa$  its isentropic exponent and  $T$  its temperature in K.

$$P_{el} = \frac{1}{\eta} \cdot \dot{m} \cdot \bar{c}_p \cdot T \cdot \left( \left( \frac{p_{out}}{p_{in}} \right)^{\frac{\kappa-1}{\kappa}} - 1 \right) \quad (14)$$

### 2.2.6. Cost model

With regard to the formulated research demand (see 1.3), we will also approach the subject from an economic perspective. A simplified investment analysis will be carried out in order to identify the optimum system configuration for various underlying conditions.

In our analysis, we allocate the annually incurring costs to two cost centers: *ladle heating* and *steam generation* (Table 2). Considered expenses for *ladle heating* are the annual costs for fuel ( $c_{NG}$ ), oxygen ( $c_{O_2}$ ), CO<sub>2</sub> emission allowances ( $c_{EA}$ ) and electricity ( $c_{EE}$ ) for product gas compression and the cooling system as well as capital costs ( $c_{IV}$ ) for the proposed plant layout (15).

$$c_{tot} = c_{NG} + c_{O_2} + c_{EA} + c_{EE} + c_{IV} - (r_{WHR} + r_{CCU}) \quad (15)$$

The savings generated in the steel mill by the utilization of waste heat ( $r_{WHR}$ ) and carbon dioxide ( $r_{CCU}$ ) are assigned to the cost center as revenues that are calculated using equations (16) and (17), where  $c_{NG, SG}$  as well as  $c_{EA, SG}$  are the fuel and emission allowance costs for steam generation,  $c_{CO_2, WT}$  as well as  $c_{CO_2, EAF}$  are the carbon dioxide costs for water treatment and the oxygen costs for the EAF, and  $SR_{NG}$  as well as  $SR_{CO_2}$  are the substitution rates for natural gas and carbon dioxide.

$$r_{WHR} = SR_{NG, SG} (c_{NG, SG} + c_{EA, SG}) \quad (16)$$

$$r_{CCU} = SR_{CO_2, WT} (c_{CO_2, WT} + c_{EA, WT}) + SR_{CO_2, EAF} \cdot c_{O_2, EAF} \quad (17)$$

In scenario F2, the additional investment costs for waste heat recovery from the EAF hot gas duct as well as the costs for natural gas and emission allowances for steam generation are allocated to a separate cost center (*steam generation*).

For the calculation of investment costs of the implemented technologies, the *percentage on delivered-equipment cost* method (Peters et al., 2004) is applied. In a first step, the costs of the individual pieces of equipment are either derived from the regression models given in (Peters et al., 2004) or provided by our project partners. In the second step,

**Table 2**  
Cost centers including allocated costs and revenues.

Ladle heating	Steam generation
Operational expenditures	<b>Operational expenditures</b>
Natural gas cost	Natural gas cost
+ oxygen cost	+ emission allowance cost
+ emission allowance cost	
+ electricity cost	
Capital expenditures	<b>Capital expenditures</b>
Investment cost	Investment cost
Revenues	
- carbon dioxide revenue	
- waste heat revenue	
Total cost	Total cost

**Table 3**

Simulation results: theoretical potentials for natural gas savings, waste heat recovery and carbon dioxide utilization.

Scenario	Reference scenario	Demo scenario	Future scenario 1	Future scenario 2
Acronym	R	D	F1	F2
Share of Oxyfuel ladle heaters	–	50%	100%	100%
Natural gas consumption ladle heaters	100%	- 32%	- 46%	- 46%
Overall oxygen consumption	100%	+55%	+79%	+79%
Natural gas consumption steam generator	100%	- 14%	- 20%	- 100%
CO <sub>2</sub> consumption water treatment	100%	- 100%	- 100%	- 100%
O <sub>2</sub> consumption electric arc furnace	100%	- 28%	- 45%	-45%

the remaining direct and indirect plant costs such as installation ( $f_{inst}$ ), instrumentation and controls ( $f_{contr}$ ), piping ( $f_{pipe}$ ), electrical installations ( $f_{electr}$ ), engineering ( $f_{eng}$ ) and construction ( $f_{constr}$ ) are added to the equipment cost ( $E_n$ ) by using multiplying factors (equation (18)).

$$I_n = E_n \cdot \sum (1 + f_{inst} + f_{contr} + f_{pipe} + f_{electr} + f_{eng} + f_{constr}) \quad (18)$$

Finally, we adjust the investment costs to the year 2021 using the chemical engineering plant cost index (CEPCI) (Access Intelligence LLC, 2021). Prior to the preparation of this study, we verified the plausibility of the calculated investment costs in cooperation with our industrial partners. A summary of the estimated capital expenditures is listed in the Appendix (A1, Table 5). According to the annuity method (19), the capital expenditures are determined by allocating the investment costs for the implemented equipment ( $I$ ) over the payback period ( $n$ ) based on a calculative interest rate ( $i$ ).

$$c_{IV} = I \cdot \frac{(1+i)^n \cdot i}{(1+i)^n - 1} \quad (19)$$

Prices for natural gas and European Union emission allowances are based on market data from the European Energy Exchange (EEX) (European Energy Exchange AG, 2021a). The oxygen and carbon dioxide price used in the study are provided by our project partner and represent the mean prices for the investigated steel mill in the year 2019. The assumed prices for energy and gases are summarized in A1, Table 4.

## 3. Results

This section covers the presentation of the simulation results and comparison with the reference case. First, we present an overview of the theoretical potentials (3.1.1) for natural gas savings, waste heat recovery and carbon dioxide utilization, followed by an analysis of the technical potentials depending on the capacity of carbon dioxide and thermal energy storages (3.1.2, 3.1.3). Finally, we determine the economically optimized system layout for each individual scenario (3.2).

### 3.1. Technical assessment

#### 3.1.1. Theoretical potential

Table 3 summarizes the theoretical potential for natural gas and emission savings, as well as for waste heat and carbon dioxide recovery. Since the values were obtained from an existing steel mill and may not be published, they are stated here in relation to their respective reference values. Moreover, this approach facilitates scaling of the results to other steel mills. This potential determination does not include considerations regarding the temporal balance of supply and demand or

technical limitations such as temperature levels, material properties, heat exchanger surface, carbon dioxide purity and losses due to storage and transport.

The simulation results indicate that the natural gas consumption for ladle heating decreases significantly for all scenarios. One reason is the higher combustion efficiency due to the conversion from natural gas/air-fired burners to natural gas/oxygen burners due to decreased exhaust gas losses. Secondly, the deployment of vertical ladle heaters leads to an enhanced transfer efficiency compared to the horizontal version. However, it must be noted that the energy consumption of the ladle heaters also includes the proportion required for ladle drying still using conventional natural gas/air burners.

The total natural gas consumption of the ladle heating processes decreases by 32% (D) and 46% (F) respectively, which corresponds to a reduction of direct carbon dioxide emissions by the same percentage. Further savings in fuel and carbon dioxide emissions are achieved by exploiting the exhaust gas heat of the ladle heaters. Starting from the demonstration scenario, the complete conversion to Oxyfuel ladle heaters equipped with waste gas heat exchangers will increase the amount of waste heat by 42%. The integration of the EAF hot gas duct into the system (F2) substantially increases the available waste heat compared to scenario F1.

Regarding the carbon dioxide balance, we can conclude that the generation of carbon dioxide at the ladle heaters is sufficient to cover the consumption for waste and cooling water neutralization in any case. Assuming mixed blowing of oxygen and carbon dioxide at 25 %<sub>vol</sub> CO<sub>2</sub>, the demand of the electric arc furnace is covered partially in scenario D and completely in scenario F1. However, the additional mass of oxygen required for the ladle heaters significantly exceeds the savings resulting from the potential substitution of oxygen at the EAF.

3.1.2. Carbon dioxide utilization

As mentioned, the ladle heaters produce sufficient carbon dioxide for the water treatment plant in all scenarios. Thus, we examine the utilization of the excessive amount of CO<sub>2</sub> for mixed blowing of carbon dioxide and oxygen at the EAF in scenario F1. However, due to the batch operation in the steel mill, the carbon dioxide demand for both wastewater neutralization as well as EAF blowing is subject to strong fluctuations. In order to balance the temporal variations in supply and consumption, the installation of a buffer storage is necessary.

By the integration of the storage sub-model described in chapter 2.2.4 into our energy system model of the steel mill and simulation for a range of different storage sizes, we can determine the CO<sub>2</sub> utilization

ratio as a function of the installed storage capacity. With increasing CO<sub>2</sub> utilization ratio, the consumption of purchased carbon dioxide and oxygen decreases.

For example, the installation of a 200 kg storage tank, indicated in the diagram by the vertical line, enables the system to consume 34% of the CO<sub>2</sub> generated at the Oxyfuel ladle heaters in scenario D (Fig. 6A). This design can provide sufficient carbon dioxide for water treatment, thus making the purchase of CO<sub>2</sub> obsolete. Given the increased available volume of carbon dioxide from the higher number of Oxyfuel ladle heaters, the utilization ratio in the future scenarios amounts to 72% for the same storage capacity, whereas oxygen consumption at the EAF is cut down by 15% (Fig. 6B). Accordingly, the substitution ratios in the economic assessment will equal 100% for carbon dioxide and 15% for oxygen (see equation (17)).

3.1.3. Waste heat recovery

According to the proposed process design, the ladle heaters serve not only as a source for carbon dioxide but also for waste heat. Another potential heat source is the cooling water from the EAF hot gas duct. Due to the matching temperature level, we identified the steam generator as a suitable heat sink within the steel mill. By utilizing the available waste heat, we want to save natural gas in steam generation.

In order to balance fluctuations of heat sources and sink, the integration of a thermal energy storage is required. The installed storage capacity is a decisive factor that determines the share of recovered heat as well as the corresponding reduction in natural gas consumption and carbon dioxide emissions. In the following, we focus on the behavior of the thermal energy storage. Fig. 7 indicates the relationship between storage capacity, waste heat recovery and natural gas consumption of the steam boiler.

In the case of the waste heat recovery for feed water preheating in the demo as well as the future scenario, the storage capacity is limited by the volume of the existing feed water tank and its maximum temperature, which correspond to 650 kWh (vertical line). For this storage capacity, the natural gas consumption at the process steam boiler decreases by 10% (Figs. 7A) and 11% (Fig. 7B) while exploiting 72% and 55% respectively of the available waste heat.

The available amount of waste heat leads to a substantially higher heat recovery potential in scenario F2. The technical potential (Table 3) shows that the cooling water of the EAF hot gas duct as well as the ladle heater exhaust gas provide sufficient heat for the overall process steam generation. Assuming a storage capacity of 3000 kWh, Fig. 7 indicates natural gas savings of 97% for steam generation while exploiting 69% of

Technical analysis - carbon dioxide utilization

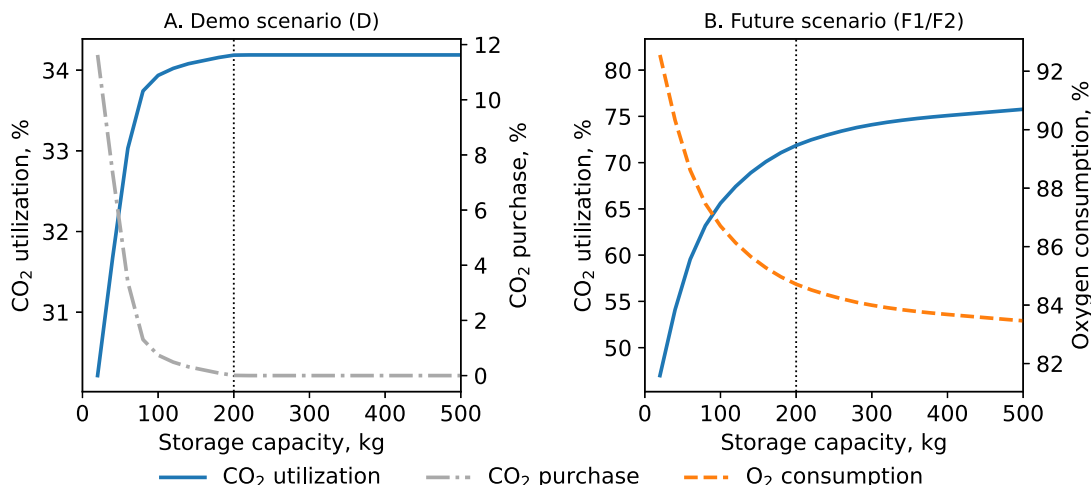


Fig. 6. Technical potential for carbon dioxide utilization for the demonstration scenario D (A) and the future scenarios F1 and F2 (B).

Technical analysis - waste heat recovery

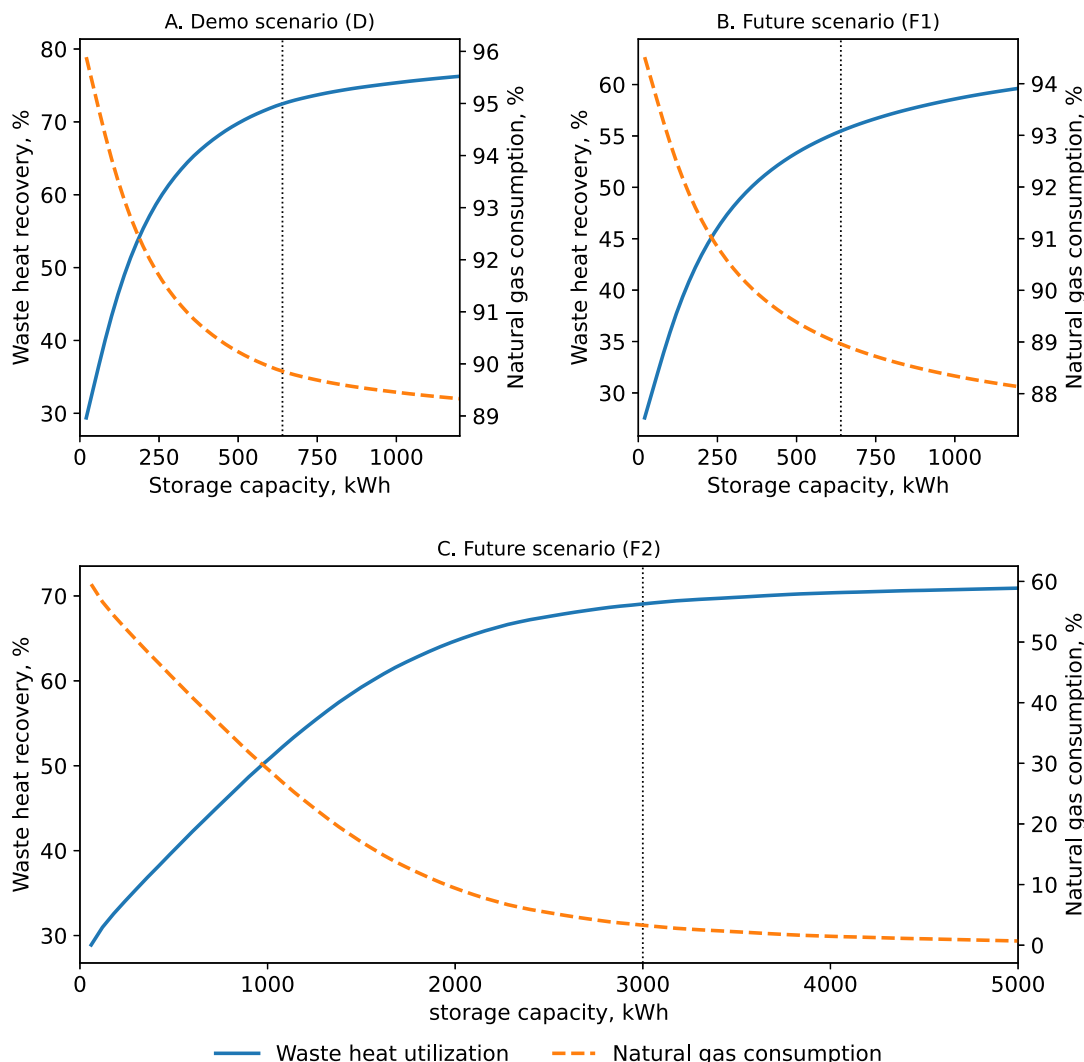


Fig. 7. Technical potential for waste heat recovery for the demonstration scenario D (A) and the future scenarios F1 (B) and F2 (C).

the available waste heat.

The presented calculations and diagrams (Figs. 6 and 7) demonstrate the technical potential for carbon dioxide and heat recovery. However, they do not provide any information about the optimal storage capacities. Therefore, we analyze the different options from an economic point of view in chapter 3.2. In order to identify the economically optimal system layout, we apply our cost model presented in section 2.2.6.

3.2. Economic assessment

The previous chapter (3.1) identified the advantages of Oxyfuel ladle heating in terms of fuel savings, the theoretical potential of carbon dioxide and waste heat recovery, and the technical requirements for their exploitation. In this section, we will investigate the conditions under which the presented technologies prove to be economically viable in the steel mill.

3.2.1. Oxyfuel combustion and CCU

By applying our cost model (section 2.2.6) to the investigated scenarios, we are able to determine the annual energy costs for the cost center ladle heating as a function of the CO<sub>2</sub> buffer storage capacity. In

order to quantify the economic benefits of the respective investments in new equipment, we present the annual costs relative to the reference scenario, which represents the status quo.

The base case for the economic assessment rests on the following assumptions: the price for emission certificates amounts to 54 EUR/t of CO<sub>2</sub> (European Energy Exchange AG, 2021b), the natural gas price is 45 EUR/MWh (E-Control, 2022a), the payback period covers 10 years and the calculative interest rate is 4% per year (see A1, Table 4). In order to analyze the impact of the volatility of underlying parameters such as prices for natural gas and carbon dioxide emission allowances, we vary them one after another. Similarly, we present the cost savings for different payback periods and at different interest rates.

Fig. 8 compares the annual energy costs of the ladle heating system under the status quo with those resulting from an investment into Oxyfuel ladle heaters equipped with carbon capture and waste heat recovery units according to scenario D. The X marks the respective cost minimum with the corresponding CO<sub>2</sub> storage capacity and the predicted annual energy cost of the ladle heating system, the base case is denoted as BC.

For scenario D, the installation of the proposed Oxyfuel and CCU equipment including a buffer storage with a capacity of 120 kg of CO<sub>2</sub> under the previously defined base case parameters decreases the annual

**Economic analysis - ladle heating (scenario D)**

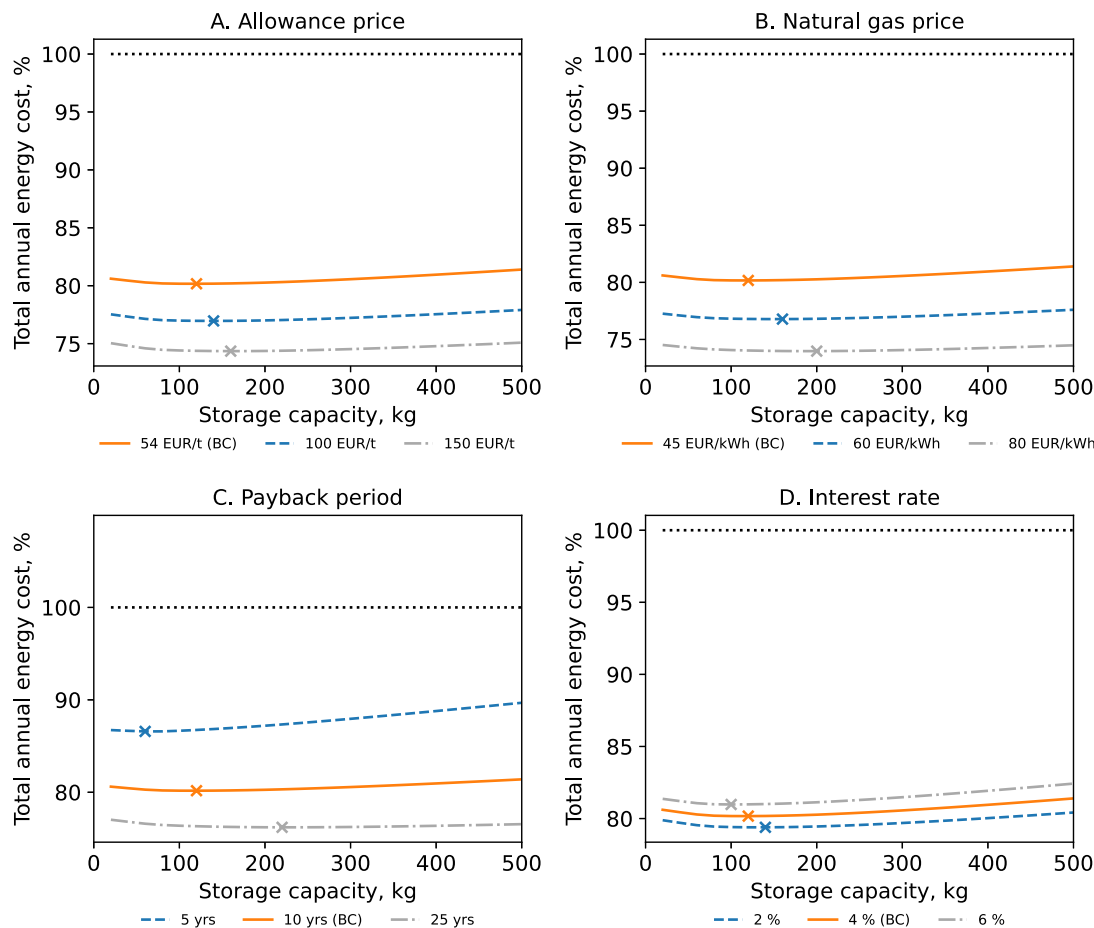


**Fig. 8.** Annual energy cost for ladle heating as a function of the CO<sub>2</sub> buffer storage capacity (scenario D).

energy costs for ladle heating by 20% (Fig. 8). In scenario F1, the analogous approach results in an optimum storage capacity of 180 kg and annual energy cost savings of 25% (Fig. 9).

**3.2.2. Waste heat recovery**

We apply a similar approach for the economic analysis of the waste heat steam generation system in scenario F2. However, in this case, the costs for investments, energy and carbon dioxide emission allowances are allocated to the cost center *steam generation*. In contrast to scenarios D and F1, in which the recovered heat is stored in the existing feed water tank, the amount of recoverable heat is dependent on the capacity of the implemented thermal energy storage. Therefore, Fig. 10 indicates the relationship between the storage capacity and the relative annual energy cost for different economic framework conditions.

As in section 3.2.1, we assume the base case parameters given in section A1, Table 4. Fig. 10B and C illustrate, that due to the high investment costs, this variant is only economically advantageous at natural gas prices exceeding 70 EUR/MWh or long assessment periods of more than 17 years. Considering a natural gas price of 80 EUR/MWh, the installation of a thermal energy storage with an economically optimized storage size of 2340 kWh results in an annual cost reduction of 10% for steam generation. Moreover, the natural gas consumption and the related CO<sub>2</sub> emissions of the steam boiler decrease by 94% (Fig. 7).

**3.3. Overall carbon dioxide reduction potential**

Our calculations demonstrate that exploiting the potential for carbon dioxide and waste heat recovery will lead to a significant reduction in

fuel consumption and direct CO<sub>2</sub> emissions. However, the actual effect of the proposed measures is limited by the previously described technical (section 3.1) and economic (section 3.2) considerations, but still leads to significant emission reductions. Fig. 11 summarizes the savings in carbon dioxide emissions for the overall steel mill, which are achievable in the individual scenarios.

The transition to Oxyfuel ladle preheating, recovery of the waste heat for feed water preheating at the steam generator and utilization of the generated carbon dioxide for cooling water treatment and wastewater neutralization results in direct emission savings of 14% in the demo scenario. Additional plant-internal utilization of CO<sub>2</sub> for EAF blowing generates emission savings of 19% in scenario F1, considering the economic optimum at the defined base case (see 3.2). Assuming the base case with an elevated natural gas price of 80 EUR/MWh, the most cost-efficient variant of the EAF waste heat recovery system would save additional 7% of the annual carbon dioxide emissions of the steel mill. While the implementation of new Oxyfuel ladle heaters implies high investment costs, the measure results in substantial CO<sub>2</sub> emission savings. In contrast, the emission reduction by carbon capture and internal utilization as well as EAF waste heat recovery is comparatively low, despite significant effort in engineering, equipment as well as the related costs.

**4. Discussion**

According to our results, the application of Oxyfuel burners as well as the transformation from horizontal to vertical ladle heaters reduces the natural gas consumption and scope 1 carbon dioxide emissions for ladle

**Economic analysis - ladle heating (scenario F1)**

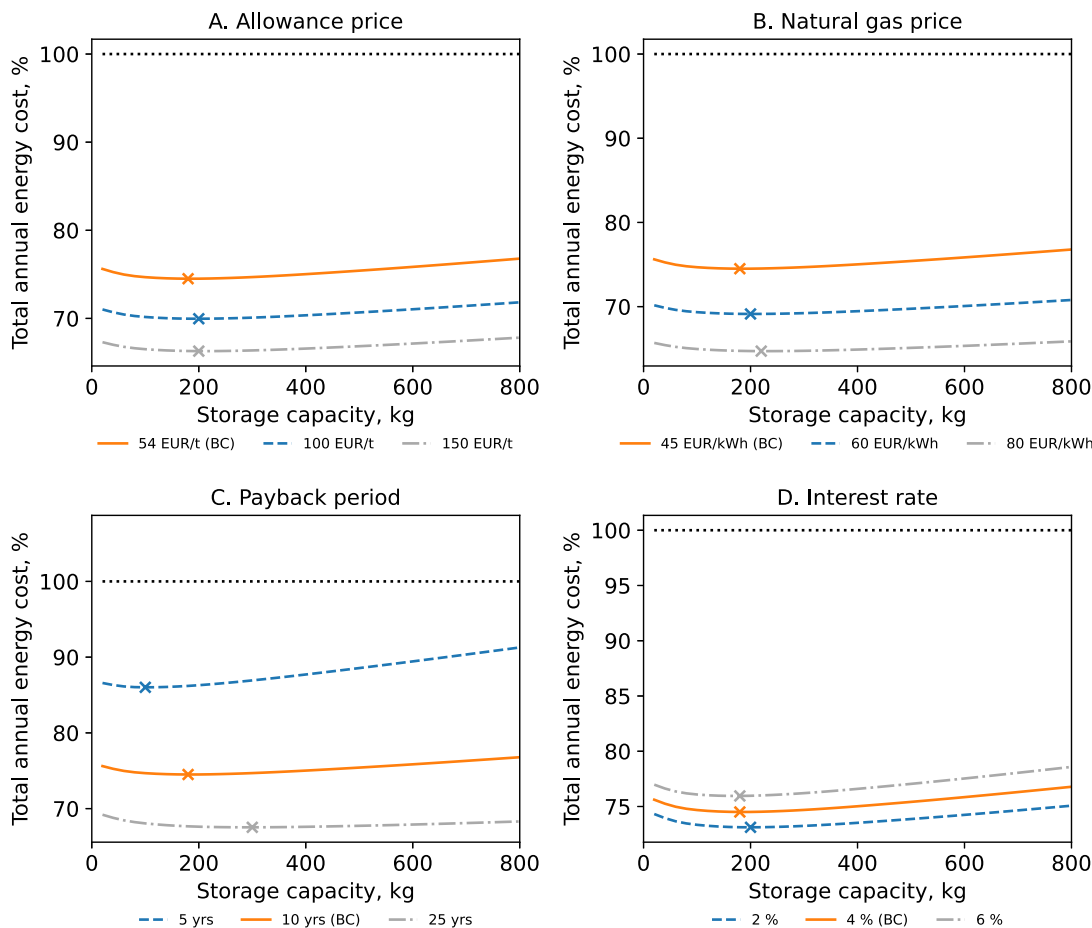


Fig. 9. Annual energy cost for ladle heating as a function of the CO<sub>2</sub> buffer storage capacity (scenario F1).

preheating in the considered steel mill by 32–46% (Table 3). The extent of the effective CO<sub>2</sub> emission cut is only dependent on the specific CO<sub>2</sub> emissions of the supplied oxygen. Moreover, our assessment of the demonstration scenario indicates that the implementation measures are economically advantageous considering reasonable framework conditions and a payback period of 10 years (Fig. 8).

The utilization ratio of recovered carbon dioxide varies significantly depending on the capacity of the buffer storage. To a certain extent, higher storage costs are compensated by savings of purchased CO<sub>2</sub> for the cooling systems and the waste water treatment plant as well as the partial substitution of oxygen by carbon dioxide in the electric arc furnace. If the carbon dioxide separation and utilization system is designed according to the economic optimum, up to 71% of the produced carbon dioxide can be exploited plant-internally (Fig. 6). In this way, the purchase of CO<sub>2</sub> for cooling water treatment and waste water neutralization is avoided and the oxygen consumption of the electric arc furnace is reduced by up to 15%. Additional emission and fuel savings are achieved by recovering the ladle heater waste heat. The existing feed water tank of the steam boiler provides a heat sink with sufficient storage capacity (Fig. 7).

The electric arc furnace produces a substantial amount of waste heat at high temperature levels. However, the recovery is difficult due to a lack of suitable heat sinks in our case study. With regard to temperature and amount of required energy, solely the process steam boiler offers potential to exploit the heat produced by the EAF hot gas duct. However, due to the batch operation both at the EAF, which acts as the heat source, and at the vacuum treatment units, which are the biggest steam consumers, heat generation and demand fluctuate substantially.

Therefore, the implementation of a thermal energy storage is crucial. In order to cut down on fuel consumption and CO<sub>2</sub> emissions of the steam generator by 95%, the installation of a pressurized hot water storage with a capacity of 2500 kWh is required. The complexity and the extent of the necessary equipment of the proposed heat recovery system lead to high investment costs. Hence, this plant is only economically feasible considering long payback periods or high natural gas prices (Fig. 10). Theoretically, it would be possible to produce the process steam almost exclusively via waste heat recovery (Fig. 7).

Since the carbon dioxide introduced into the electric arc furnace is released into the atmosphere as part of the furnace exhaust gas, it does not contribute to the mitigation of scope 1 CO<sub>2</sub> emissions. However, depending on the oxygen production process and the supplied energy, substituting oxygen at the EAF could reduce costs as well as indirect (scope 3) emissions. The potential energy and emission savings resulting from the mixed blowing of oxygen and carbon dioxide into the electric arc furnace will be the subject of subsequent studies. In order to investigate the achievable concentration of CO<sub>2</sub> in the product gas of the proposed CCU plant in an industrial environment, a demonstration project will be carried out following this study.

Finally, we discuss our results applying a sensitivity analysis. Fig. 12 demonstrates the extent by which the overall result, hence the total energy cost reduction, changes in response to individual parameter variations. The presented analyses are each built on the base case assumptions from the economic analyses in chapters 3.2.1 and 3.2.2. Introducing a 40% funding ratio ensures an economic benefit within a payback time of 10 years for the implementation of the heat recovery system (see Fig. 12). In both cases, the natural gas price and the payback

**Economic analysis - steam generation (scenario F2)**

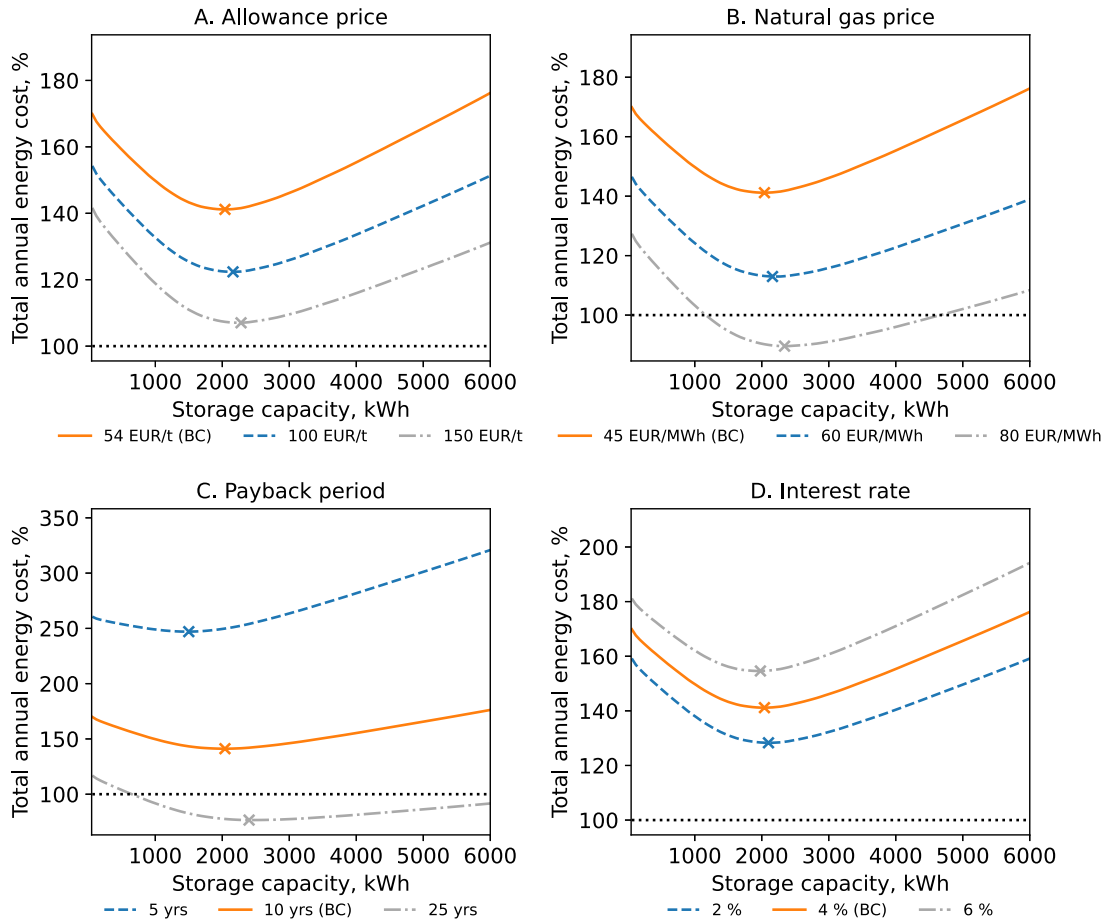


Fig. 10. Annual energy cost for steam generation as a function of the thermal energy storage capacity (scenario F2).

**Reduction of direct CO<sub>2</sub> emissions**

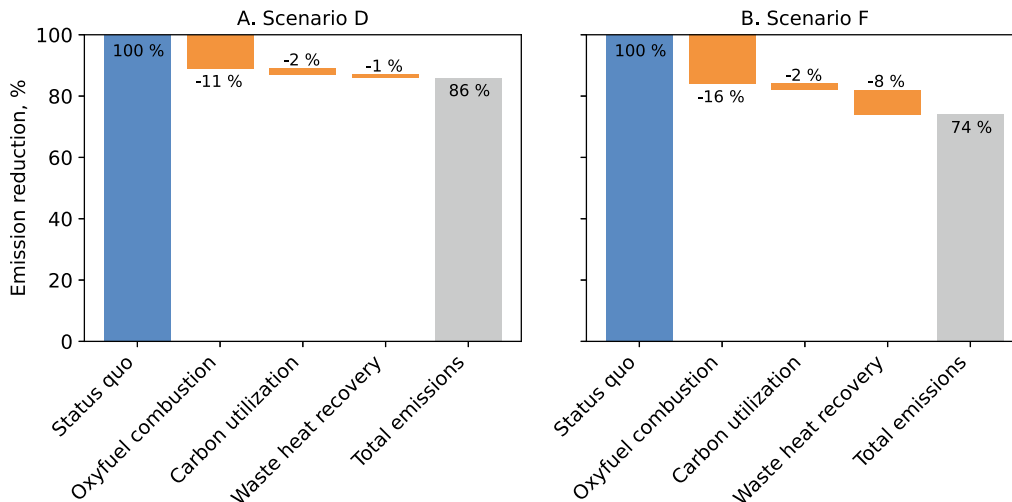


Fig. 11. Reduction of carbon dioxide emissions by scenario.

period have the strongest impact on the economic viability which calls for lifetime-based investment concepts. The CO<sub>2</sub> emission allowance price ranks only third, followed by the interest rate. However, it must be emphasized that emission allowance prices, as a policy instrument, represent the greatest uncertainty of all the analyzed parameters. In

order to reach a net-zero-emission energy system by 2050, the IEA's World Energy Outlook 2021 (International Energy Agency, 2021) anticipates carbon prices of 120 EUR/t in 2030 and 230 EUR/t in 2050, which significantly exceed the range of variation considered in the sensitivity analysis.



**Sensitivity analysis**

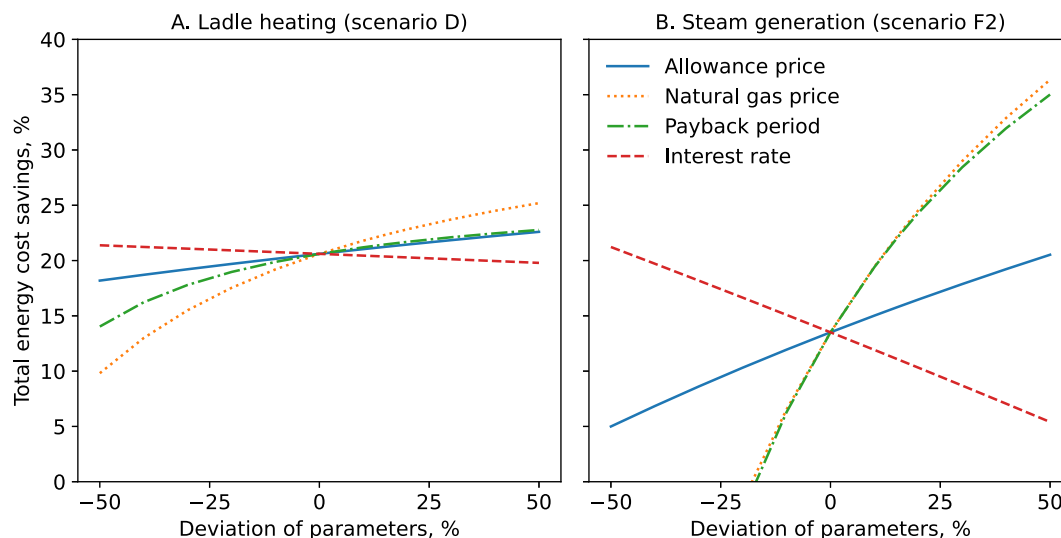


**Fig. 12.** Sensitivity analysis of the economic benefit for ladle heating (A) and steam generation (B).

**5. Conclusion**

The case study demonstrates that the implementation of the proposed technologies in the investigated steel mill leads to a significant reduction of energy consumption and direct carbon dioxide emissions. On the one hand, the transition to Oxyfuel burners reduces the natural gas consumption and related carbon dioxide emissions. On the other hand, the internal recovery of CO<sub>2</sub> further decreases emissions and saves the external purchase of carbon dioxide for the water treatment processes and enables the mixed blowing of oxygen and carbon dioxide at the electric arc furnace. Additional savings can be achieved by exploiting available waste heat sources such as the EAF or the ladle heater off-gas for water preheating or process steam production.

The first finding of our investigation is that the investments in decarbonization technologies are not only enhancing the overall energy efficiency but, in view of increasing prices for CO<sub>2</sub> emission allowances, also financially viable. However, this does not apply to all measures: the waste heat steam production from the EAF exhaust gas will not be profitable in the medium term. Therefore, the holistic analysis and thorough assessment of potential implementations on a system level is of utmost importance.

Second, the economic evaluation as well as the sensitivity analysis indicate that the substantial capital expenditures required for the implementation of novel energy-related technologies entail long payback periods, even at high fuel and emission allowance costs. From this fact, we conclude that investments in energy efficiency and decarbonization measures do not necessarily become economically feasible through an increase of the costs for carbon dioxide emissions alone. In

spite of profitability, the currently demanded amortization periods have an inhibitive effect on investments and hold the risk that investment decisions are delayed or not made at all.

Third, the investigated steel mill provides a considerable waste heat potential which can only be used to a limited extent mill-internally due to its comparably low temperature level and highly fluctuating output. In this case, external recipients such as neighboring industrial companies or district heating systems are essential to enable the efficient and economical utilization of waste heat.

Finally, the authors point out that due to its high degree of electrification, the decarbonization of EAF steelmaking is particularly dependent on electricity from renewable energy sources. Research is therefore needed not only with regard to efficient fuel utilization and avoidance of direct carbon dioxide emissions but also in terms of providing flexibility options for the increased integration of volatile renewable energy sources.

**Declaration of competing interest**

The authors declare that they have no known competing financial interests or personal relationships that could have appeared to influence the work reported in this paper.

**Acknowledgments**

This work was carried out as part of the OxySteel project. OxySteel is a subproject of NEFI – New Energy for Industry, a flagship region funded by the Climate and Energy Funds Austria.

**A1. Cost data**

**Table 4**  
Energy cost

Cost component	Unit	Cost	Reference
Electric energy	EUR/MWh	127	E-Control (2022b)
Natural gas	EUR/MWh	45	E-Control (2022a)
Oxygen	EUR/t	80	provided by industrial partners
Carbon dioxide	EUR/t	90	provided by industrial partners
Emission allowances	EUR/t	54	European Energy Exchange AG (2021b)

**Table 5**  
Capital cost

Cost component	Unit	Cost	Reference
Oxyfuel ladle heater	EUR	100	provided by industrial partners
CO <sub>2</sub> sequestration	EUR/(kg/h)	2350	provided by industrial partners, (Peters et al., 2004)
EAF waste heat recovery	EUR/kW	590	provided by industrial partners, (Peters et al., 2004)
CO <sub>2</sub> storage	EUR/kg	780	provided by industrial partners, (Peters et al., 2004)
Thermal energy storage	EUR/kWh	360	provided by industrial partners, (Peters et al., 2004)

## A2. Simulation data

**Table 6**  
Simulation parameters

Parameter	Unit	Scenario D	Scenario F	Reference
<i>Economic parameters</i>				
Payback period	a	10	10	own assumption
Interest rate	%	4.0	4.0	Greiml et al. (2021)
<i>Steam generator</i>				
Feed water temperature	°C	105	105	process requirement
Steam temperature	°C	190	190	process requirement
Steam pressure	MPa	2.0	2.0	process requirement
<i>Thermal energy storage</i>				
Min. temperature	°C	15	200	process requirement
Max. temperature	°C	105	240	process requirement
<i>CO<sub>2</sub> buffer storage</i>				
Min. pressure	MPa	0.5	1.0	process requirement
Max. pressure	MPa	1.0	2.0	own assumption
<i>CO<sub>2</sub> capture unit</i>				
Compressor efficiency		0.6	0.6	own assumption
Sequestration efficiency	–	0.8	0.8	own assumption
Heat recovery efficiency	–	0.9	0.9	own assumption

## References

- Access Intelligence LLC. Chemical engineering. <https://www.chemengonline.com/pci-home>. (Accessed 30 July 2021).
- Ahn, M., Chilakala, R., Han, C., Thenepalli, T., 2018. Removal of hardness from water samples by a carbonation process with a closed pressure reactor. *Water* 10, 54. <https://doi.org/10.3390/w10010054>.
- Arens, M., Worrell, E., Eichhammer, W., Hasanbeigi, A., Zhang, Q., 2017. Pathways to a low-carbon iron and steel industry in the medium-term – the case of Germany. *J. Clean. Prod.* 163, 84–98. <https://doi.org/10.1016/j.jclepro.2015.12.097>.
- Baehr, H.D., Kabelac, S., 2012. *Thermodynamik: Grundlagen und technische Anwendungen, fifteenth. Aufl. zwanzigstwehft.* Springer Berlin Heidelberg, Berlin, Heidelberg.
- Baukal, C.E. (Ed.), 2013. *Oxygen-enhanced Combustion, second ed.* CRC Press, Boca Raton.
- Baukal, C.E., 2013a. 2. Fundamentals. In: Baukal, C.E. (Ed.), *Oxygen-enhanced Combustion, secondnd ed.* CRC Press, Boca Raton, pp. 25–43.
- Baukal, C.E., 2013b. 10. Heat transfer. In: Baukal, C.E. (Ed.), *Oxygen-enhanced Combustion, secondnd ed.* CRC Press, Boca Raton, pp. 197–234.
- Dock, J., Janz, D., Weiss, J., Marschnig, A., Kienberger, T., 2021. Time- and component-resolved energy system model of an electric steel mill. *Cleaner Eng. Technol.* 163, 100223 <https://doi.org/10.1016/j.clet.2021.100223>.
- Docquier, N., Grant, M., Kaiser, K., 2013. 22. Ferrous metals. In: Baukal, C.E. (Ed.), *Oxygen-enhanced Combustion, secondnd ed.* CRC Press, Boca Raton, pp. 531–555.
- Dong, K., Wang, X., 2019. CO<sub>2</sub> utilization in the ironmaking and steelmaking process. *Metals* 9, 273. <https://doi.org/10.3390/met9030273>.
- E-Control, 2022a. Price Development: Natural Gas, Vienna.
- E-Control, 2022b. Price Development: Electric Energy, Vienna.
- European Energy Exchange AG. Market data. <https://www.eex.com/en/market-data>. (Accessed 30 July 2021).
- European Energy Exchange AG. Emission spot primary market auction report 2021. <https://www.eex.com/en/market-data/environmental-markets/eua-primary-auction-spot-download>. (Accessed 20 January 2022).
- Eurostat (European Commission), 2020. Energy data: 2020 edition. <https://ec.europa.eu/eurostat/web/energy/data/energy-balances>. (Accessed 20 September 2021).
- Gharib Mombeni, A., Hajidavalloo, E., Behbahani-Nejad, M., 2016. Transient simulation of conjugate heat transfer in the roof cooling panel of an electric arc furnace. *Appl. Therm. Eng.* 98, 80–87. <https://doi.org/10.1016/j.applthermaleng.2015.12.004>.
- Gibbins, J., Chalmers, H., 2008. Carbon capture and storage. *Energy Pol.* 36, 4317–4322. <https://doi.org/10.1016/j.enpol.2008.09.058>.
- Greiml, M., Fritz, F., Kienberger, T., 2021. Increasing installable photovoltaic power by implementing power-to-gas as electricity grid relief – A techno-economic assessment. *Energy* 235, 121307. <https://doi.org/10.1016/j.energy.2021.121307>.
- Hart, P., Colson, G.W., Burriss, J., 2011. Application of carbon dioxide to reduce water-side lime scale in heat exchangers. *J. Sci. Technol. Forest Products Process.* 1, 67–70.
- He, K., Wang, L., 2017. A review of energy use and energy-efficient technologies for the iron and steel industry. *Renew. Sustain. Energy Rev.* 70, 1022–1039. <https://doi.org/10.1016/j.rser.2016.12.007>.
- International Energy Agency, 2021. *World Energy Outlook 2021, Paris*.
- Keplinger, T., Haider, M., Steinparzer, T., Patrejkó, A., Trunner, P., Haselgrübler, M., 2018. Dynamic simulation of an electric arc furnace waste heat recovery system for steam production. *Appl. Therm. Eng.* 135, 188–196. <https://doi.org/10.1016/j.applthermaleng.2018.02.060>.
- Li, Z., Zhu, R., Ma, G., Wang, X., 2017. Laboratory investigation into reduction the production of dust in basic oxygen steelmaking. *Ironmak. Steelmak.* 44, 601–608. <https://doi.org/10.1080/03019233.2016.1223906>.
- Linde AG, G.D., 2017. OXYGON® XL for maximising efficiency in ladle preheating. [https://www.linde-gas.com/en/industries/steel\\_metal/steel/oxyfuel-solution-for-ladle-preheating/index.html](https://www.linde-gas.com/en/industries/steel_metal/steel/oxyfuel-solution-for-ladle-preheating/index.html). (Accessed 20 April 2022).
- Lv, M., Zhu, R., Wei, X., Wang, H., Bi, X., 2012. Research on top and bottom mixed blowing CO<sub>2</sub> in converter steelmaking process. *Steel Res. Int.* 83, 11–15. <https://doi.org/10.1002/srin.201100166>.
- Messer Americas, 2019. OXIPYR™ for Ladle Preheating: Fast and Fuel-Efficient Oxyfuel Preheating of Vessels up to 100 Tons in Size. (Accessed 20 April 2022).
- Messer North America Inc, 2021. Neutra water treatment process: neutralization of alkaline waste water with carbon dioxide. <https://www.messer-us.com/chemicals/ph-reduction>. (Accessed 11 August 2021).
- Moch, W., Adler, W., Gregor, M.A., 2008. Investigations and Measures to Reduce Emissions and Energy Consumption during the Preheating of Steel Ladles. Publications Office, Luxembourg.
- Pardo, N., Moya, J.A., Vatopoulos, K., 2015. Prospective Scenarios on Energy Efficiency and CO<sub>2</sub> Emissions in the EU Iron & Steel Industry: Re-edition. Publications Office, Luxembourg.
- Peters, M.S., Timmerhaus, K.D., West, R.E., 2004. *Plant Design and Economics for Chemical Engineers*. In: *internat (Ed.)*, fifth. McGraw-Hill, Boston.
- Quader, M.A., Ahmed, S., Ghazilla, R.A.R., Ahmed, S., Dahari, M., 2015. A comprehensive review on energy efficient CO<sub>2</sub> breakthrough technologies for sustainable green iron and steel manufacturing. *Renew. Sustain. Energy Rev.* 50, 594–614. <https://doi.org/10.1016/j.rser.2015.05.026>.
- Ramirez, M., Epelde, M., de Arceche, M.G., Panizza, A., Hammerschmid, A., Baresi, M., Monti, N., 2017. Performance evaluation of an ORC unit integrated to a waste heat

- recovery system in a steel mill. *Energy Proc.* 129, 535–542. <https://doi.org/10.1016/j.egypro.2017.09.183>.
- Ray, S.K., Chattopadhyay, G., Ray, A.K., 1997. Evaluation of dust generated from basic oxygen furnace steel making. *J. Air Waste Manag. Assoc.* 47, 716–721. <https://doi.org/10.1080/10473289.1997.10463929>.
- Remus, R., 2013. Best Available Techniques (BAT) Reference Document for Iron and Steel Production: Industrial Emissions Directive 2010/75/EU (Integrated Pollution Prevention and Control). Publications Office of the European Union, Luxembourg.
- Sasiain, A., Rechberger, K., Spanlang, A., Kofler, I., Wolfmeir, H., Harris, C., Bürgler, T., 2020. Green hydrogen as decarbonization element for the steel industry. *Berg Huettenmaenn Monatsh* 165, 232–236. <https://doi.org/10.1007/s00501-020-00968-1>.
- Stanger, R., Wall, T., Spörl, R., Paneru, M., Grathwohl, S., Weidmann, M., Scheffknecht, G., McDonald, D., Myöhänen, K., Ritvanen, J., Rahiala, S., Hyppänen, T., Mletzko, J., Kather, A., Santos, S., 2015. Oxyfuel combustion for CO<sub>2</sub> capture in power plants. *Int. J. Greenh. Gas Control* 40, 55–125. <https://doi.org/10.1016/j.ijggc.2015.06.010>.
- Steinparzer, T., Haider, M., Zauner, F., Enickl, G., Michele-Naussed, M., Horn, A.C., 2014. Electric arc furnace off-gas heat recovery and experience with a testing plant. *Steel Res. Int.* 85, 519–526. <https://doi.org/10.1002/srin.201300228>.
- Toktarova, A., Karlsson, I., Rootzén, J., Göransson, L., Odenberger, M., Johnsson, F., 2020. Pathways for low-carbon transition of the steel industry—A Swedish case study. *Energies* 13, 3840. <https://doi.org/10.3390/en13153840>.
- Verein Deutscher Ingenieure, VDI-Gesellschaft Verfahrenstechnik, Chemieingenieurwesen, VDI-Wärmeatlas, 2013. Mit 320 Tabellen, eleventh., bearb. und erw. Aufl. Springer Vieweg, Berlin.
- von Scheele, J., 2010. In: Palm, J. (Ed.), *Oxyfuel Combustion in the Steel Industry: Energy Efficiency and Decrease of CO<sub>2</sub> Emissions*. Energy Efficiency, Sciyo.
- Wall, T., Stanger, R., McDonald, D., 2013. 27. Coal-fired oxy-fuel technology for carbon capture and storage. In: Baukal, C.E. (Ed.), *Oxygen-enhanced Combustion*, secondnd ed. CRC Press, Boca Raton, pp. 631–648.
- Wang, H., Yu, H., Teng, L., Seetharaman, S., 2016. Evaluation on material and heat balance of EAF processes with introduction of CO<sub>2</sub>. *J. Min. Metall. B Metall.* 52, 1–8. <https://doi.org/10.2298/JMMB150627002W>.
- Wei, G., Zhu, R., Wu, X., Dong, K., Yang, L., Liu, R., 2018. Technological innovations of carbon dioxide injection in EAF-LF steelmaking. *JOM* 70, 969–976. <https://doi.org/10.1007/s11837-018-2814-3>.
- World Resources Institute, World Business Council for Sustainable Development. The greenhouse gas protocol. <https://ghgprotocol.org/standards>. (Accessed 19 November 2021).
- Yang, L.-z., Jiang, T., Li, G.-h., Guo, Y.-f., Chen, F., 2018. Present situation and prospect of EAF gas waste heat utilization technology. *High Temp. Mater. Process.* 37, 357–363. <https://doi.org/10.1515/htmp-2016-0218>.
- Zhu, R., Han, B.-c., Dong, K., Wei, G.-s., 2020. A review of carbon dioxide disposal technology in the converter steelmaking process. *Int. J. Miner. Metall. Mater.* 27, 1421–1429. <https://doi.org/10.1007/s12613-020-2065-5>.

## Article

# Provision of Demand-Side Flexibility through the Integration of Power-to-Gas Technologies in an Electric Steel Mill

Johannes Dock <sup>\*</sup> , Stefan Wallner, Anna Traupmann  and Thomas Kienberger

Chair of Energy Network Technology, Department of Environmental and Energy Process Engineering, Montanuniversität Leoben, A-8700 Leoben, Austria

\* Correspondence: johannes.dock@unileoben.ac.at; Tel.: +43-384-2402-5404

**Abstract:** EAF steelmaking based on renewable electricity allows for low-CO<sub>2</sub> steel production. However, the increased integration of volatile renewable energies into the energy system requires the provision of flexibility options. In view of the substantial oxygen consumption in the steel mill, flexible on-site generation and storage holds a significant potential for demand-side management. The utilization of by-product oxygen from an electrolysis plant not only contributes to load flexibility but also generates a climate-neutral fuel. In the present study, different process layouts are developed based on state-of-the-art technologies. The proposed supply systems for oxygen, hydrogen, and synthetic natural gas are subjected to design and operational optimization and assessed with respect to the overall demand-side flexibility, carbon dioxide emission reduction, and economic viability.

**Keywords:** EAF steelmaking; demand-side management; oxygen production; pressure swing adsorption; electrolysis; res integration; climate neutrality



**Citation:** Dock, J.; Wallner, S.; Traupmann, A.; Kienberger, T. Provision of Demand-Side Flexibility through the Integration of Power-to-Gas Technologies in an Electric Steel Mill. *Energies* **2022**, *15*, 5815. <https://doi.org/10.3390/en15165815>

Academic Editor: Alan Brent

Received: 14 July 2022

Accepted: 9 August 2022

Published: 10 August 2022

**Publisher's Note:** MDPI stays neutral with regard to jurisdictional claims in published maps and institutional affiliations.



**Copyright:** © 2022 by the authors. Licensee MDPI, Basel, Switzerland. This article is an open access article distributed under the terms and conditions of the Creative Commons Attribution (CC BY) license (<https://creativecommons.org/licenses/by/4.0/>).

## 1. Introduction

In view of the climate neutrality of the steel industry, steel production via the electric arc furnace (EAF) has certain advantages over the conventional blast furnace/basic oxygen furnace (BF/BOF) route. First, the reduction of iron ore using coke in the blast furnace is associated with substantial energy consumption and carbon dioxide emissions. The recycling of steel scrap, referred to as secondary production, in the EAF omits the entire reduction process step. With regard to steel production from iron ore (primary production), the processing of direct reduced iron (DRI) in the EAF offers a viable and lower-emission alternative. Consequently, EAF steelmaking plays a key role in numerous future technology scenarios in addition to carbon capture, utilization, and storage (CCUS) and smelting reduction [1–4].

Second, the EAF route is characterized by a high degree of electrification. The Greenhouse Gas Protocol defines three scopes for greenhouse gas accounting [5]. According to this definition, in the EAF steel mill, direct (scope 1) CO<sub>2</sub> emissions occur mainly in energy-intensive by-processes such as ladle heating, annealing, and steam generation [6]. In contrast, indirect (scope 2) carbon dioxide emissions of the production process depend solely on the CO<sub>2</sub> intensity of the supplied electric energy. The operation of the electric arc furnace with electricity that is certified as 100% climate neutral thus eliminates scope 2 emissions and, therefore, represents an effective emission reduction measure. However, increased integration of volatile renewable energy sources (RES) into the energy system requires flexibility options to balance both temporal and spatial fluctuations [7] and to reduce the strain on the grid infrastructure [8].

### 1.1. EAF Steel Production Process and Oxygen Demand

The remelting of steel scrap in the EAF is not only the most energy-intensive process step in electric steelmaking [9] but also causes significant oxygen consumption: During the

melting phase, chemical energy input by the introduction of oxygen, carbon, and natural gas reduces the electric energy demand and tap-to-tap time. The following refining step aims at dephosphorization, decarburization, and temperature adjustment of the steel melt. In order to protect the furnace lining, the slag is foamed by the injection of carbon and oxygen through lances [10]. For the production of stainless steel, decarburization is carried out in a separate argon oxygen decarburization (AOD) or vacuum oxygen decarburization (VOD) process to inhibit the oxidation of valuable alloying elements. Both the AOD and the VOD process involve the injection of oxygen [10]. Due to the high consumption in the steel mill, we identified the flexible oxygen production from electrical energy as a promising demand-side management option.

Further process steps, which are referred to as secondary metallurgy, include de-oxidation, desulfurization, degassing, homogenization, alloying, and temperature and composition adjustment [11]. Subsequently, the steel is casted either continuously or in ingots. Throughout secondary steelmaking, steel mill ladles are used as a transport and processing vessel. Prior to tapping of the steel melt at the electric arc furnace, they have to be preheated to more than 1000 °C. In a preceding study, the authors demonstrated that the application of Oxyfuel burners for ladle preheating rather than natural gas/air burners results in significant energy savings [6]. In Oxyfuel combustion, natural gas is burnt with oxygen, which leads to higher combustion efficiency but increases the oxygen demand in the steel mill.

## 1.2. Technology Overview

In the following section, we will discuss options for demand-side management in steel mills and the flexible operation of oxygen production and power-to-gas (PtG) plants.

### 1.2.1. Demand-Side Management in EAF Steel Mills

An efficient way to provide flexibility to the power system is to apply demand-side management (DSM). DSM describes the concept of matching the demand with the available supply, encouraging the customers in the energy market to actively manage their energy consumption [12]. Consumer-end measures include either reducing the energy consumption or shifting the energy demand to a later time [13]. According to Strbac [14], the implementation of DSM measures has the potential to reduce the generating margin, improve the operation efficiency of transmission and distribution grids, and facilitate the integration of intermittent renewable energy sources into existing energy systems.

Due to the batch operation, high nominal power, and substantial energy consumption, many studies focus on the electric arc furnace. Flexible scheduling of an EAF allows for the shifting of high power [15]. However, deferring the production schedule of the EAF impairs the subsequent processes such as secondary metallurgy and casting, degrades the asset utilization rate, and decreases the steel production volume. Zhang and Grossmann [16] give an overview of the challenges and benefits of industrial DSM. They conclude that exploiting the synergies of interdependent production processes holds potential for demand-side management. Coupling a steel mill with an oxygen production plant might serve this purpose. Another DSM option is the implementation of power-to-gas (PtG) plants that produce climate-neutral gases such as hydrogen and synthetic natural gas (SNG) from fluctuating renewable electricity [17].

### 1.2.2. Oxygen Production

Oxygen has the potential to enhance the efficiency of energy-intensive industrial processes such as glass melting, pulp bleaching, and iron, steel, and non-ferrous metal production [18]. Therefore, considerable research effort has been dedicated to its energy- and cost-efficient production. At present, two processes are commercially available for the industrial-scale production of oxygen: For the large-volume production of oxygen with high purity, cryogenic air separation (ASU) constitutes the standard process [19]. Pressure swing adsorption (PSA) offers an alternative for the production at lower throughputs [20].

The customizable plant capacity and the controllable operation of the PSA allow for the flexible on-site production of oxygen [21]. Depending on the purity, capacity, physical state and output pressure, manufacturer data for specific energy consumption ranges from 280 to 777 kWh/t O<sub>2</sub> for ASU [21] and 265 to 460 kWh/t O<sub>2</sub> for PSA [22–24].

In their study, Banaszekiewicz et al. [25] compared different oxygen production technologies for Oxyfuel combustion, including ASU, PSA, and polymer and ion transfer membranes. They concluded that for large oxy-combustion power plants, the cryogenic process is the best method due to its production capacity and energy efficiency. However, the PSA technology is suitable for small-scale Oxyfuel applications and steel mills. Sulc and Ditl [21] evaluated two different oxygen sources for a small oxy-combustion unit: Pressure swing adsorption and liquid oxygen delivery. They found that the cost and CO<sub>2</sub> emissions of oxygen supplied by the PSA unit depend mainly on the electricity price and the emission factor for electric energy. In their case study, they show that for the operation in Germany, the on-site production via PSA leads to higher costs and CO<sub>2</sub> emissions compared to the delivery of oxygen produced by a large cryogenic air separation plant.

### 1.2.3. Power to Gas

PtG technology refers to the process of gaseous fuel production from electric energy by electrolysis (hydrogen) and optional subsequent methanation (SNG). The resulting coupling of the electricity and gas grids and the storability of the generated energy carriers represents a flexibility option [26]. Key considerations for power to gas applications are the underlying electrolysis and methanation technologies.

#### Electrolysis

Due to its versatile application and the omission of direct CO<sub>2</sub> emissions, hydrogen represents an important energy carrier for future climate-neutral energy systems. Hydrogen production via electrolysis using negative residual loads in the electricity system may provide flexibility for the future electrical grid and thus contribute to the integration of fluctuating RES.

Three main technologies are available for electrolysis, which are characterized by their respective electrolyte: Alkaline water electrolysis (AEC), proton exchange membrane electrolysis (PEM-EC), and solid oxide electrolysis (SOEC). Alkaline electrolyzers consist of an aqueous potassium hydroxide electrolyte and two nickel, cobalt, or iron electrodes separated by an insulating diaphragm [27]. They operate at temperatures of 40–90 °C, pressures from atmospheric pressure to 30 bar, and production rates of 0.01–45 kg H<sub>2</sub>/h. Specific energy consumption lies in the range of 46–60 kWh/kg H<sub>2</sub>. A disadvantage of the AEC is its lower partial load limit of 20–40% [28]. In PEM electrolysis cells, a proton-conducting polymer membrane substitutes the liquid electrolyte and the diaphragm and the electrodes consist of platinum group metals. At operating temperatures of 20–100 °C, pressures of 10 to 85 bar, and hydrogen production rates of 0.02–4.50 kg/h, the energy consumption rate ranges from 53–81 kWh/kg H<sub>2</sub> [28]. The utilization of noble metals as electrode materials leads to higher capital costs for the PEM-EC. However, an expert elicitation concludes that in the future, the PEM-EC will be favored for the integration of renewables due to significant cost reductions and its higher operational flexibility [29].

Since all the considered electrolysis technologies produce oxygen as a by-product, Kato et al. [18] propose the simultaneous utilization of hydrogen and oxygen from water electrolysis. They argue that oxygen production via electrolysis is not competitive compared to the conventional technologies. However, the utilization of by-product oxygen reduces the cost for hydrogen production and the demand for oxygen produced using air separation technologies. An economic case study investigating the operation of a PEM-EC indicates that revenues from by-product oxygen significantly reduce the hydrogen production costs.

In their study, Iora and Chiesa [30] propose the combination of a solid oxide fuel cell (SOFC) with a solid oxide electrolysis cell (SOEC) for oxygen production. The process layout aims to provide part of the electric power for the electrolysis by feeding the SOFC

with the generated hydrogen. According to a finite difference model of the SOFC/SOEC stack, the system operates at a specific energy consumption of 350–500 kWh/t O<sub>2</sub> under optimized conditions [31].

### Methanation

In order to supply existing infrastructure with renewable gases, the hydrogen can be converted to synthetic natural gas (SNG) by methanation with carbon dioxide [27]. Methanation is a catalytic, exothermic process that converts carbon dioxide and hydrogen to methane at elevated temperature and pressure following the Sabatier reaction. The conversion process is favored at low temperature and high pressure and has an efficiency of around 83% based on the lower heating values of hydrogen and SNG. Due to the highly exothermic conversion reactions, the cooling of the reactor is crucial. The most common systems are sequential fixed-bed reactors using nickel as catalyst [32].

In their study, Bailera et al. [26] investigated the operation of a hybrid power plant combining a power-to-gas plant and an Oxyfuel combustion plant. The proposed PtG-plant consists of an alkaline electrolyzer with an efficiency of 68.1% based on LHV and a three-stage adiabatic methanation process operating at a pressure of 30 bar. By-product oxygen from the electrolysis is used in an oxy-combustion combined cycle power plant. The thereby generated carbon dioxide is recovered from the flue gas as a feedstock for the methanation process. This configuration allows for the storage of energy in the form of hydrogen or SNG and the substitution of oxygen produced by air separation. The results of a heat integration scenario investigating the exploitation of waste heat from the methanation process in the combined cycle power plant indicate an overall system efficiency of 67.8%. The authors conclude that the concept is particularly feasible for application in industrial energy systems. Similar research outlines combining catalytic methanisation and hydrogen production by electrolysis were also covered by the studies of Herrmann et al. [33], Chwola et al. [34], and Gorre et al. [17,35].

### 1.3. Research Need and Outline of the Article

The relevant literature covers extensive articles on commercially available and future technologies for oxygen, hydrogen, and SNG production; viable configurations for general power-to-gas plants; and technological concepts and business models for their profitable flexible operation (see Section 1.2). However, the optimal integration of such plants into an industrial production process has not yet been investigated. Therefore, we aim to identify the optimal implementation concept for the discussed technologies and evaluate their impact on the overall energy consumption, carbon dioxide intensity, and economic efficiency of the steel production process.

Therefore, we focus on the following research questions:

**Q 1.** *What are cost-optimal plant designs and operation modes for flexible O<sub>2</sub>, H<sub>2</sub>, or SNG production plants in an EAF steel mill?*

- a. Which basic plant layouts seem to be possible based on state-of-the-art technologies?
- b. Which basic operational strategies are useful under which boundary conditions?

**Q 2.** *What is their impact in terms of carbon dioxide emissions? How do they influence the overall energy systems with regard to their demand-side management potential (qualitatively and quantitatively)?*

**Q 3.** *Which economic framework conditions are required for their economically viable operation?*

In order to address these questions, we develop feasible scenarios for EAF steel mill on-site oxygen, hydrogen, and SNG production via pressure swing adsorption, electrolysis, and methanation (Section 2.1). Then, we first present an optimization model that is suited for the integration of these technologies into an existing EAF steel mill (Section 2.2); second, the deployed load profiles (Section 2.3); and third, the framework for the economical assessment (Section 2.4) are presented. Finally, we compare the scenarios based on adequate

key performance indicators (KPIs) and discuss the results from a technical and economic point of view (Section 3).

## 2. Materials and Methods

The following section covers the development of feasible scenarios and the setup of the optimization model.

### 2.1. Considered Scenarios

In order to evaluate the feasible process layout designs, we investigate the following scenarios (see Table 1):

1. The scenario PSA involves the on-site production of oxygen by a pressure swing adsorption unit. Electricity and natural gas are drawn from the grid at wholesale prices. The consumption of natural gas results in additional costs for the purchase of the related emission certificates. The implementation of the PSA into the steel mill enables the omission of oxygen purchase; however, there are additional capital costs for the installation and costs for covering the electricity demand of the oxygen production plant. The resulting levelized cost of oxygen (LCOO) serves as a benchmark for evaluating the alternative system layouts.
2. In scenario PEM, the required oxygen for the steel production process is generated as a by-product in a PEM electrolysis plant. Thus, the purchase of oxygen is obsolete in this case as well. Revenues from the sales of hydrogen aim to offset the increased expenses for investment and energy. If economically viable, a part of natural gas purchased from the grid is substituted by the produced hydrogen. Thus, we assume that the installed burners allow for the combustion of mixtures of natural gas and hydrogen up to 100% H<sub>2</sub>. In this case, the internal hydrogen utilization saves energy costs and direct carbon dioxide emissions.
3. In scenario SNG, a share of the hydrogen from the electrolysis unit is withdrawn in order to methanize the CO<sub>2</sub> produced from a mill-internal carbon capture (CCU) plant. This not only ensures sufficient oxygen supply but also reduces the amount of natural gas obtained from the grid and creates a sink for carbon dioxide. However, the limited availability of captured CO<sub>2</sub> results in a surplus of hydrogen. In this scenario, we restrict the admixture of hydrogen into the natural gas infrastructure in the EAF steel mill to 20%<sub>vol</sub> of the current natural gas load. Analogous to the scenario PEM, excess hydrogen is injected into the gas grid and, therefore, represents a source of revenue.

**Table 1.** Summary of the investigated scenarios.

Feature	PSA	PEM	SNG
Oxygen supply	VPSA	PEM electrolysis	PEM electrolysis
Oxygen purchase	no	No	no
Hydrogen sales	no	Yes	yes
Methanation	no	No	yes
Max. Hydrogen admixture <sup>1</sup>	-	100%	20%

<sup>1</sup> For each time step, the hydrogen content of the gas that is consumed in the steel mill is limited between 0–100%<sub>vol</sub> (PEM) and 0–20%<sub>vol</sub> (SNG).

### 2.2. Optimization Model

For the optimized integration of the mentioned technologies in the existing plant, we use the open-source modeling framework *oemof* (open energy modeling framework), which serves as a multi-purpose toolbox for the modeling and optimization of energy systems. The graph-based modeling framework is realized using object-oriented programming in the language Python [36]. Due to its ability to represent multi-sectoral energy systems at various scales, its transparent continuous development process, and its extensive documentation, *oemof* is suitable for a broad range of applications [37].



Within this framework, the *oemof solph* library represents a model generator for mixed-integer linear optimization problems [38]. More precisely, *solph* provides classes with associated objective expression terms, optimization variables, and constraints. These classes are used to recreate and connect components of an actual energy system. Based on their features, the components are categorized as transformers (meaning energy conversion units), sources, and sinks. Energy systems are created by interconnecting the individual components by buses. The objective of the optimization is to minimize the total energy cost ( $C_{tot}$ ) of the steel mill, which is defined in Section 2.4, within the considered time frame [37] (Equation (1)):

$$\min f = C_{tot} \quad (1)$$

$$P_{O_2}(t) - D_{O_2}(t) + S_{O_2}(t) = 0 \quad (2)$$

$$P_{CO_2} - x_{CO_2} \cdot P_{SNG} = 0 \quad (3)$$

$$SR_{H_2}(t) \leq SR_{H_2,max} \quad (4)$$

As a constraint, we predefined that the oxygen demand of the steel mill ( $D_{O_2}(t)$ ) has to be satisfied in each time step either through production ( $P_{O_2}(t)$ ) or through the storage ( $S_{O_2}(t)$ ) without venting excess production for all scenarios (2). In the SNG scenario, all the available carbon dioxide must be used for methanation (3).  $P_{CO_2}$  represents the produced amount of carbon dioxide in kg/a,  $x_{CO_2}$  the specific carbon dioxide consumption for the production of one MWh of SNG, and  $P_{SNG}$  the produced amount of SNG in MWh/a. Another constraint is the compliance of the hydrogen substitution ratio ( $SR_{H_2}(t)$ ) with the limits for hydrogen admixture into the gas system ( $SR_{H_2,max}$ ) (4). The gas storages and buses are assumed to be loss-free, and the transformers are implemented with constant efficiencies. A linear model was used for the long-term optimization runs due to the insignificant error and the reduced computation time. The predefined input parameters are listed in Table 2. The load range specifies the operation window of individual units by defining the lower and upper limit as a percentage of full load based on the oxygen, hydrogen, and SNG output. The load gradient indicates the maximum load change rate as a percentage of the full load per minute.

**Table 2.** Parametrization of the model components.

Parameter	Unit	2020	2030	2050	Reference
VPSA unit					
Specific energy demand	kWh <sub>el</sub> /kg	0.35	0.35	0.35	[22–24]
Load range	%	60–100	60–100	60–100	own assumption
Load gradient	%/min	4	4	4	own assumption
Pressure	Mpa	3	3	3	[28]
PEM electrolysis unit					
Efficiency	kWh <sub>H2</sub> /kWh <sub>el</sub> <sup>1</sup>	0.68	0.75	0.83	[39–41]
Specific energy demand H <sub>2</sub>	kWh <sub>el</sub> /kg	58.0	52.6	47.5	own calculation
Specific energy demand O <sub>2</sub>	kWh <sub>el</sub> /kg	7.3	6.6	6.0	own calculation
Load range	%	0–100	0–100	0–100	[35]
Methanation unit					
Efficiency	kWh <sub>SNG</sub> /kWh <sub>H2</sub> <sup>1</sup>	0.62	0.62	0.62	own calculation, [42]
Load range	%	20–100	20–100	20–100	[33]
Load gradient	%/min	3	3	3	[35]
Buffer storage					
Minimum pressure	MPa	1	1	1	own assumption, [35]
Maximum pressure	Mpa	3	3	3	own assumption, [35]
O <sub>2</sub> compressor					
Mean pressure	Mpa	2	2	2	own assumption
Specific energy demand H <sub>2</sub> compressor	kWh <sub>el</sub> /kgO <sub>2</sub>	0.14	0.14	0.14	own calculation

**Table 2.** *Cont.*

Parameter	Unit	2020	2030	2050	Reference
Mean pressure	Mpa	35	35	35	own assumption
Specific energy demand CO <sub>2</sub> compressor	kWh <sub>el</sub> /kg <sub>H2</sub>	2.14	2.14	2.14	own calculation
Mean pressure	Mpa	2	2	2	own assumption
Specific energy demand	kWh <sub>el</sub> /kg <sub>CO2</sub>	0.09	0.09	0.09	own calculation

<sup>1</sup> based on HHV.

The purchase of electricity, natural gas, and CO<sub>2</sub> emission allowances and the installation of production and storage capacities are associated with costs, whereas the sales of hydrogen and SNG generate revenues. The adopted specific CAPEX (capital expenditures) and OPEX (operational expenditures) and the commodity prices are listed in Tables 3 and 4. Each optimization run covers one year with a resolution of 30 min for each time-step. In order to obtain the minimum costs under these conditions, it is necessary to optimize both the sizing of the equipment and its operation.

Figure 1 gives an overview of the optimization model, which consists of buses, transformers, storages, sinks, and sources. The model covers the commodities electricity, hydrogen, natural gas, SNG, oxygen, and carbon dioxide, which are represented by energy buses. The production plants for water and oxygen and the methanation unit are implemented into the model as transformers. Furthermore, every commodity bus is connected to a storage and to either external sources (purchase) or sinks (sales).

### 2.3. Load Profiles

The load profiles for electricity demand and for the demand for natural gas and oxygen consumed in the steel mill are obtained from an energy system model developed and extended by the authors in previous studies [6,9]. This model describes a steel mill that produces heat-treated high-alloyed steel ingots from 100% steel scrap using a 65 t alternating current (AC) EAF. Figure 2 gives a rough overview of the production process and the most important energy consumers.

While the electricity demand results mainly from the EAF operation, the natural gas demand is due to the following consumers:

- Ladle heaters;
- Annealing furnaces;
- Other consumers.

The oxygen demand profile results from the oxygen demands at the following consumers:

- Electric arc furnace;
- Vacuum oxygen decarburization units;
- Ladle heaters;
- Other consumers.

Considering the operation of the electric arc furnace, oxygen demand occurs during two process phases that require different oxygen flow levels: low mass flow rate for the melting phase and high mass flow during refining. The oxygen demand for the VOD process is to be constant during the VOD treatment time while the demand of the Oxyfuel ladle heaters is proportional to their natural gas consumption and is defined by the oxidant/fuel ratio. For the mill size-independent system analysis, we use normalized load profiles. Therefore, we relate the demand in each time step to the peak demand. Figure 3 shows the normalized demand profiles of electric power, natural gas, and oxygen for one week generated by the energy system model of the EAF steel mill.

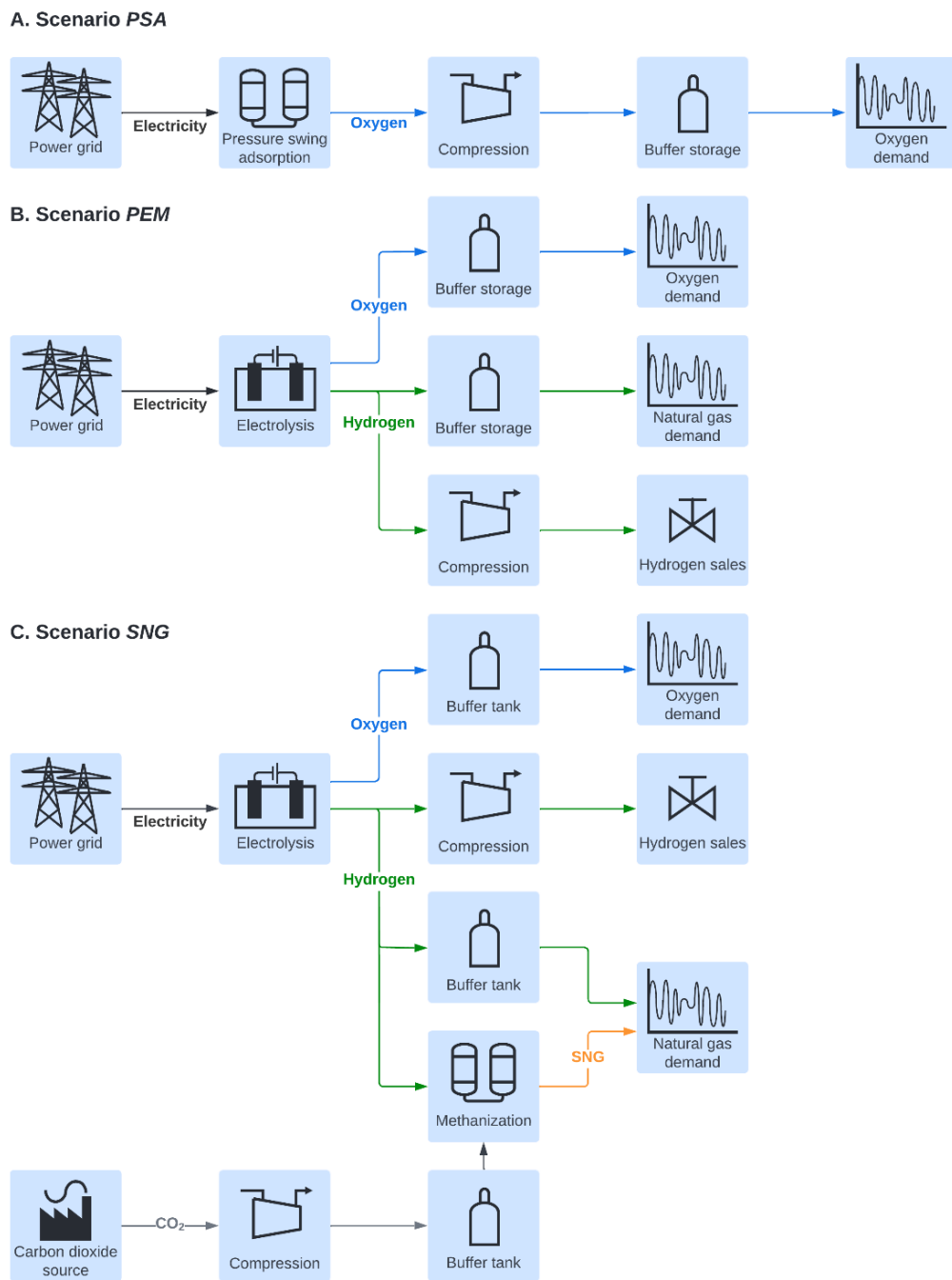


Figure 1. Configuration of the optimization model for the individual scenarios.

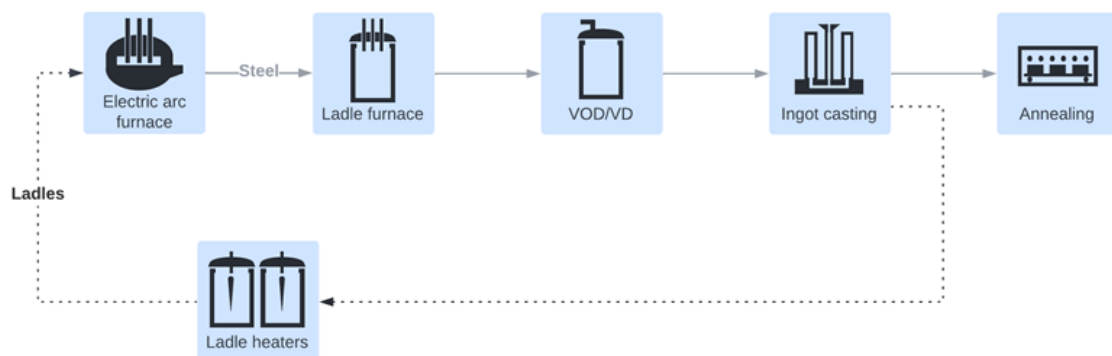
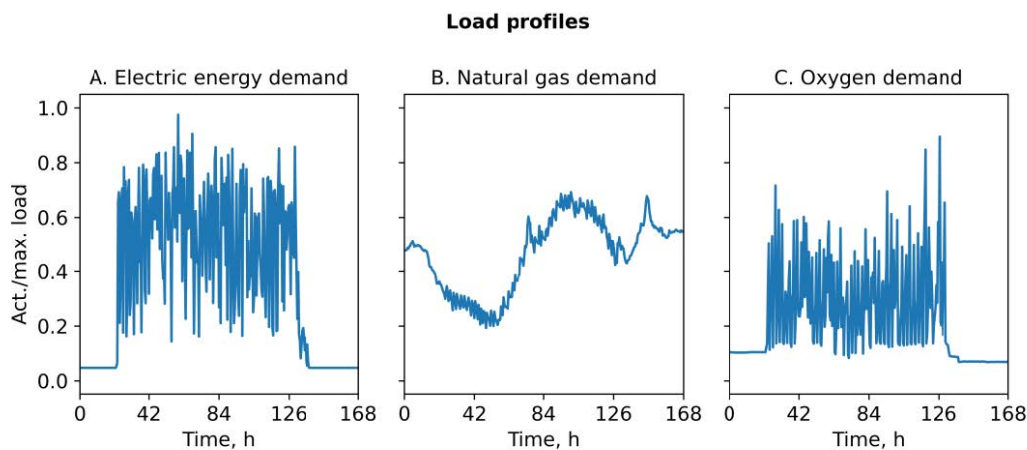


Figure 2. Production process scheme of the considered EAF steel mill.



**Figure 3.** Demand profiles for electric power (A), natural gas (B), and oxygen (C).

#### 2.4. Cost Model

The optimization aims at minimizing the total energy costs ( $C_{tot}$ ) of the steel mill in MEUR within the considered period of a year. Therefore, the cost model includes annual capital ( $A_{CAPEX}$ ) and annual operational expenditures ( $C_{OPEX}$ ) for production, compression, and storage of the product gases and the energy costs ( $C_{energy}$ , Equation (10)) for the overall steel mill reduced by the revenues from hydrogen sales ( $R_{H2\ sales}$ ) (see Equation (5)):

$$C_{tot} = A_{CAPEX} + C_{OPEX} + C_{energy} - R_{H2\ sales} \quad (5)$$

Additionally, the economic performance of the hydrogen scenarios (PEM and SNG) is compared based on the levelized cost of hydrogen (LCOH) and levelized cost of methane (LCOM) in EUR/MWh<sub>HHV</sub> ( $c_{H2}$  and  $c_{SNG}$ ). The LCOH is obtained from Equation (6), where  $A_{CAPEX, H2}$ ,  $A_{CAPEX, O2}$ ,  $C_{OPEX, H2}$ , and  $C_{OPEX, O2}$  are the annual capital and operational expenditures for the oxygen and hydrogen supply equipment.  $c_{O2}$  represents the LCOO in the PSA scenario (see Equation (8)) and  $P_{H2}$  and  $P_{O2}$  are the annual hydrogen and oxygen production in MWh/a and t/a, respectively. The LCOM is determined using Equation (7), where  $A_{CAPEX, SNG}$ ,  $A_{OPEX, SNG}$ , and  $C_{energy, SNG}$  are the annual capital, operational, and energy costs for SNG production.  $M_{H2}$  is the amount of hydrogen supplied to the methanation plant and  $P_{SNG}$  is the annual SNG production:

$$c_{H2} = \frac{A_{CAPEX, H2} + A_{CAPEX, O2} + C_{OPEX, H2} + C_{OPEX, O2} + C_{energy, H2} - c_{O2} \cdot P_{O2}}{P_{H2}} \quad (6)$$

$$c_{SNG} = \frac{A_{CAPEX, SNG} + A_{OPEX, SNG} + C_{energy, SNG} + c_{H2} \cdot M_{H2}}{P_{SNG}} \quad (7)$$

$$c_{O2} = \frac{A_{CAPEX, O2} + C_{OPEX, O2} + C_{energy, O2}}{P_{O2}} \quad (8)$$

Most of the studies cited in this article anticipate that both energy and capital costs for power-to-gas technologies will change substantially over the period between 2020 and 2030. The volatility of energy costs is underlined by the 2022 distortions on global energy markets, caused by the Russian attack on Ukraine. In order to analyze the impact of variable commodity prices and investment costs, we assess all scenarios based on the historical costs of 2020 and on projected costs for the years 2030 and 2050. All projections are based on high-level studies for the European energy markets [43,44].

##### 2.4.1. Equipment Cost

Table 3 provides a breakdown of the costs and lifetimes of individual plant components. In 2013, with specific investment costs of around 2000 EUR/kW, PEM electrolysis plants were about twice as expensive as their alkaline counterparts [28], whereas more recent data

from 2018 cites costs from 1000 to 1500 EUR/kW for both alkaline and PEM systems [45]. A report commissioned by the Fuel Cells and Hydrogen Joint Undertaking estimates that the system costs for PEM electrolysis will decrease from 700–1300 EUR/kW in 2020 to 250–1270 EUR/kW by the year 2030 [46]. For the methanation unit, specific investment costs of 450 EUR/kW of synthetic natural gas are estimated [35]. For the calculation of the annual capital costs for the implemented equipment, we assume an interest rate of 4% [8]. Typical operational costs for the implemented equipment are fixed at 1 to 3% of CAPEX per year [35,46].

**Table 3.** Specific equipment costs for the years 2020, 2030, and 2050.

Cost Component	Unit	2020	2030	2050	Reference
VPSA unit					
CAPEX	EUR/kW <sub>el</sub>	3000	3000	3000	calculated from [21] own assumption [21]
OPEX	%CAPEX	2	2	2	
Lifetime	a	10	10	10	
PEM electrolysis unit					
CAPEX	EUR/kW <sub>el</sub>	1000	750	500	[39,46]
OPEX	%CAPEX	2.75	2.75	2.75	[35]
Lifetime	a	20	20	20	[35]
Methanation unit					
CAPEX	EUR/kW <sub>SNG</sub>	450	450	450	[35]
OPEX	%CAPEX	3	3	3	[35]
Lifetime	a	20	20	20	[35]
Buffer storage					
CAPEX	EUR/m <sup>3</sup>	50	50	50	[35,45]
OPEX	%CAPEX	1	1	1	[35]
Lifetime	a	20	20	20	[35]
O <sub>2</sub> compressor					
CAPEX	EUR/kW <sub>el</sub>	1100	1100	1100	calculated from [47] own assumption
Lifetime	a	10	10	10	
H <sub>2</sub> compressor					
CAPEX	EUR/kW <sub>el</sub>	700	700	700	calculated from [47] own assumption
Lifetime	a	10	10	10	
CO <sub>2</sub> compressor					
CAPEX	EUR/kW <sub>el</sub>	1480	1480	1480	calculated from [47] own assumption
Lifetime	a	10	10	10	

Investment costs for the PSA, electrolysis, and methanation plants and the storage tanks and compressors are allocated to the assessment period by applying the annuity method (9). The annuity ( $A_{CAPEX}$ ) is calculated by multiplying the investment costs for the individual assets ( $I$ ) by an annuity factor, which depends on the interest rate ( $i$ ) and the depreciation period ( $n$ ). The individual assets are depreciated over their useful life to facilitate the economic comparison of different technologies using leveled costs:

$$A_{CAPEX} = I \cdot \frac{(1+i)^n \cdot i}{(1+i)^n - 1} \quad (9)$$

#### 2.4.2. Energy Costs

In terms of energy costs, we take into account the purchase of electrical energy, natural gas, and carbon dioxide emission allowances (see Equation (10)).  $p_{EE}$ ,  $p_{NG}$ , and  $p_{EA}$  represent the prices for electric energy, natural gas, and emission allowances in EUR/kWh and EUR/tCO<sub>2</sub>, respectively;  $D_{EE}$  and  $D_{NG}$  are the respective demand both in kWh/h, and  $SR$  is the substitution rate of natural gas either by hydrogen or SNG in %<sub>HHV</sub>. SCE represents the specific carbon dioxide emissions of natural gas in kg/kWh<sub>CH<sub>4</sub></sub>:

$$C_{energy} = \sum_t D_{EE}(t) \cdot p_{EE}(t) + D_{NG}(t) \cdot (1 - SR(t)) \cdot (p_{NG} + SCE \cdot p_{EA}) \quad (10)$$

In our model, surplus hydrogen in kg/h ( $M_{H_2 \text{ surplus}}$ ) is sold at a fixed price in EUR/kg<sub>H2</sub> ( $p_{H_2}$ ), generating annual revenues in EUR/a ( $R_{H_2 \text{ sales}}$ ) that contribute to covering the total costs (11):

$$R_{H_2 \text{ sales}} = \sum_t M_{H_2 \text{ surplus}}(t) \cdot p_{H_2} \quad (11)$$

For the 2020 scenario, we adopt the historical 2020 spot market prices, whereas for the future scenarios, estimated prices for the year 2030 are applied. In 2020, the average day-ahead electricity price at the Energy Exchange Austria (EXAA) was 33 EUR/MWh with a standard deviation of 17 EUR/MWh [48]. The development of electricity prices between 2020 and 2050 reflects the higher demand of flexibility options to balance demand and production, the rising primary energy demand, and the anticipated price surge for CO<sub>2</sub> emission allowances [43]. To cope with the mentioned influence factors on electricity prices, two aspects are considered for the estimated electricity price forecasts for 2030 and 2050:

- The development of the annual mean value of the electricity price [44]; and
- The development of the number of extreme price situations (higher than 100 €/MWh and lower than 0 €/MWh) [43].

However, the current (2022) situation on the energy markets makes it necessary to mention the high degree of uncertainty of such price projections. In the approach proposed by Taupmann et al. [49], first, the historical quarter-hourly spot market price profile from 2020 is scaled based on the predicted annual mean prices in 2030 and 2050 obtained from the EU Energy Outlook [44]. However, extreme price situations are not sufficiently represented by this scaling. To depict them, the duration curves of the scaled price profiles are additionally fitted. The resulting duration curves not only reflect the annual mean values but also the number and duration of extreme price situations estimated in the literature [43,44]. Finally, the individual quarter-hourly electricity prices in the annual profile are adjusted according to the fitted duration curve. This approach results in a mean electricity price of 62 EUR/MWh with a standard deviation of 37 EUR/MWh for 2030 and a mean electricity price of 82 EUR/MWh with a standard deviation of 66 EUR/MWh for 2050. Figure 4 compares the day-ahead prices traded at the EXAA in 2020 with those predicted for 2030 and 2050. Both the price profile (A) and the ordered duration curve (B) reflect the rising average and the increasing extreme prices through 2050.

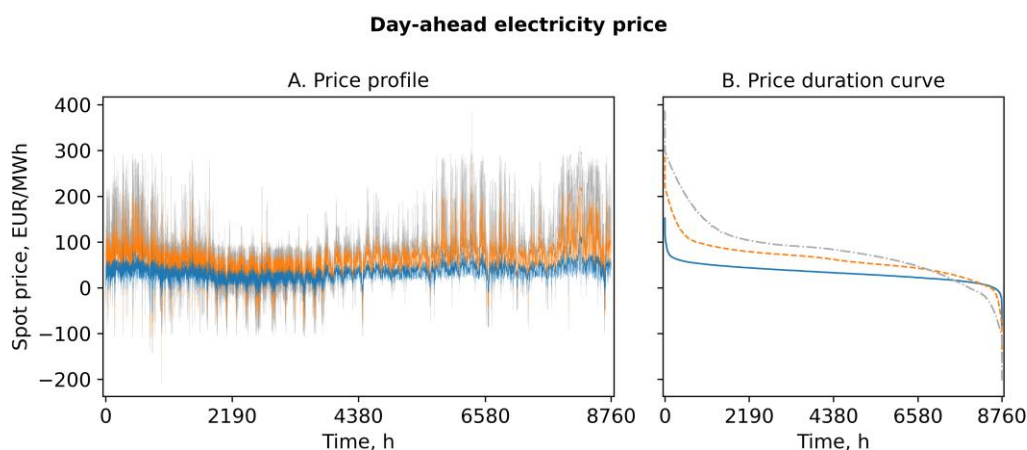


**Figure 4.** Comparison of the historical and forecasted (FC) electricity wholesale price profiles (A) and duration curves (B) for 2020 (blue), 2030 (orange), and 2050 (grey).

In its World Energy Outlook 2021, the IEA [50] provides forecasts on natural gas prices in the European Union. Starting from 13 EUR/MWh in 2020, the net-zero emissions scenario projects a slight decrease in wholesale prices to 12 EUR/MWh in 2030 and 11 EUR/MWh in 2050. Additionally, here, it needs to be said that the actual uncertainty on the natural gas market leads to a lack of meaningful price prognoses. The prices used for

this work are based on data published before the Ukrainian war and should, therefore, be treated as data with high uncertainty.

The mean prices for emission allowances are assumed to increase from 24 EUR/t CO<sub>2</sub> in 2020 [51] to 130 EUR/t CO<sub>2</sub> in 2030 [50,52] and 250 EUR/t CO<sub>2</sub> in 2050 [50]. In their study on the integration of hydrogen into the natural gas system, Cvetkovska et al. [53] expect the cost of hydrogen to fall from 146 EUR/MWh in 2020 to 61 EUR/MWh in 2050. Table 4 summarizes the estimated wholesale prices for different energy carriers, gases, and emission allowances.

**Table 4.** Commodity wholesale prices for the years 2020, 2030, and 2050.

Cost Component	Unit	2020	2030	2050	Reference
electric energy (mean)	EUR/MWh	33	62	82	[43,44,48]
natural gas	EUR/MWh <sub>HHV</sub>	13	12	11	[50]
hydrogen	EUR/MWh <sub>HHV</sub>	146	101	61	[53]
emission allowances	EUR/t	24	130	250	[50–52]

The listed prices for natural gas are surcharged by grid charges of 2.2 EUR/MWh [54], a natural gas levy of 5.8 EUR/MWh, and a value added tax of 20% [55]. Regarding the electricity prices, these differ between PSA and electrolysis units: For the PSA unit, the electricity costs include grid charges of 18 EUR/MWh [56], an electricity levy of 15 EUR/MWh, and a value added tax of 20% [57], whereas for the electrolysis unit (scenario PEM and SNG), only the wholesale power price is considered. This approach is based on the assumption that production plants for green gases are not subject to grid charges [58]. Moreover, we stipulate that due to their system-serving operation, all the gas production facilities are exempt from other fees and taxes on electric energy.

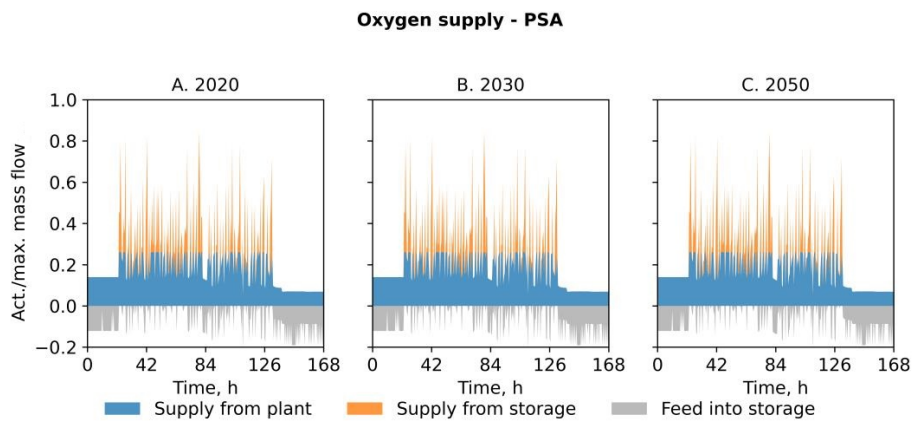
### 3. Results and Discussion

In the following section, we will present the results of our optimization-based investigations. According to our research questions (see Section 1.3), we will analyze the scenarios, with a focus on demand-side management and carbon dioxide emissions. We will formulate feasible strategies for an economically viable operation of the explained technologies to be integrated.

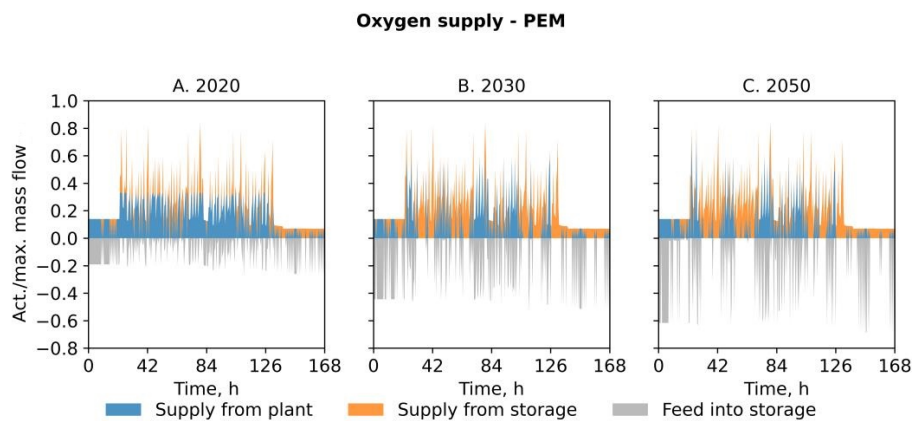
#### 3.1. General Results

Figure 5 describes the supply of the time-resolved oxygen demand by the PSA unit for one week in the years 2020, 2030, and 2050. Owing to its limited load range, the PSA unit is continuously in operation, with the demand peaks that occur between hour 30 and 130 being covered by the storage tank. In addition, the high share of CAPEX in the LCOO and the lack of opportunities for product sales obliges the plant to operate at high full-load hours, regardless of the electricity prices. This is substantiated by the fact that the plant operates at full load during periods of low demand and on weekends. Hence, the mode of operation does not change throughout the years 2020 to 2050.

In contrast, the electrolysis implemented in scenario PEM operates over the full load range, depending on the hydrogen and oxygen demand and electricity prices. As indicated by Figure 6, it shuts down during periods of high electricity prices, meets the oxygen demand from the storage, and refills it during periods of lower prices. Therefore, the increase in electricity price volatility from 2020 to 2050 results in more frequent and longer periods of production interruptions and an extensive exploitation of the available load range.



**Figure 5.** Covering the oxygen demand of the steel mill deploying a PSA for oxygen production in the years 2020 (A), 2030 (B) and 2050 (C).



**Figure 6.** Covering the oxygen demand of the steel mill deploying PEM electrolysis for hydrogen and oxygen production in the years 2020 (A), 2030 (B) and 2050 (C).

The oxygen supply profile in the scenario SNG, which is depicted in Figure 7, features individual production peaks that increase with a growing number of extreme price situations and a decreasing specific CAPEX towards 2050. The constant operation of the electrolysis unit, which is particularly visible in the year 2050, is caused by the limited operating window of the methanation unit and the boundary condition that all CO<sub>2</sub> must be used for methanation. Apart from that, this configuration provides a comparable degree of flexibility as the PEM scenario.

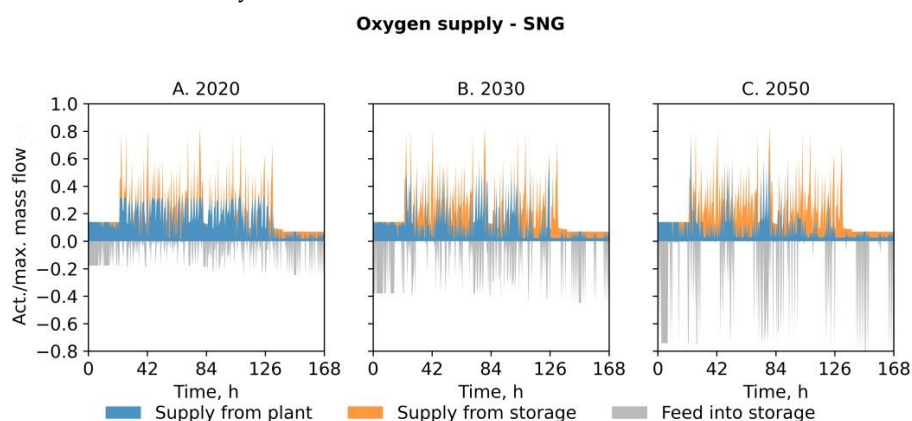


**Figure 7.** Covering the oxygen demand of the steel mill deploying PEM electrolysis for oxygen and hydrogen and a subsequent methanation unit for SNG production in the years 2020 (A), 2030 (B) and 2050 (C).



Table 5 lists the indicators derived from the time series that were obtained from the optimization model. The nominal power of the electrolysis system (scenario PEM and SNG) clearly exceeds that of the PSA unit in all scenarios. On the one hand, the specific energy demand for electrolysis is about ten times higher than for pressure swing adsorption. On the other hand, the latter produces the same amount of oxygen at less full-load hours. The annual net production of 42 GWh of hydrogen in scenarios PEM and SNG offsets the higher energy consumption of the PEM unit. Since the production units have to meet the specified oxygen demand profile without venting excess oxygen, the production volumes of oxygen, hydrogen, and SNG in the PEM and SNG scenarios remain constant over the investigated years.

**Table 5.** Resulting key performance indicators for the optimization scenarios.

KPI	Unit	2020			2030			2050		
		PSA	PEM	SNG	PSA	PEM	SNG	PSA	PEM	SNG
Scenario	-	PSA	PEM	SNG	PSA	PEM	SNG	PSA	PEM	SNG
Nominal power	kW <sub>el</sub>	400	10,600	10,185	400	16,900	15,100	400	20,000	23,300
Full-load hours	hrs	7439	5876	6119	7439	3325	3738	7439	2567	2202
H <sub>2</sub> production	MWh <sub>HHV</sub> /a	-	42,400	42,400	-	42,400	42,400	-	42,400	42,400
SNG production	MWh <sub>HHV</sub> /a	-	-	8600	-	-	8600	-	-	8600
CAPEX share	%	45	30	30	37	31	28	34	32	36
Fuel substitution	% <sub>HHV</sub>	-	0	15	-	0	15	-	45	19

The electrolysis operation depends not only on the electricity price and oxygen demand but also on the natural gas demand. The fuel substitution is a measure for the internal utilization of the produced hydrogen and SNG in the steel mill. In the years 2020 and 2030, it is more profitable to sell the hydrogen and procure natural gas from the grid. In the absence of economic alternatives, merely the produced SNG is consumed as a fuel. Conversely, in the PEM 2050 scenario, 45% of the gas demand is covered by on-site produced hydrogen. In scenario SNG, the restriction of the limited admixture of natural gas into the internal gas network implies that the major share of hydrogen must be sold, even if the on-site substitution of natural gas was more cost efficient. However, this leads to higher flexibility and thus the improved exploitation of favorable electricity prices. As a result, the SNG 2050 scenario achieves lower full-load hours than the PEM 2050 scenario.

### 3.2. Demand-Side Management Potential

A comparison of both the supply profiles (Figures 5–7) and the full-load hours (Table 5) indicates that the electrolysis-based scenarios (PEM, SNG) provide more flexibility with respect to a power price-driven operation schedule compared to the PSA scenario. However, the number of full-load hours alone is not a sufficient indicator for evaluating the plant concepts regarding the demand-side management potential. For CAPEX-intensive plants (scenario PSA), the optimizer tends to meet the specified oxygen demand with the minimum installed production and storage capacity, without considering the electricity price. In this case, the oxygen load profile determines the full-load hours rather than the electricity price signal.

Therefore, the mean price of purchased electrical energy, referred to as the effective average price ( $p_{effective\ average}$ ), for the individual gas production units was considered to assess the flexibility potential of the different scenarios (see Table 6).  $p_{effective\ average}$  is determined according to Equation (12), where  $p_{EE}(n)$  represents the electricity price and  $D_{EE}(n)$  is the demand for electric energy for each time step  $n$ :

$$p_{effective\ average} = \frac{\sum_{n=1}^t p_{EE}(n) \cdot D_{EE}(n)}{\sum_{n=1}^t D_{EE}(n)} \quad (12)$$

**Table 6.** Annual, ordered, and effective electricity prices for 2020, 2030, and 2050.

Electricity Prices	Scenario	Unit	2020	2030	2050
Annual average	-	EUR/MWh	33	62	82
Ordered average	PSA	EUR/MWh	28	51	62
	PEM	EUR/MWh	24	29	11
	SNG	EUR/MWh	25	32	4
Effective average	PSA	EUR/MWh	49	76	94
	PEM	EUR/MWh	28	38	34
	SNG	EUR/MWh	28	41	33

For orientation, the effective average price and the annual average price defer in terms of the number of time steps being used for their calculation: For the calculation of the annual average price, all time steps of a year ( $15 \times 8760$ ) are taken into account. For the calculation of the effective average price, only these time steps are used in which the respective plant is actually operating. The ordered average price, however, takes into account only the cheapest electricity prices for the same number of time steps. Equation (13) specifies the relationship between the price duration curve ( $DC$ ) and its ordered average ( $p_{ordered\ average}$ ) at any given number of load hours ( $t$ ):

$$p_{ordered\ average}(t) = \frac{1}{t} \cdot \sum_{n=1}^t DC(n) \quad (13)$$

The difference between the effective and ordered average price is a measure of how effective the respective plant is operated in terms of using low electricity prices for its operation. For the comparison of the three supply systems, the presented effective average price of the PSA was adjusted by subtracting taxes and grid charges (see Section 2.4.2).

Figure 8 depicts the ordered average price as a function of the number of full-load hours that is derived from the price duration curve. Moreover, the optimization results for the three scenarios are marked in the diagram, based on the mean purchased electricity price and full-load hours. The closer the points in Figure 8 are to the mean price curve, the more effectively the plant exploits periods of low power prices. In this context, the curve represents the border case: When the effective average price equals the ordered average for the considered number of full-load hours, the plant provides the maximum flexibility. The data in Tables 5 and 6 supports the previously observed findings: The electrolysis-based scenarios feature the highest degree of flexibility. This is reflected by significantly less full-load hours and a lower effective average price compared to the PSA unit throughout the years 2020, 2030, and 2050.

### 3.3. Carbon Dioxide Emissions

For the calculation of carbon dioxide emissions, we assume that the oxygen and hydrogen production plants are supplied solely with zero-emission electricity from renewable generation. Regarding the oxygen production, the CO<sub>2</sub> emissions attributable to scope 2, which are dependent on the specific emissions of electricity generation, are cut down to zero in the scenario PSA by this measure. Under the same assumption, scope 2 emissions are eliminated and in scenario PEM and SNG. In addition, due to the generation of CO<sub>2</sub>-neutral energy carriers such as hydrogen and SNG, fossil fuels such as natural gas are substituted.

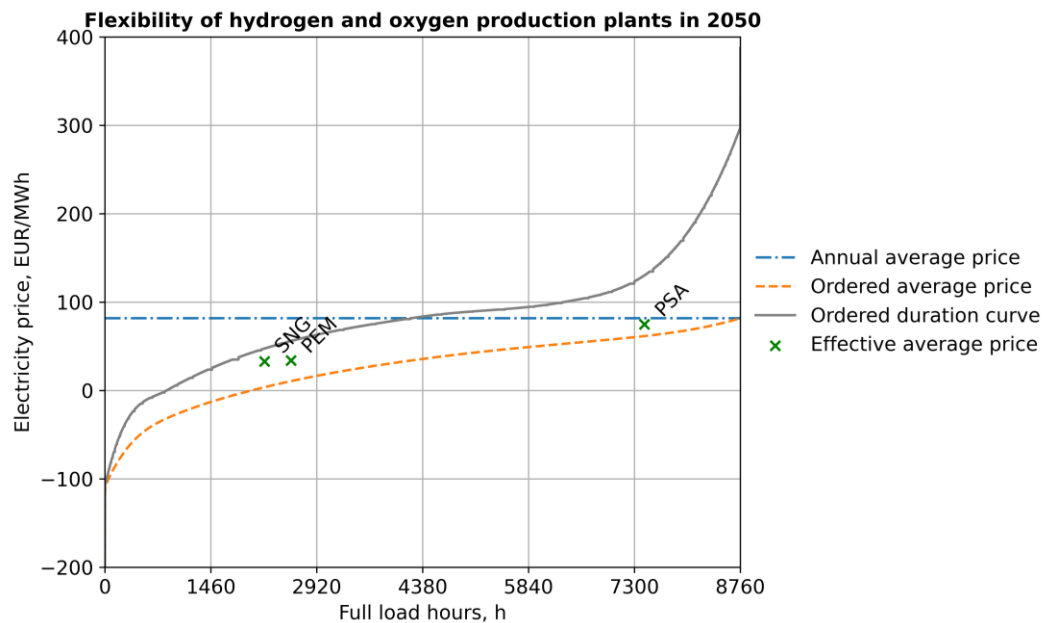


**Figure 8.** Purchased electricity price in relation to full-load hours.

Figure 9 shows the normalized gas demand profile that is covered by natural gas from the grid and SNG and hydrogen from on-site production for one week. In scenario PEM, the unlimited range for hydrogen admixture results in the substitution of the entire natural gas demand by hydrogen in several time steps. In scenario SNG, the specified maximum hydrogen content in the fuel and the availability of carbon dioxide for methanation are limiting the substitution of natural gas by hydrogen and SNG. Both scenarios, however, lead to substantial natural gas and carbon dioxide emission savings.

#### Direct fuel substitution

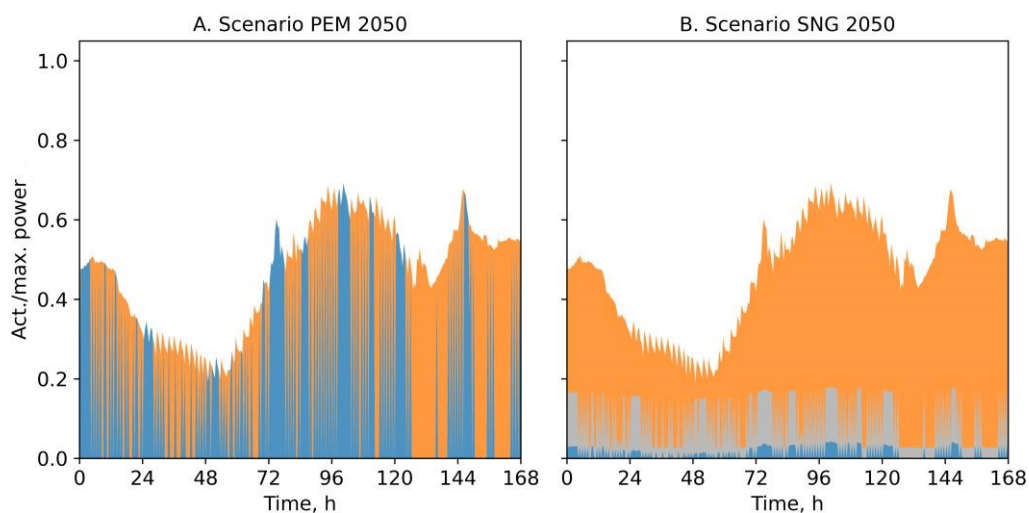


**Figure 9.** Substitution of natural gas (orange) by hydrogen (blue) and SNG (grey) for the scenarios PEM 2050 (A) and SNG 2050 (B).

Depending on where the produced gases are deployed, CO<sub>2</sub> emissions are reduced either within the steel mill (internal reduction) and/or in the higher-level energy system (external reduction). If hydrogen and SNG are consumed directly in the steel mill, scope 1 emissions of the steel mill are reduced. The injection of climate-neutral gases into the public gas grid reduces the specific emissions of the overall gas system. Since the amount of produced hydrogen and therefore that of substituted natural gas is constant over the

years, the total annual CO<sub>2</sub> emission savings amount to 7100 t for all PEM scenarios (see Table 7). In 2020 and 2030, the sale of hydrogen is more profitable than internal admixture, thus emissions are only reduced externally. In scenario PEM 2050, due to the internal utilization of hydrogen, 4600 t were saved as scope 1 emissions within the EAF steel mill and an additional 2500 t in the higher-level energy system. In the SNG scenarios, the total annual emission cut decreases to 6300 t due to the energy losses related to the methanation process. The mill-internal SNG admixture reduces internal emissions by 1500 t. Compared to scenario PEM 2050, the hydrogen admixture limit in scenario SNG 2050 constrains the steel mill-internal scope 1 emission reduction to an additional 300 t. However, the injection of excess hydrogen into the gas grid results in annual CO<sub>2</sub> emission savings of 4500 t CO<sub>2</sub> in the higher-level energy system.

**Table 7.** Reduction of internal (scope 1) and external (grid) CO<sub>2</sub> emissions.

KPI	Unit	2020		2030		2050	
		PEM	SNG	PEM	SNG	PEM	SNG
Scenario	-	PEM	SNG	PEM	SNG	PEM	SNG
Internal	t <sub>CO2</sub>	7100	4800	7100	4800	2500	4500
External	t <sub>CO2</sub>	0	1500	0	1500	4600	1800
Total	t <sub>CO2</sub>	7100	6300	7100	6300	7100	6300

### 3.4. Economic Assessment

In our case study, the specific costs for on-site production of oxygen via PSA will increase through 2050 due to growing electricity prices (Table 5). The scenarios involving the operation of an electrolysis plant (PEM and SNG) are also affected by increasing electricity prices. In addition, they cause substantially higher investment and energy costs. However, revenues from the hydrogen sales and savings from the substitution of natural gas by hydrogen or SNG compensate for higher costs. Consequently, the prices for electricity, natural gas, and CO<sub>2</sub> emission allowances are crucial for an economical operation of a power-to-gas plant. Table 6 demonstrates that the higher flexibility of the electrolysis will result in lower effective average electricity costs under highly fluctuating electricity prices in 2050 than under moderate power prices and less price volatility in 2030. In addition, specific CAPEX, especially for electrolysis units, will decrease over time.

Table 8 compares the levelized cost of hydrogen (LCOH) and SNG (LCOM) at the investigated power-to-gas plant against a reference LCOH (LCOH<sub>REF</sub>). The LCOO is determined by the PSA scenario, which is excluded from the following analysis due to the absence of hydrogen production. As a benchmark, we take into account the levelized costs that are achieved by the electrolysis units with the capacities and full-load hours specified in Table 5 without oxygen utilization. For this purpose, we assume that the units operate under nominal load and obtain electricity at the respective ordered average price (see Table 6).

**Table 8.** Comparison of the levelized cost of oxygen, hydrogen, SNG, and the reference LCOH.

KPI	Unit	2020		2030		2050	
		PEM	SNG	PEM	SNG	PEM	SNG
Scenario	-	PEM	SNG	PEM	SNG	PEM	SNG
LCOO	EUR/MWh <sub>HHV</sub>	77	77	93	93	103	103
LCOH	EUR/MWh <sub>HHV</sub>	52	52	65	66	47	50
LCOM	EUR/MWh <sub>HHV</sub>	-	94	-	120	-	97
LCOH <sub>REF</sub>	EUR/MWh <sub>HHV</sub>	77	78	87	90	43	35

In the years 2020 and 2030, the LCOH in both the PEM and SNG scenario significantly undercuts the reference price due to the additional oxygen utilization. Only in 2050, the LCOH of these scenarios exceeds the reference value. In view of the given oxygen demand, the PtG plant is increasingly incapable of optimally exploiting the highly fluctuating and, above all, seasonally varying electricity price. The rising average electricity price leads to

an increasing LCOO for the relatively inflexible operation of the PSA. This also increases the cost savings from the oxygen utilization in the electrolysis scenarios. Owing to the higher CAPEX and OPEX and the energy losses, the LCOM clearly exceeds the LCOH.

Figure 10 indicates the estimated LCOH; the natural gas price, including CO<sub>2</sub> emission allowances, charges, and taxes as described in Section 2.4.2; and the hydrogen prices for 2020, 2030, and 2050. In 2020 and 2030, the spread between the LCOH and the anticipated sales price suggests a highly profitable operation of the electrolyzer. However, in reality, there is a lack of the necessary infrastructure and the market for renewable hydrogen. The cost-efficient substitution of natural gas by internal admixture of hydrogen or injection into the gas grid is impeded by the low natural gas prices. Finally, starting at point P1, the substitution of natural gas with hydrogen is economically viable; from point P2, internal hydrogen utilization is more cost efficient than sales. Since LCOM exceeds the price of natural gas, including the emission costs, in all years, SNG production is not profitable based on the underlying conditions.

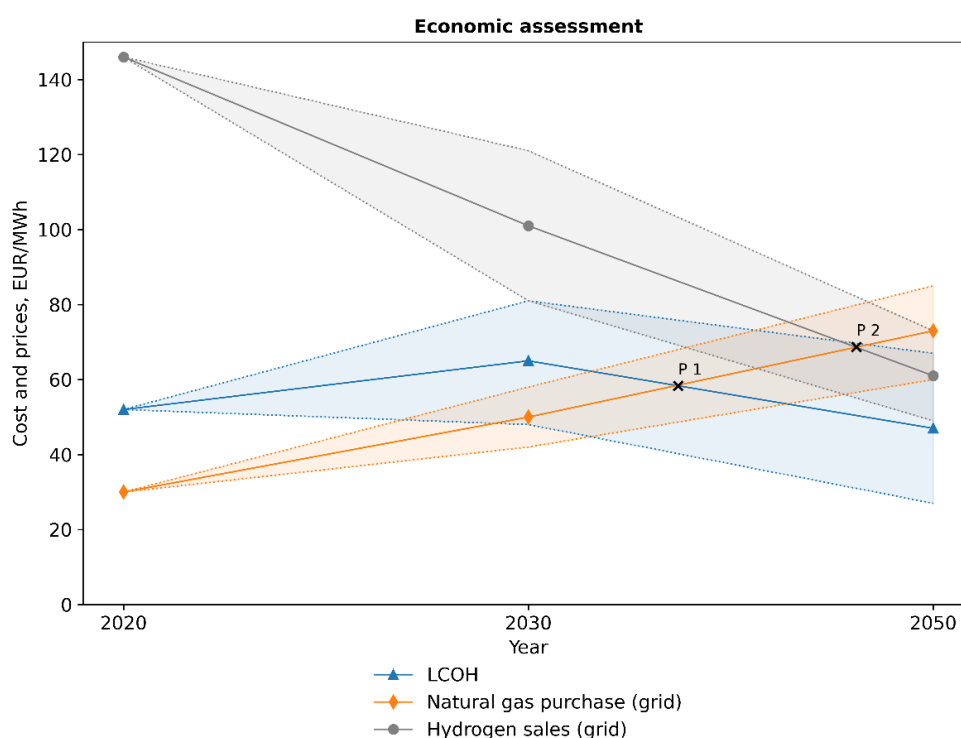


**Figure 10.** Comparison of the levelized cost of hydrogen and SNG with natural gas and hydrogen prices.

In view of the high degree of uncertainty regarding the assumptions for future years, we performed a sensitivity analysis: The prices for electricity on the day-ahead spot market, CO<sub>2</sub> emission allowances, natural gas, and hydrogen sales each varied by 20%. The dashed lines in Figure 10 represent the maximum deviations from the anticipated costs and prices from the original scenarios. According to our analysis, the substitution of natural gas by hydrogen based on PEM electrolysis while utilizing the by-product oxygen is economically viable under the condition of rising CO<sub>2</sub> certificate prices, highly volatile electricity prices, and declining electrolyzer CAPEX. Under the stated assumptions, this situation is likely to occur between 2030 and 2050. In contrast, due to the higher levelized cost, the replacement of natural gas with SNG is only economically viable in the event of an extreme rise in natural gas and/or CO<sub>2</sub> emission allowance prices (see Table 8). Therefore, the current surge of emission certificate and natural gas prices might enable investments in technologies for a climate-neutral energy supply.

#### 4. Conclusions

In the conclusion, we present concise qualitative and quantitative answers to the research questions formulated in Section 1.3:

**Q 1.a.** *Which basic plant layouts seem to be possible based on state-of-the-art technologies?*

The results of the optimization suggest that all of the three investigated system layouts, including the implementation of a PSA unit, a PEM electrolysis plant, and a combination of electrolysis and methanation, are feasible options for the oxygen supply of the steel mill. If the gas infrastructure such as burners, piping, and fittings are compatible with natural gas-hydrogen mixtures, the co-production of hydrogen and oxygen by electrolysis followed by the direct utilization of both product gases is the best option in terms of energy efficiency, carbon dioxide reduction, and economic viability. From the point at which the LCOH falls below the price of natural gas, including the cost for emission allowances, the admixture of hydrogen into the gas network becomes viable. Exchanging gas with the grid eliminates the need to implement storage and allows for arbitrage operation. After subtracting the costs for oxygen supply resulting from the PSA scenario, the optimized plant configuration yields an LCOH of 47 EUR/MWh in 2050. If the implemented infrastructure is not hydrogen compatible, the methanation of CO<sub>2</sub> offers an alternative. The use of CO<sub>2</sub> from combustion processes for methanation enables the production of a carbon-neutral fuel. However, the conversion of hydrogen to methane implies higher capital and operational expenditures and energy losses, resulting in LCOM of 97 EUR/MWh in 2050. Moreover, ensuring sufficient availability of carbon dioxide is a critical prerequisite. Therefore, SNG production is not profitable under the defined framework conditions but qualifies as a bridging technology facing the limited hydrogen compatibility of the gas infrastructure.

**Q 1.b.** *Which basic operational strategies are useful under which boundary conditions?*

Considering the high share of electricity cost in the levelized cost of oxygen and hydrogen, it is essential to minimize the effective average electricity prices. Therefore, with increasing electricity price fluctuations and decreasing specific CAPEX for the electrolysis plant over time, larger hydrogen production capacities are advantageous, despite lower full-load hours. Adequate buffer storage capacity for produced gases is required in all scenarios not only to balance supply and demand but also to ramp up production in periods of favorable electricity prices and thus cut down on effective electricity prices.

**Q 2.** *What is their impact on the overall energy system in terms of demand-side management potential and carbon dioxide emissions?*

Due to the narrow load range and the high specific investment costs, the PSA offers limited demand-side flexibility. The potential CO<sub>2</sub> emission savings are restricted to the reduction of specific CO<sub>2</sub> emissions of the supplied power (scope 2). The scenarios based on electrolysis (PEM and SNG), however, show a high degree of flexibility. This is reflected by less full-load hours in the range of 3300–3700 h in 2030 and 2200–2600 h in 2050 and 46–65% lower effective average electricity prices compared to the PSA scenario. Assuming that the electrolysis process is supplied with CO<sub>2</sub>-emission-neutral electricity, the substitution of natural gas with hydrogen and synthetic methane results in considerable emission savings in the steel mill and in the higher-level energy system. Depending on the system configuration, the absolute emission reduction corresponds to 40–50% of the scope 1 CO<sub>2</sub> emissions of the steel mill.

**Q 3.** *Which economic framework conditions are required for their economically viable operation?*

Low electricity prices and specific investment costs favor the use of power-to-gas technologies. Furthermore, increasing emission allowance prices are decisive for the substitution of natural gas by green gases such as hydrogen or SNG. In their long-term strategy for a climate-neutral economy [59], the European Commission emphasizes the relevance of the ETS in achieving its climate goals. As demonstrated in our study, emission allowance

prices serve as a price signal that triggers investments in climate-neutral technologies. For an emission reduction between 80 and 100%, carbon dioxide prices in the range of 250 to 350 EUR/tCO<sub>2</sub> are expected by 2050. Hence, the decreasing specific capital expenditures, the increase in situations with extremely low electricity prices, and the expected surge of emission certificate prices towards the year 2050 make PEM electrolysis not only a viable flexibility option for the future electricity grid but also an effective enabler for a climate-neutral energy system.

**Author Contributions:** Conceptualization, J.D. and T.K.; methodology, J.D. and T.K.; software, S.W.; validation, J.D.; formal analysis, J.D., S.W. and A.T.; investigation, J.D. and S.W.; resources, J.D.; data curation, J.D., S.W. and A.T.; writing—original draft preparation, J.D., T.K. and A.T.; writing—review and editing, T.K.; visualization, J.D.; supervision, T.K.; project administration, J.D.; funding acquisition, T.K. All authors have read and agreed to the published version of the manuscript.

**Funding:** This work was carried out as part of the OxySteel project. OxySteel is a subproject of NEFI—New Energy for Industry, a flagship region funded by the Climate and Energy Funds Austria.

**Institutional Review Board Statement:** Not applicable.

**Informed Consent Statement:** Not applicable.

**Data Availability Statement:** Not applicable.

**Conflicts of Interest:** The authors declare no conflict of interest.

## References

1. Material Economics. Industrial Transformation 2050—Pathways to Net-Zero Emissions from EU Heavy Industry. 2019. Available online: <https://materialeconomics.com/publications/industrial-transformation-2050> (accessed on 21 October 2021).
2. International Energy Agency. Iron and Steel Technology Roadmap, Paris. 2020. Available online: <https://www.iea.org/reports/iron-and-steel-technology-roadmap> (accessed on 22 October 2021).
3. The Boston Consulting Group (BCG), Steel Institute VDEh. Steel's Contribution to a Low-Carbon Europe 2050: Technical and Economic Analysis of the Sector's CO<sub>2</sub> Abatement Potential. 2013. Available online: <https://www.bcg.com/publications/2013/metals-mining-environment-steels-contribution-low-carbon-europe-2050> (accessed on 13 January 2022).
4. ICF Consulting Services Limited, Fraunhofer Institute for Systems and Innovation Research. Industrial Innovation: Pathways to Deep Decarbonisation of Industry: Part 2: Scenario Analysis and Pathways to Deep Decarbonisation. 2019. Available online: <https://www.isi.fraunhofer.de/de/competence-center/energietechnologien-energiesysteme/projekte/pathways.html#3> (accessed on 28 October 2021).
5. World Resources Institute, World Business Council for Sustainable Development. The Greenhouse Gas Protocol. Available online: <https://ghgprotocol.org/standards> (accessed on 19 November 2021).
6. Dock, J.; Kienberger, T. Techno-economic case study on Oxyfuel technology implementation in EAF steel mills—Concepts for waste heat recovery and carbon dioxide utilization. *Clean. Eng. Technol.* **2022**, *9*, 100525. [\[CrossRef\]](#)
7. Bussar, C.; Stöcker, P.; Cai, Z.; Moraes Jr., L.; Magnor, D.; Wiernes, P.; van Bracht, N.; Moser, A.; Sauer, D.U. Large-scale integration of renewable energies and impact on storage demand in a European renewable power system of 2050—Sensitivity study. *J. Energy Storage* **2016**, *6*, 1–10. [\[CrossRef\]](#)
8. Greiml, M.; Fritz, F.; Kienberger, T. Increasing installable photovoltaic power by implementing power-to-gas as electricity grid relief—A techno-economic assessment. *Energy* **2021**, *235*, 121307. [\[CrossRef\]](#)
9. Dock, J.; Janz, D.; Weiss, J.; Marschnig, A.; Kienberger, T. Time- and component-resolved energy system model of an electric steel mill. *Clean. Eng. Technol.* **2021**, *4*, 100223. [\[CrossRef\]](#)
10. Madias, J. Electric furnace steelmaking. In *Treatise on Process Metallurgy*; Elsevier: Kidlington, Oxford, UK; Waltham, MA, USA, 2014; pp. 271–300. ISBN 978-0-08-096988-6.
11. Holappa, L. Secondary steelmaking. In *Treatise on Process Metallurgy*; Elsevier: Kidlington, Oxford, UK; Waltham, MA, USA, 2014; pp. 301–345. ISBN 978-0-08-096988-6.
12. Warren, P. A review of demand-side management policy in the UK. *Renew. Sustain. Energy Rev.* **2014**, *29*, 941–951. [\[CrossRef\]](#)
13. Paulus, M.; Borggreffe, F. The potential of demand-side management in energy-intensive industries for electricity markets in Germany. *Appl. Energy* **2011**, *88*, 432–441. [\[CrossRef\]](#)
14. Strbac, G. Demand side management: Benefits and challenges. *Energy Policy* **2008**, *36*, 4419–4426. [\[CrossRef\]](#)
15. Marchiori, F.; Belloni, A.; Benini, M.; Cateni, S.; Colla, V.; Ebel, A.; Lupinelli, M.; Nastasi, G.; Neuer, M.; Pietrosanti, C.; et al. Integrated dynamic energy management for steel production. *Energy Procedia* **2017**, *105*, 2772–2777. [\[CrossRef\]](#)
16. Zhang, Q.; Grossmann, I.E. Enterprise-wide optimization for industrial demand side management: Fundamentals, advances, and perspectives. *Chem. Eng. Res. Des.* **2016**, *116*, 114–131. [\[CrossRef\]](#)

17. Gorre, J.; Ortlhoff, F.; van Leeuwen, C. Production costs for synthetic methane in 2030 and 2050 of an optimized Power-to-Gas plant with intermediate hydrogen storage. *Appl. Energy* **2019**, *253*, 113594. [CrossRef]
18. Kato, T.; Kubota, M.; Kobayashi, N.; Suzuoki, Y. Effective utilization of by-product oxygen from electrolysis hydrogen production. *Energy* **2005**, *30*, 2580–2595. [CrossRef]
19. McGuinness, R.M.; Kleinberg, W.T. Oxygen production. In *Oxygen-Enhanced Combustion*, 2nd ed.; Baukal, C.E., Ed.; CRC Press: Boca Raton, FL, USA, 2013; pp. 44–74. ISBN 978-1-4398-6230-8.
20. Kerry, F.G. Noncryogenic oxygen production. In *Oxygen-Enhanced Combustion*, 2nd ed.; Baukal, C.E., Ed.; CRC Press: Boca Raton, FL, USA, 2013; pp. 77–87. ISBN 978-1-4398-6230-8.
21. Šulc, R.; Ditzl, P. A technical and economic evaluation of two different oxygen sources for a small oxy-combustion unit. *J. Clean. Prod.* **2021**, *309*, 127427. [CrossRef]
22. Air Liquide Engineering and Construction. Standard Plants: Fully Packaged Modular Solutions. Available online: <https://www.engineering-airliquide.com/standard-plants> (accessed on 7 January 2022).
23. PCI Oxygen Solutions. On-Site Oxygen Solutions: Industrial. Available online: <https://www.pcgases.com/oxygen-solutions/marketing-literature/> (accessed on 7 January 2022).
24. Adsorptech. EcoGen™ Oxygen VPSA Onsite Generator. Available online: <https://adsorptech.com/wp-content/uploads/2021/Adsorptech-EcoGen-2111-2.pdf> (accessed on 7 January 2022).
25. Banaszkiwicz, T.; Chorowski, M.; Gizicki, W. Comparative analysis of oxygen production for oxy-combustion application. *Energy Procedia* **2014**, *51*, 127–134. [CrossRef]
26. Bailera, M.; Kezibri, N.; Romeo, L.M.; Espatolero, S.; Lisbona, P.; Bouallou, C. Future applications of hydrogen production and CO<sub>2</sub> utilization for energy storage: Hybrid power to gas-oxycombustion power plants. *Int. J. Hydrogen Energy* **2017**, *42*, 13625–13632. [CrossRef]
27. Schiebahn, S.; Grube, T.; Robinius, M.; Tietze, V.; Kumar, B.; Stolten, D. Power to gas: Technological overview, systems analysis and economic assessment for a case study in Germany. *Int. J. Hydrogen Energy* **2015**, *40*, 4285–4294. [CrossRef]
28. Mergel, J.; Carmo, M.; Fritz, D. Status on technologies for hydrogen production by water electrolysis. In *Transition to Renewable Energy Systems*; Wiley-VCH: Weinheim, Germany, 2013; pp. 425–450. ISBN 978-3-527-33239-7.
29. Schmidt, O.; Gambhir, A.; Staffell, I.; Hawkes, A.; Nelson, J.; Few, S. Future cost and performance of water electrolysis: An expert elicitation study. *Int. J. Hydrogen Energy* **2017**, *42*, 30470–30492. [CrossRef]
30. Iora, P.; Chiesa, P. High efficiency process for the production of pure oxygen based on solid oxide fuel cell–solid oxide electrolyzer technology. *J. Power Sources* **2009**, *190*, 408–416. [CrossRef]
31. Iora, P.; Taher, M.A.A.; Chiesa, P.; Brandon, N.P. A one dimensional solid oxide electrolyzer-fuel cell stack model and its application to the analysis of a high efficiency system for oxygen production. *Chem. Eng. Sci.* **2012**, *80*, 293–305. [CrossRef]
32. Ghaib, K.; Nitz, K.; Ben-Fares, F.-Z. Chemical methanation of CO<sub>2</sub>: A review. *ChemBioEng Rev.* **2016**, *3*, 266–275. [CrossRef]
33. Herrmann, F.; Grünwald, M.; Meijer, T.; Gardemann, U.; Feierabend, L.; Riese, J. Operating window and flexibility of a lab-scale methanation plant. *Chem. Eng. Sci.* **2022**, *254*, 117632. [CrossRef]
34. Chwoła, T.; Spietz, T.; Więclaw-Solny, L.; Tatarczuk, A.; Krótki, A.; Dobras, S.; Wilk, A.; Tchórz, J.; Stec, M.; Zdeb, J. Pilot plant initial results for the methanation process using CO<sub>2</sub> from amine scrubbing at the Łaziska power plant in Poland. *Fuel* **2020**, *263*, 116804. [CrossRef]
35. Gorre, J.; Ruoss, F.; Karjunen, H.; Schaffert, J.; Tynjälä, T. Cost benefits of optimizing hydrogen storage and methanation capacities for Power-to-Gas plants in dynamic operation. *Appl. Energy* **2020**, *257*, 113967. [CrossRef]
36. Van Rossum, G. The Python Library Reference. Release 3.7.8rc1. 2020. Available online: <https://docs.python.org/3.7/library/index.html> (accessed on 24 June 2020).
37. Hilpert, S.; Kaldemeyer, C.; Krien, U.; Günther, S.; Wingenbach, C.; Plessmann, G. The open energy modelling framework (oemof)—A new approach to facilitate open science in energy system modelling. *Energy Strategy Rev.* **2018**, *22*, 16–25. [CrossRef]
38. Krien, U.; Schönfeldt, P.; Launer, J.; Hilpert, S.; Kaldemeyer, C.; Plessmann, G. Oemof.solph—A model generator for linear and mixed-integer linear optimisation of energy systems. *Softw. Impacts* **2020**, *6*, 100028. [CrossRef]
39. Buttler, A.; Spliethoff, H. Current status of water electrolysis for energy storage, grid balancing and sector coupling via power-to-gas and power-to-liquids: A review. *Renew. Sustain. Energy Rev.* **2018**, *82*, 2440–2454. [CrossRef]
40. Carmo, M.; Fritz, D.L.; Mergel, J.; Stolten, D. A comprehensive review on PEM water electrolysis. *Int. J. Hydrogen Energy* **2013**, *38*, 4901–4934. [CrossRef]
41. International Energy Agency. The Future of Hydrogen: Seizing Today’s Opportunities, Paris. 2019. Available online: <https://www.iea.org/reports/the-future-of-hydrogen> (accessed on 3 January 2022).
42. Mutz, B.; Carvalho, H.W.P.; Mangold, S.; Kleist, W.; Grunwaldt, J.-D. Methanation of CO<sub>2</sub>: Structural response of a Ni-based catalyst under fluctuating reaction conditions unraveled by operando spectroscopy. *J. Catal.* **2015**, *327*, 48–53. [CrossRef]
43. Energy Brainpool. Trends in the Development of Electricity Prices—EU Energy Outlook 2050. Available online: <https://blog.energybrainpool.com/en/trends-in-the-development-of-electricity-prices-eu-energy-outlook-2050/> (accessed on 16 February 2022).
44. Energy Brainpool. Update: EU Energy Outlook 2050—How will Europe Evolve over the Next 30 Years? Available online: <https://blog.energybrainpool.com/en/update-eu-energy-outlook-2050-how-will-europe-evolve-over-the-next-30-years/> (accessed on 16 February 2022).



45. van Leeuwen, C.; Mulder, M. Power-to-gas in electricity markets dominated by renewables. *Appl. Energy* **2018**, *232*, 258–272. [CrossRef]
46. E4tech, E.E. Development of Water Electrolysis in the European Union: Final Report. 2014. Available online: <https://www.fch.europa.eu/node/783> (accessed on 20 December 2021).
47. Peters, M.S.; Timmerhaus, K.D.; West, R.E. *Plant Design and Economics for Chemical Engineers*, 5th ed.; McGraw-Hill: Boston, MA, USA, 2004; ISBN 0-07-239266-5.
48. Austrian Power Grid AG. EXAA Day-Ahead Prices 2020. Available online: <https://www.apg.at/de/markt/Markttransparenz/Uebertragung/EXAA-Spotmarkt> (accessed on 21 December 2021).
49. Traupmann, A.; Greiml, M.; Steinegger, J.; Kühberger, L.; Kienberger, T. Sector coupling technologies as re-purposing options for coal-fired power plants in the austrian grids—A MES approach. *Sustain. Energy Technol. Assess.* **2022**; under review.
50. International Energy Agency. World Energy Outlook 2021, Paris. 2021. Available online: <https://www.iea.org/reports/world-energy-outlook-2021> (accessed on 4 January 2022).
51. European Energy Exchange AG. Emission Spot Primary Market Auction Report 2020. Available online: <https://www.eex.com/en/market-data/environmental-markets/eua-primary-auction-spot-download> (accessed on 21 December 2021).
52. Pietzcker, R.C.; Osorio, S.; Rodrigues, R. Tightening EU ETS targets in line with the European Green Deal: Impacts on the decarbonization of the EU power sector. *Appl. Energy* **2021**, *293*, 116914. [CrossRef]
53. Cvetkovska, R.; Nagovnak, P.; Kienberger, T. Pathways for ramping-up hydrogen into the natural gas system. In Proceedings of the 17th Symposium Energieinnovation, Future of Energy: Innovationen für Eine Klimaneutrale Zukunft, Graz, Austria, 16–18 February 2022.
54. Gas-Systemnutzungsentgelte-Verordnung. Available online: <https://www.ris.bka.gv.at/GeltendeFassung.wxe?Abfrage=Bundesnormen&Gesetzesnummer=20007992&FassungVom=2022-06-02> (accessed on 28 June 2022).
55. E-Control. Natural Gas: Taxes and Surcharges. Available online: <https://www.e-control.at/en/industrie/gas/gaspreis/stuern-und-abgaben> (accessed on 28 June 2022).
56. Systemnutzungsentgelte-Verordnung 2018. Available online: <https://www.ris.bka.gv.at/GeltendeFassung.wxe?Abfrage=Bundesnormen&Gesetzesnummer=20010107&FassungVom=2022-01-01> (accessed on 28 June 2022).
57. E-Control. Electricity: Taxes and Surcharges. Available online: <https://www.e-control.at/en/industrie/strom/strompreis/stuern> (accessed on 28 June 2022).
58. Electricity Industry and Organization Act: ElWOG. 2010. Available online: <https://www.ris.bka.gv.at/GeltendeFassung.wxe?Abfrage=Bundesnormen&Gesetzesnummer=20007045> (accessed on 5 April 2022).
59. European Commission. A Clean Planet for All—A European Long-Term Strategic Vision for a Prosperous, Modern, Competitive and Climate Neutral Economy: In-Depth Analysis in Support of the Commission Communication COM (2018) 773, 28th 2018. Available online: [https://ec.europa.eu/clima/eu-action/climate-strategies-targets/2050-long-term-strategy\\_en](https://ec.europa.eu/clima/eu-action/climate-strategies-targets/2050-long-term-strategy_en) (accessed on 30 June 2022).